The role of proteasome dysfunction in the mechanisms of motor neuron degeneration in a mouse model of familial amyotrophic lateral sclerosis

Thesis

"THE ROLE OF PROTEASOME DYSFUNCTION IN THE MECHANISMS OF MOTOR NEURON DEGENERATION IN A MOUSE MODEL OF FAMILIAL AMYOTROPHIC LATERAL SCLEROSIS"

The Open University, UK

— Advanced School of Pharmacology —
Dean, Enrico Garattini M D

Mario Negri Institute for
Pharmacological Research

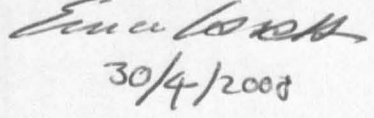

30/4/2008

Cristina Cheroni

Thesis submitted for the degree of Doctor of Philosophy

The Open University of London

Laboratory of Molecular Neurobiology

Department of Neuroscience

Mario Negri Institute for Pharmacological Research Milano

Submitted: September 2007

ABSTRACT

Amyotrophic lateral sclerosis (ALS) is a neurodegenerative disease characterized by the loss of the motor neurons. One consistent neuropathological feature of ALS patients and models of the disease is the formation of proteinaceous inclusion bodies; for this reason, alterations in the proteolytic ubiquitin-proteasome pathway (UPP) have been suggested to be implicated.

The purpose of this thesis was to analyze the role of the UPP in ALS pathogenesis studying the G93A mouse model. The activity of UPP was evaluated in G93A mice carrying the Ub^{G76V}-GFP reporter protein for proteasomal functionality. Furthermore, the expression of different constitutive proteasome and immunoproteasome subunits was measured during disease progression.

In symptomatic G93A lumbar spinal cord, a mild increase of Ub^{G76V}-GFP protein, but not of its transcript, was found in the motor neuronal population and was partly associated with high levels of ubiquitin and perikarial presence of phosphorylated neurofilaments. At the end stage, the increase of the reporter protein was prevalent in other neurons besides motor neurons, but also the mRNA levels were augmented.

Constitutive catalytic subunits of the 20S proteasome were reduced in end stage G93A lumbar spinal cord, while an increase of their inducible counterparts and a decrease of the non-catalytic α5 subunit were evident at the symptomatic phase. Components of 19S and 11S complexes were significantly reduced prior to symptom onset. The changes in proteasome composition were accompanied by a substantial increase of glial markers and TNFα.

Altogether, these data suggest that a subtle dysfunction of the ubiquitin-proteasome pathway occurs in the spinal cord of a mouse model of ALS in a phase in which the first signs of motor impairment are detectable. This pairs with alterations in the transcriptional rate of various proteasome subunits, resulting in a decrease of constitutive proteasome and an increase of immunoproteasome.

ACKNOWLEDGMENTS

I would like to express my gratitude to Dr. Caterina Bendotti for the great academic and personal support given me in all these years spent in her laboratory and to my supervisor Prof. C. Shaw.

My sincere thanks also go to Dr. Nico Dantuma and Dr. Christa Maynard for their advice and suggestions about this project, and for the warm welcome in Stockholm.

I thank the Mario Negri Institute for Pharmacological Research, for giving me the opportunity to undertake my PhD

Finally, the most special thought to all the people that have been the body and the soul of the laboratory of in the last seven years.

I dedicate this thesis to all the people who believe in me and bring happiness in my life, and to a special person among them.

INDEX

LIST OF ABBREVIATIONS

AD	Alzheimer's Disease
ALS	Amyotrophic Lateral Sclerosis
AMPA	α-Amino-3-Hydroxy-5-Methyl-4-Isoxazole Propionic Acid
ANOVA	Analysis of Variance
ATF-3	Activating Transcription Factor 3
ATF-6	Activating Transcription Factor 6
ATP	Adenosine Triphosphate
BCA	Bicinchoninic Acid Assay
bp	Base pair
BSA	Bovine Serum Albumin
CCS	Copper Chaperone for Superoxide Dismutase
CD11β	Cluster of Differentiation 11β
CD68	Cluster of Differentiation 68
CD8	Cluster of Differentiation 8
CDK5	Cyclin-Dependent Kinase 5
cDNA	Complementary DNA
ChAT	Choline Acetyl Transferase
CHIP	Carboxyl terminus of Hsc-70 Interacting Protein
CHOP	C/EBP Homologous Protein
CMV	Cytomegalovirus
CNS	Central Nervous System
COX-2	Cyclooxygenase 2
CRA mice	Cramping mice
CSF	Cerebrospinal Fluid

CTP	Cytidine Triphosphate
DAB	3'-3-Diaminobenzidine Tetrahydrocholride
DNA	Deoxyribonucleic Acid
DNase	Deoxyribonuclease
dNTP	Deoxynucleotide Triphosphates
DTT	Dithiothreitol
DUB	Deubiquitinating enzyme
E1	Ubiquitin-activating enzyme
E2	Ubiquitin-conjugating enzyme
E3	Ubiquitin-protein ligase
EAAT	Excitatory Amino Acid Transporter
ECL	Enhanced Chemiluminescence
EDTA	Ethylenediamine-N,N,N',N'-Tetraacetic Acid
ER	Endoplasmic Reticulum
ERAD	ER-associated Degradation
fALS	Familial ALS
FTD	Frontotemporal Dementia
FTDP	Frontotemporal Dementia with Parkinsonism
FTLD	Frontotemporal Lobar Degeneration
G93A mice	Mice transgenic for human SOD1 with Gly93Ala substitution
GDP	Guanosine-5'-Diphosphate
GEF	Guanine Exchange Factor
GFAP	Glial Fibrillary Acidic Protein
GFP	Green Fluorescent Protein
GFP1 mice	Mice transgenic for Ub^{G76V}-GFP line 1
GFP2 mice	Mice transgenic for Ub^{G76V}-GFP line 2

GTP	Guanosine Triphosphate
H	Hour
HECT	Homologous to E6-AP carboxyl terminus
HRP	Horseradish Peroxidase
IFNγ	Interferon γ
ISH	*In Situ* Hybridization
IGF	Insulin Growth Factor
IgG	Immunoglobulin G
Kb	Kilobase
Kda	KiloDalton
LMN	Lower Motor Neurons
LMP10	Low Molecular Mass Polypeptide 10
LMP2	Low Molecular Mass Polypeptide 2
LMP7	Low Molecular Mass Polypeptide 7
LOA mice	Legs-at-Odd-Angles mice
MAPK	Mitogen Activated Protein Kinase
MHC I	Major Histocompatibility Complex class I
Min	Minute
MND	Motor Neuron Disease
MND mice	Motor Neuron Degeneration mice
mRNA	Messenger RNA
mSOD1	Murine SOD1
MuLV RT	Moloney Murine Leukaemia Virus Reverse Transcriptase
NEM	N-Methyl d-Aspartate
NF-H	High molecular weight Neurofilament
NFkB	Nuclear Factor-Kappa B
NF-L	Low molecular weight Neurofilament

NGS	Normal Goat Serum
NMD mice	Neuromuscular Degeneration mice
NO	Nitric Oxide
NOS	Nitric Oxide Synthase
NTg mice	Non-Transgenic mice
PBS	Phosphate Buffered Saline
PBST	Phosphate Buffered Saline + 0.1 Tween-20
PCR	Polymerase Chain Reaction
PD	Parkinson's Disease
PDI	Protein-Disulfide Isomerase
PKA	Protein Kinase A
PMN mice	Paralyzé Natural Mutant mice
Poli-Q	Poliglutamine-extension
POMP	Proteasome Maturation Protein
RNA	Ribonucleic Acid
RNase	Ribonuclease
ROS	Reactive Oxygen Species
RT	Room Temperature
RT-PCR	Reverse-Transcriptase Polymerase Chain Reaction
S.E.	Standard error
sALS	Sporadic ALS
SDS	Sodium Dodecyl Sulfate
Sec	Second
SETX	Senataxin
SOD1	Superoxide Dismutase 1
SOD2	Superoxide Dismutase 2
SOD3	Superoxide Dismutase 3

SSC	Saline-Sodium Citrate Buffer
SUMO	Small Ubiquitin-like Modifier
TBS	Tris Buffered Saline
TBST	TBS + 0.1% Tween-20
TDP-43	TAR-DNA-binding Protein 43
TNB	TBS 0.1 M, Blocking reagent 0.5%
TNFα	Tumor Necrosis Factor α
TNT	TBS 0.1 M, Triton X-100 0.05%
Tris	Tris(hydroxymethyl)methylamine
Ub	Ubiquitin
UBC	Ubiquitin Conjugating Domain
UCHL1	Ubiquitin Carboxy-terminal Hydrolase-1
UFD	Ubiquitin-Fusion Degradation
UMN	Upper Motor Neurons
UPP	Ubiquitin-Proteasome Pathway
UPR	Unfolded Protein Response
UTP	Uridine Triphosphate
VAPB	Vesicle-Associated Membrane Protein B
VEGF	Vascular Endothelial Growth Factor
VPS 54	Vacuolar Vesicular Protein Sorting 54
WT SOD1 mice	Mice transgenic for human wild type SOD1

LIST OF TABLES

LIST OF FIGURES

CHAPTER I

OVERALL INTRODUCTION

The existence of clinical conditions characterized by progressive muscular weakness and wasting became clearly recognized by the mid 19th century. In 1869 the famous French neurobiologist and physician Jean-Martin Charcot, studying the pathological features of this syndrome, described the characteristic alterations of the corticospinal tract and the loss of motor neurons and proposed the term *amyotrophic lateral sclerosis* (ALS). "Amyotrophic" refers to the muscle atrophy, weakness and fasciculation that derive from the degeneration of the motor neurons, whereas "lateral sclerosis" refers to the hardness to palpation of the lateral columns of the spinal cord in autopsy specimens, where gliosis follows degeneration of the corticospinal tracts.

The term *motor neuron disease* (MND) is commonly used in the United Kingdom to indicate the ALS syndrome. In the United States, ALS is often known as *Lou Gehrig's disease* after the great baseball player who developed this disorder in the 1930s.

Nowadays, amyotrophic lateral sclerosis is defined as a progressive and fatal neurodegenerative disease resulting from the selective degeneration of upper motor neurons (UMN) in the motor cortex and lower motor neurons (LMN) in the brainstem and in the spinal cord (Fig. 1.1). When the motor neurons die, the nervous system becomes unable to initiate and control muscle movements. Because muscles no longer receive the input they need in order to function, they gradually weaken and deteriorate, producing deep atrophy.

ALS is the most frequent of the motor neuron disorders, representing 85-90% of cases of this kind of pathologies. The majority of ALS patients present a sporadic form (sporadic ALS, sALS) but in 5-10% of cases the disease is inherited (familial ALS, fALS).

Regrettably, at the moment, no primary therapy for this disorder is available and the only drug approved for its treatment (riluzole) only slightly promotes survival; therefore symptomatic measures are the mainstay of management of ALS.

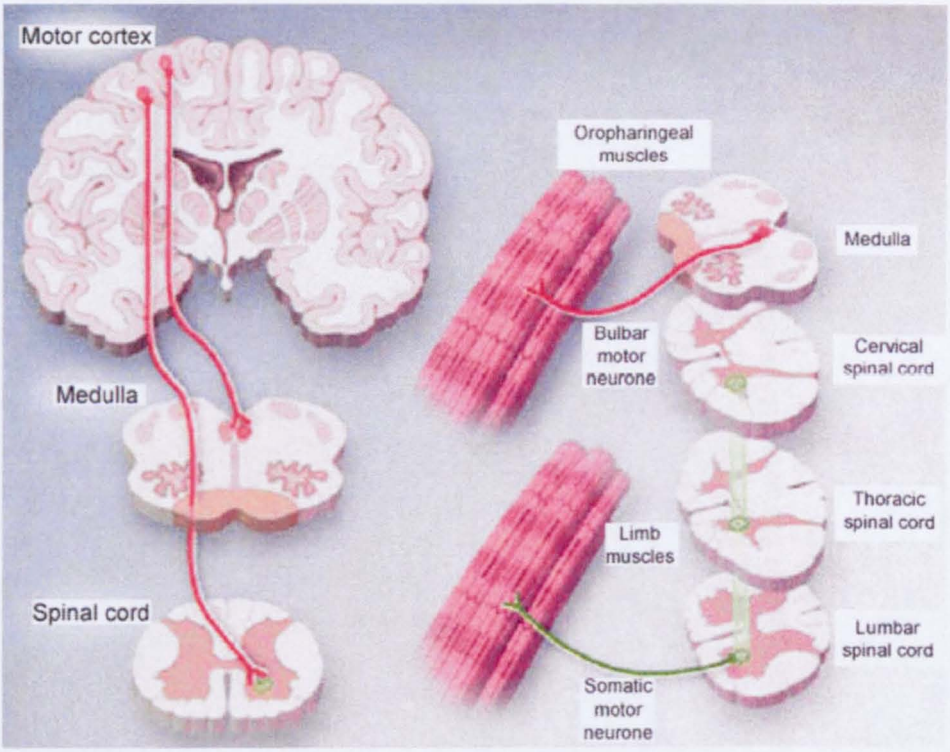

Figure 1.1 The human motor system. Adapted from Rowland L.P. and Shneider N.A., N. Engl. J. Med., 2001.

1.1 Clinical phenotype of Amyotrophic Lateral Sclerosis

By definition, the features of ALS are signs and symptoms of lower motor neuron dysfunction associated with upper motor neuron dysfunction. LMN involvement determines weakness and fatigue, associated to progressive muscular atrophy, fasciculation (muscular twitching and shaking of contiguous groups of muscle fibers) and fibrillation (muscular twitching and shaking involving individual muscle fibers acting without coordination), reduced muscle tone and absence of tendon reflex. UMN involvement causes weakness, incoordination, stiffness and slowing of movement, with spasticity (persistent contraction of muscle), increased tendon reflexes, clonus (alternating contractions and relaxations) and extensor plantar responses.

ALS probably begins a long time before its clinical manifestations, given that a substantial number of motor neurons can be lost before any clinical signs develop. In fact, several studies on animal models have shown that motor neuron dysfunction precedes the onset of symptoms and that compensatory reinnervation from nearby motor neurons permits a good maintenance of the motor function, although with an enlargement of motor units, until more than 50% of motor units have been lost; at this point symptoms appear and the number of motor units declines rapidly (Cote et al., 1993; Kennel et al., 1996).

No neuropathological, neurophysiological or biochemical markers are yet available to identify a patient as potentially susceptible for ALS prior to symptom onset.

The different extent and localization of motor system involvement determines various early clinical features in different patients but ultimately, as the

disorder progresses, the clinical expression of ALS is quite uniform, with extreme muscular wasting, spasticity and paralysis.

At the onset, ALS presents with lower motor neuron involvement, upper motor neuron involvement or bulbar involvement. Limb onset is the most frequent, and is found in 75-80% of cases, while bulbar onset is evidenced in only 20-25%. The most common initial presentation of ALS is focal asymmetric distal weakness and muscular atrophy. For example, the patient may present himself with a history of unexpected tripping, dragging of a foot and ultimately more diffuse weakness of the leg. Difficulty with buttoning clothes, turning keys in doors or simply poor coordination while performing fine movements are the symptoms of involvement of upper limbs. Bulbar motor neuron degeneration leads to difficulty in swallowing (dysphagia) and speaking or forming words (dysarthria), associated to fasciculation of the tongue. Bulbar signs are often closely related to respiratory deficits, due to the involvement of diaphragmatic muscular weakness. This leads to a poor prognosis and to a shorter life expectancy.

With the progression of the illness, the disease spreads to contiguous muscle segments. The progressive loss of motor function results in increasing disability and paralysis, ultimately leading to a bed-bound state.

Recent findings have revealed that the selectivity of ALS for the motor system is not absolute. In fact, some reports describe cognitive impairment in a subgroup of ALS patients. A battery of neuropsychological tests has shown a cognitive impairment in about 30% of ALS patients, ranging from mild impairment to frontotemporal lobar degeneration (FTLD). The main symptoms are executive dysfunction with deficits in verbal and non-verbal fluency and concept formation (Lomen-Hoerth et al., 2003; Kilani et al., 2004; Abrahams et al., 2005; Schreiber et al., 2005; Rippon et al., 2006). However, in the majority

of the cases, the rate of cognitive decline is very slow as compared to the devasting motor deterioration.

Respiratory deficits, due to the progressive atrophy of respiratory muscles, appear during the progression of the disease. When respiratory muscle activity is insufficient, patients need to use mechanised ventilatory support. Respiratory failure finally leads to the death of almost all ALS patients without mechanised assistance.

In 50% of cases the death occurs within three years from diagnosis.

1.2 Diagnosis of Amyotrophic Lateral Sclerosis

Diagnosis of ALS is often critical, since many different clinical conditions may resemble this disease. To date, no test or specific marker can provide a definitive diagnosis of ALS; thus, it is primarily based on the symptoms and signs that the physician observes in the patient and on a series of tests to rule out other diseases.

Criteria for clinical and pathological diagnosis have been defined during the ALS meeting held in El Escorial, Spain, in 1994 and updated at Airlie House, Virginia, four years later.

Based on these criteria, the diagnosis of ALS requires the presence of:

1) evidence of LMN degeneration by clinical, electrophysiological or neuropathological examination,

2) evidence of UMN degeneration by clinical examination, and

3) progressive spread of symptoms or signs within a region or to other regions, as determined by history or examination,

together with the absence of:

1) electrophysiological and pathological evidence of other disease processes that might explain the signs of LMN and/or UMN degeneration, and
2) neuroimaging evidence of other disease processes that might explain the observed clinical and electrophysiological signs.

As shown in table 1.1, the El Escorial scale classifies the probability of a patient having ALS according to the degree of clinical certainty in relation to other pathologies. It includes four degrees of certainty for the diagnosis of ALS. A careful history, physical and neurological examination must search for clinical evidence of UMN and LMN signs in four regions (brainstem, cervical, thoracic or lumbosacral spinal cord) of the central nervous system (CNS).

LEVEL OF CERTAINTY	CHARACTERISTIC FEATURES
Clinically Possible ALS	• UMN and LMN signs together in one region; or • UMN signs in two or more regions; or • UMN and LMN signs in two regions with no UMN signs rostral to LMN signs
Clinically Probable – Laboratory supported ALS	• UMN and LMN dysfunction in only one region; or • UMN signs alone are present in one region, and LMN signs defined by electromyography criteria are present in at least two regions
Clinically Probable ALS	• UMN and LMN signs in at least two regions with some UMN signs rostral to LMN signs
Clinically Definite ALS	• UMN as well as LMN signs in three regions.

Table 1.1: El Escorial scale for ALS diagnosis

1.3 EPIDEMIOLOGY OF AMYOTROPHIC LATERAL SCLEROSIS

ALS is considered as a rare disease: it occurs in about 1-3 people per 100,000 per year with a *prevalence* (number of surviving patients at any given time) of about 5-7 per 100,000. However, its personal and socioeconomic impact is greater and it has been calculated that its lifetime risk is approximately 1 in 1000 (McGuire et al., 1996; Mitsumoto et al., 1998). The frequency of ALS appears to have been rising moderately over the past 50 years. Although this rise may indicate the increasing effect of some unidentified exogenous factors, more probably it simply reflects the greater life expectancy of the population, which allows longer survival of a subpopulation susceptible to ALS.

The average survival for sporadic ALS patients is approximately 3-5 years after the first symptoms. Onset of ALS in patients younger than 50 years of age is generally associated with a longer survival.

The incidence of ALS increases with age (Kurtzke, 1991), with a peak occurring between 55 and 75 years of age; therefore, aging is the most significant risk factor.

ALS occurs predominantly in males, with a male to female ratio of 1.4 to 2.5; however, with increasing of age, this difference tends to diminish (Kurtzke, 1991).

Environmental risk factors are inconsistently reported in ALS; this may reflect a complex interaction between several environmental risk factors and specific genetic susceptibilities.

People of all races and ethnic backgrounds are affected by ALS and, with the exception of specific endemic areas in the Western Pacific, its worldwide frequency is uniform. Four geographic areas with a high prevalence (approximately 100-150 fold higher than the other regions) of ALS are described (Kurland and Molgaard, 1982; Oyanagi and Wada, 1999):

- Guam and Rota islands
- 2 areas in the Kii peninsula
- Irian Jaya (Indonesia)
- Area of the Gulf of Carpentaria (North Australia)

Western Pacific ALS is considered a distinct disease because it is often associated to Parkinsonism dementia, with pathological alterations resembling Alzheimer's disease (neurofibrillary tangles). This syndrome is not considered further in this thesis.

Although familial ALS is almost indistinguishable from the sporadic form in terms of clinical phenotype, some features differentiate it from an epidemiological point of view (Mitsumoto et al., 1998). The average onset of fALS cases is approximately 47 years, a decade earlier than the sporadic type, and the mean survival is shorter; moreover, it occurs equally in males and females. Finally, in fALS, symptoms more frequently begin in the lower extremities compared to sporadic ALS.

1.4 Neuropathology of Amyotrophic Lateral Sclerosis

Immunohistochemical and ultrastructural studies performed on post mortem tissues of ALS patients have helped to describe better the neuropathology of the disease. However, post-mortem examinations are conducted on tissues representing the final stage of the pathology; thus the alterations observed reflect a very advanced state of neuronal degeneration and give little information about the triggering events causing the cell death. It is also true that patients have different degrees of neuronal degeneration in various areas of their central nervous system; for example, many patients with aggressive form of bulbar onset ALS at the time of death often have relatively spared motor neurons in the spinal cord.

1.4.1 Motor system pathology

The major pathological features of ALS are:

I. Upper motor neuron abnormalities

II. Myelin pallor in the corticospinal tracts

III. Reduction in both size and number of lower motor neurons in the spinal ventral horns and in the bulbar nuclei.

I. UMN involvement

Upper motor neurons are defined as the neurons, localized in the motor cortex, that exert supranuclear control over lower motor neurons.

The degree of degeneration observable at autopsy in the motor cortex of ALS patients is quite variable and may not be always evident, even in the presence of clear upper motor neuron signs. In the most severely affected cases, an evident loss of giant Betz cells in cortical layer 5, associated with an extensive astrogliosis and microgliosis, is reported. Since there are not good markers to distinguish upper motor neurons and other pyramidal cell types in the cortex, the identification of the Betz cell is often based on morphological and size criteria. Neuron cell bodies appear atrophied (Kiernan and Hudson, 1991), with shorter fragmented dendrites (Hammer et al., 1979). Intracellular alterations are rarely identified in the spared Betz cells in classical ALS; occasionally, ubiquitinated neurofilament inclusions are reported.

Pathological changes are rarely evident in somatosensory cortex, prefrontal cortex and premotor areas (Kiernan and Hudson, 1991).

II. Corticospinal tract alterations

Axonal degeneration of the descending corticospinal tract results in clear demyelination of the tract. As a consequence, the spinal cord of ALS cases shows a pallor with myelin stain. Corticospinal fibers also show marked

axonal swelling and spheroids (Chou, 1992). An extensive gliosis is present, causing the typical sclerosis of lateral spinal cord tracts.

III. LMN involvement

Loss of large motor neurons localized in the lower brainstem and in the spinal cord is clearly observed at autopsy. Shrinkage and atrophy of the cell body precede neuronal death (Kiernan and Hudson, 1991); the phenomenon is associated with alterations of axon and dendrite structures, which become thinner (Nakano and Hirano, 1987).

Certain motor neuron groups, such as those controlling eye movements and the Onuf's nucleus of the sacral spinal cord (that regulates the pelvic floor musculature) are largely spared by the disease.

The remaining motor neurons present several abnormalities, listed below.

Ubiquitinated inclusions

Ubiquitin-positive inclusions are found very frequently in the susceptible LMN groups of the spinal cord and brainstem of most cases and are defined as skein-like inclusions or Lewy body-like accumulations. The first are a specific hallmark of ALS whereas Lewy body-like inclusions are found also in other disorders. Both inclusions probably represent two different morphological stages of protein aggregation, from diffuse filamentous forms to dense and compact inclusions. Besides phosphorylated neurofilaments and ubiquitin, Lewy body-like inclusions also contain cyclin-dependent kinase 5 (CDK5) (Nakamura et al., 1997); dorfin, a RING finger-type E3 ubiquitin ligase, has also been found (Hishikawa et al., 2003). More recently, the nuclear factor TDP-43 (TAR-DNA-binding protein 43) has been identified as a major component of ubiquitinated inclusions in sporadic ALS cases (Neumann et al., 2006); TDP-43 is thought to function as a regulator of transcription and

alternative splicing (Buratti and Baralle, 2001; Buratti et al., 2004; Mercado et al., 2005).

Ubiquitin-positive inclusions are localized both in normal appearing motor neurons and in some shrunken cells.

Bunina bodies

Bunina bodies are described as small, eosinophilic, irregularly shaped inclusions localized in the soma of motor neurons; probably they have a lysosomal derivation (Sasaki and Maruyama, 1993). At the ultrastructural analysis, they appear like electron-dense, amorphous structures surrounded by vesicles, endoplasmic reticulum (ER) fragments, lipofuscin granules and are shown to contain cystatin C.

Bunina bodies are reported to be present in 30-50% of cases; since they are not described in other disorders, they seem to be specific for ALS. Their pathogenesis and their relationship to neurodegeneration have not yet been unravelled.

Hyaline conglomerate inclusions

Hyaline conglomerate inclusions consist of large aggregates of phosphorylated and non phosphorylated neurofilaments associated with other "entrapped" cytoplasmic proteins and organelles (Schochet et al., 1969; Leigh et al., 1989; Sasaki and Maruyama, 1991). They have been identified in sporadic and familial ALS; however, they seem to be less specific for this pathology, since they have been found in other neurological disorders (Sobue et al., 1990).

Globules and spheroids

Phosphorylated neurofilaments are also found packed in axonal swellings in the anterior horns of ALS patients (Corbo and Hays, 1992; Toyoshima et al., 1998).

Spheroids are larger and tend to be localized in proximal axons and dendrites, while globules are smaller and usually are more peripheral in the ventral horn. Both are presumed to represent focal abnormalities of axonal cytoskeletal regulation with a failure of axonal transport.

Diffuse somatic phosphorylation of neurofilaments

Diffuse accumulation of phosphorylated neurofilaments has been observed in the perikarya of motor neurons, especially in sporadic ALS (Hirano et al., 1984).

Golgi fragmentation

Both upper and lower motor neurons of ALS cases show signs of fragmentation of the Golgi apparatus, that is dispersed into numerous small isolated elements (Mourelatos et al., 1994; Fujita and Okamoto, 2005).

Mitochondrial alterations

In recent years, morphological alterations of mitochondria in the motor neurons of ALS patients have been observed. These include dense conglomerates of aggregates, dark mitochondria, swelling and vacuolization (Hirano et al., 1984; Swerdlow et al., 1998).

VI. Involvement of other cell types

Remarkable morphological and neurochemical evidence demonstrates the proliferation and activation of the microglial and astrocytic populations in the areas characterized by motor neuronal loss (Kawamata et al., 1992).

The concept of selective motor neuronal death has been challenged by studies reporting the loss of small neurons in the spinal cord of ALS cases (Oyanagi et al., 1989; Raynor and Shefner, 1994). In a recent report by Stephens and colleagues, the morphometric examination of the lumbar spinal cord of sporadic ALS patients revealed a substantial loss of ventral interneurons in addition to motor neurons. Therefore, the interneuronal population may

degenerate to a similar extent and contemporary with the motor neuronal one (Stephens et al., 2006).

1.4.2 Non-motor system pathology

Autopsy examination revealed in some ALS patients alterations in extra-motor regions of the CNS, such as in the sensory system (Hudson, 1981), substantia nigra and hippocampus (Wharton, 2003).

1.4.3 Non-CNS pathology

Profound atrophy of the skeletal muscles is one of the earliest pathological changes in ALS patients (Mitsumoto et al., 1998). Other alterations are reported in the skin, in which the collagen cross-linking results altered (Kolde et al., 1996).

1.5 Genetics of Amyotrophic Lateral Sclerosis

ALS is considered a multifactorial disease, with a complex interaction between genetic and environmental factors.

As already explained, in 90-95% of ALS cases, there is no apparent genetic linkage (sporadic ALS), but in the remaining 5-10% the disease is inherited (familial ALS); the transmission is, in most cases, dominant, with rare cases of recessive inheritance.

1.5.1 Mendelian genetics of ALS

So far, as shown in table 1.2, five mendelian gene defects have been reported to cause ALS (Pasinelli and Brown, 2006).

fALS type	Gene	Genomic region	Clinical features
		Mendelian genes	
ALS1	SOD1	21q22	Autosomal dominant; typical ALS
ALS2	ALS2	2q33	Autosomal recessive; juvenile onset, slowly progressive form
ALS4	SETX	9q34	Autosomal dominant; juvenile onset, slowly progressive non-fatal form
ALS8	VAPB	20q13	Autosomal dominant; heterogeneous disease phenotype
ALS	Dynactin	2p13	Autosomal dominant; adult onset, slowly progressive form with vocal cord paralysis
FTDP	Tau	17q21	Autosomal dominant, frontotemporal dementia and parkinsonism with some amyotrophy
		Mendelian loci	
ALS3	Unknown	18q21	Autosomal dominant
ALS5	Unknown	15q12-21	Autosomal recessive; juvenile onset, slowly progressive
ALS6	Unknown	16q12	Autosomal dominant
ALS7	Unknown	20p13	Autosomal dominant
ALS-FTD	Unknown	9q21-22	Autosomal dominant; ALS associated with frontotemporal dementia (FTD)
ALS-FTD	Unknown	9p	Autosomal dominant; ALS associated with frontotemporal dementia

Table 1.2: Mendelian genetics of ALS

The protein products of these mutated genes are:

- **ALS1: Cu,Zn superoxide dismutase (SOD1):**

  In 1993, Rosen and colleagues reported that mutations in the gene coding for the soluble, cytoplasmic enzyme Cu,Zn superoxide dismutase (SOD1) were associated with a subset of familial ALS patients (Rosen et al., 1993). This is the most common form of inherited ALS, accounting for about 20% of all familial ALS forms and corresponding to 2-3% of all ALS cases.

  SOD1 is a 153 amino acid, cytoplasmic homodimer that converts superoxide, produced as a by-product of oxidative phosphorylation, to oxygen and hydrogen peroxide; it is very abundant, representing up to 2% of the soluble proteins of the brain.

  To date, more than 125 mutations have been identified in SOD1 gene and are localized in all the five exons, with no region of the polypeptide escaping from disease-causing mutations; 114 of them result in amino acid substitution and are known to cause the disease, whereas six silent mutations and five intronic variants do not. Although most mutations are missense, 12 are nonsense or deletion mutations that produce a truncated protein (Andersen et al., 2003). Fig. 1.2 shows human SOD1 three-dimensional structure and some mutations that cause ALS. All mutations are associated with autosomal dominant fALS, except for D90A and D96N, which can cause both dominant and recessive ALS (Andersen et al., 1995; Robberecht et al., 1996; Orrell, 2000). The most frequent SOD1 mutation is A4V.

  Penetrance, clinical manifestations, age of onset, disease progression and survival vary greatly among specific mutations. For example, A4V and A4T are associated with an aggressive fALS type, (Aksoy et al., 2003), while slow

progression over 10-15 years is reported for mutations such as G37R, D90A, G93C and G93V (Arisato et al., 2003).

It was initially proposed that the toxicity of mutated SOD1 was associated with the loss of superoxide dismutase activity. However, most mutated SOD1 forms appear to fully retain their enzymatic property. The creation of transgenic mice expressing SOD1 with some of the mutations found in the human patients, which develop a motor syndrome similar to human ALS, showed that the catalytic activity is unchanged or elevated (Gurney et al., 1994; Ripps et al., 1995; Wong, 1995; Bruijn et al., 1997). Furthermore, SOD1 knockout mice do not develop spontaneous motor neuron disease (Reaume et al., 1996). The conclusion is that SOD1 mutants acquire one or more toxic properties, irrespective of the amount of superoxide dismutase activity that each of them retains.

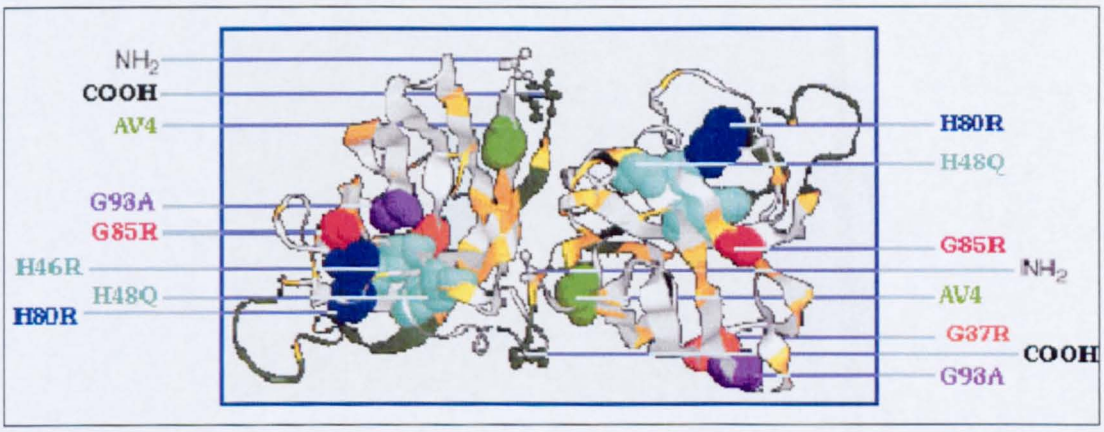

Figure 1.2 Position of some SOD1 mutations in the three-dimensional structure of human SOD1.

- **ALS2: alsin**

A new gene linked to a rare, recessively inherited form of ALS characterized by juvenile onset and slow progression has been identified in 2001 (Hadano et al., 2001; Yang et al., 2001); ALS2 variant is distinguished by the predominance of spasticity of facial and limb muscles. The ALS2 gene is

localized to chromosome 2 and encodes a 184 KDa protein named alsin. Alsin is ubiquitously expressed and is abundant in neurons, where it is localized to the cytosolic portion of the endosomal membrane. The amino-terminal region of alsin contains sequence motifs that are characteristic of guanine exchange factors (GEFs), involved in the recycling of a specific small G protein from its GDP-bound state to its GTP-state. The carboxy-terminal half of alsin contains two further domains, which are similar to those of the Rho G-protein family that modulates dynamic actin assembly. The function of alsin is not fully understood, but it is known that it acts as exchange factor for the small GTPase Rab5a *in vitro* (Otomo et al., 2003; Topp et al., 2004), suggesting a possible involvement in the organization of the cytoskeleton and in vesicle trafficking. In addition, alsin can interact with the small Rho GTPase Rac1 (Topp et al., 2004; Tudor et al., 2005). Interestingly, alsin is also able to bind specifically to different mutant variants of SOD1 through the RhoGEF domain (Kanekura et al., 2004) and, in a cell culture paradigm, it has been shown to suppress mutant SOD1 toxicity.

All the disease-causing alsin truncation mutations are highly unstable (Hadano et al., 2001); this has led to the hypothesis that the disease is caused by loss of activity of the protein.

- **ALS4: Senataxin (SETX)**

The gene encode a 303 KDa protein that contains a DNA/RNA helicase domain with strong homology to human RENT1 and IGHMBP2, two proteins known to have roles in RNA processing (Chen et al., 2004). Missense mutations in SETX cause an autosomal dominant, juvenile onset motor neuron disease with very slow progression of distal limb atrophy and motor neuron loss; the lifespan is not reduced.

- **ALS8: vesicle-associated membrane protein B (VAPB)**

  VAPB gene encodes a ubiquitously expressed homodimer, which belongs to a family of intracellular vesicle-associated/membrane-bound proteins that can associate with microtubules and are presumed to regulate vesicle transport. In particular, VAPB has been shown to act during the transport through the endoplasmic reticulum, Golgi apparatus and secretion. The P56S mutation dramatically disrupts the sub-cellular distribution of VAPB and induces the formation of intracellular protein aggregates (Nishimura et al., 2004).

- **Dynactin**

  This protein is a component of the dynein complex, implicated in the retrograde axonal transport of organelles and proteins. Dominantly transmitted mutations cause an adult onset, slowly progressive atypical motor neuron disorder with vocal cord paresis. The mutations appear to affect the binding of the dynactin-dynein motor to microtubules.

- **FTDP: Tau**

  Tau is a member of the microtubule-associated protein family, which has the principal functions of stabilizing microtubules and promoting their assembly by binding to tubulin. In addition, tau is likely to regulate motor protein-mediated transport of vesicles and organelles along the microtubules by modulating their stability (Sato-Harada et al., 1996; Ebneth et al., 1998). In frontotemporal dementia with parkinsonism (FTDP), the mutation of tau gene affects the alternative splicing of exon 10, resulting in an excess of four repeat tau isoforms; this may cause a reduced binding of tau to microtubules in axons. No pure ALS case has been associated with tau mutations.

Although all these forms have in common the degeneration of motor neurons, only ALS1 represents the classic late-onset neurodegenerative disease with selective death of upper and lower motor neurons.

Besides these genes, other loci linked to ALS have been identified and are reported in table 1.2.

1.5.2 Susceptibility genes

Susceptibility genes are defined as genes that can potentially contribute to the development of ALS; in other words, mutations in these genes may lead to ALS interacting with other genetic or environmental risk factors.

Among the genetic alterations that may confer a higher predisposition to the development of ALS, have been described mitochondrial DNA micro deletions encoding for cytochrome-C oxidase (Borthwick et al., 1999), RNA processing errors in the glutamate transporter EAAT2 (Excitatory Amino Acid Transporter) (Lin et al., 1998), an abnormal copy number of the survival motor neuron gene (Corcia et al., 2002) and gene deletions of the chromosome 5q13-linked neuronal apoptosis inhibitory protein gene (Jackson et al., 1996). An increased frequency of the cytochrome P450 debrisoquine hydroxylase CYP2D6(B) allele, encoding a cytochrome P450 monooxygenase involved in drug metabolism and associated with a "poor metabolizer" phenotype, has been also reported (Siddons et al., 1996). Frequently, these alterations were described in only few cases or the results of different studies are conflicting.

Some evidence suggests that vascular endothelial growth factor (VEGF) acts as a modifier of ALS in both human and mice. In a study conducted by Oosthuyse et al., ALS–like symptoms and neuropathology were observed in mice bearing a targeted deletion that eliminates the ability of VEGF gene to respond to tissue hypoxia (Oosthuyse et al., 2001). These mice show a normal baseline expression of VEGF, but have a pronounced deficit in the ability to

induce it in response to hypoxia. The motor deficits appear between 5 and 7 months of age and gradually progress; various classical features of ALS are observed, such as accumulation of neurofilaments in the motor neurons, degeneration of motor axons and muscle atrophy. As regards to the human pathology, in a large European study three single nucleotide polymorphisms in the promoter region of the VEGF gene have been associated with an overall 1.8–fold increased risk of developing ALS. The promoter variants in the VEGF gene in these patients coincided with reduced levels of plasma VEGF (Lambrechts et al., 2003).

Also neurofilament variants are probable modifying risk factors in sporadic ALS and may modulate disease expression. A set of small in-frame deletions or insertions in the repetitive tail domain of the large neurofilament subunit NF-H has been identified in about 1% of 1,300 sporadic ALS patients examined (Al-Chalabi et al., 1999). Although the known neurofilament sequence variants are not responsible by themselves for producing disease with high penetrance, it is likely that they are at least important risk factors for apparently sporadic disease.

The studies that link sALS to particular genetic variants so far known account only for a small number of the total cases; the causes could be a complex pattern of inheritance with very low penetrance, a high degree of heterogeneity and/or the existence of environmental factors predisposing to ALS. In conclusion, high genetic heterogeneity and complex interactions between genetic and environmental factors are the main obstacles in the process of finding new ALS genetic determinants.

1.6 Experimental Models of Amyotrophic Lateral Sclerosis

One of the major breakthroughs in the field of ALS research derives from the development of animal models of disease, that proved useful both for the study of pathogenetic mechanisms and to test potential pharmacological approaches.

Histopathological studies performed on post-mortem tissues obtained from ALS patients at autopsy may give important information about the status of motor neurons and other cells involved in the pathology at the final stage of the disease, but they provide a poor contribution to the understanding of the pathogenic mechanisms. Thus, the study of experimental models of ALS is useful to investigate the triggering events occurring earlier in the pathology.

Nowadays, many models of motor neuron degeneration have been discovered or developed. However, even if some of them are associated with gene mutations found in human ALS or considered risk factors for the disease, they recapitulate only some of the features of the human disease.

Nevertheless, these models may provide useful insights in deciphering the mechanisms of selective motor neuron degeneration as potential therapy targets.

1.6.1 Spontaneous models of ALS

Mice carrying naturally occurring mutations on identified or unidentified genes provide animal models of motor system impairment.

I. MND mouse

MND (motor neuron degeneration) is a spontaneous, dominant mutation localized to chromosome 8 in the coding region of the gene Cln8, belonging to the family of neuronal ceroid lipofuscinose-related genes (Ranta et al., 1999).

MND mice exhibit an adult-onset, progressive deterioration of motor function with spastic paralysis moving from caudal to cranial spinal cord levels. They undergo a premature death at 10-12 months (Messer et al., 1987). However, the number of choline acetyl transferase (ChAT) immuno-positive lumbar motor neurons is not different from normal mice (Mennini et al., 2002).

Neuropathological hallmarks are inclusion bodies containing ubiquitin, mitochondrial alterations, lipofuscin accumulation and neurofilament abnormalities. However, the presence of abnormal autofluorescent cytoplasmic inclusions rich in lipofuscin found in neurons, as well as in many other somatic organs, makes these animals a useful model for human neuronal ceroid lipofuscinosis rather than for ALS (Bronson et al., 1993).

II. PMN mouse

PMN (paralysé natural mutant) mice carry a recessive mutation on chromosome 13, (Brunialti et al., 1995). Two groups identified the PMN mutation as a Trp to Gly substitution at the last residue of the tubulin-specific chaperone protein (Bommel et al., 2002; Martin et al., 2002), that is essential for the proper tubulin assembly and for the maintenance of microtubules in motor axons. Distal axonopathy with paralysis of the limbs and muscular atrophy are the most relevant clinical signs, while motor neuron cell bodies and proximal axons are relatively preserved (Schmalbruch et al., 1991). Symptomatic phase begins at 2 weeks of age and evolves rapidly to death.

III. Wasted mouse

It carries a recessive mutation on chromosome 2, in the gene coding for the translational elongation factor eEF1A2 (Chambers et al., 1998).

The symptom onset is around 2 weeks of age and the progression is very fast, leading to death within a month. Spinal and brainstem motor neurons are lost, while UMN are not affected (Doble and Kennel, 2000).

IV. Wobbler mouse

The wobbler mouse represents another model of motor neuron disease (Mitsumoto and Bradley, 1982). It shows a progressive forelimb weakness and atrophy, accompanied by a marked decrease of muscular strength and motor ability; the symptoms are associated with proximal axonal degeneration and vacuolar changes within the motor neurons of the cervical spinal cord with little involvement of the brain.

In this case, the autosomal recessive genetic defect responsible for this syndrome has been mapped on chromosome 11 and it has recently been identified as a missense mutation in a Vacuolar Vesicular Protein Sorting (Vps 54) involved in the transport of vesicles from late endosomes to Golgi apparatus (Schmitt-John et al., 2005).

V. NMD mouse

Mice showing neuromuscular degeneration, with autosomal recessive mutation localized on the gene coding for the ATPase/DNA helicase have been described (Cook et al., 1995; Cox et al., 1998). Called NMD (neuromuscular degeneration) mice, they present rapidly progressive hind limb weakness and motor neuron cell body degeneration and have a life span that range from 2 to 20 weeks.

1.6.2 Artificial models of ALS

The discovery of mutations linked with fALS has made possible the development of etiological models of the disease.

I. SOD1 mutant mice

To obtain transgenic mice, exogenous genes are introduced by microinjection of purified DNA in the male pronucleus of fertilized mouse eggs. The integration of foreign DNA is random, with multiple copies of DNA usually integrating at a single site. Using the above described technology, several

transgenic mouse strains were created by the introduction of the sequence coding for human mutant SOD1 under the control of a promoter that enables ubiquitous expression of the transgene (Shibata, 2001). Investigators have generated different lines over-expressing human SOD1 with G93A, G37R or G85R mutations (Dal Canto and Gurney, 1994; Wong, 1995), or mouse SOD1 with G86R mutation (Ripps et al., 1995). These animals develop a phenotype that closely resembles ALS, with an adult onset progressive motor paralysis, muscle wasting and reduced lifespan. Pathological changes mainly consist of depletion of motor neurons in the spinal cord, atrophy, gliosis, axonal swelling and presence of ubiquitin-positive inclusions. By contrast, mice over-expressing wild type SOD1 remain clinically normal, although some changes have been reported at two years of age (Jaarsma et al., 2000).

Transgenic mice carrying 23 copies of human SOD1 with Gly93Ala mutation (G93A mice) are considered the standard model of ALS in therapeutic studies (Bendotti and Carri, 2004). The model develops a motor system disease prevalently affecting lower motor neurons. Ultrastructural and microscopical analysis reveals that the earliest pathological sign in these mice is the vacuolization of large neurons in the anterior horns of the spinal cord (Bendotti 2001); it has been hypothesized that these vacuoles originate from the dilation of rough endoplasmic reticulum and from degenerating mitochondria. At the end stage, motor neuronal depletion is evident and hyaline, filamentous inclusions immuno-positive for ubiquitin and neurofilaments are present in some of the surviving neurons (Gurney et al., 1994; Migheli et al., 1999).

Transgenic mice expressing low levels of SOD1 G37R mutant show a motor disease restricted to lower motor neurons, whereas higher copy number causes more severe abnormalities and affects a variety of other neuronal

populations. The most obvious cellular abnormality is the presence in axons and dendrites of membrane-bounded vacuoles, which appear to be derived from degenerating mitochondria (Wong, 1995).

Transgene expression of mutant human SOD1 G85R or its murine counterpart G86R develops a very aggressive pathology with a rapid progression to paralysis and death within two weeks from the first symptoms. In G85R mice, motor neurons and astrocytes present inclusions immuno-positive for ubiquitin and SOD1 as the most relevant pathological feature (Bruijn et al., 1997).

Differences on disease progression and survival in various SOD1 mutant mice depend on the mutation and the copy number of the transgene. The age of onset, the duration and several pathological features also vary in dependence of the mouse strain in which the mutation is expressed; this background effect suggests the existence of strong modifying genetic factors.

More recently, the transgenic technology has also permitted the creation of transgenic rats expressing the G93A mutant. In this model, the onset of the disease occurs early and the progression is very rapid. Pathological abnormalities are similar to those observed in the mouse model; vacuolization and gliosis are evident before clinical onset and before motor neuron death in the spinal cord and brainstem (Howland et al., 2002).

II. LOA mice

Recently, Ahmad-Annuar and colleagues have described another mutant mouse model of motor neuron disease, the legs-at-odd-angles (LOA) mutant. In these mice, mutations in the cytoplasmic dynein heavy chain gene cause motor neuron degeneration. Mice exhibiting the LOA phenotype suffer progressive loss of locomotor function and homozygous animals have neuronal

inclusion bodies that are positive for SOD1, CDK5, neurofilaments and ubiquitin (Ahmad-Annuar et al., 2003).

III. ALS2 mice

ALS2 knock out mice have been obtained recently by two groups (Hadano et al., 2006; Lai et al., 2006). The study of their phenotype revealed a mild motor dysfunction characterized by age-dependent deficits in motor coordination, slow progressive loss of cerebellar Purkinjie cells, reduction in ventral motor axons, astrogliosis and evidence of deficits in endosome trafficking (Hadano et al., 2006; Lai et al., 2006).

IV. Tau mice

Different transgenic mouse models over-expressing various human tau isoforms have been generated (Ishihara et al., 1999; Spittaels et al., 1999; Lewis et al., 2000; Santacruz et al., 2005)

These mice acquire an age-dependent CNS pathology, similar to FTDP, and show axonal degeneration in brain and spinal cord, progressive motor disturbance and behavioural impairment.

1.7 Pathogenetic Hypotheses in Amyotrophic Lateral Sclerosis

To date, the mechanisms underlining the motor neuron death in ALS still remain unknown; this is true also for fALS cases, in which single gene mutations have been identified. In fact, most of the current knowledge on disease mechanisms in ALS has come from the study of the effect of SOD1 mutations, but even in this defined genetic subgroup the pathways of degeneration appear to be complex and multifactorial; indeed, mutations in

SOD1 provoke motor neuron disease through the acquisition of one or more toxic properties.

Studies performed on human ALS autopsy samples or on SOD1 mutant mice have suggested the involvement of various processes as possible triggers or secondary events in ALS pathology. Thus, most researchers consider ALS as a multifactorial disease in which a complex interplay between multiple mechanisms including genetic factors, oxidative stress, excitotoxicity, protein aggregation, damage to mitochondria and axonal transport determines the motor neuronal death.

Because the clinical and pathological profiles of sporadic and familial ALS are similar, it can be predicted that insight from studies on ALS-causing gene mutations apply also to sporadic ALS.

1.7.1 Oxidative damage

The role of oxidative stress as primary or secondary event in the pathogenesis of ALS still remains controversial. Increase in markers of oxidative damage has been reported in human patients affected by both sporadic and inherited forms of ALS (Beal et al., 1997; Ferrante et al., 1997; Liu et al., 1999) and in transgenic mouse models of the disease (Ferrante et al., 1997; Andrus et al., 1998). However, in other studies, no significant differences in markers of oxidative damage were found (Shaw et al., 1995; Bruijn et al., 1997).

Concerning the ALS form linked to SOD1 mutation, some studies suggested that a possible source of oxidative insult may be represented by the gain of toxic function of mutated SOD1 (Cleveland and Rothstein, 2001): it has been hypothesized that the mutation of SOD1 alters the enzyme activity through aberrant copper catalysis or improper metal binding. Mutant SOD1 may accept abnormal substrates such as peroxynitrite, provoking aberrant tyrosine nitration and numerous toxic events (Beckman et al., 1993), or hydrogen

peroxide (Wiedau-Pazos et al., 1996). In the latter case, the use of hydrogen peroxide as substrate might produce the extraordinarily reactive hydroxyl radical (OH^-), leading to a cascade of peroxidation (Wiedau-Pazos et al., 1996). Another hypothesis suggests that SOD1 mutations may reduce the zinc bound, allowing a rapid reduction of Cu^{2+} to Cu^{1+}. The reduced SOD1 mutant would then run the normal catalytic step backwards, converting oxygen to superoxide; the superoxide so produced would react with nitric oxide producing peroxynitrite, which would promote intracellular damage, including protein nitration (Estevez et al., 1999).

Several experiments have raised questions as to whether the toxicity of mutant SOD1 can be explained by copper-dependent oxidative mechanisms.

In G85R mice, genetic manipulation of the levels of wild type SOD1 did not affect the age of onset, the survival or the rate of progression (Bruijn et al., 1998); by contrast, the forced expression of high levels of wild type SOD1 in G93A, L126Z and A4V mice accelerates the onset of the disease (Jaarsma et al., 2000; Deng et al., 2006).

SOD1 with mutation of the four histidines that bound copper into the active site, that losses the dismutase activity, also develop motor neuron disease (Wang et al., 2003). Moreover, transgenic mice with the knock out of the gene encoding the copper chaperone normally required for the insertion of copper into SOD1 (CCS), possess only minute levels of SOD1-bound copper and have drastically reduced dismutation activity, but still develop motor neuron disease (Subramaniam et al., 2002). On the contrary, CCS over-expression in G93A mice produces severe mitochondrial pathology and strongly accelerates disease course (Son et al., 2007).

1.7.2 Mitochondrial dysfunction

Mitochondrial alteration is an attractive candidate for involvement in ALS pathogenesis because of its occurrence at the pre-symptomatic stage in SOD1 mutant mice (Bendotti et al., 2001; Jung et al., 2002) and in cultured cells expressing the mutant protein (Carri et al., 1997; Beal et al., 2000). Interestingly, mitochondrial abnormalities have also been observed in motor axon terminals of muscle biopsies from patients with early-diagnosed sporadic ALS (Siklos et al., 1996; Beal et al., 2000) and in proximal axons (Hirano et al., 1984) and in anterior horns of the spinal cord in sALS patients (Sasaki and Iwata, 1996).

Observations on the function of mitochondria have produced evidence consistent with the morphological data: biochemical studies have highlighted defects in the activity of the respiratory chain complex IV in sALS spinal motor neurons (Borthwick et al., 1999) and in complexes I and IV in spinal cord and brainstem homogenates of G93A mice (Browne et al., 1998).

Recent studies have indicated that mutant SOD1 could directly damage mitochondria. The presence of SOD1 in mitochondria of eukaryotic cells has been confirmed by several groups using a variety of experimental approaches. In particular, using immuno-gold electron microscopy, it has been demonstrated that both wild type and mutant SOD1 localize in the mitochondria of motor neurons in the spinal cord of transgenic mice (Jaarsma et al., 2001; Higgins et al., 2002).

Liu and colleagues proposed that mutant SOD1 progressively accumulates and aggregates on the mitochondrial outer membrane, altering the protein translocation machinery of the organelle (Liu et al., 2004). It has also been hypothesized that mutant SOD1 aggregates could damage the mitochondrion

through abnormal interaction with mitochondrial proteins such as Bcl-2 (Pasinelli et al., 2004).

1.7.3 Alterations of cytoskeleton and axonal transport

The idea that cytoskeleton abnormalities may play a role in ALS pathology arises from early reports of neurofilament accumulations in the cell bodies and proximal axons of motor neurons of both sporadic and familial ALS (Hirano et al., 1984). Subsequently, it has been shown that in mice the over-expression of NF-H or NF-L subunits causes the selective degeneration and death of motor neurons (Cote et al., 1993; Xu et al., 1993). However, it has not yet been clarified whether neurofilament disorganization represents a secondary product of pathological processes or whether it directly contributes to the death of the motor neurons. Other studies on transgenic mice have demonstrated that neurofilament content and organization strongly influence the disease induced by mutant SOD1 (Couillard-Despres et al., 1998; Williamson et al., 1998; Couillard-Despres et al., 2000; Kong and Xu, 2000). In particular, eliminating neurofilaments by deletion of the NF-L subunit increases the survival of SOD1 mutant mice, while enhancing the expression of the NF-L or NF-H subunits slows SOD1 mutant-mediated disease. The protective effects of increased NF-H content in perikarya may be due to the ability of neurofilaments to "buffer" against a cascade of aberrant and harmful events in the cell body (Couillard-Despres et al., 1998).

Another intermediate filament protein, peripherin, may be implicated in motor neuron degeneration. In fact, mice that over-express peripherin develop a late onset motor neuron degeneration and show disruption of neurofilament assembly (Beaulieu et al., 1999). On the other hand, alteration of peripherin levels in SOD1 mutant mice does not modify the disease course (Lariviere et al., 2003).

In neurons, the transport of molecules and organelles is dictated by the highly polarized anatomy of these cells: axonal proteins are synthesized in the cell body and must be transported in an anterograde manner along the axons and dendrites to reach synapses, whereas substances such as peripherally located trophic factors must be transported centrally from the synaptic regions by retrograde transport. The molecular motors for anterograde and retrograde transport are kinesin and the dynein-dynactin complex, respectively.

Several factors indicate that defects in axonal transport might contribute to the degeneration of motor neurons in ALS. First, anterograde transport is slowed in G93A and G37R transgenic mice prior to disease onset and the deficit are exacerbated as the disease progresses (Zhang et al., 1997; Borchelt et al., 1998; Williamson et al., 1999). Also retrograde transport is disrupted in SOD1 mutant mice (Murakami et al., 2001).

Several authors suggest that the aggregation of neurofilaments in proximal axons (spheroids) might physically compromise the transport apparatus (Sasaki and Iwata, 1996). Diminution of retrograde transport in ALS mice has been attributed to the mis-localization and disruption of dynein function (Ligon et al., 2005). In two lines of mice (LOA and CRA) point mutations in the dynein heavy chain impair motor neuron functionality and viability (Witherden et al., 2002; Hafezparast et al., 2003). Finally, aberrant vesicular sorting, which is relevant to successful axonal transport, has been implicated in the wobbler mouse.

1.7.4 Excitotoxicity

Glutamate-induced excitotoxicity is considered another major mechanism that may contribute to the aetiology of ALS. An over-stimulation of neuronal glutamate receptors can cause neuron death by increasing the cytosolic free calcium and activating the death cascades. This phenomenon may be

exacerbated by the regulation of the activity or of the subunit composition of glutamatergic receptors, which can render them more permeable to Ca^{2+} and Zn^{2+}. Glutamate transporters play an important role in preventing an aberrant activation of these receptors, removing glutamate from the synaptic cleft. Thus, changes in the equilibrium of this system may result in harmful events to the motor neurons in ALS.

The first indication of an involvement of glutamate-mediated excitotoxicity in ALS arose from studies showing increased levels of glutamate in the plasma (Plaitakis and Caroscio, 1987) and in the cerebrospinal fluid of a subset of ALS patients (Rothstein et al., 1990; Shaw et al., 1995).

Furthermore, several line of evidence point out an involvement of the most abundant astrocytic glutamate transporter EAAT2. In fact, in animal models of ALS, there are changes in EAAT2 levels and activity in the spinal cord (Alexander et al., 2000; Bendotti et al., 2001), and its expression has been found impaired also in ALS patients (Fray et al., 1998).

It is likely that the regulation of the expression of calcium-permeable AMPA (α-amino-3-hydroxy-5-methyl-4-isoxazole propionic acid) receptors is related to motor neuron degeneration in ALS patients and in SOD1 mutant mice. Indeed, motor neurons probably have a greater proportion of calcium-permeable AMPA receptors and the relative abundance of their subunits might change during the progression of the disease.

1.7.5 Inflammation

An increasing body of evidence suggests the involvement of inflammatory processes in ALS. Accumulation of reactive microglia and astrocytes has been documented in the spinal cord and in the motor cortex of ALS patients and animal models of the disease (Kawamata et al., 1992; Hall et al., 1998). A broad spectrum up-regulation of pro-inflammatory genes, such as COX-2

(Cyclooxygenase 2), NOS (nitric oxide synthase) and cytokines, for example TNFα, is reported in the spinal cord of G93A mice (Hensley et al., 2002).

1.7.6 Non cell-autonomous death

In recent years, various findings have emerged indicating that the cross-talk between neurons and non-neuronal cells may be crucial for the induction of motor neuronal death.

Experiments with transgenic mice have shown that the specific expression of mutant SOD1 in motor neurons or glia fails to trigger motor neuron degeneration (Gong et al., 2000; Pramatarova et al., 2001); however, as a major drawback of these experimental paradigms, the levels of SOD1 may have been below the threshold necessary to provoke disease. Transgenic mice possessing SOD1 G37R cDNA under the prion gene promoter express mutant SOD1 in neurons, astrocytes and muscles, but not in the macrophage lineage, and develop motor neuron disease (Wang et al., 2005), thus indicating that the presence of the mutant protein in the motor neuron/muscle circuit, along with supporting astrocytes, is sufficient to induce the disease.

In an elegant work using chimeric mice with mixed population of cells expressing either endogenous or transgenic mutant SOD1, it has been demonstrated that the toxicity to motor neurons requires damage from mutant SOD1 acting within non-neuronal cells. In fact, motor neurons expressing mutant SOD1 did not degenerate if they were surrounded by wild type glia; reciprocally, wild type motor neurons surrounded by SOD1 mutated glia showed ubiquitin-positive inclusions (Clement et al., 2003). The importance of microglia for the pathological processes has been unravelled by recent new studies. Experiments with deletable transgenes has demonstrated that the lack of mutant SOD1 only in microglia and peripheral macrophages does not change the onset of the disease, but increases the survival (Boillee et al.,

2006); the deletion of mutant SOD1 only within motor neurons extend survival by delaying the onset and the early phase of disease progression. The role of microglia was confirmed, using a different approach, by Beers et al., who established that the presence of G93A only in microglia is not capable of inducing motor neuron disease, while in G93A mice the substitution of mutated microglia with the wild type one significantly slowed the motor neuron loss, prolonging the disease duration and the survival (Beers et al., 2006).

Also the role of astrocytes in ALS has recently been highlighted: experiments in co-culture systems provided evidence that astrocytes expressing mutant SOD1 are able to cause the death of both wild type and mutant motor neurons (Di Giorgio et al., 2007; Nagai et al., 2007).

1.7.7 Protein aggregation

Many neurodegenerative disorders have in common the sequestration of aberrant proteins into inclusions and amyotrophic lateral sclerosis does not represent an exception. As already described in the section 1.4.1, one of the most relevant pathological features of ALS cases, as well as of SOD1 mutant mice, is the formation of proteinaceous inclusions in the motor neurons and sometimes in the surrounding astrocytes (Migheli et al., 1990; Bruijn et al., 1997; Kato et al., 1999). These inclusions are composed of different proteins, such as SOD1, ubiquitin, dorfin, neurofilaments, peripherin and p38 MAPK; additionally, chaperones and proteasome subunits may also be sequestered (Watanabe et al., 2001; Strong et al., 2005).

Given that ubiquitin-containing aggregates are a frequent feature both in sporadic and familial cases, this could link the mechanisms of the two forms of ALS. As regards to fALS cases linked to SOD1 mutations, one major pathogenetic hypothesis concerns the idea that mutant SOD1 becomes

unfolded and prone to aggregate; this theory has been deeply analyzed, with various experimental approaches, in *in vivo* and *in vitro* models.

I. Structural characteristics of wild type SOD1

The evolution of aerobic organisms that can survive in oxygen-rich environments requires an effective defence against reactive oxygen species (ROS). The superoxide dismutase enzymes are the first line of antioxidant defence against ROS, and particularly superoxide anion radicals, since they catalyze the reaction of dismutation of the superoxide anion, in which two molecules of superoxide are turned into molecular oxygen and hydrogen peroxide. Each eukaryotic cell has several types of SODs: mitochondrial SOD (SOD2), cytosolic SOD (SOD1) and extracellular SOD (SOD3).

In humans, SOD1 gene has been localized to chromosome 21. The protein is a ubiquitously expressed homodimer with a molecular mass of about 32 KDa; the two subunits are held together primarily with hydrophobic contacts (Tainer et al., 1982).

The secondary structural elements of SOD1 are illustrated in Fig. 1.3. From a structural point of view, SOD1 is part of the immunoglobulin-fold family (Richardson et al., 1976) and each monomer consists primarily of an eight-stranded β-barrel with two large loops, the so-called "electrostatic loop" and the "metal-binding" loop (residues 49-84) (Tainer et al., 1982). The latter region contains the residues necessary for binding one copper, which plays a catalytic role, and one zinc, with a structural function (Rodriguez et al., 2005). The Cu^{2+} and Zn^{2+} ions are coordinated in close proximity (Strange et al., 2003).

Human SOD1 contains four cystidine residues; of these, Cys57 and Cys146 form an intersubunit disulphide bond, whose presence is quite unexpected in a cytosolic enzyme localized in the reducing environment of the cytoplasm. It

is therefore evident that SOD1 displays a complex folding and maturation pathway; indeed, to acquire their final structure, newly translated molecules have to undergo at least four steps: copper insertion, zinc insertion, disulfide formation and dimerization.

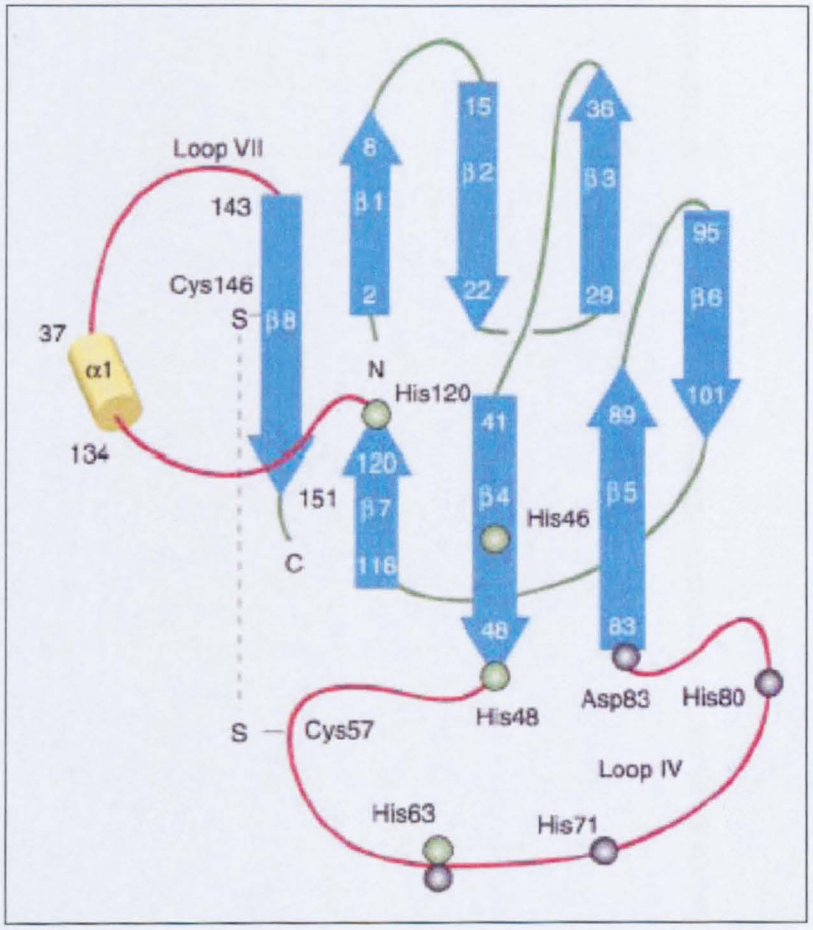

Figure 1.3 Secondary structural elements of human SOD1. The β-strands are shown as blue arrows and the short α-helix as a cylinder. The Zn-coordinating residues are shown as grey spheres and the Cu-coordinating residues as green spheres. The disulfide bond between Cys 57 and Cys 146 is indicated with a broken line. The two large loops (IV and VII) are coloured red. Adapted from B.F. Shaw, J.S. Valentine, Trends Biochem. Sci. 2007.

SOD1 is one of the most stable proteins known and remains active under a broad range of harsh denaturing conditions (Forman and Fridovich, 1973; Lepock et al., 1985). Its stability seems to be linked to its structural

characteristics, in particular the metal coordination and the presence of the disulfide bond. The maintenance of the disulfide linkage is critical both for the dimeric and the monomeric stability, since its reduction weakens the dimeric interactions and increases the proportion of denaturated and potentially aggregation-prone species (Furukawa and O'Halloran, 2005). Also the dimerization, reducing the solvent accessible surface area, contributes to render the molecule stable (Goodsell and Olson, 2000).

Although originally thought to be a cytosolic protein, recently SOD1 has been localized also in other cell compartments such as nucleus, mitochondria and microsomes (Keller et al., 1991; Crapo et al., 1992).

II. Mutant SOD1 alterations and aggregation

In the last decade, more than one hundred mutations of SOD1 linked to ALS have been discovered. These mutations are localized in all the regions of the primary sequence and in all the functional domains of the protein. The various mutants can differ for some features, for example the catalytic activity, the net charge and the metal affinity. For this reason, it has been difficult to describe precisely the properties that distinguish the mutant proteins from the wild type one.

Based on their biophysical characteristics, SOD1 mutants have been divided into two groups (Hayward et al., 2002):

1. wild type-like mutants, with a metal content similar to wild type and structural perturbations in the region of the mutation (for example G93A)
2. metal-binding region mutants, that are deficient in zinc and/or copper.

Different studies have tried to find the alterations shared by the pathological mutants that could be responsible for the acquired toxicity. An increasing body of observations suggests that the ALS disease mechanism is coupled to destabilization or misfolding of the SOD1 structure, manifested ultimately by

the presence of cellular inclusions. Actually, SOD1 mutants display a general structural instability (Lindberg et al., 2002) and result to be less thermostable than the wild type enzyme (Rodriguez et al., 2002). In this regard, particularly important is the increased sensitivity to the reduction of the disulfide bond, given its role in maintaining the integrity of the dimeric structure (Lindberg et al., 2002; Tiwari and Hayward, 2003); indeed, disulfide reduction was shown to prevent dimerization, increasing the presence of instable monomers (Lindberg et al., 2004). Also demetallation leads to structural destabilization of SOD1 mutants (Lindberg et al., 2002).

Particular attention has been focused on the monomeric apo protein as a precursor state for noxious gain of function (Rakhit et al., 2004). Some studies suggest that SOD1 mutations perturb the folding pathway of the protein by destabilizing the precursor monomers or weaken the dimer interface; the result is a shift of the folding equilibrium toward poorly structured monomers (Lindberg et al., 2005). Furthermore, in an *in vitro* model of reticulocyte extracts, it has been shown that different fALS-associated mutations are significantly impaired in their ability to fold to a native-like dimeric state; this delayed folding should be expected to increase the fraction of instable folding intermediates (Bruns and Kopito, 2007). Conversely, the SOD1 monomer can be produced from the native heterodimer in a variety of ways, all of which involve disulfide reduction and demetallation (Tiwari and Hayward, 2003; Arnesano et al., 2004; Furukawa and O'Halloran, 2005).

Another characteristic that could promote aggregation of mutant SOD1 is the decrease of the net negative charge of the polypeptide observed in several ALS-associated mutations; this phenomenon is further exacerbated in environments that are more acidic than the cytosol, such as mitochondria and the trans-Golgi network (Lindberg et al., 2005).

SOD1 misfolding could also be the result of its oxidation: when treated with mild oxidation systems, mutant SOD1 display greater aggregation propensity than wild type (Rakhit et al., 2002).

Generalizing, the mutation can determine both local perturbations of the secondary, tertiary or quaternary structure and the loss of metal ion binding; the common result is a destabilization of the enzyme that leads to non-native interactions with itself, or other proteins, and aggregation.

Many *in vitro* and *in vivo* data support this hypothesis.

In cell cultures, studies have shown that, in contrast to the stable wild type protein, the mutant one oligomerizes to form small pore-like structures (Chung et al., 2003; Ray et al., 2004; Matsumoto et al., 2005; Matsumoto et al., 2006). Inclusions of SOD1 are found in primary cultured motor neurons expressing several different SOD1 mutations; the formation of such inclusions correlates with loss of viability (Durham et al., 1997).

Analyzing the clinical course of familial ALS cases, it has been reported a correlation between protein aggregation and clinical phenotype: mutations that cause a more severe disease have a shorter half-life and are more likely to form aggregates (Lindberg et al., 2005; Sato et al., 2005).

As regards to SOD1 mutant mice, the formation of large inclusion bodies is a relatively late event in the disease progression. In a time course immunohistochemical study in the spinal cord of G93A mice, aggregates appeared progressively in dendrites, periaxonal processes of oligodendrocytes and neuronal and astrocytic perikarya (Stieber et al., 2000). Conversely, the presence of insoluble complexes of SOD1 much smaller than the visible inclusions has been detected much earlier during disease progression. Johnston et al. showed that the aggregation of SOD1 into insoluble high molecular weight species is an early event occurring in G93A mice (Johnston

et al., 2000) and their abundance increases as the disease progresses. Using another approach, accumulation of mutant SOD1 complexes that can be trapped by cellulose acetate filtration was confirmed in brain and spinal cord of SOD1 mutant mice; although expressed to the same level in non-nervous tissues, mutant SOD1 was not found in high molecular weight structures (Wang et al., 2002).

SOD1 species with reduced disulfide bond are detected in the mouse model and their concentration is considerably higher in the CNS compared to the peripheral tissues (Jonsson et al., 2006). Moreover, a significant fraction of insoluble SOD1 aggregates found in the symptomatic spinal cord contains multimers cross-linked via uncorrected intermolecular disulfide bonds. These data suggest that the formation of insoluble aggregates of mutant SOD1 may derive from the formation of incorrect disulfide cross-linking of immature misfolded proteins (Deng et al., 2006).

III. Potential toxicity of SOD1 aggregates

The role of proteinaceous aggregates in ALS pathogenesis remains controversial; however, although large inclusion bodies may not themselves be toxic, they are at least a sign that something is wrong in the cell with respect to the stability and solubility of the mutant protein. Aggregate formation could be a primary event in the disease pathogenesis and underlie neurotoxicity. Otherwise, aggregation could occur secondary to the primary neurotoxic event: indeed, it has been hypothesized that inclusions could be the ultimate product of a cellular defence mechanism that occurs when the burden of misfolded or damaged protein exceeds the capacity of the protein degradation machinery to eliminate them. Finally, the formation of inclusion bodies may act as a cellular defence mechanism in the attempt to actively reduce the concentration of smaller, more toxic aggregates (Ross and Poirier, 2005). Actually, whether the

final protein aggregates are themselves toxic, or whether some soluble precursors are the major toxic species, is a hotly debated subject. Considerable data implicates smaller aggregates and oligomers as the primary cytotoxic agent in many diseases associated with protein aggregation (Lashuel et al., 2002; Ross and Poirier, 2005) .

Various hypotheses have been proposed regarding the citotoxicity of SOD1 aggregates, including the disruption of axonal transport (Stokin et al., 2005), the aberrant binding of apoptosis regulators (Pasinelli et al., 2004; Tomik et al., 2005), perturbations in mitochondrial function and calcium homeostasis (Hervias et al., 2006; Sumi et al., 2006) and inhibition or overload of the ubiquitin-proteasome pathway (Cleveland and Rothstein, 2001). Consistent with the latter hypothesis, accumulation of ubiquitinated aggregates have been detected in SOD1 mutant mice (Stieber et al., 2000; Watanabe et al., 2001; Bendotti et al., 2004). Since one of the roles of ubiquitin is to label and target misfolded and no more active proteins to the proteasome machinery, it has been hypothesized that proteasome activity could be inhibited by SOD1, leading to accumulation of aberrantly folded forms of SOD1 and other proteins (Cleveland and Rothstein, 2001).

The possible involvement of dysfunctions of the ubiquitin-proteasome pathway in ALS has been the focus of this thesis; for this reason, the constitution and the physiological and pathological roles of the ubiquitin-proteasome pathway are discussed in the next chapter.

CHAPTER II

THE UBIQUITIN-PROTEASOME PATHWAY

In the last decades, a major breakthrough in cell biology has been the discovery that protein turnover is a highly regulated process orchestrated by the ubiquitin-proteasome pathway (UPP). The pioneering research of Rose, Hersko and Ciechanover during the early '80s led to the discovery of the ubiquitin–mediated protein degradation and was awarded with the Nobel prize in chemistry in 2004. Nowadays, UPP is known as a versatile mechanism that plays a vital role in a great variety of cellular functions. For example, UPP controls the temporal and spatial inactivation of key proteins that regulate processes such as cell cycle progression, apoptosis, transcription and development; moreover it is involved in the immune response, since it generates the majority of the peptides presented by MHC I (major histocompatibility complex class I) (Goldberg et al., 2002), and is responsible for the clearance of aberrant proteins in the cellular environment. Finally, there are many non-proteolytic functions associated with UPP, such as DNA repair, membrane transport, chromatin-remodelling, transcription and signalling pathways (Ferdous et al., 2001; Gillette et al., 2001; Krogan et al., 2004).

The dual function of UPP as a sentinel of protein quality control and as a regulator of vital cellular processes places the system in a delicate position. This situation may be particularly relevant under conditions that cause a rapid accumulation of misfolded and damaged proteins.

As shown in figure 2.1, the degradation of a protein via the ubiquitin-proteasome pathway involves two steps:

1. the substrate is tagged by the covalent attachment of multiple ubiquitin molecules;
2. the tagged protein is degraded by the 26S proteasome .

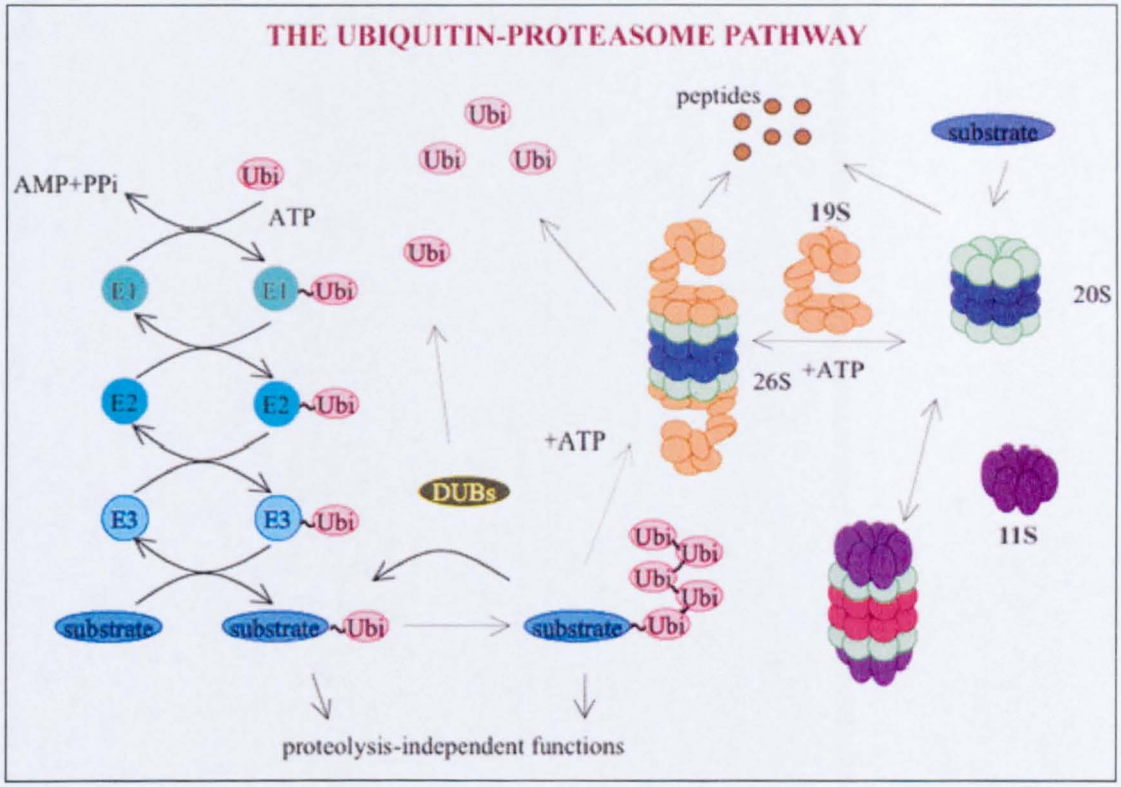

Figure 2.1 The ubiquitin- and proteasome-dependent system of protein degradation. E1, E2 and E3 enzymes cooperate to tag the target protein with a poly-ubiquitin chain. Poly-ubiquitinated substrates can then be destroyed by 26S proteasome. Adapted from Wojcik C., Di Napoli M., Stroke 2004.

2. 1 Ubiquitin

Ubiquitin (Ub) is a small protein of 76 amino acids expressed in all the eukaryotic cells and it was the first protein discovered to be covalently attached to other proteins by an isopeptide bond (Goldknopf and Busch, 1977). Protein modification by ubiquitin can be mediated either by the attachment of a single ubiquitin (mono-ubiquitination) or a poly-ubiquitin chain (poly-ubiquitination), in which a new ubiquitin is conjugated to the preceding ubiquitin molecule; the latter modification was shown to serve as a signal that targets proteins for degradation (Ciechanover et al., 1980a; Ciechanover et al., 1980b; Hershko et al., 1980; Wilkinson and Rose, 1980).

Beyond its role in protein degradation, ubiquitin is increasingly recognized to be a key post-translational modification that regulates target protein localization and activity in processes such as endocytosis, signal transduction, chromatin remodelling and DNA repair (Schnell and Hicke, 2003; Welchman et al., 2005); many of these functions are controlled by mono-ubiquitination or by the formation of non-canonical ubiquitin chains (Pickart and Eddins, 2004; Hicke, 2001).

2.2 UBIQUITINATION

Ubiquitination refers to the post-translational modification of a protein by the covalent attachment of one or more ubiquitin monomers. Conjugation of ubiquitin to the protein substrate proceeds via a three-step cascade mechanism:

1. initially, E1 enzyme activates ubiquitin;
2. the activated ubiquitin is transferred to a Cys residue of one of the several E2 enzymes;
3. finally, the concerted action of E2 and E3 results in the attachment of ubiquitin to the substrate.

The ubiquitin molecule is generally transferred to an ε-NH_2 group of an internal lysine residue in the substrate to generate the isopeptide bond with the C-terminal glycine of the ubiquitin (Gly76).

Once the first ubiquitin is attached to the substrate, its internal Lys residues can become the acceptor for a new ubiquitination cycle and, through successive rounds of ubiquitination, the poly-ubiquitin chain is formed; since ubiquitin has several Lys residues, several linkages could occur that would result in chains with different structures and functions (Peng et al., 2003).

Most commonly, poly-ubiquitin chains are linked through Lys 48 as canonical signal for proteolysis.

2.2.1 E1: the Ubiquitin-Activating Enzyme

E1 activates ubiquitin, via a two-step ATP-dependent reaction, to generate a high-energy linkage between the C-terminal carboxyl group of the ubiquitin and the thiol group of a cysteine residue within the catalytic site of E1. In mammals, E1 exists as two isoforms, resulting from alternative translation initiation sites (Cook and Chock, 1992; Handley-Gearhart et al., 1994).

2.2.2 E2: the Ubiquitin-Conjugating Enzymes

E2s catalyze the covalent attachment of ubiquitin to the target proteins, or, when acting along with HECT-domain E3s, the transfer of the activated ubiquitin moiety to a high-energy E3-ubiquitin intermediate. More than 30 different E2s have been described in higher organisms. All E2 enzymes share a catalytic core domain, that contains the ubiquitin-binding Cys residue, and are distinguished by the presence of a UBC (ubiquitin conjugating) domain required for binding distinct E3s. Typically, each E2 interacts with a number of ligases, thus being involved in targeting numerous substrates.

2.2.3 E3: the Ubiquitin-Protein Ligase

E3s, which are responsible for the specific recognition of the multitude of substrates of the ubiquitin system, are the least defined components of the pathway and display the greatest variety. The mechanism by which E2s and E3s mediate the ubiquitination varies for different E3s.

E3s belong to two main sub-families:

1. HECT-domain E3s: E3 accepts the ubiquitin transferred from E2 by forming another high-energy bond; ubiquitin is then transported to the ligase-bound substrate. HECT-domain proteins are characterized by a C-terminal domain that contains the conserved Cys residue to which the

ubiquitin is transferred from E2 (Scheffner et al., 1995). The NH_2-terminal domain, which varies among the different HECT-domain proteins, is probably involved in specific substrate recognition.

2. RING-finger domain E3s: RING-finger E3s act as scaffolds to bring together the E2 and the substrate, allowing the efficient transfer of ubiquitin from E2 to the substrate (Lorick et al., 1999; Tyers and Willems, 1999; Jackson et al., 2000; Joazeiro and Weissman, 2000). RING-finger domain is a small domain characterized by a pattern of conserved Cys and His residues that form a cross-brace structure and bind Zn^{2+}; it is involved in the interaction between E2 and E3.

An additional subset of E3s, termed E4s, serves as a scaffold to aid in the transfer of ubiquitin from E2 to a previously conjugated ubiquitin moiety, in effect elongating poly-ubiquitin chains. From a structural point of view, this family of protein is characterized by a modified version of the RING-finger motif, named U-box (Hatakeyama and Nakayama, 2003). It is still a debated subject whether E4 proteins have intrinsic E3 activity and should be considered a subfamily of E3 enzymes.

The specificity of the ubiquitin-proteasome system is largely determined at the E3 level, since the substrates must be specifically recognized by an appropriate E3 as a prerequisite to their ubiquitination. In most cases, however, substrates are not recognized in a constitutive manner. In some instances, the E3 must be "switched on" by undergoing post-translational modifications to yield an active form that recognizes the substrate; in other cases, it is the substrate that must undergo a certain change that renders it susceptible for recognition. These phenomena are essential for an accurate spatial and temporal regulation of the substrate fate.

2.2.4 DUB: Deubiquitinating Enzymes

Deubiquitinating enzymes (DUBs) are an heterogeneous and not fully characterized group of proteins that catalyzes the cleavage of ubiquitin moieties after the glycine 76. Their activity plays an important role for UPP functionality; for example, DUBs maintain the free ubiquitin pool in the cell by processing ubiquitin precursors and recycling ubiquitin from poly-ubiquitinated substrates.

2.3 THE PROTEASOME

The 26S proteasome is a large, multicatalytic protease that degrades poly-ubiquitinated proteins to small peptides. As shown in Fig. 2.2, it is composed of two sub-complexes: a 20S core particle, that carries the catalytic activity, and a 19S regulatory particle. One or two regulatory particles attach to the surface of the outer α-rings of the 20S to form the 26S proteasome holoenzyme.

2.3.1 The 20S particle

The 20S core particle is a barrel-shaped structure composed of four stacked rings, two identical outer α-rings and two identical inner β-rings. Each ring is composed of seven distinct subunits; in the two β-rings, three of the seven subunits have the threonine-protease activity, meaning that each proteasome has six (three different) proteolytic active sites (Lowe et al., 1995; Groll et al., 1997). The protease active sites face an inner cavity, termed proteolytic chamber, that can be accessed through a narrow channel formed by the α-rings (Groll et al., 2000; Kohler et al., 2001). Indeed, the NH_2 termini of the α-subunits obstruct the access to the proteolytic chamber, suggesting that the proteasome channel is gated (Groll et al., 1997; Groll et al., 2000).

Overall, the 20S can cleave peptide bonds after any amino acid. However, each of the three active sites preferentially cleaves after different amino acids: β1 (post-glutamil peptide hydrolase) cleaves after acidic amino acids, β2 (trypsin-like) cuts after basic amino acids, while β5 (chymotrypsin-like) hydrolyzes the peptide bond after hydrophobic residues (Dick et al., 1998). The rules that govern the cleavage rate of the same peptide bond can be significantly altered when put into the context of the primary structure of the polypeptide (Holzhutter et al., 1999).

2.3.2 The 19S particle

The 19S regulatory particle is composed of at least 18 different subunits and can assemble at either end of the 20S core particle to form the 26S proteasome.

The 19S itself can be further dissected into two multisubunit substructures: the lid and the base (Glickman et al., 1998). The base is connected to the α subunits of the 20S by a ring formed by six ATPase subunits (named Rpt 1-6 in S. Cerevisiae); two additional components of the base are the non-ATPase subunits Rnp1 and Rnp2 (Davy et al., 2001; Fu et al., 2001). The lid contains nine of the remaining non-ATPase subunits (Rpn3, -5, -6, -7, -8, -9, -10, -11, -12) and can be released from the proteasome or rebound under certain conditions. The role of the lid is still unclear, although it is necessary for the proper degradation of poly-ubiquitinated proteins (Glickman et al., 1998).

The 19S complex serves multiple roles in regulating proteasomal activity. First, it is responsible for the recognition of the substrates that should be degraded; in particular, Rnp10 and Rpt 5 subunits have been shown to bind poly-ubiquitinated chains (Young et al., 1998; Hofmann and Falquet, 2001). The subsequent removal of the poly-ubiquitin chain from the substrate is mediated by subunits that display a de-ubiquitinating activity (Verma et al.,

2002; Yao and Cohen, 2002). A second function of 19S is to open an orifice in the α-ring, allowing the substrate to enter into the proteolytic chamber. In addition, because a folded protein would not be able to fit through the narrow proteasomal channel, it is assumed that the 19S particle unfolds substrates and inserts them into the 20S channel. Both the channel opening function and the unfolding of the substrate require energy, and therefore are probably mediated by the ATPase subunits.

It is well known that the 26S complex is responsible for the clearance of the bulk of cellular ubiquitinated proteins. However, the 20S particle constitutes a major portion of the total amount of the proteasome present in cells and it has recently emerged that it is able to degrade some proteins in a ubiquitin-independent manner (Orlowski and Wilk, 2003). Natural unfolded, damaged, misfolded and oxidized proteins are all susceptible to degradation by the 20S proteasome. It is probable that the delivery of such proteins to the 20S proteasome is mediated by the exposure of hydrophobic patches (Inai and Nishikimi, 2002; Shringarpure et al., 2003).

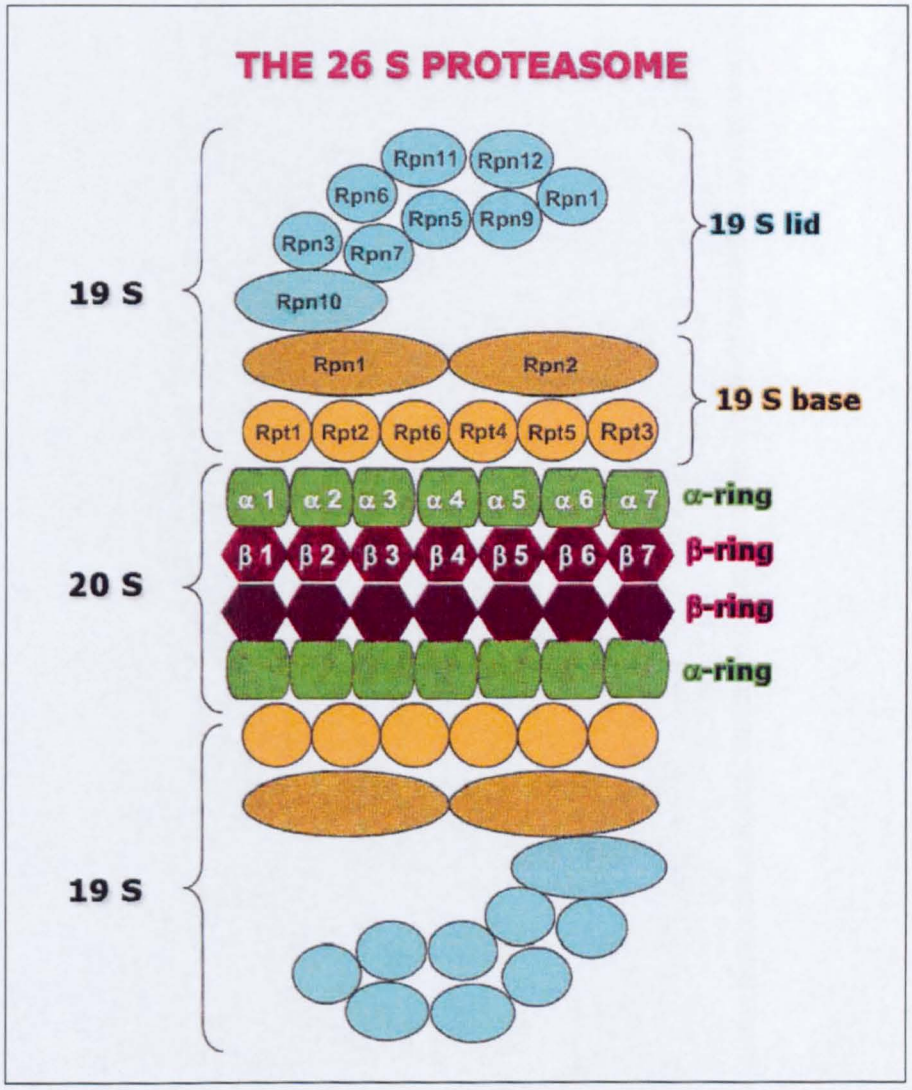

Figure 2.2 The subunit composition of 26S proteasome. The different 19S subunits are indicated using the nomenclature of S. Cerevisiae 26S proteasome. Rnp: regulatory particle non-ATPase; Rtp: regulatory particle ATPase. Adapted from Pickart and Cohen, Nat. Rev. Mol. Cell. Biol., 2004

2.3.3 Proteasome plasticity

I. The immunoproteasome

An important function of protein breakdown in mammalian cells is to generate the peptides that are presented in association with MHC class I molecules to the immune system, and in particular to the T cell receptor of cytotoxic CD8+ T cells. Each antigenic peptide is bound by an MHC I molecule; MHC genes are highly polymorphic, with several hundred alleles and each allele binds a unique set of peptides with an average length of 8–10 amino acids.

Cells display intracellular antigens, from both self proteins and intracellular pathogens, at the cell surface to distinguish between infected and uninfected cells. Peptide fragments derived form self proteins are usually ignored by the host immune system, whereas epitopes derived from foreign or mutated self-antigens trigger a cytotoxic T cell response. MHC I plays also an important role as ligand for the receptor of natural killer cells, thereby controlling the functional state of these lymphocytes (Moretta et al., 2004; Lanier, 2005; Parham, 2005).

The clearest evidence that most antigentic peptides are generated by the proteasome was the finding that inhibitors of proteasome reduce or prevent antigenic presentation (Rock et al., 1994).

During infections, the release of the cytokine IFNγ (interferon γ), a critical antiviral mediator in the CNS (Komatsu et al., 1996), optimizes the antigen presentation by the replacement of the proteolytically active β-subunits with alternative, so-called LMP or βi, subunits. β1i/LMP2 replaces its constitutive β1-homolog, β5i/LMP7 replaces β5, and β2i/LMP10 (or MECL-1) replaces β2 (Bochtler et al., 1999). Since the proteasome complex with inducible subunits is more prone to generate peptides suitable for the antigen presentation, it is often referred to as "immunoproteasome". Indeed, experiments with small

fluorogenic substrates have shown that immunoproteasome has a greater capability to cleave after hydrophobic and basic amino acids, and lower to cleave after acidic ones. This tendency should enhance the production of peptides able to bind MHC molecules (Van Kaer et al., 1994).

Another molecule able to elicit changes in proteasomal composition is the pro-inflammatory cytokine TNFα (tumor necrosis factor α) (Hallermalm et al., 2001).

II. 11S regulatory particle

IFNγ induces also the up-regulation of PA28α and PA28β, which form an heptameric ring (α3β4) known as 11S regulatory particle, or PA28 (Schwarz et al., 2000). Similarly to 19S, 11S can assemble with the 20S core particle and is believed to open the α gate; on the other hand, 11S does not have ATPase activity or ubiquitin-binding sites. The precise role of 11S in MHC I presentation is still not well understood. It is known that it is able to greatly stimulate the ability of 20S to hydrolyze small peptides (Ma et al., 1992). 11S can also associate with 26S particles containing one 19S cap to generate hybrid 19S-20S-11S (Cascio et al., 2002); these hybrid complexes generate a distinct set of peptide products, that presumably exit from the 11S-bound end.

III. Post-translational modifications

Besides the shift from constitutive proteasome to immunoproteasome, other and more subtle modifications can regulate the catalytic activity of the proteasome. In fact, western blot analysis demonstrated that frequently proteasome inhibition is not associated with a decrease of proteasome levels (Keller et al., 2000a; Keller et al., 2000c); therefore, it appears that post-translational modifications can play an important role. For example, it has been shown that, under severe stress conditions, 26S dissociates into 19S and 20S components causing a rapid decrease in cellular proteolysis. In addition,

various 19S and 20S subunits can be phosphorylated; it is thought that phosphorylation plays a positive role in proteasome function, favouring its assembly and stability. The subunits can also be modified by glycosylation at the same residues as phosphorylation, with antagonistic outcomes.

In vitro experiments demonstrated that mild oxidative stress inactivates the 26S proteasome, whereas the 20S one seems to be more resistant (Shang and Taylor, 1995; Jahngen-Hodge et al., 1997; Grune et al., 1998; Grune, 2000).

2.3.4 Proteasome biogenesis

All the different proteasome subunits of the 20S catalytic core are usually synthesized in stochiometric amounts. 20S is formed following a sophisticated biogenesis pathway; the 3 β-catalytic subunits are synthesized as inactive precursors and are activated by intramolecular proteolysis after the incorporation into 20S (Chen and Hochstrasser, 1996; Ditzel et al., 1998). The assembly is a multistep process that occurs via the formation of precursor complexes and requires accessory proteins to promote maturation steps. Among these various factors, a fundamental role is played by POMP (proteasome maturation protein), that is directly associated with proteasome precursors and is degraded as a first substrate when the 20S is fully assembled and activated (Ramos et al., 1998; Burri et al., 2000; Witt et al., 2000). POMP transcript levels are increased after IFNγ treatment (Burri et al., 2000) and the interaction between POMP and LMP7 is thought to accelerate immunoproteasome biogenesis (Heink et al., 2005); indeed, in POMP-depleted cells, a decrease of MHC I surface expression is found.

2.4 The Ubiquitin-Proteasome Pathway In Neurodegenerative Diseases

Accumulation of ubiquitin conjugates and inclusion bodies has been reported in a broad array of chronic neurodegenerative diseases, such as the neurofibrillary tangles of Alzheimer's disease (AD), Lewy bodies in Parkinson's disease (PD), Bunina bodies in ALS and nuclear inclusions in polyglutamine-extension disorders (Poli-Q diseases, for example Huntington's disease, spinocerebellar ataxia and spinal bulbar muscular atrophy). Since the pathogenetic significance of these aggregates has remained still mysterious, the appearance of inclusion bodies has emerged as a common but poorly understood mechanistic theme in neurodegenerative disorders (Fig. 2.3).

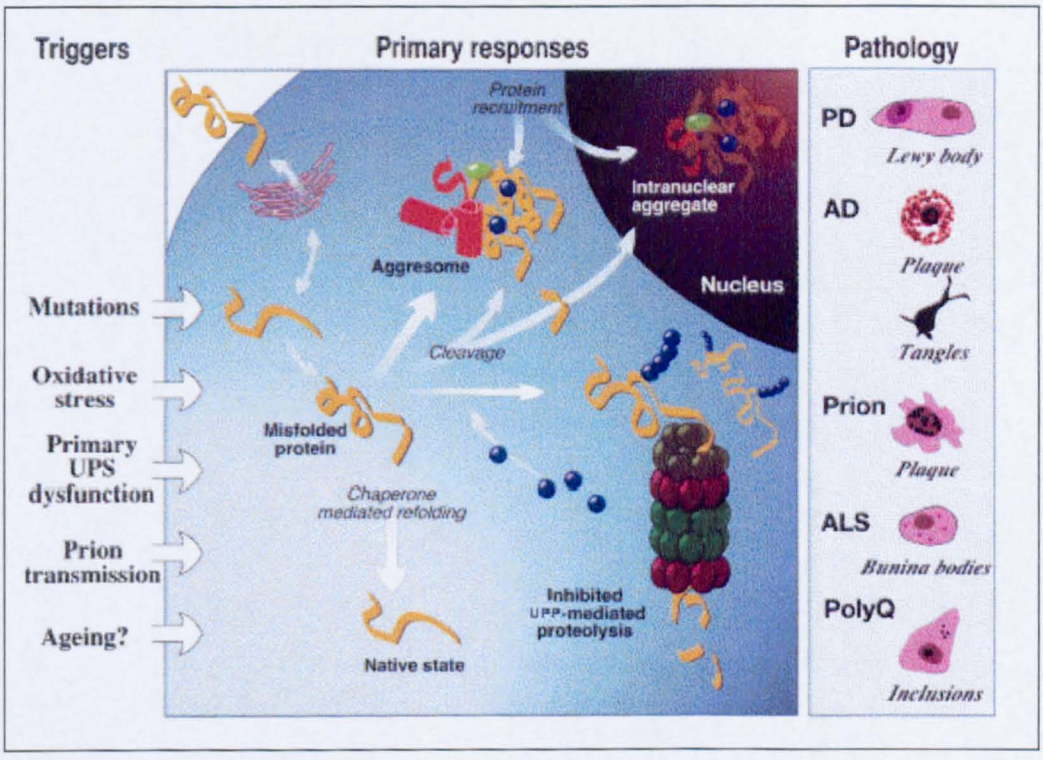

Figure 2.3 The involvement of the ubiquitin-proteasome pathway in neurodegenerative diseases. The figure describes different aspects related to protein misfolding and neurodegeneration: the triggers that can cause the accumulation of misfolded proteins, the primary responses to their accumulation and the types of neuropathological protein deposits that can be found in the patients. Adapted from Ciechanover A., Brundin P., Neuron 2003.

It has been suggested that alterations in UPP functionality can be involved in this phenomenon. In fact, the proteins that accumulate in neurons are apparently tagged for degradation, but amass rather than be destroyed. Therefore, an important, unanswered question is why UPP fails to destroy aggregation-prone proteins and allows their accumulation over time. Bence and co-worker (Bence et al., 2001) demonstrated that UPP function is directly impaired by protein aggregates. Following their hypothesis, the proteasome could become engaged by ubiquitinated aggregates that can neither unfold nor degrade, and would thus be unavailable for degrading other substrates. Indeed, proteasome subunits co-localize in inclusion bodies associated with neurodegenerative diseases (Kwak et al., 1991; Cummings et al., 1998; Seilhean et al., 2004). A decline in UPP activity would result in increased production of aggregated proteins, that, in turn, would lead to a further decline of UPP function, determining a feed-back mechanism. Such phenomenon is more dramatic in post-mitotic cells, possibly explaining the vulnerability of neurons (Sitte et al., 2000).

The failure of UPP can occur at different levels, for example it could derive from a decrease of proteasome catalytic activity, a mis-regulation of ubiquitinating enzymes, a mis-regulation of the delivery of the substrates to the proteasome, or alterations in the activity of 19S particle. It is important to highlight that even subtle perturbations of the UPP could compromise the neurons by rendering them more susceptible to other stresses.

The strongest support for the possibility that UPP has a primary role in the pathogenesis of neurodegenerative diseases comes from mutations in UPP components that provoke disease insurgence. In fact, mutation in the E3-ligase parkin causes an early onset parkinsonism in humans (Kitada et al., 1998). Ubiquitin carboxy-terminal hydrolase-1 (UCHL1) is a neuron-specific

deubiquitinating enzyme that also displays a secondary dimerization-dependent ubiquitin-ligase activity. A point mutation affecting the ligase activity of UCHL1 has been linked to Parkinson's disease (Liu et al., 2002), while an internal deletion in the same gene is responsible for murine gracile axonal dystrophy, which is characterized by axonal degeneration and formation of spheroids in nerve terminals (Saigoh et al., 1999).

There is also indirect evidence implicating UPP in neurodegeneration. Decreased proteasome activity seems to be a feature that characterizes many cell models in which aggregates are formed, for example *in vitro* models of Parkinson's disease (Rideout et al., 2001; Tofaris et al., 2001; Liu et al., 2002), of prion disease (Ma and Lindquist, 2001; Yedidia et al., 2001; Ma et al., 2002) and Poli-Q diseases (Jana et al., 2001; Chan et al., 2002). Additionally, Aβ oligomers, as well as prion oligomers, were shown to inhibit proteasome function (Kristiansen et al., 2007; Tseng et al., 2007). Not always, these *in vitro* findings mirror the *in vivo* situation. For example, in some poli-Q disease mouse models, proteasome impairment was not detected at the symptomatic stage (Diaz-Hernandez et al., 2003; Bowman et al., 2005). On the other hand, a direct relationship between prion neuropathology and a dysfunction of the UPP was demonstrated in prion-infected mice (Kristiansen et al., 2007). Analyses of AD and PD human brain showed modest decrease of proteolytic activity of the proteasome (Keller and Markesbery, 2000; McNaught and Jenner, 2001) and 20S complex isolated from AD brain revealed post-translational modifications such as acetylation and dephosphorylation (Gillardon et al., 2007).

CHAPTER III

AIM

OF THE THESIS

The purpose of this thesis is to study in depth the role of the ubiquitin-proteasome pathway in the pathogenesis of amyotrophic lateral sclerosis, analysing the mice transgenic for human SOD1 with G93A mutation.

As a first objective, I have evaluated the time course of ubiquitinated protein accumulation in the spinal cord of G93A mice during disease progression. Then, the activity of the ubiquitin-proteasome pathway has been monitored by cross-breeding G93A mice with a mouse model that expresses a protein reporter of UPP activity.

Another aim of the study is the investigation of the shift from constitutive proteasome to immunoproteasome in the mechanisms that lead to motor neuron degeneration. Therefore I examined the levels of the transcripts for constitutive and inducible proteasome subunits in the spinal cord of G93A mice at different stages of disease progression.

CHAPTER IV

METHODS

In this chapter are provided the general procedures adopted in the experiments described in this thesis. When necessary, further methodological details are given for specific experiments before the presentation of the results.

4.1 Mouse Models

Procedures involving animals and their care were conducted in according to the institutional guidelines, that are in compliance with national (D.L. no. 116, G.U. suppl. 40, Feb. 18, 1992, Circolare No.8, G.U., 14 luglio 1994) and international laws and policies (EEC Council Directive 86/609, OJ L 358, 1 DEC.12, 1987; NIH Guide for the Care and use of Laboratory Animals, U.S. National Research Council, 1996). The animals were housed under standard conditions (22 ± 1°C, 60% relative humidity, 12 hour light/dark schedule), 3-4 per cage, with free access to food (Altromin, MT, Rieper) and water.

4.1.1 G93A transgenic mice

Transgenic mice expressing about 20 copies of mutant human SOD1 with a Gly93Ala substitution (G93A mice) were originally obtained from Jackson Laboratories (B6SJL-TgNSOD-1-G93A-1Gur); the line is hemizygous for the transgene. Male G93A mice were repeatedly backcrossed with non transgenic female C57BL/6 mice, obtaining transgenic mice on the homogeneous C57BL/6 genetic background. These mice develop the first signs of neuropathology at the motor neuronal level around one month of age, while the first symptoms of muscular dysfunction appear around three months of age, with tremors and a progressive reduction in the extension reflex of the hind limbs, when the mice are raised by the tail. At about four months of age, the mice start to show a progressive muscular weakness, revealed by the increasing difficulty in staying on a rotating bar and by a reduction in stride length on an inclined ramp. At this stage, about 50% of motor neurons of the

lumbar spinal cord are lost and two months later these mice die (Ciavarro et al., 2003).

Mitochondrial vacuolisation and swelling are among the earliest events and are accompanied by a decreased function of the mitochondria. Later, but still at the asymptomatic stage, G93A mice show signs of cytoskeletal disorganization in the motor neurons, with the accumulation of phosphorylated neurofilaments in the perykaria (Tortarolo et al., 2003). Reactive gliosis, which involves hypertrophy and the activation of astrocytes and the proliferation and activation of microglia, is detectable with the degeneration of motor neurons and becomes prominent when the cell loss is remarkable (Tortarolo et al., 2003; Veglianese et al., 2006).

For the present study, female mice have been sacrificed at 12, 16 and 22-23 weeks of age, corresponding respectively to pre-symptomatic, early symptomatic and end stage of the progression of the motor dysfunction. Age-matched non transgenic littermates (NTg mice) and, for some experiments, transgenic mice expressing wild type human SOD1 (WT SOD1 mice) have been used as controls.

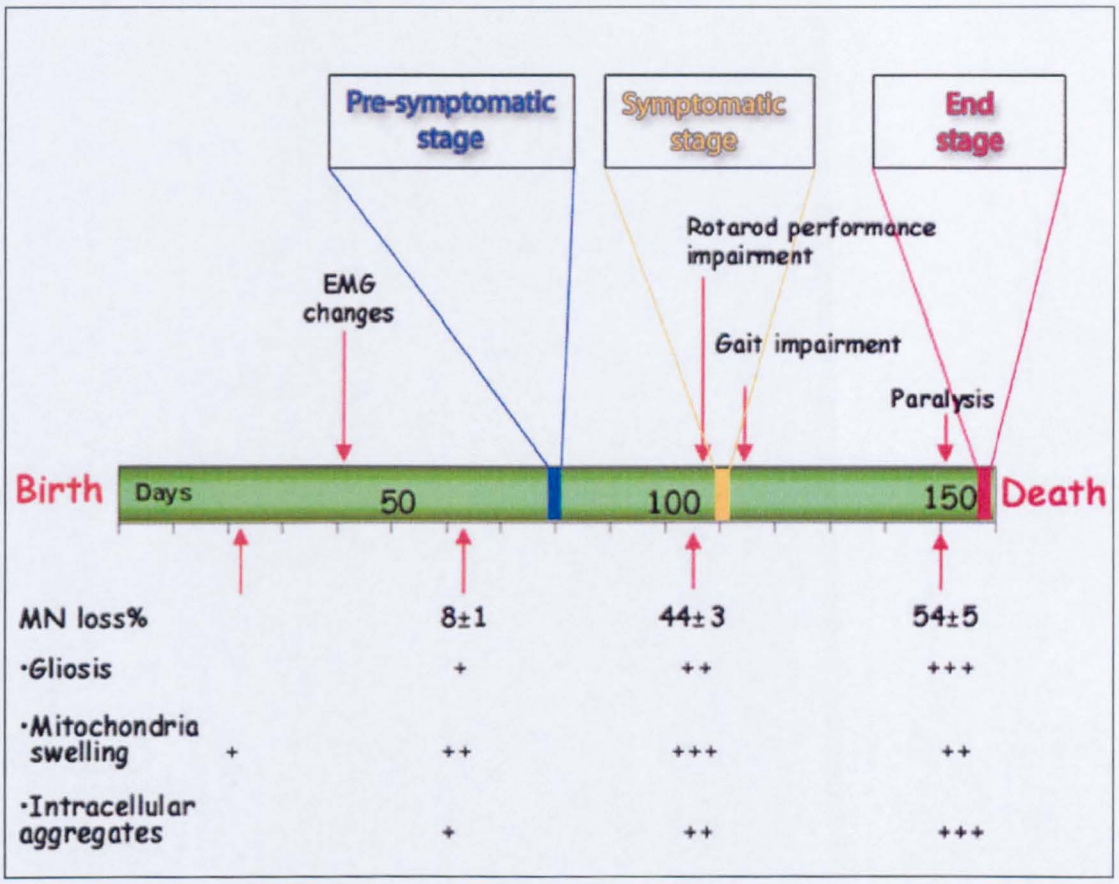

Figure 4.1 The disease progression in G93A mouse model.

4.1.2 Ub^{G76V}-GFP transgenic mice

Ub^{G76V}-GFP mice are available in our laboratory thanks to a collaboration with Dr. Dantuma (Dept. Cell and Molecular Biology, Karolinska Institute, Stockholm, Sweden), who generated them.

This model is based on the constitutive expression of the Ub^{G76V}-GFP reporter protein for the activity of the ubiquitin-proteasome pathway (see section 5.1.4), that was selected because its short half-life and low toxicity in cell cultures. The transgene is expressed from a chicken β-actin promoter with a cytomegalovirus (CMV) immediate early enhancer, which normally gives high

constitutive expression in all the tissues (Sato-Harada et al., 1996). Two mouse strains, named Ub^{G76V}-GFP1 (GFP1) and Ub^{G76V}-GFP2 (GFP2) were generated with the reporter construct and were characterized by the presence of the transcript in all the examined tissues (Lindsten et al., 2003); both lines are hemizygous for the transgene. Degradation of the substrate was so efficient that inhibition of the UPP was required in order to detect the reporter protein. For the maintenance of these lines, GFP1 or GFP2 males were bred with C57BL/6 (NTg) females.

4.1.3 Double transgenic mice

Since G93A females are sterile, to obtain double transgenic GFPG93A mice G93A males and GFP1 or GFP2 females were cross-bred. Both G93A and GFP mice are derived from the same strain C57BL/6, thus minimizing the confounding effects of different genetic backgrounds. The genotyping of the litters was conducted by polymerase chain reaction (PCR) on DNA extracted from tail biopsies. In the experiments, double transgenic mice were evaluated in comparison with single transgenic and non transgenic littermates.

4.1.4 Mouse genotyping

I. DNA extraction

Tail biopsies were treated with 0.1 µg/µl of Proteinase K (Promega Corporation, Madison, WI, USA) over-night at 55°C for tissue digestion. Total genomic DNA extraction was performed using Wizard genomic DNA purification kit (Promega). Nuclei lysis and protein precipitation were carried out according to manufacturer's instructions; DNA was precipitated by adding 40 µl (10 % of volume) of sodium acetate 3M, pH 5 and 1 ml of cold ethanol. The pellet was dried at room temperature, then resuspended in 100 µl of distilled water; samples were then incubated for 1 h at 65°C to allow complete resuspension. DNA concentration was measured by spectrophotomer

(Eppendorf International, Hamburg, Germany) and samples were diluted to reach the final concentration of 50 ng/µl.

II. PCR screening

The conditions for qualitative PCR experiments were established using GoTaq (Promega). 50 ng of DNA from each animal were used as a substrate for the PCR reaction, in a mix containing 1X PCR buffer, GoTaq (0.25 U), deoxyNTPs (250 µM each), specific forward and reverse primers (0.5 µM each) in a final volume of 10 µl. All the reagents were purchased by Promega, except for primers that were synthesized by Invitrogen (Invitrogen Corporation, Carlsbard, CA, USA).

The thermocycling profile used for amplification is reported below:

1.	94°C for 2 min	
2.	94°C for 45 sec T annealing for 45 sec 72°C for 1 min	For 34 cycles
3.	72°C for 10 min	

PCRs were performed in a MJ thermocycler (distributed by Bio-rad laboratorie, Hercules, CA, USA). Amplicons were resolved in agarose gel usually containing 1.5% of agarose, 2 µg/ml ethidium bromide in Tris-Acetate-EDTA (40 mM Tris, 0.35% vol/vol acid acetic, 1 mM EDTA).

In the table 4.1 are reported the primer sequences and their annealing temperatures.

Gene	Forward (5'->3')	Reverse (5' 3')	T annealing
SOD1	CATCAGCCCTAATCCATCTGA	CGCGACTAACAATCAAAGTGA	56 °C
GFP	ACCACATGAAGCAGCACGACT	CTTGTACAGCTCGTCCATGC	58°C

Table 4.1: Primer sequences for SOD1 and GFP genotyping.

4.2 IMMUNOHISTOCHEMISTRY

4.2.1 Tissue obtainment

Mice were anesthetized with Equithesin (1% Phenobarbital, 4% chloral hydrate) and transcardially perfused with 20 ml of phosphate buffered saline (PBS, phosphate buffer 0.01M, 0.9% NaCl) followed by 50 ml of 4% para-formaldehyde solution in PBS. Brains and spinal cords were rapidly removed, post-fixed in fixative for 2 h, transferred to 20% sucrose solution in PBS overnight, then to 30% sucrose solution until they sank, and finally frozen in 2-methylbutane at −45°C and conserved at -80°C until the experiments. Before freezing, spinal cord was divided in cervical, thoracic and lumbar segments and included in OCT (Tissue-tek, Sakura Finetek, Torrance, CA, USA).

Tissues were cut on a cryostat at -20°C to obtain sections of 30 µm. The brain was sectioned in the sagittal plane, whereas the spinal cord in the coronal plane. The lumbar level of the spinal cord was chosen for the experiments, because the hind legs of G93A mice are affected earlier and more severely compared to the forelegs.

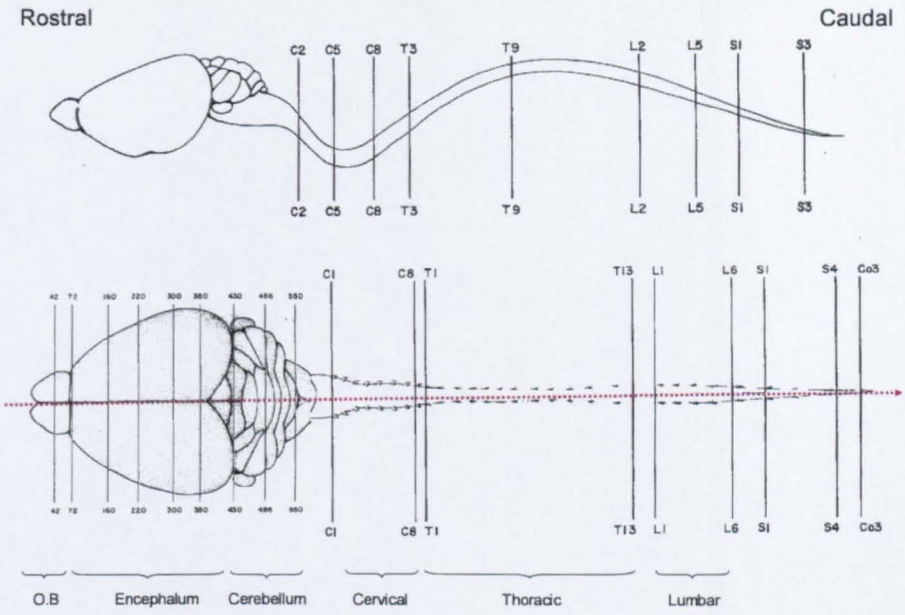

Figure 4.2 The mouse central nervous system.

4.2.2 Diaminobenzidine immunostaining

Free floating sections were treated for 10 min with 1% hydrogen peroxide in PBS 0.01M to inhibit endogenous peroxidases, blocked in PBS containing normal goat serum (NGS) and Triton X-100 at the appropriate concentration for 60 min at room temperature (RT) and then incubated overnight at 4°C with the primary antibody diluted in PBS containing NGS and Triton X-100. The following day, after three washing in PBS 0.01 M, sections were incubated with biotinylated secondary antibody (1:200, Vectastain kit, Vector Laboratories, Burlingame, CA, US) for 1 h, washed and incubated in avidine-biotin-peroxidase solution (Vectastain kit, Vector Laboratories). Immunostaining was revealed by the reaction with 3'-3-diaminobenzidine tetrahydrochloride (DAB, 10 mg/20 ml in TBS + 6 µl hydrogen peroxide 30%). Subsequently, sections were washed, dried and mounted on poly-L-lysine coated slides, dehydrated through graded alcohols, fixed in xylene and coverslipped using DPX

mountant (BDH, Poole, UK). Control sections were incubated without the primary antibody.

4.2.3 Indirect immunofluorescence

Free-floating sections were treated for 1 h with a blocking solution composed of NGS and Triton X-100 at the appropriate concentration in PBS. Subsequently, the sections were incubated overnight at 4°C with the primary antibody diluted in PBS containing NGS and Triton X-100. Then, after three washes in PBS, samples were treated for 1 h with the appropriate secondary antibody conjugated to fluorochromes with various wavelengths (Alexa 488, 546 and 647, Molecular Probes, Invitrogen), diluted 1:500 in PBS added with NGS 2%. Finally, sections were mounted on slides and coverslipped with Fluorsave (Calbiochem, Notthingam, UK).

Control sections were incubated without the primary antibody.

4.2.4 Amplified immunofluorescence by tyramide

Sections were pre-treated for 10 min with hydrogen peroxide 1% in PBS. Blocking was performed for 1 h at RT with NGS and Triton X-100 at appropriate concentration in PBS. Subsequently, samples were probed overnight at 4°C with the primary antibody, diluted in PBS containing NGS and Triton X-100. The following day, after three washes in PBS, sections were incubated with biotinylated secondary antibody (1:200, Vectastain kit, Vector Laboratories) for 1 hour, washed with TNT (TBS 0.1 M; Triton 0.05%) and incubated with for 90 min in TNB (TBS 0.1 M, Blocking reagent 0.5%). Subsequently, the sections were again washed with TNT and treated with streptavidin (1:100, Perkin Elmer, Waltham, MA, USA) in TNB for 30 min, washed with TNT and incubated for 10 min with tyramide conjugated with Cy5 fluorochrome (1:500, Perkin Elmer) in amplification diluent provided by the

kit. Processed sections were mounted on slides and coverslipped with Fluorsave.

The amplification technique was utilized to detect faint signal or reveal two antibodies of the same specie on the same section, taking advantage of the sensibility of this technique for one of the antibodies. In the latter case, it was verified that, in the established conditions, no direct reaction was detectable between the secondary fluorescent antibody and the primary antibody amplified with tyramide procedure.

In each immunohistochemical experiment, some of the sections were processed without the primary antibody, in order to verify the specificity of the staining.

4.2.5 Image analysis

Sections immunolabelled with diaminobenzidine were examined under an Olympus BX61 light microscope. Images were collected with a camera, using AnaliSYS software (Soft Imaging Systems, ver. 3.2).

Fluorescence-labelled sections were analyzed under an Olympus Fluoview laser scanning confocal microscope, using three lasers: Ar with a 488 nm emission line to acquire Alexa 488 signal, He-Ne green laser with a 546 emission line to acquire Alexa 546 signal and He-Ne red laser with a 647 emission line to acquire Cy5 signal. Analysis in double or triple staining was made by sequential scanning in order to avoid cross talk between the channels.

For some immunohistochemical experiments, with the aim to obtain quantitative data, co-localization studies were performed on serial sections (1 every 10 sections, for a total of 10 sections for animal) from the spinal cord. Samples were examined under an Olympus BX61 light microscope and images of the dorsal and ventral spinal cord were collected with a camera, using

AnaliSYS software (Soft Imaging Systems, ver. 3.2); cells that resulted stained for one or both of the analyzed markers were recorded.

4.3 CELL CULTURES

4.3.1. Culture Preparation

Primary spinal neurons were prepared from 14-day-old mouse embryos deriving from the cross-breeding of GFP2 males with NTg females; genotyping of the embryos was performed by PCR as described above (paragraph 4.1.4) using the DNA extracted from the liver.

Spinal cords were isolated by dissection and the meninges were removed. The tissue was then mechanically dissociated using a fire-polished glass Pasteur pipette in phosphate-buffered saline (PBS, Ca^{2+} and Mg^{2+} free) supplemented with glucose (33 mM). The cell suspension was layered onto a 4% BSA cushion, centrifuged at 1000 rpm for 10 min, and the cells from the pellet were resuspended in culture medium composed of Neurobasal (Gibco, Invitrogen) supplemented with 10% inactivated horse serum, 16.5 mM glucose, 1 ng/ml BDNF, 2 mM glutamine, 100 µg/ml streptomycin and 60 µg/ml penicillin. A mixture of hormones and salts composed of insulin (25 µg/ml), transferrin (100 µg/ml), putrescine (60 µM), progesterone (20 nM) and sodium selenate (30 nM) was also added to the culture medium. In order to improve neuronal viability and resistance, neurons from GFP2 embryos were plated into wells previously coated with a layer of confluent non-transgenic astrocytes; the growth of Ub^{G76V}-GFP glial cells was minimized by adding to the culture medium the anti-mitotic drug Ara-c.

Cells were cultured at 37°C in a humidified atmosphere of 95% air and 5% CO_2 and were used after 5-6 days *in vitro*.

4.3.2 Treatment with proteasome inhibitor

Proteasome inhibition was obtained adding to the medium the drug MG132. Actually, primary neurons resulted to be very sensitive to proteasome inhibition and the administration of MG132 in concentration suitable for overnight treatment in cell lines demonstrated to be toxic. For this reason, experiments were done with decreasing quantities of MG132 and shorter periods of treatment; the best range was chosen to be in 0.5-4.5 μM for 6 hours of incubation.

At the end of the treatment, cells were rinsed in PBS, fixed with 4% para-formaldehyde in PBS for 30 min at RT and labelled by immunofluorescence techniques as already described.

4.4 BEHAVIOURAL ANALYSES

Starting from the age of 84 days, mice were tested once a week for motor behavioural deficits using the grid test. Animals were posed on a horizontal grid and supported until they grabbed the grid with both their fore and hind paws; the grid was then inverted so that the mice were allowed to hung upside down. At this point, time was started for a maximum of 90 sec. The time (sec) at which the animal fell from the grid was recorded. Animals performed three trials with at least 5 min of rest among them; the time of the best trial was considered for the statistical analysis. Body weight of each animal was recorded before the test.

Mice at the end stage of the disease that were unable to right themselves within 30 sec after being placed on one side were euthanized by a high dose of anaesthetic; the age of death was recorded as time of survival.

For the statistical analyses, the results from each group of animals at each test session were expressed as mean ± standard error (S.E.). Missing data, due to death of animals, were taken into account in the statistic analysis as follows: when an animal died, its performance was considered equal to the last recorded value for all subsequent test sessions, until the death of the last animal of the group. The patterns in the progression of motor deficits and body weight were evaluated by a repeated measure two-way ANOVA. The survival of G93A and GFP1G93A mice was analyzed by the log-rank test. All the statistical analyses were done using Prism 4 for Windows, version 4.03 (GraphPad Software Inc.).

4.5 WESTERN BLOT

Western blot experiments were performed in collaboration with Dr. C. Maynard and Dr. N. Dantuma (Dept. Cell and Molecular Biology, Karolinska Institute, Stockholm, Sweden).

4.5.1 Tissue obtainment

Mice were killed upon ethical procedures by decapitation. The spinal cord was fluxed from the vertebral column employing sterile physiological solution (0.9% NaCl) and sectioned into the cervical, thoracic and lumbar segments; the samples were immediately frozen on dry-ice and stored at -80°C.

4.5.2 Protein extraction

Frozen spinal cord tissues were thawed on ice and homogenized in 500 µl of ice-cold homogenization buffer (20 mM Hepes pH 7.4, 100 mM NaCl, 10 mM NaF, 1% Triton X-100, 1 mM orthovanadate and 10 mM EDTA) containing freshly added 20 mM NEM (N-methyl d-aspartate) to block deubiquitination enzymes, and complete mini-protease inhibitor cocktail (Roche).

Homogenisation was carried out by sonication (30 pulses of 1 sec at 15% intensity) on a Bandelin Sonopuls ultrasonic homogenizer, and samples were centrifuged at 10,000 g for 10 min at 4°C; supernatants were transferred to a fresh tube and stored on ice. Protein concentration was determined by BCA Proteain Assay (Pierce Biotechnology, Rockford, IL, USA) against BSA standards and homogenates were adjusted to equal protein concentration in homogenization buffer.

4.5.3 SDS-poly-acrylamide gel elecrophoresis (SDS-PAGE)

Prior to electrophoresis, aliquots of homogenate were boiled in SDS sample buffer (1.2% SDS, 5% β-mercaptoethanol, 5% glycerol, 25.5 mM Tris/HCl pH6.8, 0.6% glycine) at 95-100°C for 10 min Equal amounts of total protein (30 μg) were separated on 12% Tris-glycine polyacrylamide gels and electroblotted onto 0.2 μM nitrocellulose membranes, 100V for 1h using a BioRad mini-transfer system. To check for even protein loading and transfer, membranes were briefly immersed in Ponceau-S stain (0.2% Ponceau-S in 3% trichloro-acetic acid) and rinsed in water. Membranes were then placed between plastic sheets and scanned for later analysis.

4.5.4 Immunoblotting

Membranes were rinsed in PBS to remove Ponceau-S stain and immersed in blocking buffer (5% non-fat milk in PBS pH 7.4, 0.1% Tween). Membranes were then probed with the primary antibody diluted in blocking buffer, washed 4 times in PBST, and incubated with HRP-conjugated secondary antibody (GE Helathcare, UK) 1:4000 for 1h at RT. Membranes were washed 4 times in PBST for 10 min and the signal detected by enhanced chemioluminescence (ECL) using Fuji Super RX film for various exposure times to obtain signal within the linear range. Films were scanned on a CanoScan 5200F scanner (Canon) and band intensities measured using Image J (public domain

software). The obtained values were normalized to Ponceau staining quantity and expressed as percentage of the basal value registered in the control samples (i.e. single transgenic tissues). Mean values were used for statistical analysis by Student's t-test. The statistical analysis was done using Prism 4 for Windows, version 4.03.

4.6 Real Time PCR

4.6.1 Tissue obtainment

The analysis of mRNA expression was performed on total RNA extracted from fresh tissues. Mice were killed upon ethical procedures by decapitation. The spinal cord was fluxed from the vertebral column employing sterile physiological solution (0.9% NaCl) and sectioned in the cervical, thoracic and lumbar tracts. The brain was sectioned, isolating the hippocampus, the cerebellum and the cortex. The samples were immediately frozen on dry-ice to avoid endogenous RNases to degrade the RNA and stored at -80°C.

4.6.2 RNA extraction

Total RNA was extracted using the Trizol method (Invitrogen), purified according to the manufacturers' recommendation and resuspended in sterile water.

RNA was quantified by spectrophotometer. Moreover, to check its quality, 2 μg of each sample were loaded in electrophoresis gel and 18S and 28S ribosomial bands were considered as indicators of RNA integrity.

4.6.3 DNase I treatment

Prior to retrotranscription, RNA samples were treated with DNaseI (Deoxyribonuclease I Amplification Grade, Invitrogen) in order to minimized genomic DNA contamination.

DNase I treatment was performed upon the manufacturer's instructions: 2 µg of total RNA were added to the mix containing 1X DNase I reaction buffer and 2U of DNAse I, in a total volume of 10 µl. The mixture was incubated for 15 min at RT, then DNase I was inactivated by adding EDTA (pH 8.0) to a final concentration of 2.5 mM, and heating the sample at 65°C for 10 min. To assure that the treatment with DNAse I was efficient, a portion of each sample was tested with a qualitative PCR in order to verify possible DNA contaminants; this was obtained using the standard conditions described above (paragraph 4.1.4) and a set of primers able to amplify the genomic sequence of murine SOD2 gene (primer sequences in table 4.2).

4.6.4 Synthesis of cDNA

I. cDNA for SYBR Green experiments

The cDNA used for real time PCR experiments with the SYBR Green chemistry was obtained by reverse transcription of total RNA with a Moloney murine leukaemia virus reverse transcriptase (MuLV RT) from Gene Amplification RNA PCR-core kit (Applied Biosystems, Foster City, CA, USA). It was decided to employ oligo d(T)16 to allow retro-transcription of any messenger harbouring the polyA tail. Practically, 2 µg of DNase-treated RNA from each sample were used as a substrate for cDNA synthesis in a mix containing 1X PCR Buffer, MuLV reverse transcriptase (2.5 U/µl), RNAsi inhibitor (1U/µl) oligo dT (2.5 µM), and deoxyNTP (1 mM each) in a final volume of 40 µl.

The mixture was stored at RT for 10 min, then incubation was performed in the thermocycler at 42°C for 15 min, at 99°C for 5 min, and at 4°C for at least 5 min.

II. cDNA for TaqMan experiments

For real-time quantification using the TaqMan technology, it was decided to modify the conditions of retro-transcription in order to accomplish the

guidelines of the manufacturers for this kind of experiments. Reverse transcription was therefore carried out using the High Capacity reverse transcription kit (Applied Biosystems): 2 µg of DNase-treated RNA from each sample were added in a mix containing 1X RT Buffer, Multiscribe MuLV reverse transcriptase (1.25 U/µl), RNAsi inhibitor (1U/µl) Random Primers 1X, and 4 mM deoxyNTP mix in a final volume of 40 µl.

The mixture was incubated in the thermocycler at 25°C for 10 min, at 37°C for 120 min, and at 85°C for 5 sec.

III. cDNA quality control

The quality of the obtained cDNA was tested with qualitative PCR using primers able to recognize the transcript of murine SOD2 (sequence in table 4.2)

Gene	Forward (5'->3')	Reverse (5' 3')	T annealing
SOD2 DNA	GGCAGCAGGTGCAGGAGAG	GATATCCAAGGGGTCAGGGAG	60 °C
SOD2 cDNA	TGCACTGAAGTTCAATGGTGG	TAGAGCAGGCAGCAATCTGT	56°C

Table 4.2 Primer sequences for the gene and the transcript of SOD2

4.6.5 Real time PCR with SYBR Green

For the majority of the transcripts analyzed, the levels of expression of mRNAs were determined by real time quantitative PCR, performed with 7300 Real time PCR system (Applied Biosystems), exploiting SYBR Green as fluorescent dye.

In order to reach high efficiency rate of amplification, the steps to optimize the reaction of amplification were accomplished according to the manufacturer of the real-time PCR instrument. Indeed, amplicon and primer design were

achieved by Primer Express software (Applied Biosystems) set with default parameters. Thus, the annealing temperature of each primer was restricted to 58-60°C, which corresponds to the optimal working conditions for the used DNA polymerase enzyme (AmpliTaq Gold, Applied Biosystems).

The specificity of SYBR Green dye for a certain DNA target is entirely determined by primers, since this dye binds any double stranded nucleotide sequence; for this reason, a dissociation curve analysis (analysis of melting temperature profiles) was performed upon completion of each PCR run. Moreover, agarose gel analysis was done to further verify the lack of any spurious band due to non-specific amplification.

Real time PCR on cDNA specimens, standards and not-template control (in triplicate) was performed in a 25-µl reaction mixture containing 25 ng of cDNA template, 1X SYBR Green PCR master mix and specific primers (0.3 µM each). The quantification of the samples was done using the standard scale method; the efficiency and reproducibility of the PCR were assessed evaluating the slope and correlation coefficient of the standard curve.

The thermocycling profile used for the amplification is reported below:

1.	95°C for 10 min	
2.	95°C for 5 sec 60°C for 1 min	For 40 cycles

4.6.6 Real time PCR with TaqMan

For some transcripts, the evaluation of their levels was done in real time PCR using the TaqMan technology. The principle of TaqMan reaction is based on the use of fluorogenic probes designed to hybridize to the gene target sequence of two PCR primers. Each probe contains a 5' fluorescent reporter dye and a 3' quencher dye; in the intact probe, the presence of the 3' quencher inhibits the 5' reporter emission. During the extension phase of PCR cycling, the annealed probe is cleaved by the 5'→3' exonuclease activity of Taq polymerase, thus producing an increase in the fluorescence emission of the reporter dye. This event occurs in each PCR cycle and leads to an increase of fluorescence proportional to the initial concentration of target sequences in the sample.

Real time PCR on cDNA specimens, standards and not-template control (in triplicate) was performed in a 20-µl reaction mixture containing 50 ng of cDNA template, 1X Universal PCR master mix and 1X mix containing specific primers and probe (TaqMan Gene expression assays, Applied Biosystems). The quantification of the samples was done using the standard scale method; the efficiency and reproducibility of the PCR were assessed evaluating the slope and correlation coefficient of the standard curve.

The thermocycling profile used for the amplification is the same reported above for SYBR Green experiments.

4.6.7 Statistical analysis

The quantity of the measured transcript was normalized to β-actin quantity and expressed as percentage of the basal value registered in the control samples (i.e. NTg or single transgenic tissues). Mean values were used for statistical analysis by Student's t-test. The statistical analysis was done using Prism 4 for Windows, version 4.03.

4.7 *In Situ* Hybridization

4.7.1 Tissue obtainment

Mice were killed using ethical procedures by decapitation and brain and spinal cord rapidly removed. Tissues were immediately frozen in 2-methylbutane at -45°C and conserved at –80° until the experiments.

4.7.2 Slide preparation and pre-hybridization procedure

Frozen lumbar spinal cords were cut on a cryostat at -20°C and sections (14 µm) mounted on poly-L-lysine coated microscope slides. Sections were then fixed in 4% para-formaldehyde for 15 min followed by two 10 min incubations in PBS, acetylated (0.1 M triethanolamine and 0.25% acetic anhydride in 0.9% NaCl), dehydrated through a graded series of ethanol, delipidated for 5 min in chloroform, air dried and stored frozen at -80°C.

4.7.3 *In vitro* transcription

^{35}S-labelled RNA probes were obtained by *in vitro* transcription (Bendotti et al., 1990).

The reaction mixture for the *in vitro* transcription contained: 1 µg of DNA, 1X transcription buffer, 10 mM dithiothreitol (DTT), 15 U of RNA polymerase,15 U of RNase inhibitor, 0.5 mM ATP, 0.5 mM GTP, 0.5 mM CTP, 10 µM UTP (all the reagent were purchased from Promega) and 2.5 µM ^{35}S-UTP (1000 Ci/mM; Amersham Biosciences, Little Chalfont, Buckinghamshire, UK). After 90 min incubation at 37°C for T7 or at 40°C for SP6 , the templates were digested with 1 U of DNase I - RNase free (Promega) for 15 min at 37 °C.

The templates were hydrolysed in mild alkaline buffer (80 mM $NaHCO_3$ and 120 mM Na_2HCO_3) at 60°C to obtain fragments of about 200 base pairs in length. The mixtures were neutralized and the ^{35}S-labelled riboprobes were purified by G-50 Sephadex Quick Spin Columns (Roche, Basel, Switzerland).

Probes were diluted to 4000 cpm/µl with hybridization buffer containing 50% formamide, 2X sodium saline citrate buffer (SSC), 10 mM Tris/HCl pH 7.5, 1X Denhart's solution, dextran sulfate 10%, 0.2% SDS, 100 mM DTT, 500 µg/ml double-strand Salmon Sperm DNA (Roche).

4.7.4 Hybridization and post-hybridization procedures

On the day of the experiment, the slides were brought to room temperature and hybridized with the ^{35}S-labelled RNA probes. Sections were incubated overnight at 55°C in sealed humidified chambers using Parafilm coverslips. After hybridization, coverslips were removed and sections were incubated in 1X SSC for 10 min at RT. Sections were then washed for 30 min at 37°C in 20 µg/µl of RNase A in RNase buffer (0.5 M NaCl, 1 mM EDTA and 10 mM Tris/HCl, pH 8.0) followed by 30 min at 37°C in RNase buffer alone. Sections were then washed in 1X SSC for 30 min at RT, 0.5X SSC for 30 min at 65°C and 0.5X SSC for 10 min at RT before dehydrating through a graded series of ethanol. The slides were exposed to Beta-max film (Amersham Biosciences) for 7 days, dipped in photographic emulsion (Ilford K5 diluted 1:1 with 0.1% Tween 20) and exposed for 15 days at 4°C. Sections were then developed, counterstained with cresyl violet and examined by light and dark field microscope before the quantitative analysis of the grain density. The specificity of the *in situ* hybridisation for the transcript was verified by the absence of the signal using sense radiolabelled probes.

4.7.5 Image analysis

Grain density in single cell was quantitatively evaluated using AnaliSYS software (Soft Imaging Systems, ver. 3.2).

Cresyl violet stained cells were used to define the circular frame outlining the cell and the grain density over a single cell was expressed as number of grains/µm^2 cell area. At least two sections from each animal were analyzed

and the cells were subdivided on the basis of their size. Mean values of grain density for each size category in each animal were used for statistical analysis by Student's T-test. The statistical analysis was done using Prism 4 for Windows, version 4.03.

4.8 MATERIAL

Unless otherwise stated, the reagents used for the experiments were obtained from Sigma-Aldrich (Poole, U.K.).

CHAPTER V

EVALUATION OF THE FUNCTIONALITY OF THE UBIQUITIN-PROTEASOME PATHWAY

5.1 INTRODUCTION

As already discussed in the second chapter, altered functionality of UPP as a pathogenetic event has been proposed in various neurodegenerative diseases. Also in the field of ALS research, several studies have evaluated this hypothesis.

5.1.1 Clearance of mutant SOD1 by the ubiquitin-proteasome pathway

In a recent study carried out by our group, it was established that the accumulation of mutant SOD1 observed in the spinal cord of G93A mice during disease progression did not involve changes in the transcription of the transgene: mRNA levels were unchanged at ages in which the amount of protein was already markedly increased and were even reduced at the final stage of the disease, although the protein was still at high levels (Cheroni et al., 2005). For this reason, we hypothesised that the accumulation of SOD1 was due to an inhibition of its degradation. Additionally, in agreement to other data (Shinder et al., 2001), we found that increased levels of mutant SOD1 correlated with a decrease of its solubility and with the presence of high molecular weight forms. It is known that *in vivo* the propensity of mutant SOD1 to aggregate is linked to the rate of turnover of native and misfolded species by the protein degradation machinery.

All these data pointed out a possible involvement of alterations of UPP functionality in the processes of accumulation and aggregation of mutant SOD1.

Indeed, studying cell lines stable transfected with wild type or mutant SOD1, Hoffman and colleagues verified that the mutation increases the rate of protein turnover; however, the half-life of mutant SOD1 could be prolonged by blocking the UPP, demonstrating that the mutant protein is degraded by the

proteasome (Hoffman et al., 1996; Johnston et al., 2000). These findings were confirmed also by Urushitani and co-workers (Urushitani et al., 2002), who showed that mutant SOD1 was degraded by the UPP in cultured cells and that oxidative damage increased the degree of ubiquitination of the mutant but not of the wild type protein.

Partial inhibition of the proteasome is sufficient to provoke the formation of large aggregates in cultured cells that express SOD1 mutants (Johnston et al., 2000; Hyun et al., 2003), thus suggesting that proteasome activity is limiting and its decrease prevents the appropriate removal of the mutant protein and/or of other components. In addition, the presence of mutated SOD1 enhances the vulnerability to proteasome dysfunction: exposure to proteasome inhibitors resulted in increased cell death in cell lines expressing mutant SOD1 (Aquilano et al., 2003; Hyun et al., 2003) and, in primary cultures, caused the selective death of motor neurons (Urushitani et al., 2002).

These data are supported by studies carried out in organotypic cultures from G93A mice, which demonstrated that the ubiquitin-proteasome system is critically involved in the generation of SOD1-positive complexes. In fact, treatment of G93A spinal cord slices with proteasome inhibitor induced the formation of high molecular weight SOD1 complexes identical to those observed in spinal cord homogenates from symptomatic G93A mice (Puttaparthi et al., 2003). This was proved to be a reversible phenomenon, given that aggregates could be eliminated after the removal of the proteasome inhibitor. From these experiments, proteasomal processing of mutant SOD1 appeared to be finely tuned, since also modest perturbations of its activity were able to generate aggregates in a short period.

In a similar experimental paradigm, selective damage and death of motor neurons were reported after a short-term exposure (36 and 72 hours) to

proteasome inhibitor (Tsuji et al., 2005); however, a longer term treatment determined the degeneration of motor neurons and interneurons in a similar amount (Vlug and Jaarsma, 2004).

Besides the degradation pathway by the 26S complex, it has been shown that, at least *in vitro*, purified SOD1 in its metal-free form can be degraded directly by the 20S proteasome without requiring ATP or ubiquitin; for mutant SOD1, the susceptibility to degradation through the 20S particle correlates with the amount of structural perturbation caused by the mutation (Di Noto et al., 2005). Moreover, in a recent work, the use of specific inhibitors has permitted to reveal that wild type and mutant SOD1 are degraded both by the UPP and macroautophagy in a comparable percentage (Kabuta et al., 2006).

In vivo, 20S proteasome activity measured by fluorogenic peptides is reduced in adult mouse spinal cord compared to other tissue types, maybe contributing to the propensity of SOD1 to accumulate and form aggregates in this region (Puttaparthi et al., 2003). Furthermore, proteasome activity in the spinal cord decreases with age (Keller et al., 2000b).

5.1.2 Interaction of mutant SOD1 with UPP components

In ALS patients and mouse models, proteinaceous inclusions are often labelled with antibodies that recognize members of the UPP, pointing out their potential involvement in ALS. The possible interactions of mutant SOD1 with some of these molecules have been investigated more in detail.

I. Dorfin

The RING finger-type E3 ligase dorfin was found localized in inclusion bodies in familial and sporadic ALS cases. In cell cultures, dorfin was demonstrated to be able to selectively interact with mutant SOD1, promoting its poly-ubiquitination and degradation and protecting cells against the toxic effects of the mutant protein (Niwa et al., 2002). Interestingly, dorfin expression is

increased in the spinal cord of sporadic ALS patients (Ishigaki et al., 2002); this may suggest an attempt to enhance the clearance of altered proteins.

II. NEDL-1

NEDL-1 is an HECT-type E3, preferentially expressed in the CNS, that physiologically interacts with Trapδ, a component of the ER system. In neuroblastoma cells, mutant SOD1, but not the wild type enzyme, interacts with the NEDL1-Trapδ complex, that mediates SOD1 ubiquitination. NEDL-1 is contained in inclusion bodies in the motor neurons of fALS patients and SOD1 mutant mice (Miyazaki et al., 2004).

III. CHIP

Also the E4 protein CHIP (carboxyl terminus of Hsc-70 interacting protein) is localized in the proteinaceous inclusions of G93A mouse spinal cord (Urushitani et al., 2004). CHIP is a chaperone-dependent E4 that ubiquitinates unfolded proteins, thus representing a link between the chaperone system and UPP (Meacham et al., 2001). In cell line paradigms, CHIP, together with Hsp/Hsc 70, is able to selectively bind mutant SOD1 and to promote its degradation. CHIP over-expression modulates the ubiquitination pattern of SOD1, surprisingly increasing the species linked with short ubiquitin chains (Choi et al., 2004). Probably, the augmented clearance of SOD1 is mediated by the poly-ubiquitination of Hsp/Hsc70 rather than of mutant SOD1 itself (Urushitani et al., 2004).

IV. SUMO

SUMO (small ubiquitin-like modifier) is a family of ubiquitin-like proteins; the link of SUMO on a lysine residue of the target protein blocks the ubiquitination of the same site, resulting in the inhibition of protein degradation and in the alteration of its function (Desterro et al., 1998; Huang et al., 2003; Steffan et al., 2004). Human SOD1 is a substrate of SUMO-1, that

modifies the protein on Lys75; SUMO-1 modification of SOD1 enhances its stability and its steady-state level. Furthermore, in a cell culture paradigm, over-expressed SUMO-1 increases the aggregation of SOD1 and co-localizes onto SOD1 aggregates (Fei et al., 2006).

V. UCHL1

Although the interaction of this protein with mutant SOD1 has not been studied so far, depletion of the transcript of the deubiquitinating enzyme UCHL1 was found in the motor cortex of patients affected by sporadic ALS (Lederer et al., 2007).

5.1.3 Levels of constitutive proteasome subunits

In a recent published study, analysing by western blot the spinal cord of G93A mice, we found reduced levels of the three constitutive catalytic subunits β1, β2 and β5 at the late stage of disease progression. Immunohistochemical experiments highlighted a decrease of 20S immunostaining selectively in some spinal motor neurons of pre-symptomatic G93A mice; with disease progression, a more diffuse and marked decrease of both 20S and 19S was observed in ventral and intermediate zones of spinal cord sections and correlated with the accumulation of mutant SOD1 and ubiquitin (Cheroni et al., 2005). In line with these findings, Kabashi's study reported a decrease of 20S proteasome α subunit in motor neurons of symptomatic G93A mice (Kabashi et al., 2004). However, some inclusions moderately labelled by the antibody recognizing 20S proteasome were reported in the spinal cord of G93A and G85R mice (Watanabe et al., 2001). As regards to sporadic human samples, the results are contradictory: no inclusions were found immunoreactive for proteasome in two studies (Ii et al., 1997; Watanabe et al., 2001) while Mendoca and colleagues highlighted, in some neurons and astrocytes, the presence of areas of intense focal 20S staining, in which the

proteasome could be co-localized with aggregates (Mendonca et al., 2006). Finally, the proteasome complex was found down-regulated in a microarray study on the motor cortex of sALS patients (Lederer et al., 2007).

5.1.4 Proteasomal activity in *in vitro* and *in vivo* models of ALS

Various studies have tried to analyze the activity of the ubiquitin- proteasome pathway in *in vitro* and *in vivo* models of amyotrophic lateral sclerosis. However, the complex nature of UPP renders the evaluation of its functionality a difficult task; in the last years, various methods have been developed to try to accomplish it.

I. Methods for measuring the activity of the ubiquitin-proteasome pathway

Two are the major approaches that have been used to analyze the activity of the UPP:

1. Small fluorogenic peptides:

   The individual activities of purified proteasome can be quantified with the use of synthetic peptide substrates linked to a fluorogenic group, that measure the ability of the proteasome present in the tissue extract to catabolize an additional substrate load (the fluorogenic peptide). This assay is simple and reliable, but it has certain limitations. First, it provides information only about the proteolytic process and does not take into account upstream events such as ubiquitination, deubiquitination and unfolding. Second, fluorogenic substrates cannot be used for the study of qualitative variations, such as changes in the subcellular distribution of components of the UPP. Finally, this assay does not provide information of the functional impairment *in vivo* or on cell type differences.

2. Fluorescent reporter proteins:

To overcome the above reported limits, several groups have developed assays that allow the functional analysis of UPP *in vivo*. All these reporter substrates are based on the targeting of a fluorescent protein for proteasomal degradation by the introduction of constitutive degradation signals; the latter are defined as motifs that recruit specific E3s, resulting in the ubiquitination and proteasome degradation of the target protein. Kopito's group coupled green fluorescent protein (GFP) to the short degron CL1, generating the GFP^{u} reporter (Bence et al., 2005). Dantuma's group has designed different substrates, among which the Ub^{G76V}-GFP, that is constitutively degraded by the ubiquitin-fusion degradation (UFD) pathway (Salomons et al., 2005). UFD signal is characterized by the presence of an N-terminal ubiquitin moiety that, due to the G76V substitution, cannot be cleaved by DUBs; in these circumstances, ubiquitin is recognized as a degradation signal, leading to poly-ubiquitination and degradation of the UFD-containing protein (Johnson et al., 1992; Johnson et al., 1995). The use of fluorescent reporter proteins offers the great advantage to permit the evaluation of the global activity of the UPP *in vivo* and at the cellular level. However, also this methodology has its own limitations: first, only ubiquitin-dependent proteolysis is monitored; moreover, high level inhibition of proteasome activity is required to observe a substantial increase of GFP fluorescence. Fluorescent reporter proteins have been used also for the generation of animal models that allow the study of UPP in the contest of different diseases; Ub^{G76V}-GFP mice, that were used in this study, have been already described in the method section of this thesis (4.1.2).

II. The activity of the ubiquitin-proteasome pathway in models of ALS

Several studies measured the total proteasomal proteolytic activity by analysing the hydrolysis of fluorogenic peptides in cell lines transfected with mutant SOD1. The results obtained, however, are controversial, since total proteasomal activity was found decreased by some investigators (Urushitani et al., 2002; Allen et al., 2003; Hyun et al., 2003) and increased by others (Casciati et al., 2002; Aquilano et al., 2003).

Our group used the same technical approach with the purpose to analyse the proteasomal catalytic activity in homogenates from the spinal cord of G93A mice compared to NTg littermates; the results showed no change of the three proteolytical activities (Cheroni et al., 2005). Analysing the spinal cord of late onset G93A mice at advanced stage of disease progression, an increase of chymotripsin-like and caspase-like activities of the proteasome has been revealed (Puttaparthi and Elliott, 2005); similar data were described in G93A rats (Ahtoniemi et al., 2007). Conversely, Durham and colleagues reported in the lumbar spinal cord of G93A mice a significant decrease in proteasome activity already at a pre-symptomatic stage (Kabashi et al., 2004); the discrepancy with the other data may rely on the fact that these authors focused on the lumbar region of the spinal cord.

Two recent studies have taken advantage of the reporter proteins for UPP activity to analyze the functionality of the entire ubiquitin-proteasome system in cell cultures expressing mutant SOD1. Matsumoto and colleagues reported increased level of Ubi-YFP reporter in cells containing G85R or G93A aggregates (Matsumoto et al., 2005); similarly, the presence of mutant SOD1 in NSC34 cells determined a strong accumulation of the YFP^{u} reporter (Sau et al., 2007).

5.1.5 Link between ER stress and UPP functionality

The endoplasmic reticulum is the main site of the synthesis of secreted proteins. Given the substantial protein load in the ER, it is of great importance to promptly eliminate abnormal and potentially hazardous proteins that accumulate in this organelle (Bachmair et al., 1986). In fact, there is a tight connection between the protein quality control in the ER and the ubiquitin-proteasome pathway (Aviel et al., 2000): in a process known as ER-associated degradation (ERAD), proteins that fail the ER quality control are transported back to the cytosol where they are rapidly destroyed by the UPP (Aviel et al., 2000). Under conditions that negatively affect the environment in the ER, the pool of aberrant proteins rapidly increases, resulting in the induction of the unfolded protein response (UPR). The UPR is a cellular program which involves at least three different mechanisms to re-establish the homeostasis: attenuation of protein synthesis, optimization of chaperone-assisted protein folding and augmentation of protein degradation (Bachmair et al., 1986). Stimulation of translocation of aberrant ER proteins to the cytosol followed by UPP-dependent degradation is an integrated part of the UPR and it is necessary to relieve the burden of abnormal proteins in the ER (Bachmair et al., 1986; Bachmair and Varshavsky, 1989); cells that fail to restore a proper ER homeostasis will eventually be eliminated by ER stress-induced cell death (Baumeister et al., 1998; Bebok et al., 1998). CHOP, also named GADD153, is a stress transcription factor linked to cell death and controls the transition from pro-survival to pro-apoptotic signalling during ER stress (Rutkowski and Kaufman, 2004), but its mode of action and its downstream pathways are still essentially obscure. With unknown mechanisms, CHOP is able to decrease Bcl-2 levels and to provoke glutathione depletion (Oyadomari and Mori, 2004). Its regulation is essentially transcriptional: in physiological situations, the

protein is expressed at very low levels and localizes in the cytosol; during ER stress, CHOP is strongly inducted and accumulates in the nucleus (Oyadomari and Mori, 2004). Phosphorylation of CHOP by p38 MAPK is able to enhance its transcriptional activity (Wang and Ron, 1996). p38 is a member of a large family of serine/threonine kinases that has been implicated in the responses to a variety of cellular stresses, including pro-inflammatory cytokines and excitotoxicity. A selective accumulation and activation of p38 has recently been demonstrated by our group in the spinal motor neurons of G93A mice at an early stage of the disease; this effect persisted until the end stage, becoming prominent in the reactive glial cells (Tortarolo et al., 2003).

A recent study has pointed out a subtle effect of ER stress on the functionality of UPP (Menendez-Benito et al., 2005). In fact, the administration in cell cultures of drugs that act as ER stressor provoked a robust induction of CHOP; this phenomenon was accompanied by a modest accumulation of Ub^{G76V}-GFP reporter protein for UPP functionality. The effect was about 10% of that accomplished by a full obstruction of the pathway, but it could be important to determine an increased sensitivity of the system to other stresses (Menendez-Benito et al., 2005). These data suggest that the pressure to keep the ER operative while facing large amounts of aberrant proteins may alter the UPP functionality, causing a chronic imbalance between generation and clearance of misfolded proteins.

5.1.6 ER stress in ALS

SOD1 is an essentially cytosolic protein that lacks organelle targeting sequences and is synthesized by free ribosomes (Hirano et al., 1985). Nonetheless, recent and surprising data have revealed that both mutant and wild type SOD1 are present also in the ER compartment. It has been shown that SOD1 co-localizes with ER markers in COS7 and neuro2A cells (Tobisawa

et al., 2003; Urushitani et al., 2006); furthermore, in mice spinal cord, both wild type SOD1 and mutant ones have been identified in the ER, where the mutant proteins accumulate during disease progression and form high molecular weight species (Kikuchi et al., 2006). How SOD1 is post-translationally imported within the ER compartment remains enigmatic; also the reasons of the physiological presence of SOD1 in the ER is unclear, although one possibility is to form native disulfide bonds before transit to other locations. Indeed, the disulfide status of the proteins is largely regulated by ER stress-inducible enzymes. Protein-disulfide isomerase (PDI) is an ER chaperone that catalyzes the formation and rearrangement of intra- and inter-molecular disulfide bonds (Roth and Koshland, 1981; Turano et al., 2002). PDI was found in association with SOD1 in cellular and animal models of fALS; furthermore, the pharmacological inhibition of PDI triggered the formation of SOD1 inclusions (Atkin et al., 2006).

Another important issue regards the consequences of the presence of the mutated protein in the endoplasmic reticulum. ER abnormalities have been reported in human ALS patients and transgenic mice (Dal Canto and Gurney, 1995; Engelhardt et al., 1997); moreover, in the spinal cord of SOD1 mutant mice, UPR-induced chaperones, stress sensor kinases and apoptotic effectors are up-regulated. For instance, in low expressor G93A mice, induction of ATF-3 has been highlighted in the motor neurons at a relatively early stage of disease progression (Vlug et al., 2005); another study, in early onset G93A mice, reported an increase of ATF-6 and IRE-1 at the symptomatic stage (Kikuchi et al., 2006).

As regards to CHOP, contrary results come from studies on G93A mice, in which its expression has been reported both as unchanged (Wootz et al., 2004)

or up-regulated at disease onset in low expressor line (Vlug et al., 2005) and at symptomatic stage in high expressor line (Atkin et al., 2006).

Given these results, it seems possible that, over the course of the disease, motor neurons expressing ALS-linked SOD1 mutants undergo a UPR aimed at improving their capacity to withstand the ER accumulation of misfolded mutant SOD1; therefore, ER stress may play a role in SOD1 mediated neurodegeneration.

5.2 AIMS

As just discussed, an eminent literature has been produced regarding the possible involvement of alterations of the ubiquitin-proteasome pathway in the events that lead to motor neuron loss in ALS. However, the obtained data are contradictory and neither prove nor exclude a pathogenic role of UPP in the disease.

The first aim of this section was to analyze by immunohistochemistry the time course of the accumulation of ubiquitinated proteins in the spinal cord of G93A mice during disease progression. Afterwards, I evaluated the activity of UPP in the same animal model. To achieve this goal, I took advantage from the Ub^{G76V}-GFP mouse model, that expresses a reporter protein for UPP activity; in this way, it was possible to study the overall functionality of UPP *in vivo* and at the cellular level in G93A mice, thus overcoming the limitations typical of the fluorogenic *in vitro* assays used so far on SOD1 mutant mice.

In order to characterize the expression of the reporter protein in the area of interest, the first investigations were focussed on the analysis of Ub^{G76V}-GFP basal levels in the spinal cord of Ub^{G76V}-GFP mice and on the confirmation of its accumulation in the motor neurons in response to the administration of proteasome inhibitors. Then, the breeding between G93A and Ub^{G76V}-GFP mice permitted to obtain double transgenic mice; since the presence of Ub^{G76V}-GFP in the spinal cord of G93A mice may have been a further element of stress for motor neurons, the disease progression in double transgenic mice was evaluated. Finally, UPP functionality was studied in double transgenic GFPG93A mice by assessing the levels of the reporter protein both in the homogenate and in the cell populations of the spinal cord.

5.3 METHODS

5.3.1 Western blot

Western blot experiments were conducted in collaboration with Dr. C. Maynard and Dr. N. Dantuma (Dept. Cell and Molecular Biology, Karolinska Institute, Stockholm, Sweden), according to the general procedures described in the paragraph 4.5.

For the detection of GFP protein, membranes were probed overnight at 4°C with an anti-GFP mixed-mouse monoclonal antibody (Roche) diluted 1:2000 in blocking buffer.

5.3.2 Immunohistochemistry

I. Experiments of co-localization with ubiquitin

Following the general procedures described in the paragraph 4.2, the sections were first labelled for ubiquitin (polyclonal antibody from DAKO - Ely, Cambridgeshire, UK - diluted 1:750 and incubated for 30' at RT) and the signal revealed with the tyramide amplification. Then, the sections were incubated with the following primary antibodies: anti-human SOD1 rabbit polyclonal antibody, 1:2000 dilution (Upstate Biotechnology, Temecula, CA, USA); anti-GFAP mouse monoclonal antibody, 1:2500 dilution (Chemicon International, Harrow, UK) to stain the glial fibrillary acidic protein (GFAP); anti-CD11β rat monoclonal antibody, 1:1000 dilution (The Chemical Society) to label activated microglial cells; anti-choline acetyl transferase (ChAT) mouse monoclonal antibody, 1:200 dilution (Chemicon) for co-localization with the motor neuronal population. Anti-mouse, anti-rabbit or anti-rat secondary fluorescent antibodies were used as described (paragraph 4.2.3).

If not differently specified, primary antibodies were incubated overnight at 4°C.

II. DAB staining of GFP

The staining was performed as described in the section 4.2.2 using an anti-GFP rabbit polyclonal antibody (Molecular Probes) diluted 1:3500.

III. DAB staining of CHOP

The staining was performed as described in the section 4.2.2 using anti-CHOP rabbit polyclonal antibody (Santa Cruz Biotechnology, Santa Cruz, CA, USA) diluted 1:200.

IV. Experiments of co-localization with GFP

Free-floating sections were first labelled for GFP (rabbit polyclonal antibody from Molecular Probes, diluted 1:1000 and incubated for 2 h at 4°C) and the signal was revealed by tyramide amplification; then, they were incubated with the following primary antibodies: anti-SMI-32 mouse monoclonal antibody, 1:200 dilution, or anti-SMI-31 mouse monoclonal antibody, 1:5000 (both from Sternberger) for co-localization with non-phosphorylated or phosphorylated neurofilaments antigens, respectively; anti-GFAP mouse monoclonal antibody, 1:2500 dilution (Chemicon); anti-CD11β rat monoclonal antibody, 1:1000 dilution (The Chemical Society); anti-calretinin rabbit polyclonal antibody, 1:1000 dilution (Swant, Bellinzona, Switzerland) for co-localization with interneurons; anti-NeuN mouse monoclonal antibody (diluted 1:250, Chemicon) to stain the neuronal population; anti-ubiquitin rabbit polyclonal antibody (form DAKO, diluted 1:100 and incubated for 45 min at RT). Anti-mouse, anti-rabbit or anti-rat secondary fluorescent antibodies were used as already described (section 4.2.3).

If not differently specified, primary antibodies were incubated overnight at 4°C.

V. Experiments of co-localization with CHOP

Free-floating sections were first labelled for CHOP (polyclonal antibody from Santa Cruz, diluted 1:300) and the signal revealed by tyramide amplification;

subsequently, sections were incubated with the following primary antibodies: anti-NeuN mouse monoclonal antibody (1:250, Chemicon) to stain the neuronal population; anti-GFP rabbit polyclonal antibody (from Molecular Probes, diluted 1:500 and incubated for 1 h. at RT). Anti-mouse or anti-rabbit secondary fluorescent antibodies were used as already described (section 4.2.3).

If not differently specified, primary antibodies were incubated overnight at 4°C.

5.3.3 Real time PCR

Real time PCR for GFP transcript was done exploiting SYBR Green as fluorescent dye, as described in the paragraph 4.4, and using β-actin as internal standard.

In table 5.1 are reported the primer sequences.

5.3.4 *In situ* hybridization

In situ hybridization (ISH) experiments were conducted following the method described in section 4.7. Primers specific for GFP (sequence in table 5.2) were employed to amplify a 514 bp fragment from GFP mouse cDNA, following the standard procedures already illustrated (paragraph 4.1.4). The fragment was subcloned in pCDNA3 plasmid.

The plasmid was linearized with Not I for the antisense and with BamHI for the sense and purified. Radiolabelled cRNA were synthesized *in vitro* from linearized plasmid (paragraph 4.5.3), using RNA polymerase T7 for the sense and SP6 for the antisense.

Gene	Accession n°	Forward (5'→ 3')	Reverse (5'→ 3')
β-actin (Actb)	NM_007393	GCCCTGAGGCTCTTTTCCAG	TGCCACAGGATTCCATACCC
GFP	M62654	CATGCCCGAAGGCTACGT	GCTTGTGCCCCAGGATGT

Table 5.1 Primer sequences for real-time PCR experiments

Gene	Forward (5'→ 3')	Reverse (5'→ 3')
GFP	GCCGGATCCCTTGTACAGCTCGTCCATGC	AAGGAAGGCGCGCCCCATGAAGCAGCACGACT

Table 5.2 Primer sequences for ISH experiments

5.4 RESULTS

5.4.1 Ubiquitin accumulation in G93A spinal cord during disease progression

The presence of ubiquitinated inclusions is a well-known phenomenon that occurs in the spinal cord of SOD1 mutant mice. By immunohistochemical techniques, the extension of this phenomenon was analyzed in our mouse model during the progression of the disease. In Fig. 5.1 is displayed the immunolabelling for ubiquitin and the neuronal marker NeuN in the lumbar spinal cord of NTg and G93A mice. In NTg mice, a weak ubiquitin staining appears homogenously distributed in the neurons of the ventral horns. In G93A sections, rare ubiquitin-positive spots are visible at the pre-symptomatic stage in large neurons of the ventral horns and become more numerous as the motor impairment aggravates; finally, at the end stage, a massive increase of ubiquitin is found both inside neuronal cells and as large spots spread throughout the grey matter. In some cases, neurons with high ubiquitin accumulation are characterized by a weak NeuN staining.

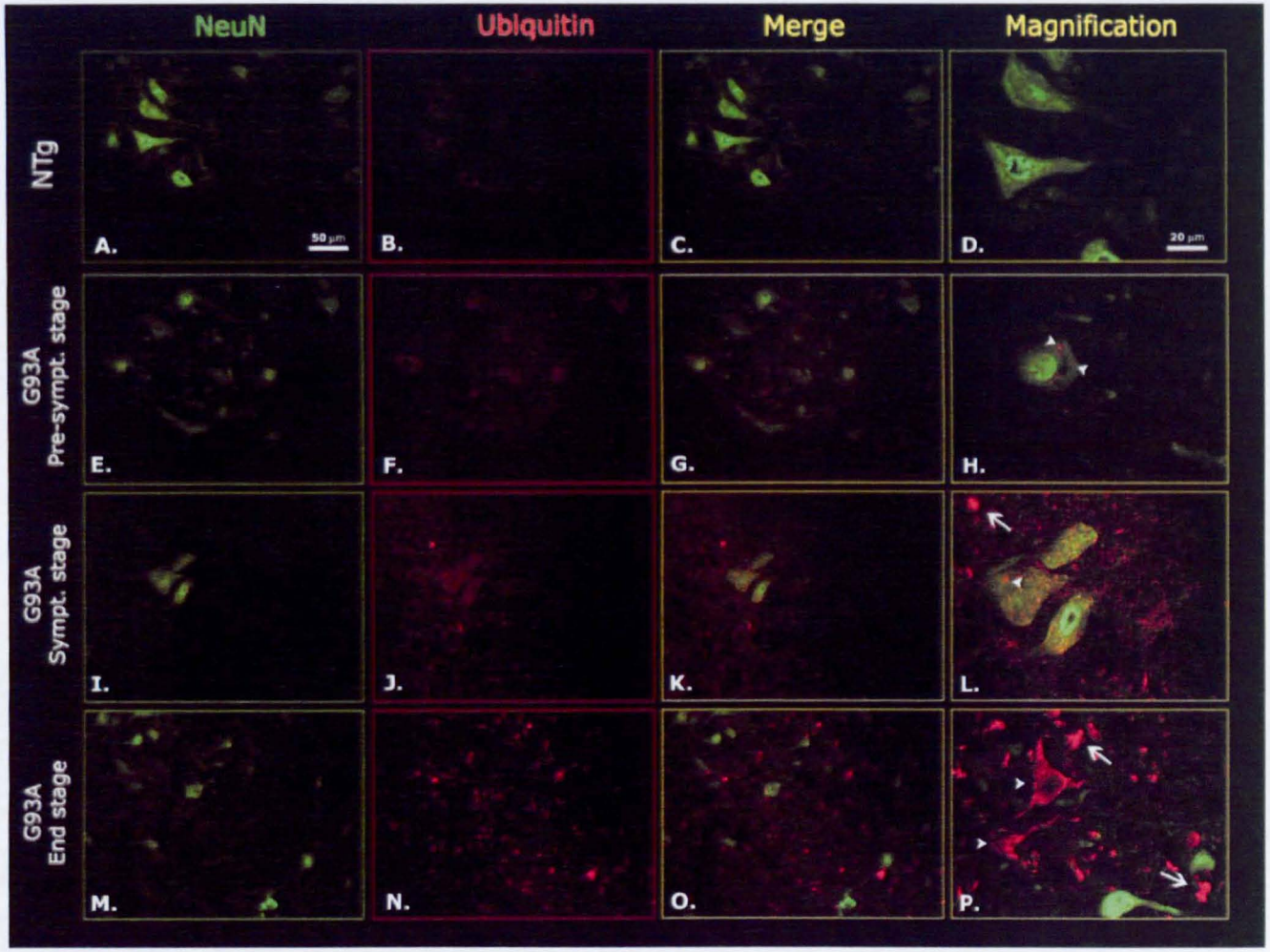

Figure 5.1 Laser scanning confocal microphotographs of NeuN and ubiquitin labelling in the ventral horn lumbar spinal cord of NTg (A-D) and G93A mice at the pre-symptomatic (E-H), symptomatic (I-L) and end stage (M-P) of disease progression. Scale bar 50 µm (A-C, E-G, I-K, M-O) and 20 µm (D, H, L, P). In NTg sections, ubiquitin staining is weak and uniform in NeuN-positive neurons. In G93A speciments, ubiquitin-positive spots are rarely visible at the pre-symptomatic stage (arrowheads in H) and become more frequent during the progression of the disease both in the grey matter (arrows in L, P) and inside neuronal cells (arrowheads in L, P).

In order to examine the cellular distribution of ubiquitin and its possible co-localization with mutant SOD1, triple immunostaining experiments were performed in lumbar spinal cord sections of end stage G93A mice in comparison to mice that over-express wild type human SOD1 (WT SOD1).

In WT SOD1 mice, both SOD1 and ubiquitin labelling resulted low and uniformly distributed in the neurons of the spinal cord, including the ChAT-immuno-positive motor neurons (Fig. 5.2 A-E). Conversely, particularly intense labelling for SOD1 was detected in G93A mice at the edge of the vacuoles characteristic of the ventral and intermediate regions of spinal cord grey matter (Fig. 5.2 arrows in I and M) and in some degenerating motor neurons (Fig 5.2 arrowheads in I and L). In the same sections of G93A mice, the ubiquitin immunoreactivity showed a pattern of distribution characterised by large spots of ubiquitin-positive accumulation scattered throughout the grey matter (Fig. 5.2 H-M), which did not co-localise with SOD1, except for very few cases. Focussing on ChAT-positive motor neurons of G93A mice, it was observed that only occasionally ubiquitin-positive spots were localized in vacuolized motor neurons where SOD1 was highly expressed (Fig 5.2 I-M).

The analysis of SOD1 and ubiquitin in GFAP labelled astrocytes of G93A mice showed that hypertrophic astrocytes do not accumulate SOD1; however, some GFAP-positive cells characterized by a round morphology display high levels of ubiquitin signal (Fig 5.2 N-S).

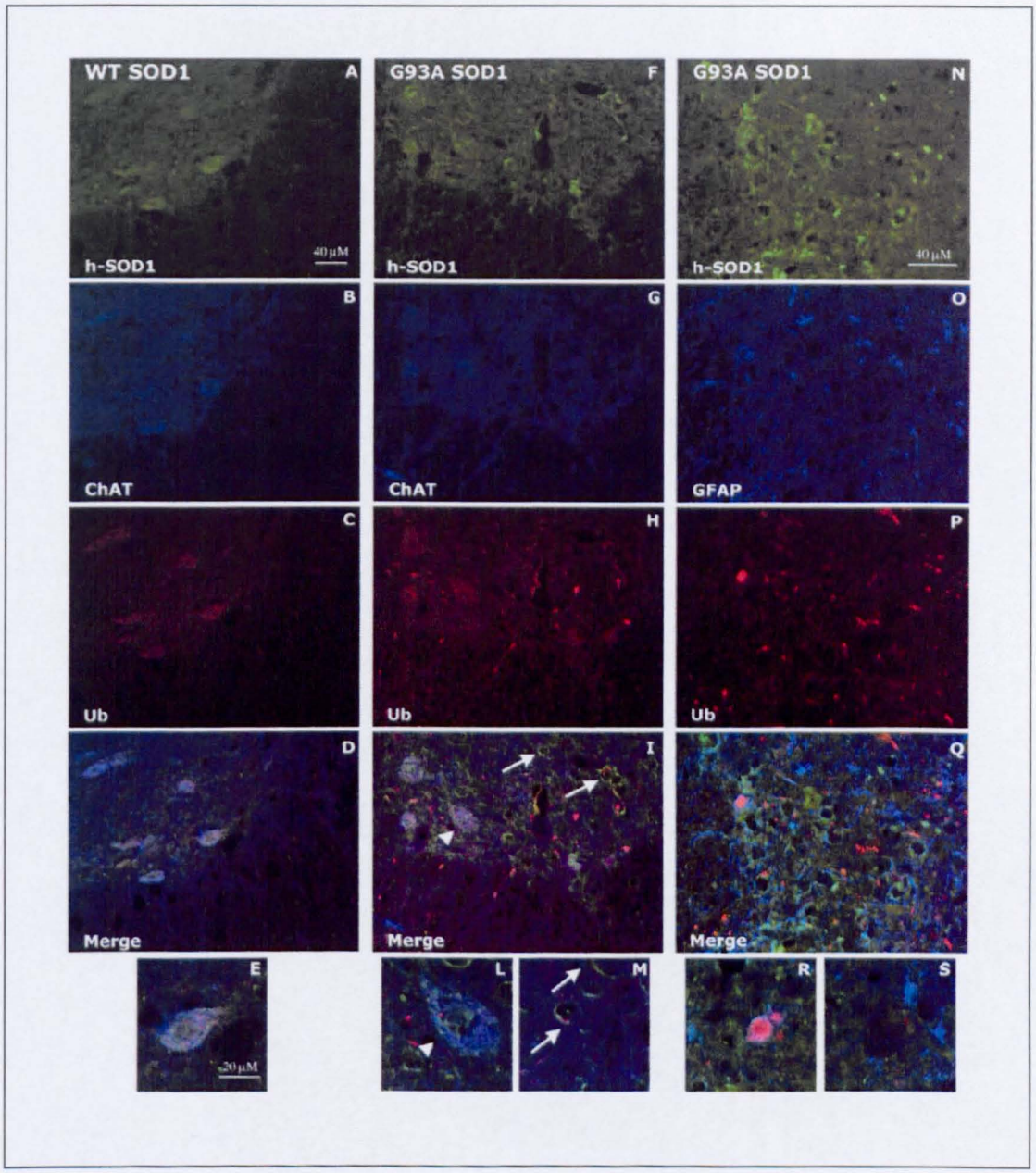

Figure 5.2 Laser scanning confocal microphotographs of SOD1, ChAT, GFAP and ubiquitin labelling in the ventral horn lumbar spinal cord of WT SOD1 (A-E) and G93A (F-S) mice at the end stage of disease progression. Scale bars 40 μm (A-D, F-I and N-Q) and 20 μm (E, L, M, R and S). In WT SOD1 mice, SOD1 and ubiquitin labelling are low and uniformly distributed in ChAT-positive motor neurons (A-E). In G93A sections, SOD1 accumulation is particularly visible on the edge of vacuoles in the grey matter (arrows in I, M) and in some motor neurons (arrowheads in I, L), with scarce co-localization with ubiquitin-positive spots. No accumulation of SOD1 occurs in GFAP-positive astrocytes (N-S), while some of them show high ubiquitin levels (O-R).

5.4.2. Immunohistochemical analysis of Ub^{G76V}-GFP distribution in the spinal cord of Ub^{G76V}-GFP mice

Both GFP1 and GFP2 lines of Ub^{G76V}-GFP mice were characterized for the presence of the reporter protein in the spinal cord, in order to establish the basal levels of Ub^{G76V}-GFP in this area.

Examining the sections from the lumbar spinal cord of GFP1 and GFP2 mice, no GFP intrinsic fluorescence was detected. Therefore, the analysis of the two transgenic lines was conducted by immunohistochemistry using an anti-GFP antibody and amplifying the immunostaining by the avidin/biotin diaminobenzidine system or the tyramide system for the immunofluorescence. The diaminobenzidine labelling revealed differences in the basal level of the reporter protein between the two transgenic lines: while in GFP2 mice GFP remained undetectable, in GFP1 sections the signal was higher and distributed in various cell populations in the ventral and dorsal horns of the spinal cord; the staining resulted being particularly evident in the motor neurons (Fig. 5.3). No differences with age progression were found in both GFP1 and GFP2 lines. No staining was visible in non-transgenic (NTg) mice.

Since in GFP2 mice the background level of the reporter protein is lower, this line was considered more appropriate to detected possible increases in neuronal Ub^{G76V}-GFP. However, before using it for the majority of the experiments, the accumulation of the reported protein was tested in response to UPP inhibition in spinal cord neurons by *in vitro* studies.

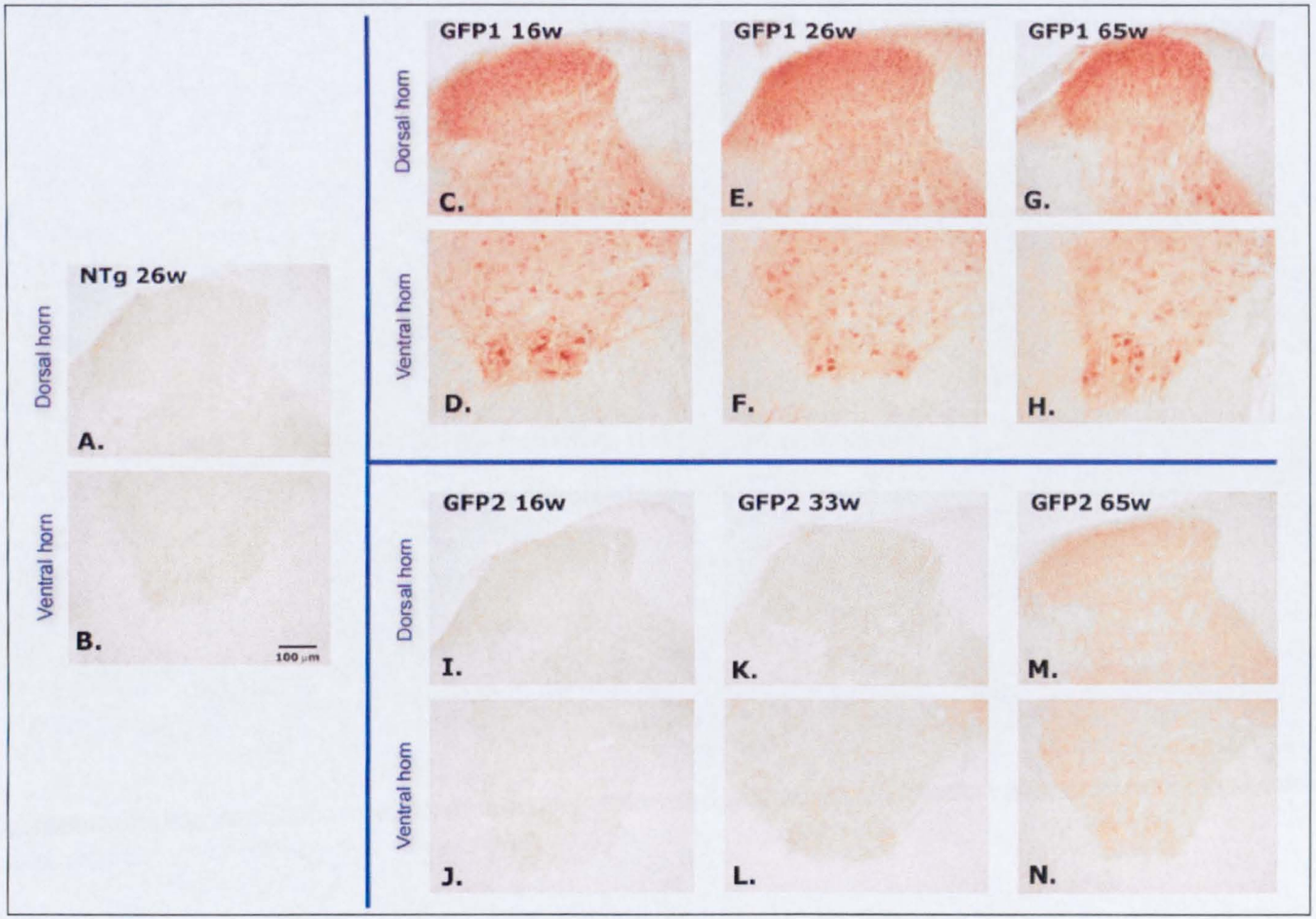

Figure 5.3 Microphotographs of GFP labelling in the dorsal and ventral horns of the lumbar spinal cord of NTg (A, B), GFP1 (C-H) and GFP2 (I-N) mice (w = weeks of age). Scale bar 100 µm. No staining is visible in NTg and GFP2 sections, while in GFP1 speciments the signal is visible in various cell populations both of the dorsal and the ventral horns. No changes are detectable with age progression in both GFP1 and GFP2 mice.

5.4.3 Proteasome inhibition in Ub^{G76V}-GFP primary cultures

Primary cultures were obtained from the spinal cord of NTg and GFP2 embryos (14 days), treated with the proteasome inhibitor MG132 0.5, 1.5 or 4.5 μM for 6 h and labelled for SMI-32 and GFP as described in the method section.

The results achieved showed that, in GFP2 neurons, the administration of MG132 was able to determine an increase in the levels of the reporter protein. The accumulation of Ub^{G76V}-GFP was clearly visible also in neurons characterized by intense SMI-32 labelling, large cell body and prominent neuritic arborisation, identified as motor neurons (Fig 5.4).

In conclusion, these experiments have demonstrated that the administration of a proteasome inhibitor is able to determine the accumulation of the reporter protein in the motor neuronal population of GFP2 embryos. Therefore, the GFP2 mouse line was used for the majority of the experiments, although the key findings were confirmed also in GFP1 line.

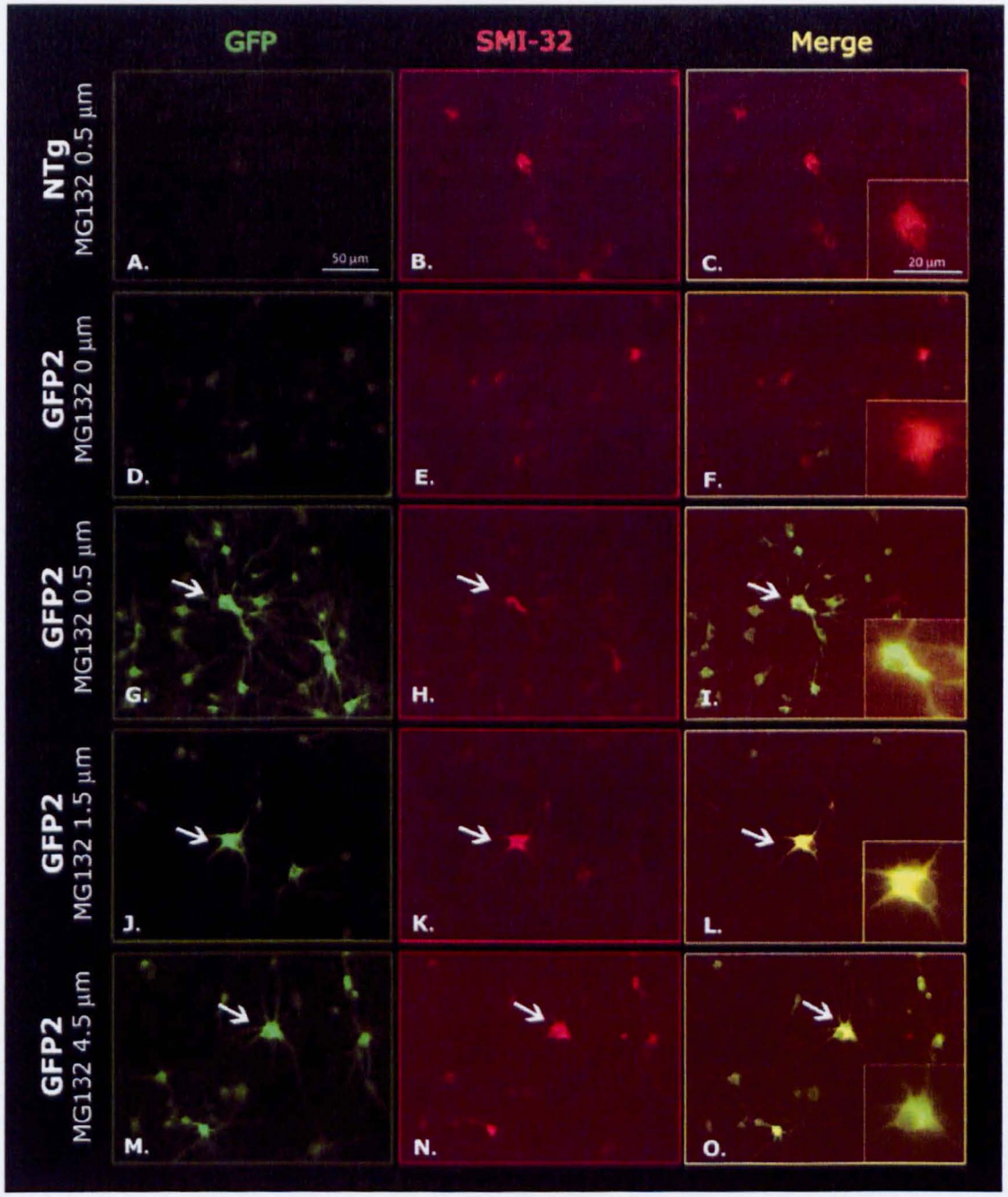

Figure 5.4 Laser scanning microphotographs of GFP and SMI-32 in spinal primary cultures from NTg (A-C) or GFP2 (D-O) embryos treated with vehicle (D-F) or the proteasome inhibitor MG132 0.5 μM (A-C, G-I), 1.5 μM (J-L) or 4.5 μM (M-O). Scale bar 50 μm, insets 20 μm. In GFP2 cultures, the inhibition of the proteasome is able to provoke an increase of GFP levels; the phenomenon is noticeable also in neurons characterized by an intense SMI-32 labelling (arrows in G-O and insets).

5.4.4 Cross-breeding of Ub^{G76V}-GFP and G93A mice

Double transgenic GFP1G93A and GFP2G93A lines were established according with the procedures reported in the method section (4.1.3).

The offspring was genotypized for both the transgenes by PCR analysis.

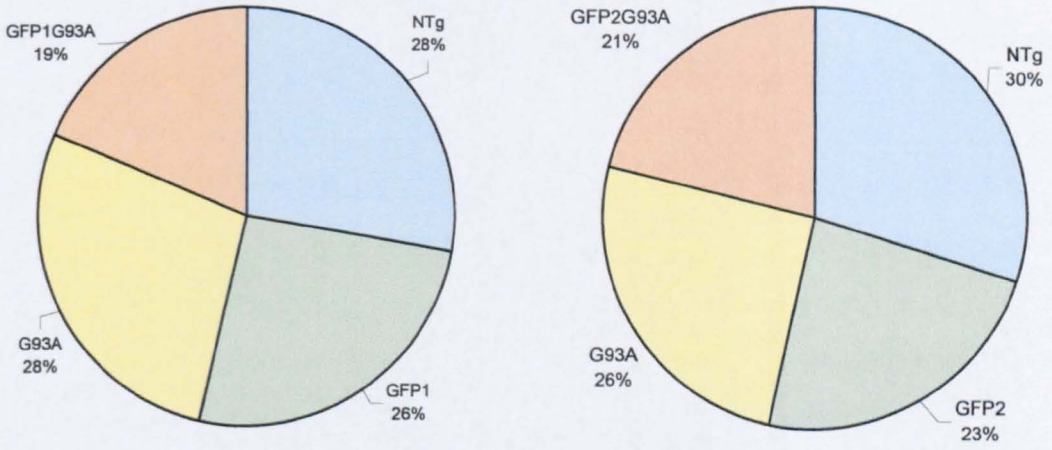

Figure 5.5: Percentage of offspring genotypes in GFP1G93A (n=300) and GFP2G93A (n=386) lines.

As shown in Fig. 5.5, the percentage of double transgenic mice in both GFP1G93A and GFP2G93A lines is lower than the expected 25%. However, the statistical analysis by χ-square test revealed that the difference was not significant ($p>0.05$).

5.4.5 Behavioural analysis of double transgenic mice

The presence of a transgene coding for a protein that is degraded by UPP could represent an additional burden for a system already facing large amounts of unfolded proteins; therefore, the expression of Ub^{G76V}-GFP in G93A mice may be able to modify the disease progression. To investigate this possibility, the motor behaviour of double transgenic mice was analyzed. Since GFP1 mice express higher levels of the reporter protein, this line was selected for the behavioural tests.

Initially, to verify that the solely expression of Ub^{G76V}-GFP was not able to influence the motor behaviour of the mice, I evaluated GFP1 mice in respect to NTg littermates (8 animals for each group). As described in the section 4.4, starting from 84 days of age, the body weight of the mice was recorded once a week; moreover, the motor function of the animals was evaluated using the grid test.

As shown in Fig 5.6 and 5.7, no differences in the body weight nor in the grid test were found between NTg and GFP1 mice.

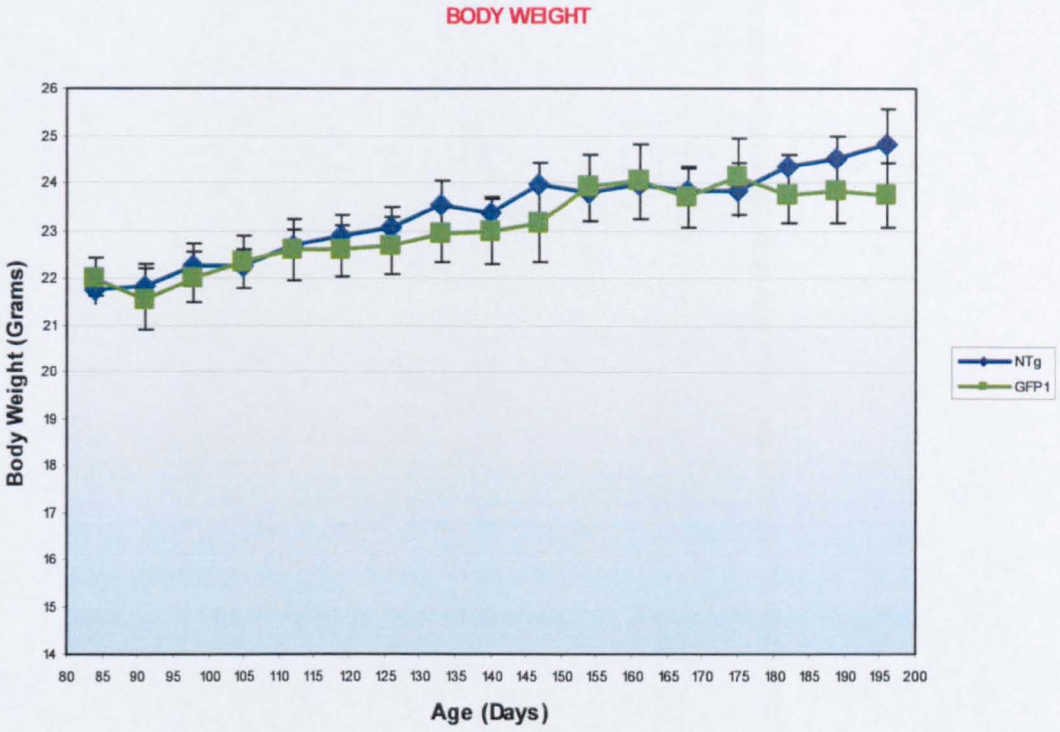

Figure 5.6 Body weight of NTg (n=8) compared to GFP1 (n=8). Each point represents the mean ± S.E. Statistical analysis was done by two-way ANOVA for repeated measures; no significant interaction was found.

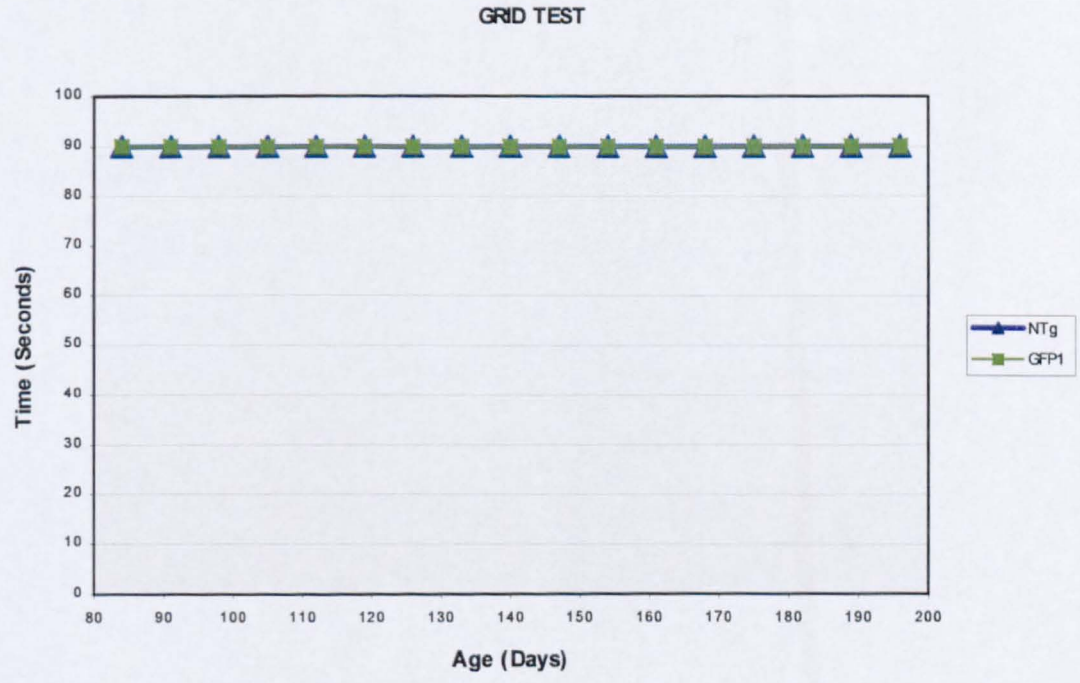

Figure 5.7 Grid test of NTg (n=8) compared to GFP1 (n=8). Each point represents the mean ± S.E. Statistical analysis was done by two-way ANOVA for repeated measures; no significant interaction was found.

Then, with the same approach, GFP1G93A mice (n=13) were evaluated in respect to G93A mice (n=13). The decline of the body weight (Fig. 5.8) and of the motor function (Fig 5.9) was not different between G93A and GFP1G93A mice; also the survival was unchanged (Fig. 5.10). It can therefore be concluded that the progression of the disease in G93A and GFP1G93A mice is contemporaneous.

Figure 5.8 Body weight of G93A (n=13) compared to GFP1G93A (n=13). Each point represents the mean ± S.E. Statistical analysis was done by two-way ANOVA for repeated measures; no significant interaction was found.

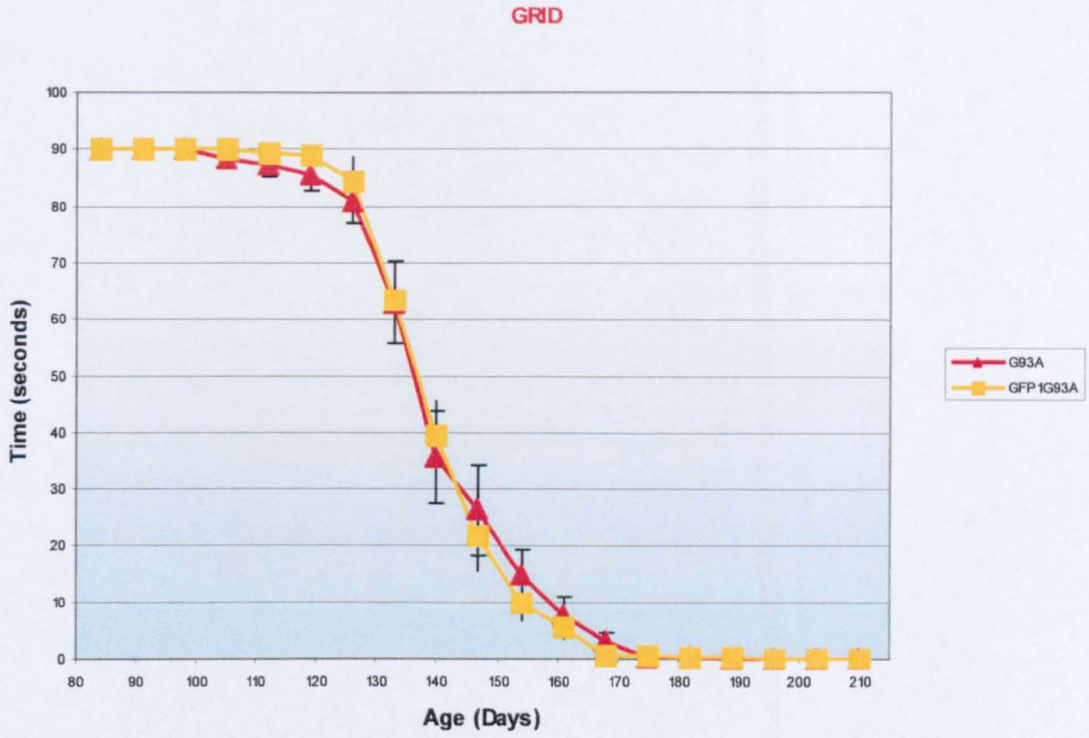

Figure 5.9 Grid test of G93A (n=13) compared to GFP1G93A (n=13). Each point represents the mean ± S.E. Statistical analysis was done by two-way ANOVA for repeated measures; no significant interaction was found.

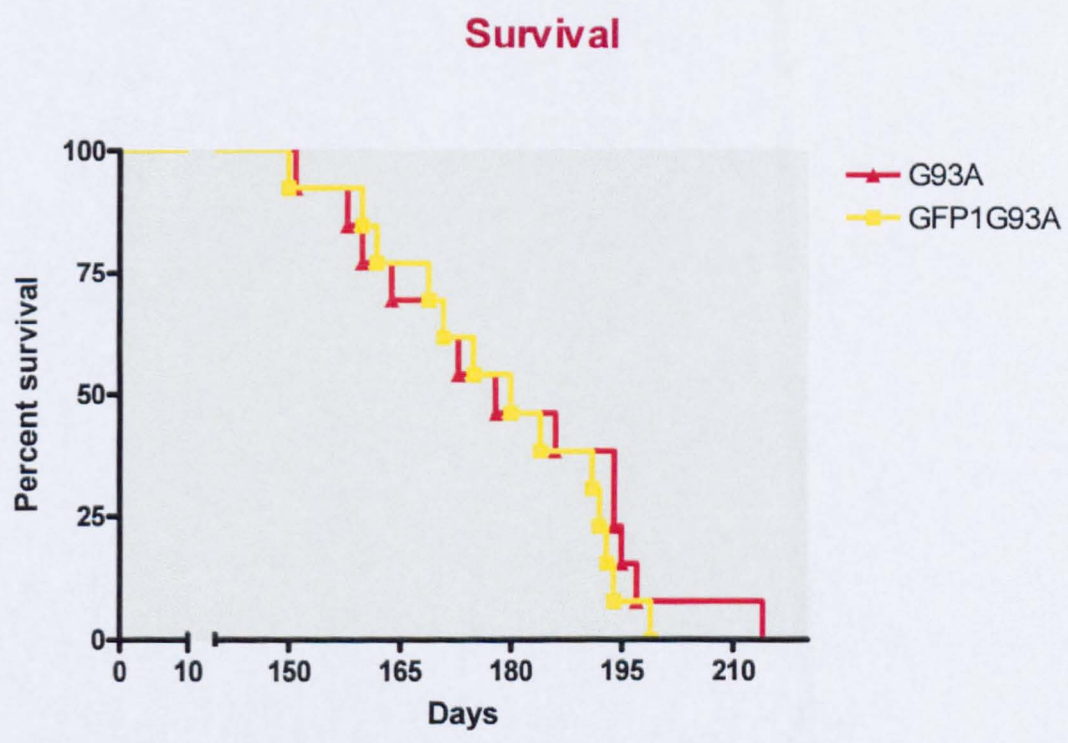

Figure 5.10 Comparison of the survival curves for G93A and GFP1G93A mice. Log-rank analysis of probabilities showed no significant difference.

5.4.6 Western blot analysis of Ub^{G76V}-GFP in the lumbar spinal cord of double transgenic mice

By western blot, the total levels of the reporter protein were evaluated in the lumbar spinal cord of GFPG93A mice in comparison to GFP littermates.

Western blot experiments were conducted in collaboration with Dr. Maynard and Dr. Dantuma (Dept. Cell and Molecular Biology, Karolinska Institute, Stockholm, Sweden).

Regarding the GFP2 line, the levels of the reporter protein were under the threshold of detection both in GFP2 and GFP2G93A mice.

Conversely, in the lumbar spinal cord of both GFP1 and GFP1G93A at the symptomatic phase, a band corresponding to Ub^{G76V}-GFP was detectable (Fig 5.11). The quantification of the optical density (Fig. 5.12) revealed an 1.2-fold increase in GFP1G93A samples compared to GFP1 ones, although the data did not reach the statistical significance ($p=0.058$).

Therefore, it can be concluded that the presence of mutant SOD1 does not determine obvious changes in the global levels of the reporter protein, thus excluding major and generalized alterations of UPP functionality. However, the trend to an augment of Ub^{G76V}-GFP in double transgenic mice put forward the possibility of a dysfunction of UPP occurring selectively in some cell populations.

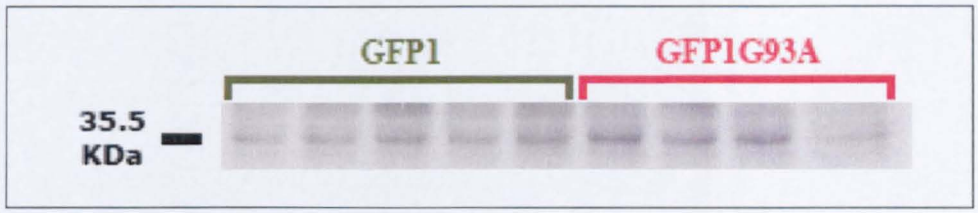

Figure 5.11 Representative immunoblot for Ub^{G76V}-GFP in the lumbar spinal cord of GFP1 and GFP1G93A mice at the symptomatic stage.

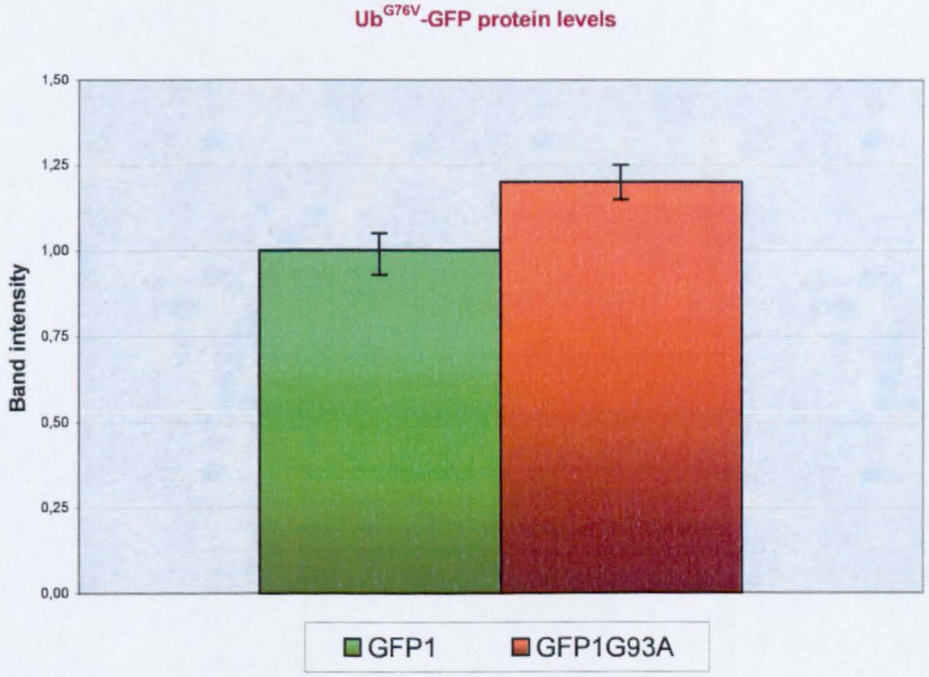

Figure 5.12 Quantitative analysis of the immunoblot. The optical density was evaluated for each autoradiographic band and values for GFP1G93A were normalized to GFP1 after correction for protein loading. Each histogram shows the mean ± S.E. of at least four mice. Data were analyzed by Student's t-test. A tendency to an increase is visible in GFP1G93A samples, but it does not reach the statistic significance.

5.4.7 Immunohistochemical analysis of Ub^{G76V}-GFP in the lumbar spinal cord of pre-symptomatic GFP2G93A mice

Western blot data suggest that UPP functionality may be altered selectively in particular cell types of the spinal cord. For this reason, immunohistochemical experiments were performed on the lumbar spinal cord of double transgenic mice at various stages of disease progression.

In sections from pre-symptomatic G93A mice, an unspecific background signal is visible; in GFP2 specimens, the reporter protein remains undetectable, as already shown in Fig. 5.3. In pre-symptomatic GFP2G93A, only sporadic cells with a mild increase of Ub^{G76V}-GFP, difficult to distinguish from the background signal found in G93A sections, are noticeable (Fig. 5.13).

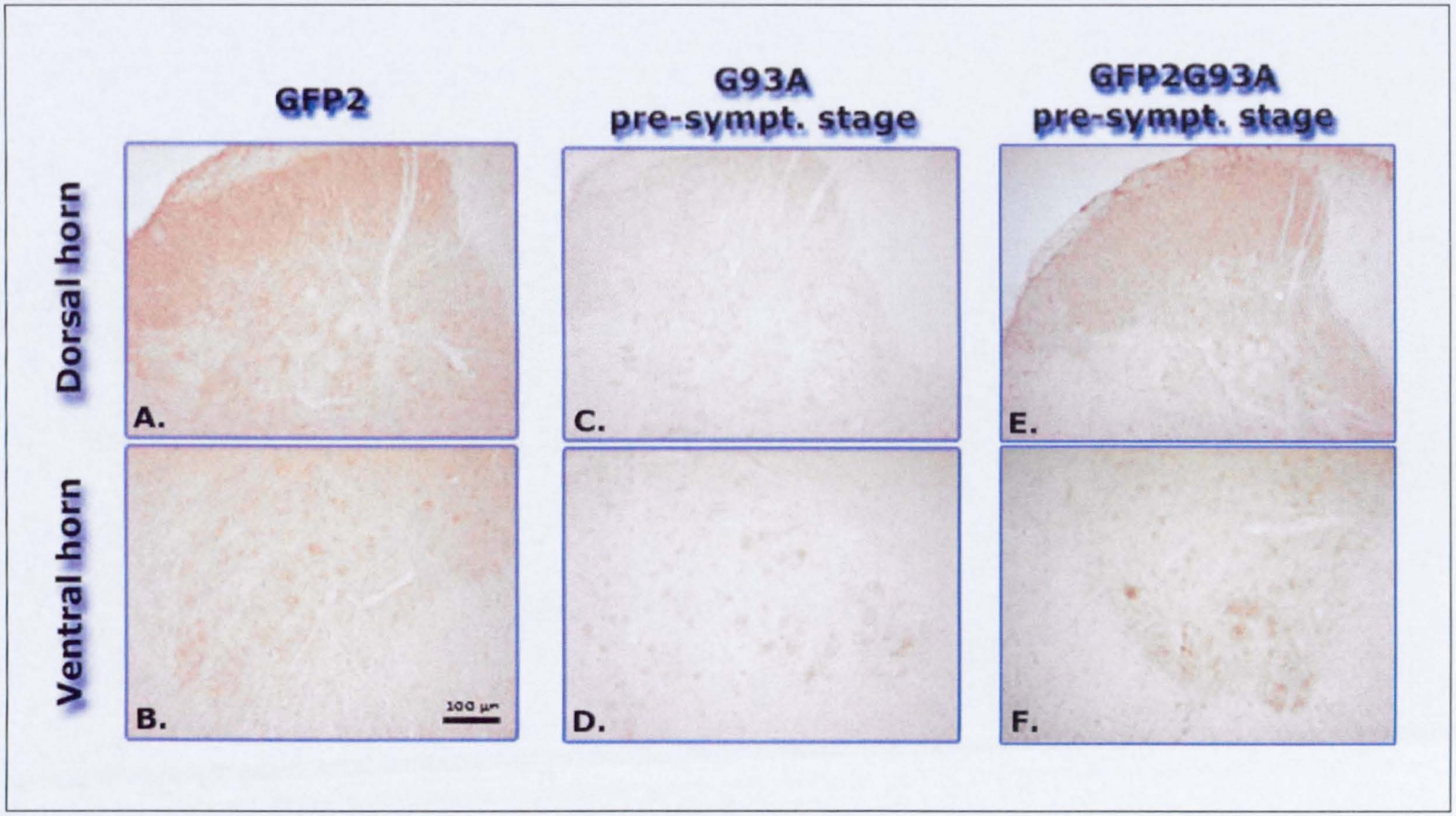

Figure 5.13 Microphotographs of GFP labelling in the lumbar spinal cord of pre-symptomatic GFP2 (A, B), G93A (C, D) and GFP2G93A (E, F) mice. Scale bar 100 µm. No clear accumulation of GFP is noticeable in the neurons of double transgenic mice.

5.4.8 Immunohistochemical analysis Ub^{G76V}-GFP in the spinal cord of symptomatic double transgenic mice

To evaluate whether a dysfunction of UPP could be more evident at later phases of disease progression, also symptomatic and end stage double transgenic mice were analyzed.

5.4.8.1 Immunohistochemical analysis of Ub^{G76V}-GFP in the lumbar spinal cord of symptomatic GFP1G93A and GFP2G93A mice

Immunohistochemical experiments were performed on the lumbar spinal cord of symptomatic GFP2G93A mice in comparison to GFP2 and G93A littermates (Fig. 5.14). As already shown, no specific GFP staining is visible in G93A and GFP2 sections. On the contrary, in GFP2G93A mice a small number of cells with a clear accumulation of the reporter protein is detectable in the grey matter; the majority of them are localized in the ventral horns and some show morphological alterations such as vacuolization.

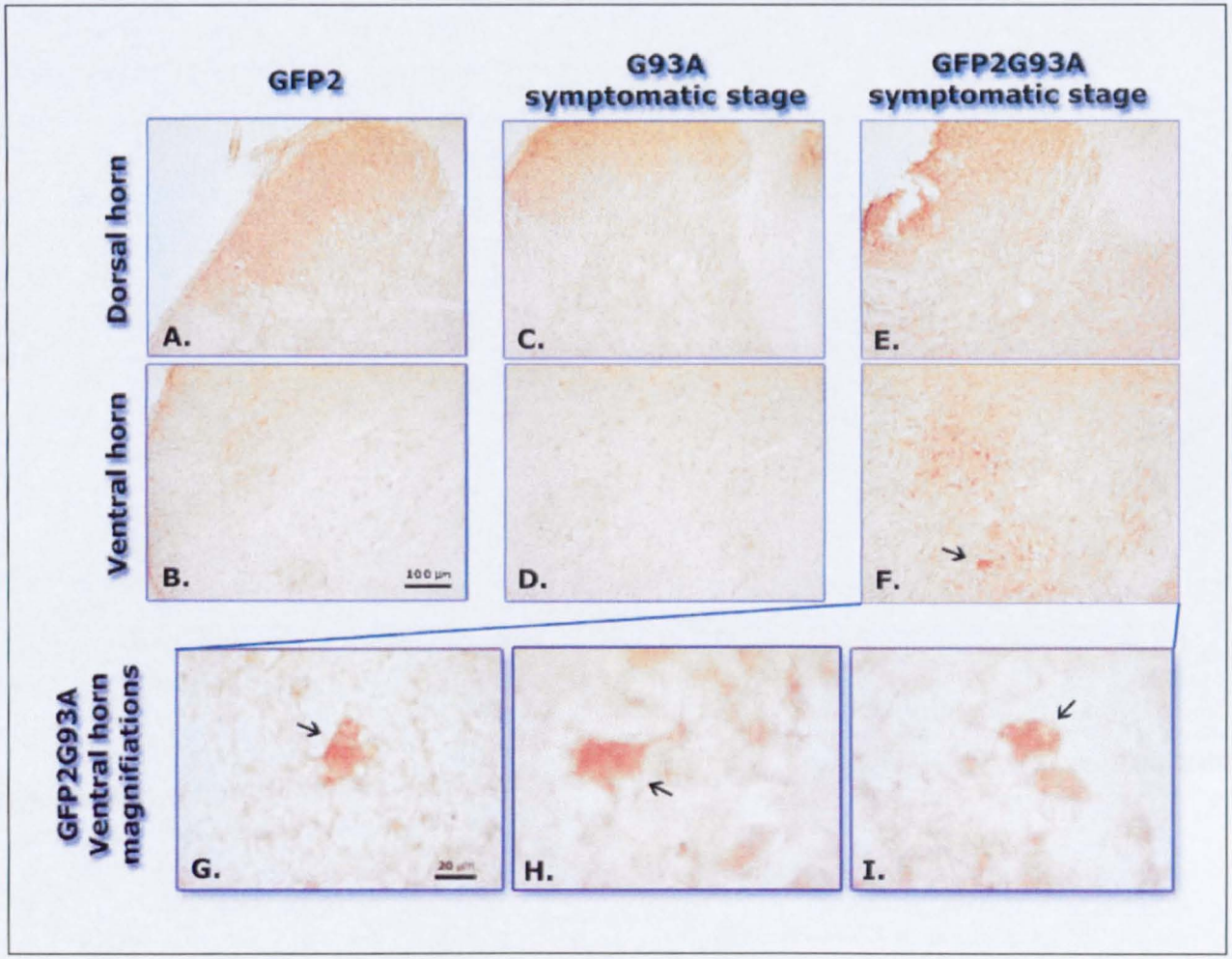

Figure 5.14 Microphotographs of GFP labelling in the dorsal and ventral horns of the lumbar spinal cord of GFP2 (A, B), G93A (C, D) and GFP2G93A (E-I) mice at the symptomatic stage of disease progression. Scale bar 100 µm (A-F) and 20 µm (G-I). While in GFP2 and G93A sections no specific staining is visible (A-D), rare cells from GFP2G93A sections display high levels of GFP (arrows in F-I).

To verify if the observed phenomenon was replicable also in line 1, symptomatic GFP1G93A mice were studied in comparison to GFP1 and G93A littermates. As already highlighted (Fig. 5.3) and shown in Fig. 5.15, in GFP1 sections the reporter protein is visible in various cell populations of the lumbar spinal cord. In GFP1G93A, a stronger GFP signal is noticeable in large cells of the ventral horns, similarly to what observed in GFP2G93A line.

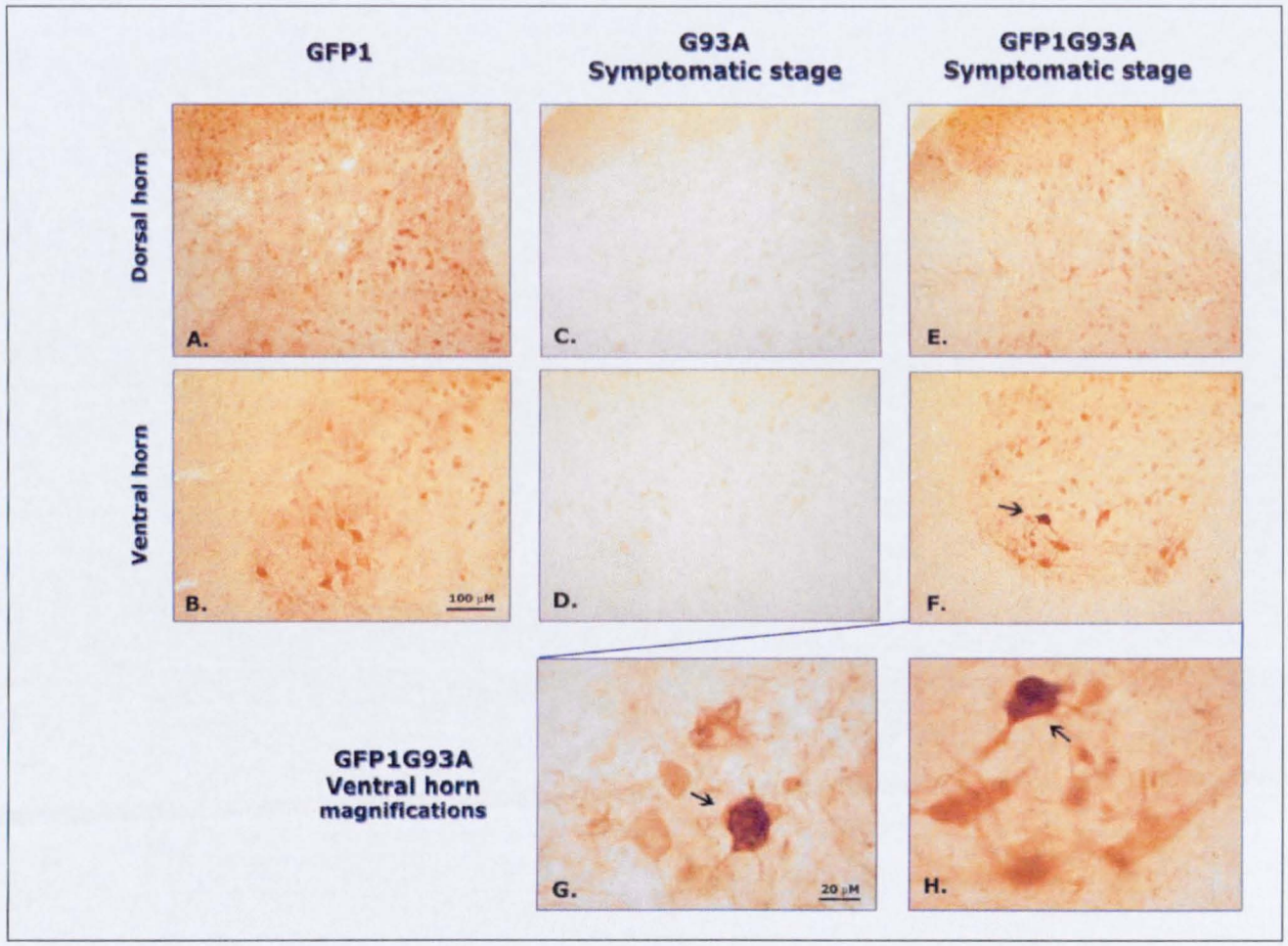

Figure 5.15 Microphotographs of GFP labelling in the dorsal and ventral horns of the lumbar spinal cord of GFP1 (A, B), G93A (C, D) and GFP1G93A (E-H) mice at the symptomatic stage of disease progression. Scale bar 100 µm (A-F) and 20 µm (G, H). G93A sections display no specific GFP staining, while in GFP1 speciments the reporter protein is localized in various cell populations of both the dorsal and the ventral horns. In the ventral horns of GFP1G93A sections some large neurons with an intense GFP staining are observable (arrows in F-H).

5.4.8.2 Co-localization between Ub^{G76V}-GFP staining and neuropathological markers in the lumbar spinal cord of symptomatic GFP2G93A mice

I. GFP and SMI-31 double staining

With the aim to obtain an estimation of the number of damaged neurons that accumulate Ub^{G76V}-GFP, double immunostaining for GFP and SMI-31 was performed on serial sections from symptomatic GFP2G93A lumbar spinal cord as described in the paragraph 4.2.5. SMI-31 antibody specifically labels phosphorylated epitopes of the neurofilaments, whose accumulation in the neuronal cell body is considered as a pathological hallmark. Neuronal cells were identified by the NeuN marker.

The co-localization between NeuN, SMI-31 and GFP is shown in Fig. 5.16. In sections from GFP2 mice, SMI-31 labelling was never found in the neuronal population stained by NeuN; on the contrary, in the ventral horns of both G93A and GFP2G93A spinal cord, some neuronal cells resulted stained with SMI-31 (arrows in Fig. 5.16). In double transgenic mice, a significant fraction of SMI-31-positive cells also displayed an accumulation of Ub^{G76V}-GFP.

The number of the cells stained only for GFP or double stained for GFP and SMI-31 was recorded; the great majority of GFP-positive cells were localized in the ventral horns. In table 5.17A are reported the data obtained analysing the ventral horns of 10 sections for each animal (5 GFP2G93A mice examined). As visible in the graph, about one third of GFP-positive cells is also SMI-31 positive.

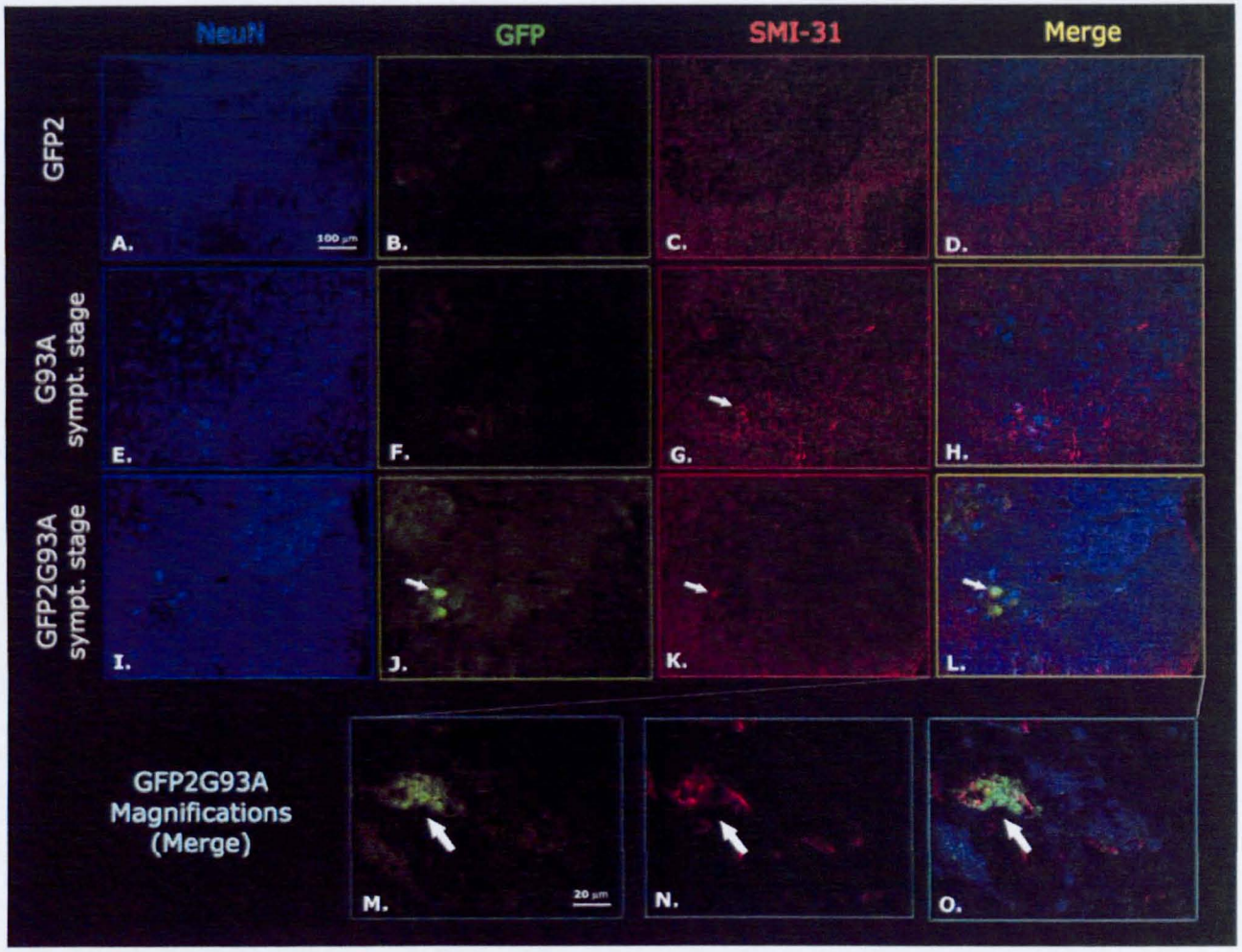

Figure 5.16 Laser scanning confocal microphotographs of NeuN, GFP and SMI-31 in the ventral horn lumbar spinal cord of GFP2 (A-D), G93A (E-H) and GFP2G93A (I-O) mice at the symptomatic stage. Scale bar 100 µm (A-L) and 20 µm (M-O). In G93A, but not in GFP2 sections, SMI-31-positive neurons are detectable (arrow in G). In GFP2G93A sections, some GFP-positive neurons are noticeable (arrow and arrowhead in J); some of these display also SMI-31 accumulation in the cell body (arrows in K-O).

A.

	Mean	S.E.
GFP+/SMI31-	15.7	4.2
GFP+/SMI31+	10.0	3.3

B.

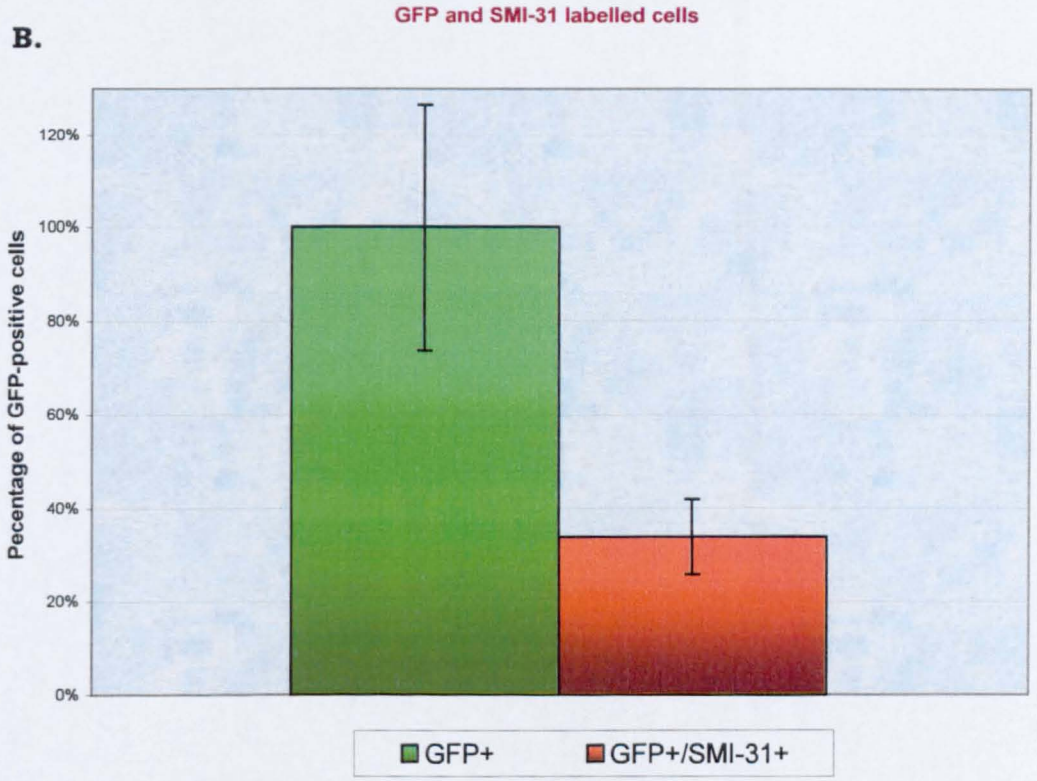

Figure 5.17 Quantitative analysis of SMI-31 labelling in the GFP-positive population of the ventral horns of symptomatic GFP2G93A lumbar spinal cord. In the table A, the mean represents the total count of positive cells in 10 sections for each sample (5 mice analyzed). The graphic B represents, expressed as percentage, the total population of GFP-positive cells (green bar, mean ± S.E. of five mice) and the fraction that is also SMI-31 positive (orange bar, mean ± S.E. of five mice).

II. GFP and ubiquitin double staining

The same approach was applied also for the co-localization between Ub^{G76V}-GFP and ubiquitin (Fig 5.18). In GFP2 mice, the staining for ubiquitin resulted low and uniformly distributed in the neurons of the ventral horns, while in symptomatic G93A mice ubiquitin-positive spots were noticeable. In GFP2G93A mice, GFP-positive cells frequently displayed also ubiquitin accumulation.

The number of cells stained only for GFP or double stained for GFP and ubiquitin was recorded. In Fig. 5.19 A are reported the data obtained analysing the ventral horns of 10 sections for each sample (5 GFP2G93A mice examined). As shown in the graph (Fig 5.19 B), about a half of GFP-positive cells showed also intense ubiquitin staining.

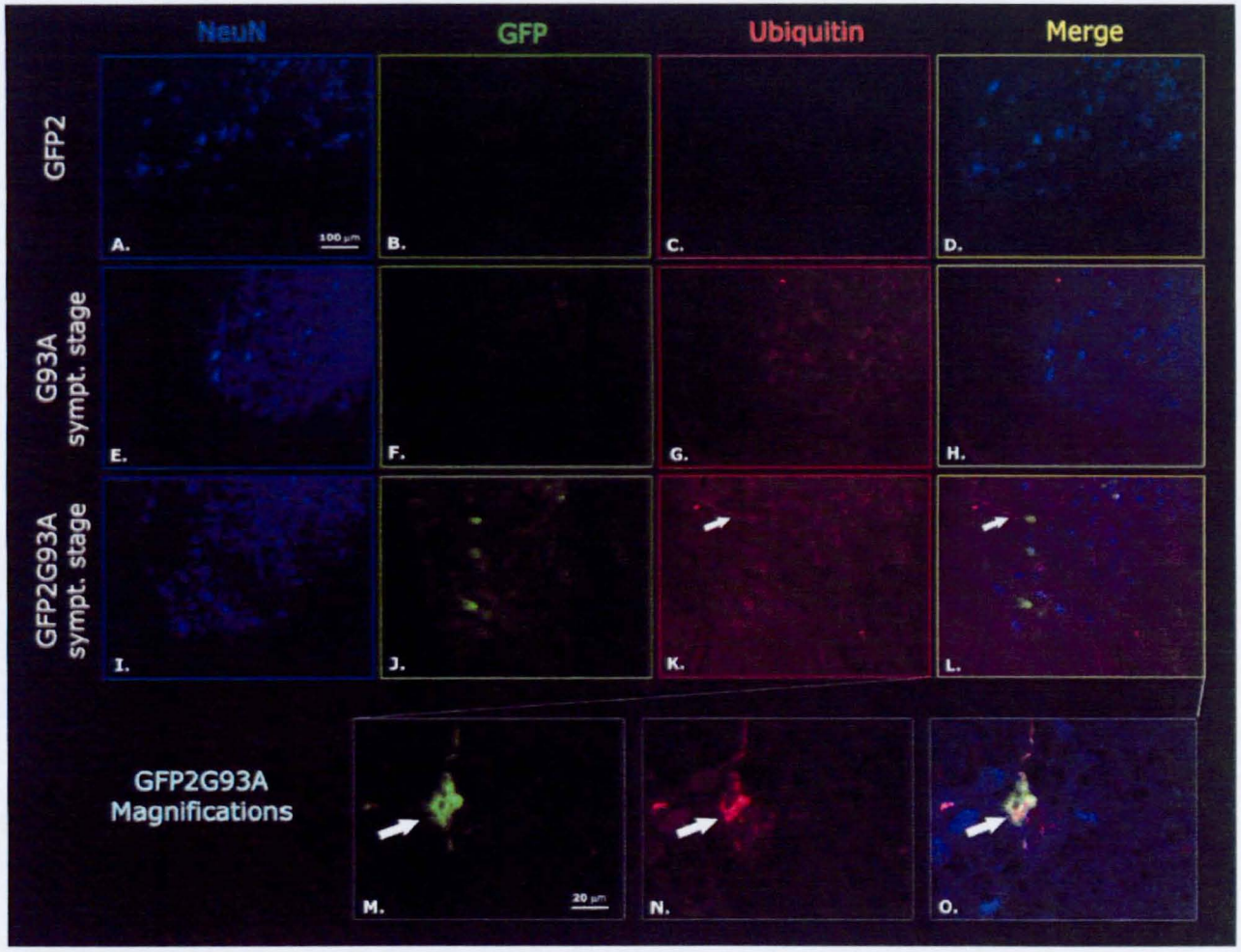

Figure 5.18 Laser scanning confocal microphotographs of NeuN, GFP and ubiquitin in the ventral horn lumbar spinal cord of GFP2 (A-D), G93A (E-H) and GFP2G93A (I-O) mice at the symptomatic stage. Scale bar 100 μm (A-L) and 20 μm (M-O). Ubiquitin-positive spots are noticeable in G93A and GFP2G93A sections (G, K), while are absent in GFP2 speciments (C). In GFP2G93A samples, GFP-positive cells frequently display an intense ubiquitin staining (arrows K-O).

A.

	Mean	S.E.
GFP+/Ubiquitin-	12.6	4.0
GFP+/Ubiquitin+	14.3	5.2

B.

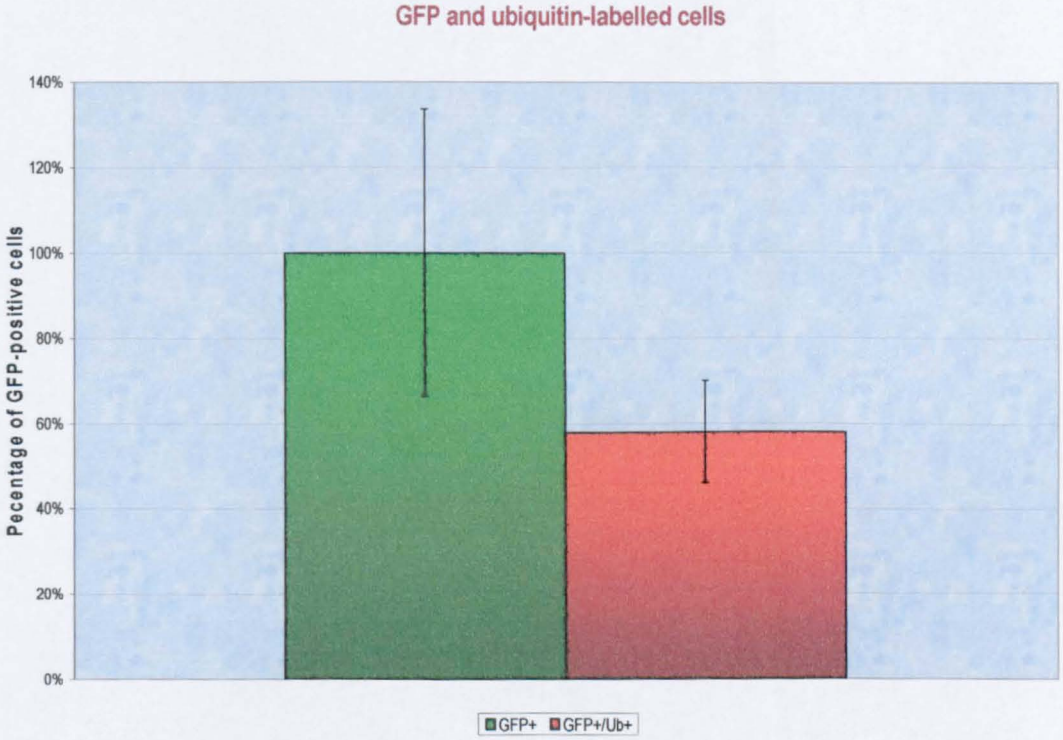

Figure 5.19 Quantitative analysis of ubiquitin labelling in the GFP-positive population of the ventral horns of symptomatic GFP2G93A lumbar spinal cord. In the table A, the mean represents the total count of positive cells in 10 sections for each sample (5 mice analyzed). The graphic B represents, expressed as percentage, the total population of GFP-positive cells (green bar, mean ± S.E. of five mice) and the fraction that is also ubiquitin-positive (orange bar, mean ± S.E. of five mice).

5.4.8.3. Analysis of CHOP staining in the spinal cord of G93A and double transgenic mice

As reported in the introduction, it has been shown that a situation of ER stress can determine subtle alterations in UPP functionality. For this reason, it was assessed if the accumulation of Ub^{G76V}-GFP in the spinal cord of symptomatic double transgenic mice correlated with the up-regulation of CHOP, a marker of ER stress.

I. Immunohistochemical analysis of CHOP distribution in the lumbar spinal cord of G93A mice during disease progression

Initially, the induction of CHOP was analyzed in the spinal cord of G93A mice at the pre-symptomatic, symptomatic and end stage. As shown in Fig. 5.20, CHOP expression is very low in NTg mice. On the contrary, in G93A mice, already at the pre-symptomatic phase is evident the presence of large cells, localized in the ventral horns, with intense CHOP staining in the nucleus. CHOP-positive cells with similar features are found more frequently in symptomatic mice; finally, at the end stage, also some smaller cells of the dorsal horns display CHOP-positive nucleus.

The results of the DAB staining were confirmed with the immunofluorescence techniques (Fig 5.21), that highlighted an intense CHOP labelling in the nucleus of large NeuN-positive cells localized in the ventral horns of G93A sections.

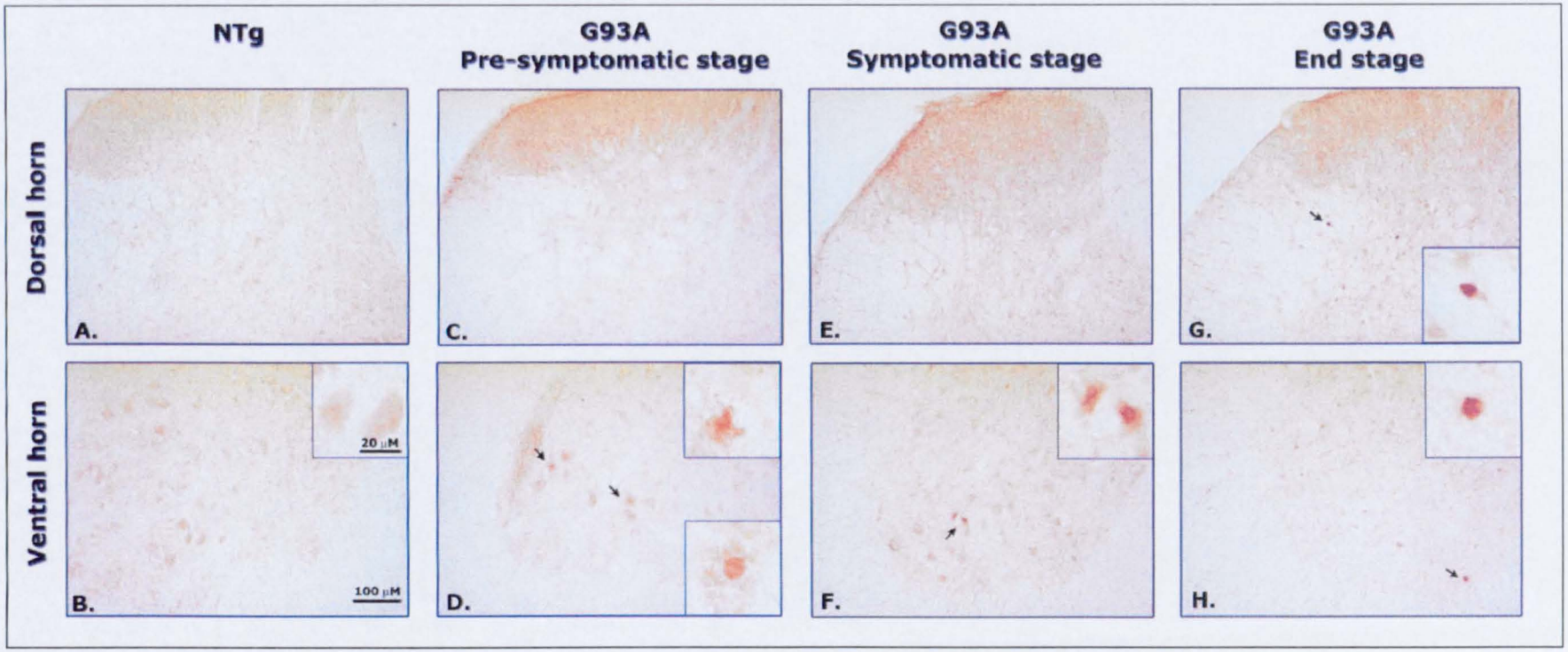

Figure 5.20 Microphotographs of CHOP labelling in the dorsal and ventral horns of the lumbar spinal cord of NTg (A, B) and G93A mice at the pre-symptomatic (C, D), symptomatic (E, F) and end stage (G, H) of the disease. Scale bar 100 µm, insets 20 µm. CHOP labelling is weak in the neurons of NTg sections, while an intense staining is visible in the nucleous of ventral horn neurons in pre-symptomatic and symptomatic G93A samples (arrows in D, F). At the end stage, CHOP-positive cells are noticeable both in the ventral andf dorsal horns (arrows in G, H).

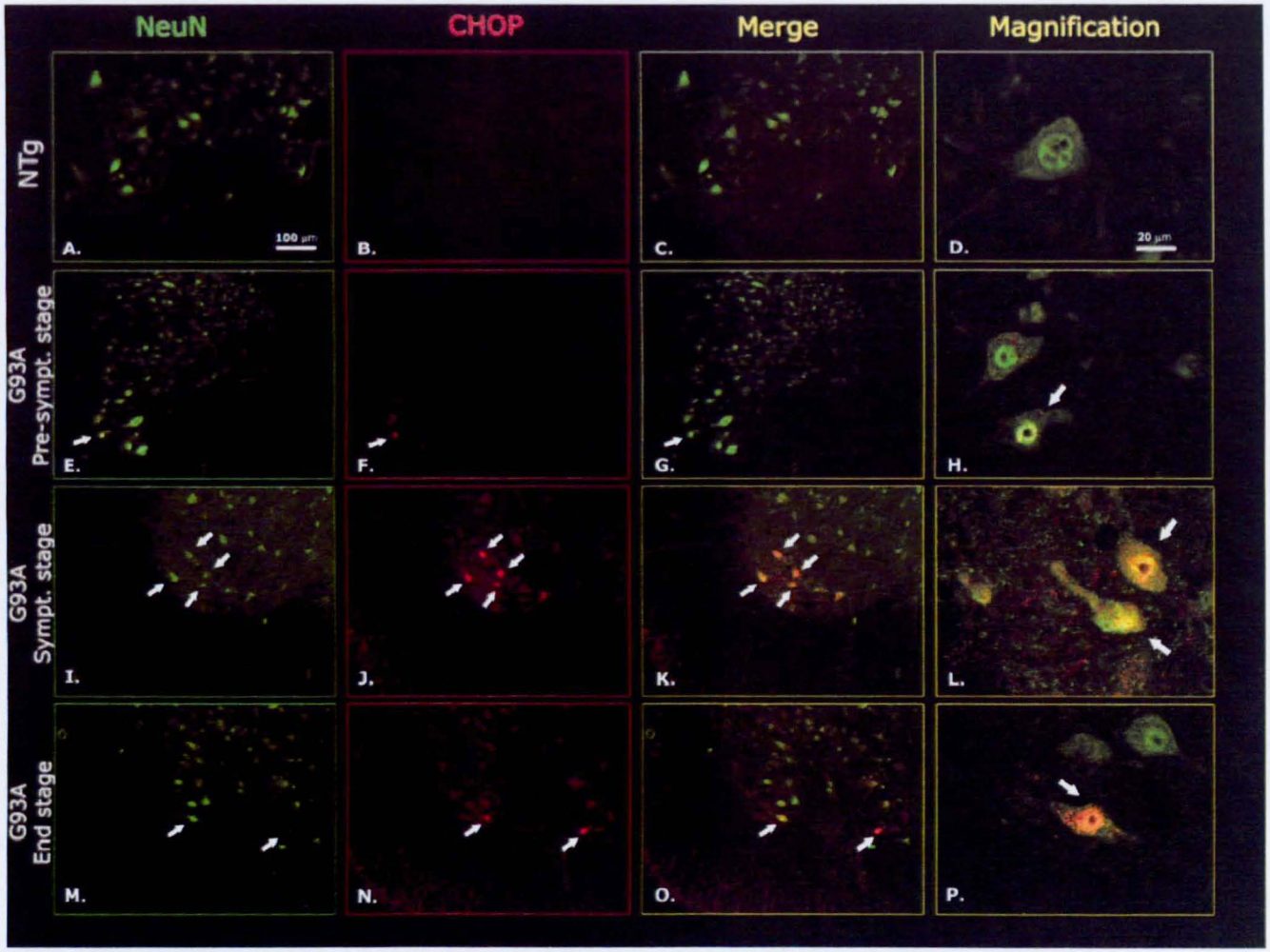

Figure 5.21 Laser scanning confocal microphotographs of NeuN and CHOP in the ventral horn lumbar spinal cord of NTg (A-D) and G93A mice at the pre-symptomatic (E-H), symptomatic (I-L) and end stage (M-P) of the disease. Scale bar 100 µm (A-C, E-G, I-K, M-O) and 20 µm (D, H, L, P). Some large neurons in the ventral horn of G93A mice at various stages of disease progression present an intense CHOP staining in the nucleous (arrows in E-P).

II. Co-localization between CHOP and Ub^{G76V}-GFP in the lumbar spinal cord of symptomatic GFP1G93A mice

Double staining for GFP and CHOP was performed on the lumbar spinal cord of symptomatic GFP1G93A mice in order to understand if the accumulation of the reporter protein correlates with signs of ER stress. For this experiment, GFP1 line was chosen for a technical reason, that is the possibility to detect Ub^{G76V}-GFP signal using a secondary fluorescent antibody; this permitted to reveal the CHOP signal using the tyramide amplification.

As shown in the Fig. 5.22, in GFP1G93A sections the majority of CHOP-positive cells does not present increased levels of Ub^{G76V}-GFP and, reciprocally, the cells with augmented GFP are not CHOP-positive.

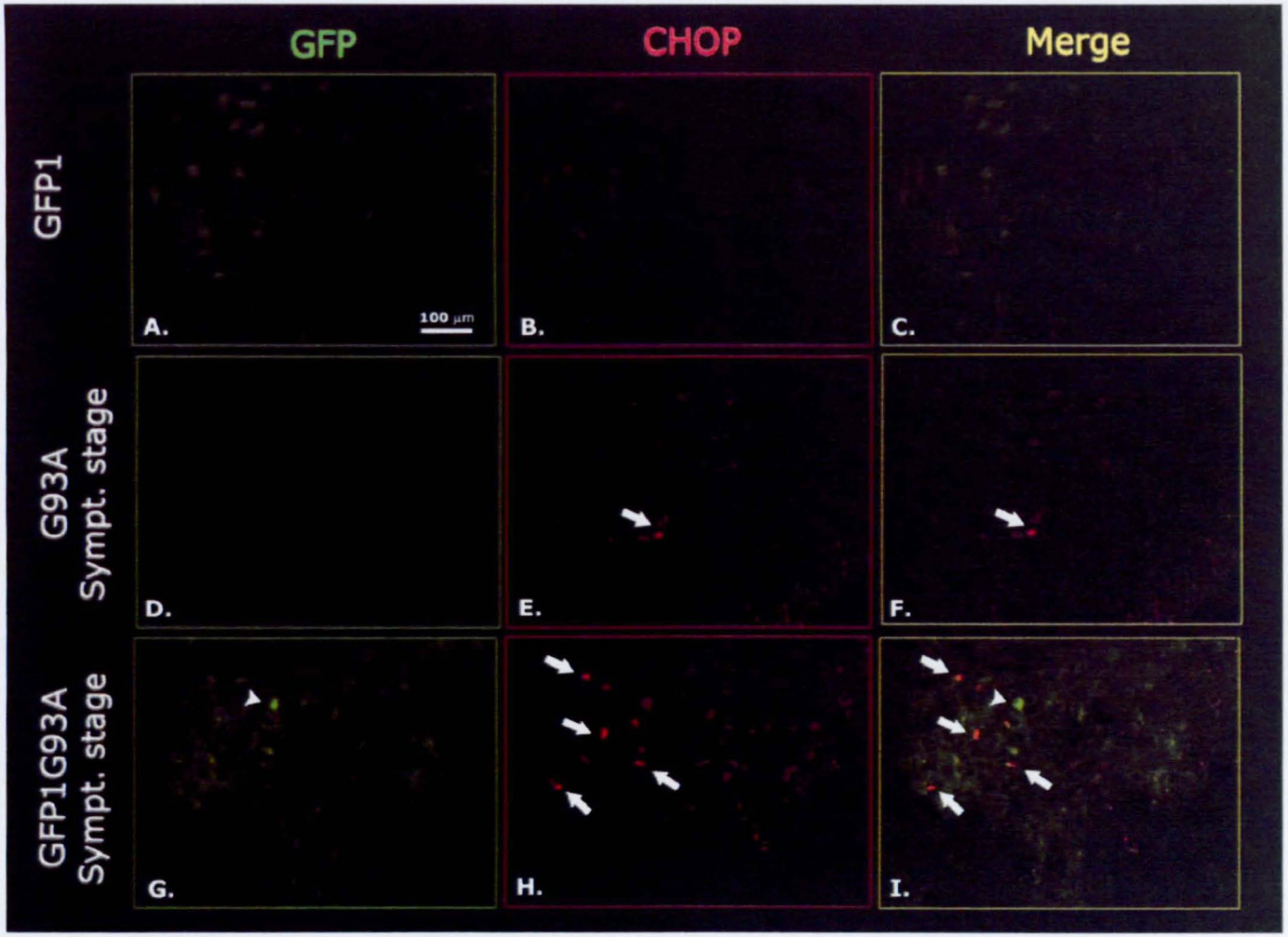

Figure 5.22 Laser scanning confocal microphotographs of GFP and CHOP in the ventral horn lumbar spinal cord of GFP1 (A-C), G93A (D-F) and GFP1G93A (G-I) mice at the symptomatic stage. Scale bar 100 µm. In the ventral horns of both G93A and GFP1G93A spinal cord, some cells with an intense CHOP-positive nucleous are noticeable (arrows in E, H). In double transgenic sections, CHOP and GFP stainings do not co-localize (arrows and arrowheads in I).

5.4.9 Immunohistochemical analysis of the spinal cord of end stage double transgenic mice

The levels of the reporter protein were examined by immunohistochemistry also in sections from end stage double transgenic mice.

5.4.9.1. Immunohistochemical analysis of Ub^{G76V}-GFP in end stage GFP1G93A and GFP2G93A lumbar spinal cord

DAB staining for GFP was performed on sections from the lumbar spinal cord of end stage GFP2G93A mice and GFP2 and G93A littermates. Some cells with stronger GFP labelling were detected in double transgenic mice; these cells were localized in the grey matter of the dorsal and the ventral horns and showed a neuronal-like morphology, with a size that, in the majority of cases, seemed lower than motor neurons (Fig. 5.23).

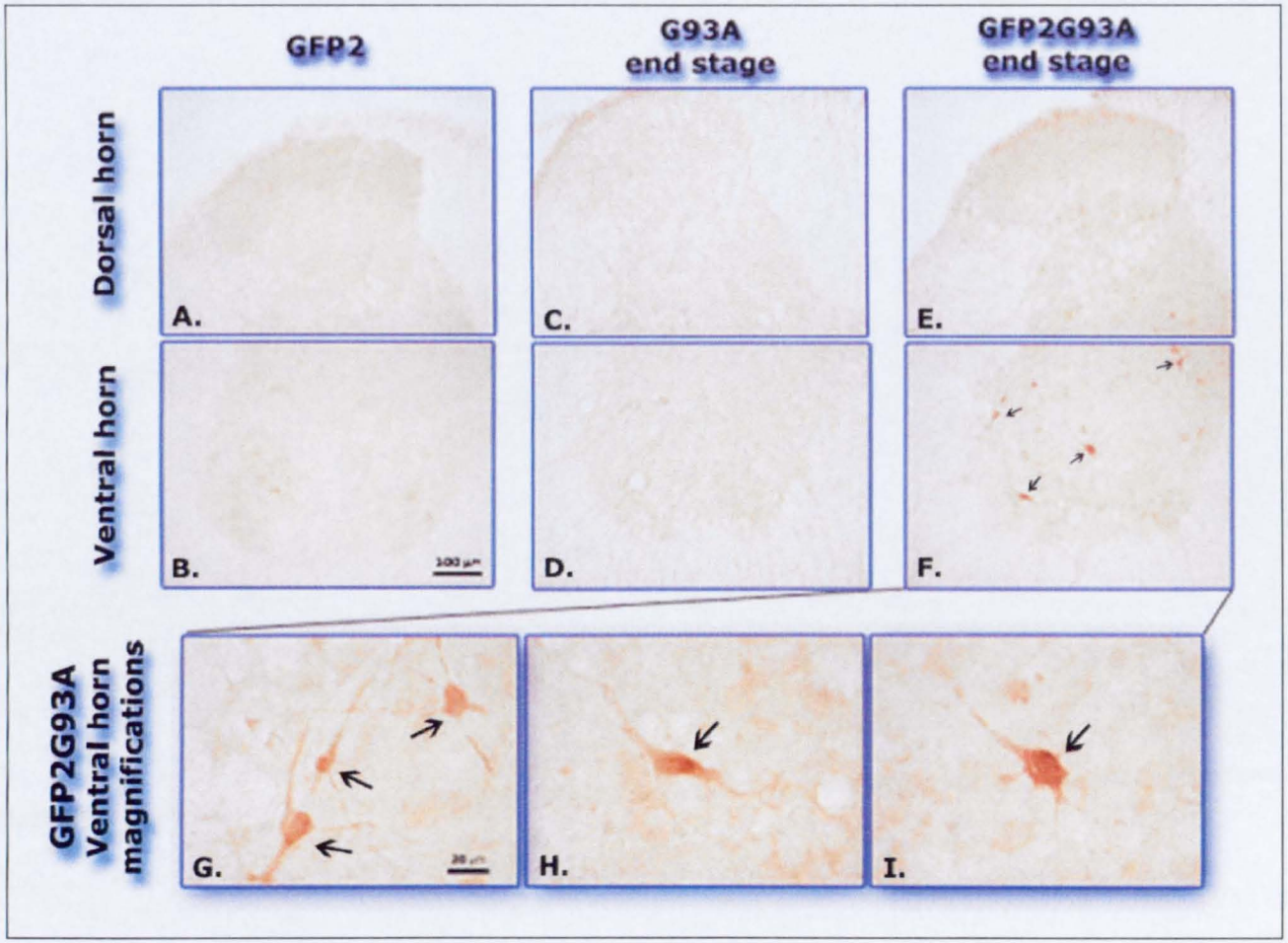

Figure 5.23 Microphotographs of GFP labelling in the dorsal and ventral horns of the lumbar spinal cord of GFP2 (A, B), G93A (C. D) and GFP2G93A (E-I) mice at the end stage of disease progression. Scale bar 100 μm (A-F), and 20 μm (G-I). GFP2 and G93A sections do not present GFP-positive cells. On the contrary, GFP2G93A samples reveal high levels of GFP in neuronal-like cells of the ventral and intermediate region of the gray matter (arrows in F-I).

To prove if the observed phenomenon was present also in the other transgenic line, the lumbar spinal cord of end stage GFP1G93A mice was also analyzed in comparison to age-matched GFP1 and G93A mice. Like in GFP2G93A mice, also in GFP1G93A ones cells with increased levels of Ub^{G76V}-GFP were found; the morphology of these cells was similar to those observed in GFP2G93A mice (Fig. 5.24).

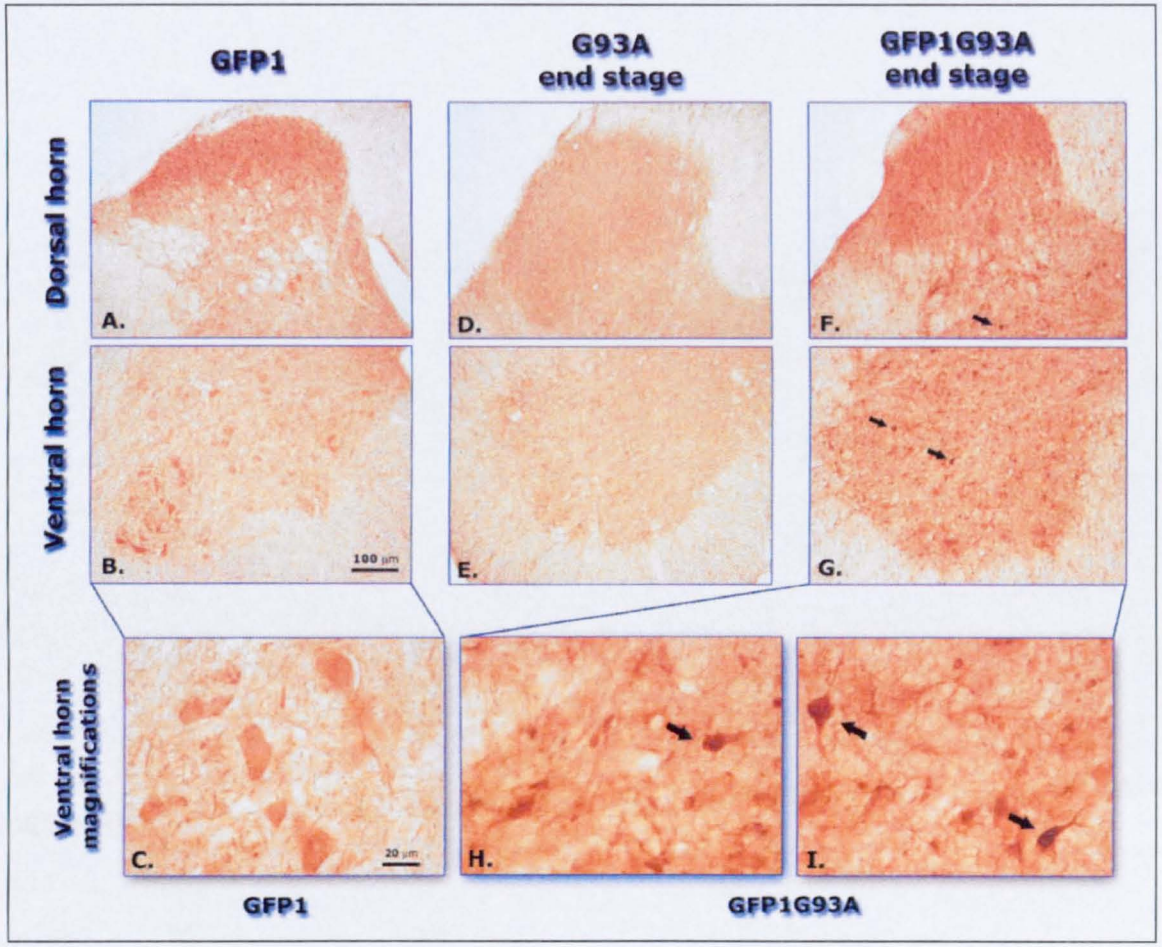

Figure 5.24 Microphotographs of GFP labelling in the dorsal and ventral horns of the lumbar spinal cord of GFP1 (A-C), G93A (D, E) and GFP1G93A (F-I) mice at the end stage of disease progression. Scale bar 100 µm (A, B, D, E, F, G) and 20 µm (C, H, I). G93A sections display no GFP staining, while in GFP1 speciments the reporter protein is present in the neuronal population of the spinal cord. In GFP1G93A sections, some small cells with an intense GFP labelling are localized both in the ventral and the dorsal horns (arrows in F-I).

5.4.9.2. Analysis of the distribution of Ub^{G76V}-GFP in the cell populations of the lumbar spinal cord of end stage GFP2G93A mice

In order to describe better the cell types showing the rise of Ub^{G76V}-GFP, double immunofluorescence experiments followed by confocal microscopy analysis were performed in the spinal cord of end stage GFP2G93A mice.

I. GFP and ChAT double staining

To examine the levels of the reporter protein in the vulnerable cell population, a double staining for GFP and the motor neuronal marker choline acetyl transferase (ChAT) was performed. As shown in Fig. 5.25, the motor neurons display differential levels of Ub^{G76V}-GFP, with only rare cells showing high quantities of the reporter protein. The majority of GFP-positive cells are not ChAT-positive, indicating that, among the cells with accumulation of Ub^{G76V}-GFP, only few motor neurons are present.

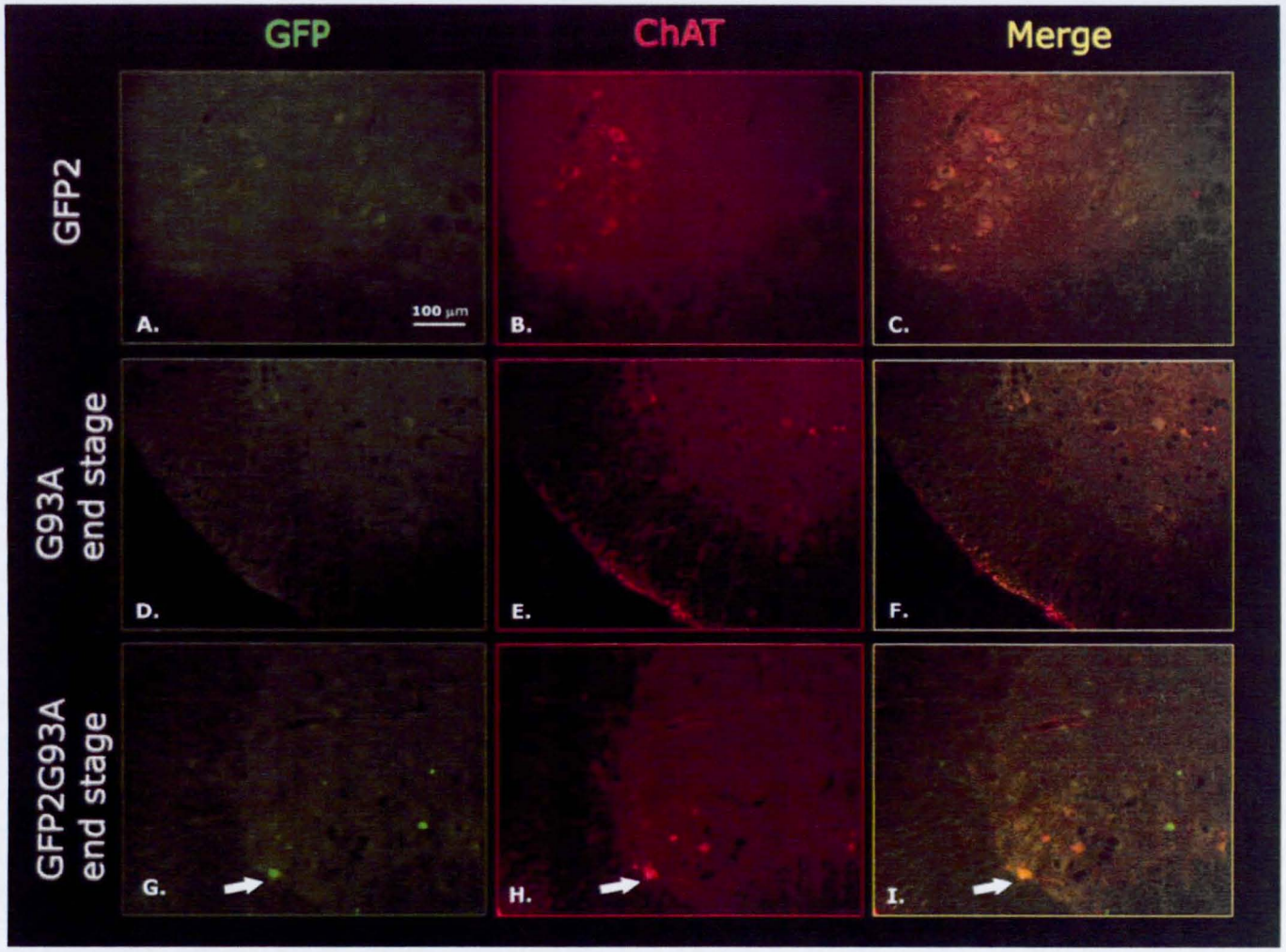

Figure 5.25 Laser scanning confocal microphotographs of ChAT and GFP in the ventral horn lumbar spinal cord of GFP2 (A-C), G93A (D-F) and GFP2G93A (G-I) mice at the end stage of disease progression. Scale bar 100 µm. GFP staining is not visible in the ChAT-positive population of GFP2 and G93A sections. In GFP2G93A samples, GFP accumulation occurs in some ChAT-positive motor neurons (arrows in G-I).

II. GFP and calretinin double staining

In order to verify if increased levels of Ub^{G76V}-GFP are detectable in other neuronal populations besides motor neurons, a double staining for GFP and calretinin was performed. Calretinin is a calcium-binding protein that specifically labels a sub-population of spinal interneurons.

As visible in Fig. 5.26, Ub^{G76V}-GFP accumulation occurs in some calretinin-positive interneurons; however, some GFP-positive cells do not co-localize with the calretinin staining.

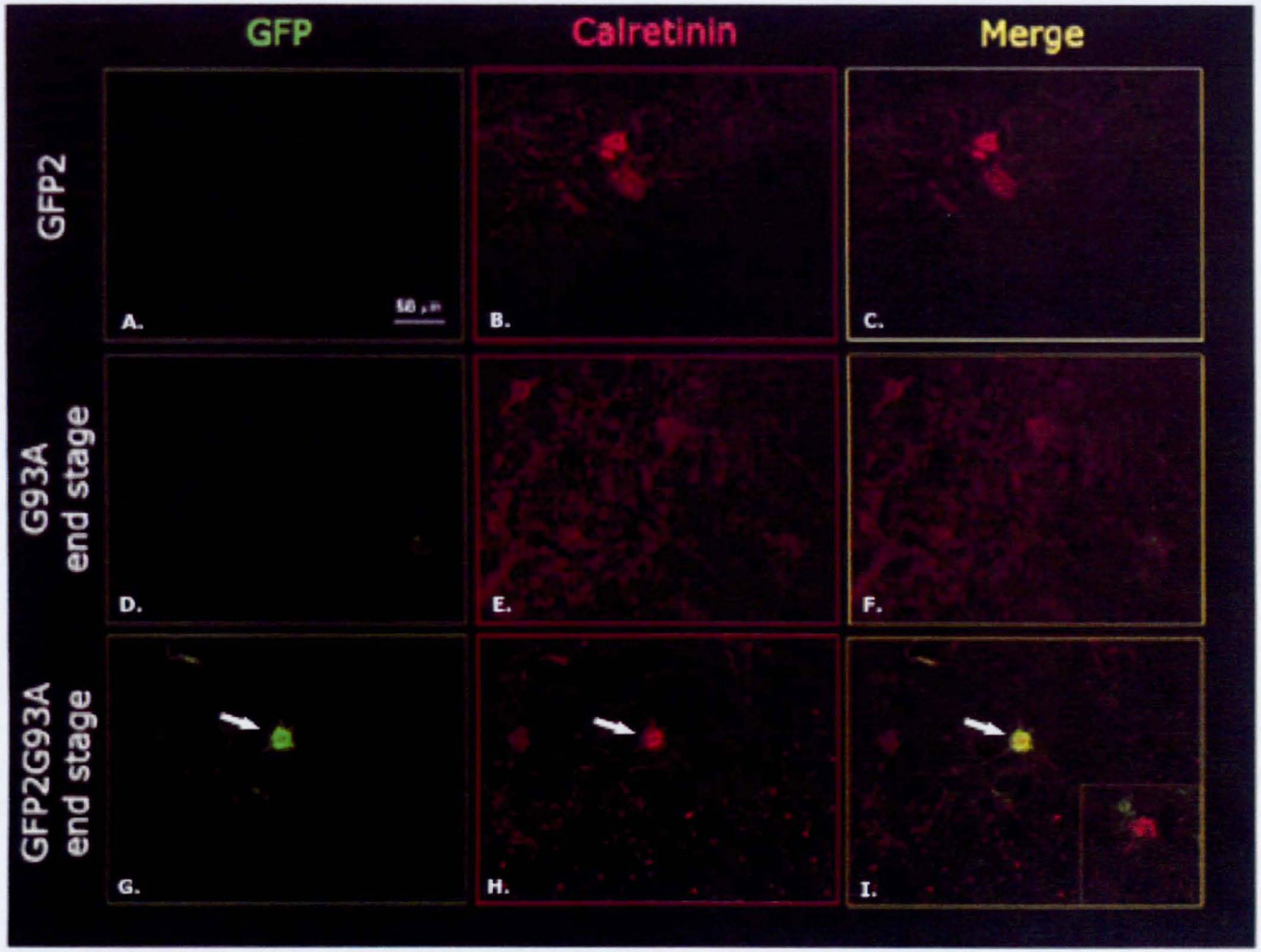

Figure 5.26 Laser scanning confocal microphotographs of calretinin and GFP in the ventral horn lumbar spinal cord of GFP2 (A-C), G93A (D-F) and GFP2G93A (G-I) mice at the end stage of disease progression. Scale bar 50 μm. Differentially from GFP2 and G93A samples, in GFP2 sections some calretinin-positive neurons display high levels of GFP staining (arrows in G-.I).

III. GFP and GFAP double staining

Since in G93A mice at the advanced stage of motor neuron degeneration both astrocytes and microglial cells are strongly activated, the levels of Ub^{G76V}-GFP were examined also in the glial population. Fig. 5.27 shows the immunofluorescent staining for GFP and for the glial fibrillary acidic protein (GFAP), which specifically labels the astrocytes. In the spinal cord of GFP2 mice, GFAP immunoreactivity is weak, while in G93A and GFP2G93A mice astrocytes become hypertrophic and intensely immunostained, a sign of their activation. However, no co-localization between GFP and GFAP was observed.

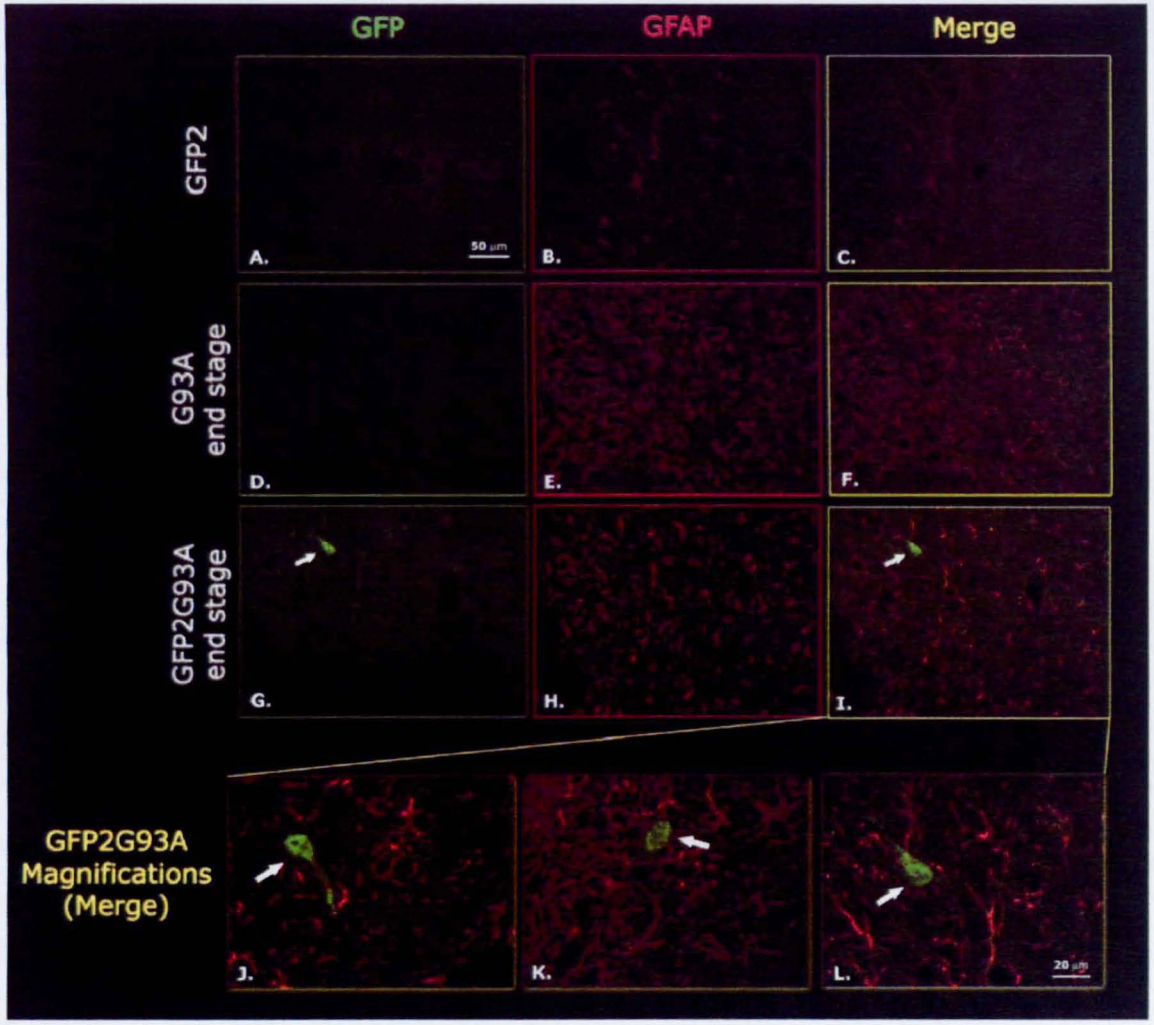

Figure 5.27: Laser scanning confocal microphotographs of GFAP and GFP in ventral horn lumbar spinal cord of GFP2 (A-C), G93A (D-F) and GFP2G93A (G-L) mice at the end stage of disease progression. Scale bar 50 μm (A-I) and 20 μm (J-L). GFP labelling reveals the proliferation and hypertrophy of the astrocytic population in the spinal cord of G93A and GFP2G93A mice (E, F, H, I). In GFP2G93A sections some neuronal-like GFP-positive cells are noticeable (arrows in G, I, J-L) while no co-localization between GFP and GFAP is observed (I-L).

IV. GFP and CD11β double staining

A remarkable increase of reactive microglial cells detected by the anti-CD11β antibody was also found in the sections from end stage G93A and GFP2G93A mice, but GFP immunoreactivity was never localised inside this cell population (Fig. 5.28).

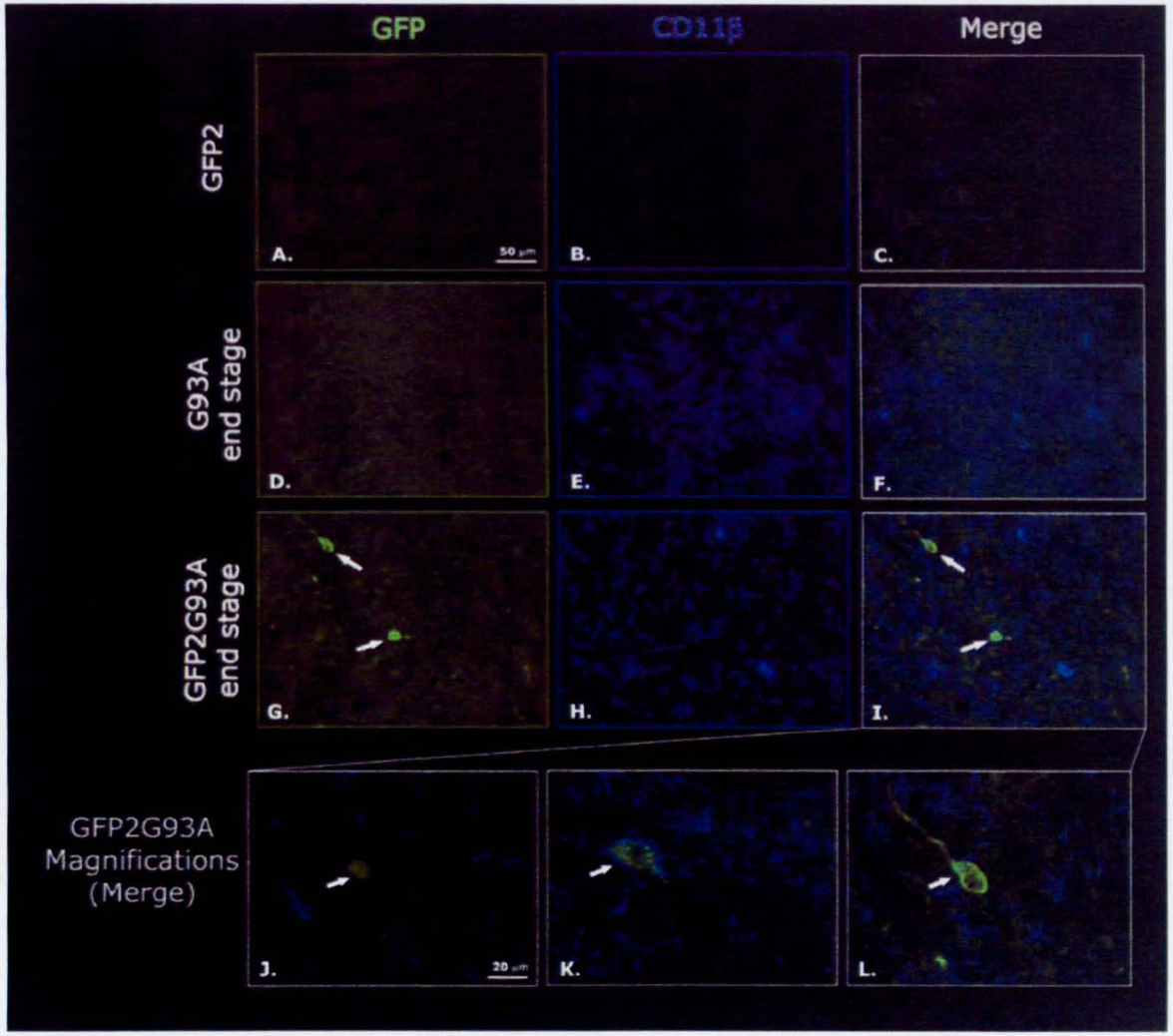

Figure 5.28 Laser scanning confocal microphotographs of CD11β and GFP in the ventral horn lumbar spinal cord of GFP2 (A-C), G93A (D-F) and GFP2G93A (G-L) mice at the end stage of disease progression. Scale bar 50 μm (A-I) and 20 μm (J-L). CD11β labelling reveals a strong activation of the microglial population in G93A (E-F) and GFP2G93A (H-I) samples. In GFP2G93A sections, GFP staining is localized inside small neuronal-like cells (arrows in G, I, J-L) and does not co-localize with CD11β.

V. GFP and ubiquitin double staining

To verify whether the cells with increased Ub^{G76V}-GFP undergo a general accumulation of ubiquitinated proteins, a double labelling for ubiquitin and GFP was performed. Large spots of ubiquitin deposits are noticeable in the sections of G93A and GFP2G93A samples (Fig. 5.29). In double transgenic mice, most of the GFP-positive cells display high levels of ubiquitin.

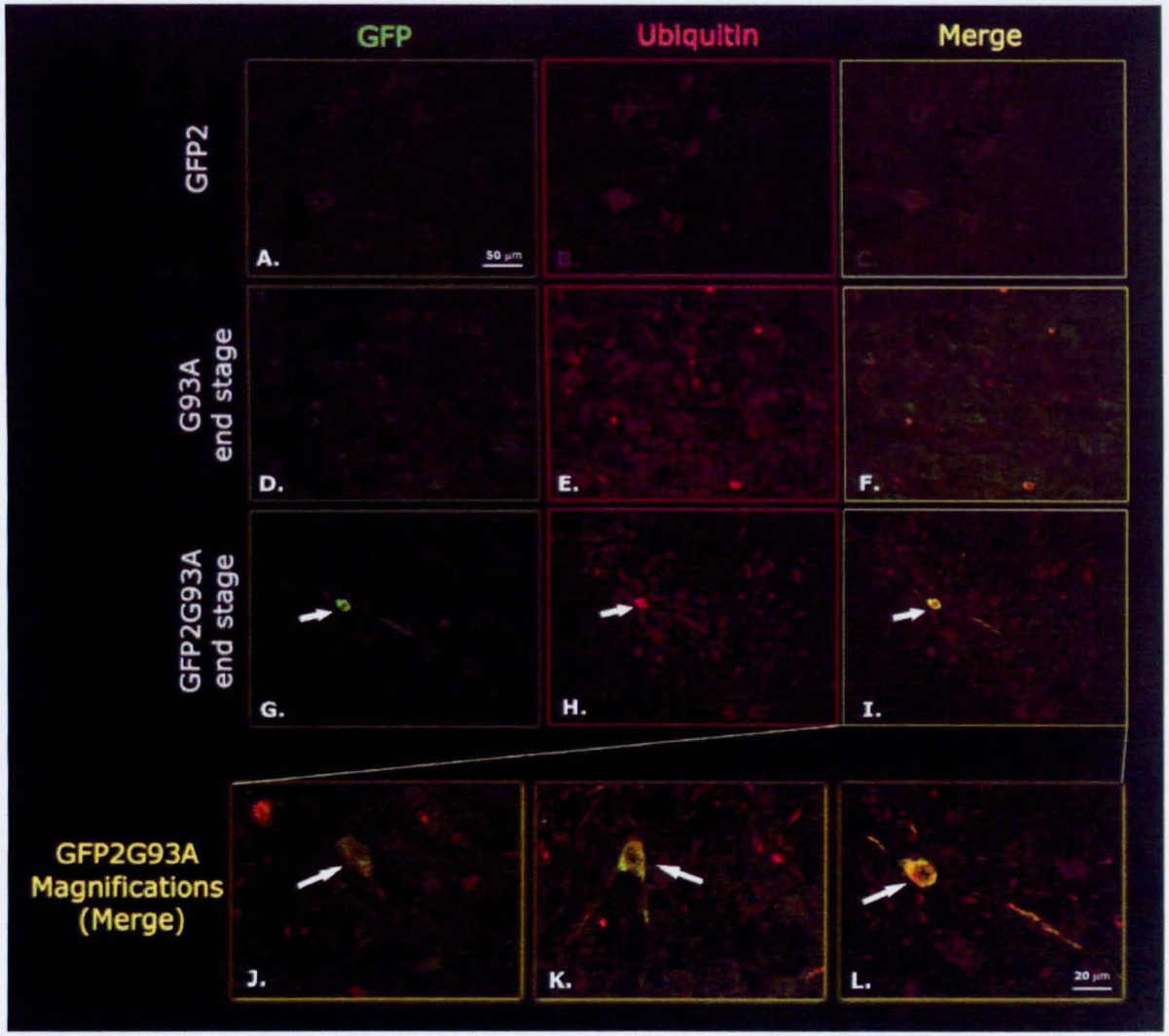

Figure 5.29 Laser scanning confocal microphotographs of GFP and ubiquitin in the ventral horn lumbar spinal cord of GFP2 (A-C), G93A (D-F) and GFP2G93A (G-I) mice at the end stage of disease progression. Scale bar 50 µm (A-I) and 20 µm (J-L). Ubiquitin-positive spots are easily noticeable in G93A and GFP2G93A sections (E, F, H-L). In double transgenic samples, ubiquitin accumulation is visible in GFP-positive cells (arrows in G-L).

5.4.10 Immunohistochemical analysis of Ub^{G76V}-GFP in the brain of GFP2G93A mice

To evaluate whether the accumulation of the reporter protein was restricted to the lumbar spinal cord or involved also other areas of the CNS, the brain of double transgenic mice was analyzed at various phases of disease progression.

I. Pre-symptomatic GFP2G93A mice

DAB staining for GFP in the brain of pre-symptomatic GFP2G93A did not reveal any difference in comparison to GFP2 or G93A mice.

II. Symptomatic GFP2G93A mice

Also in the brain of symptomatic GFP2G93A mice, no GFP signal was revealed (Fig. 5.30). Only in one sample out of five, rare GFP-positive cells were found in the brainstem.

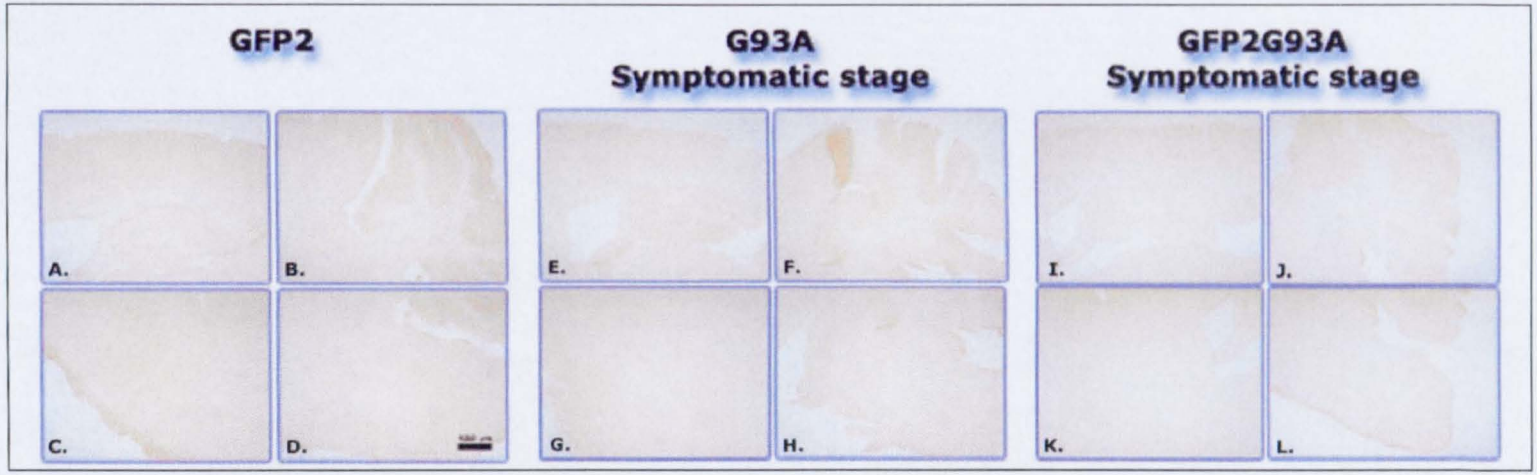

Figure 5.30: Microphotographs of GFP labelling in the brain of GFP2 (A-D), G93A (E-H) and GFP2G93A (I-L) mice at the symptomatic stage of the disease. Scale bar 500 μm. No specific GFP staining is visible in GFP2, G93A and GFP2G93A brain sections.

III. End stage GFP2G93A mice

Analyzing the brain of GFP2G93A mice at the end stage of disease progression, the levels of the reporter protein were found undetectable in most of the regions. However, a stronger signal was clearly visible in the brainstem, where it was particularly evident in neuronal-like small cells of the nuclei trigemini and facialis (Fig. 5.31).

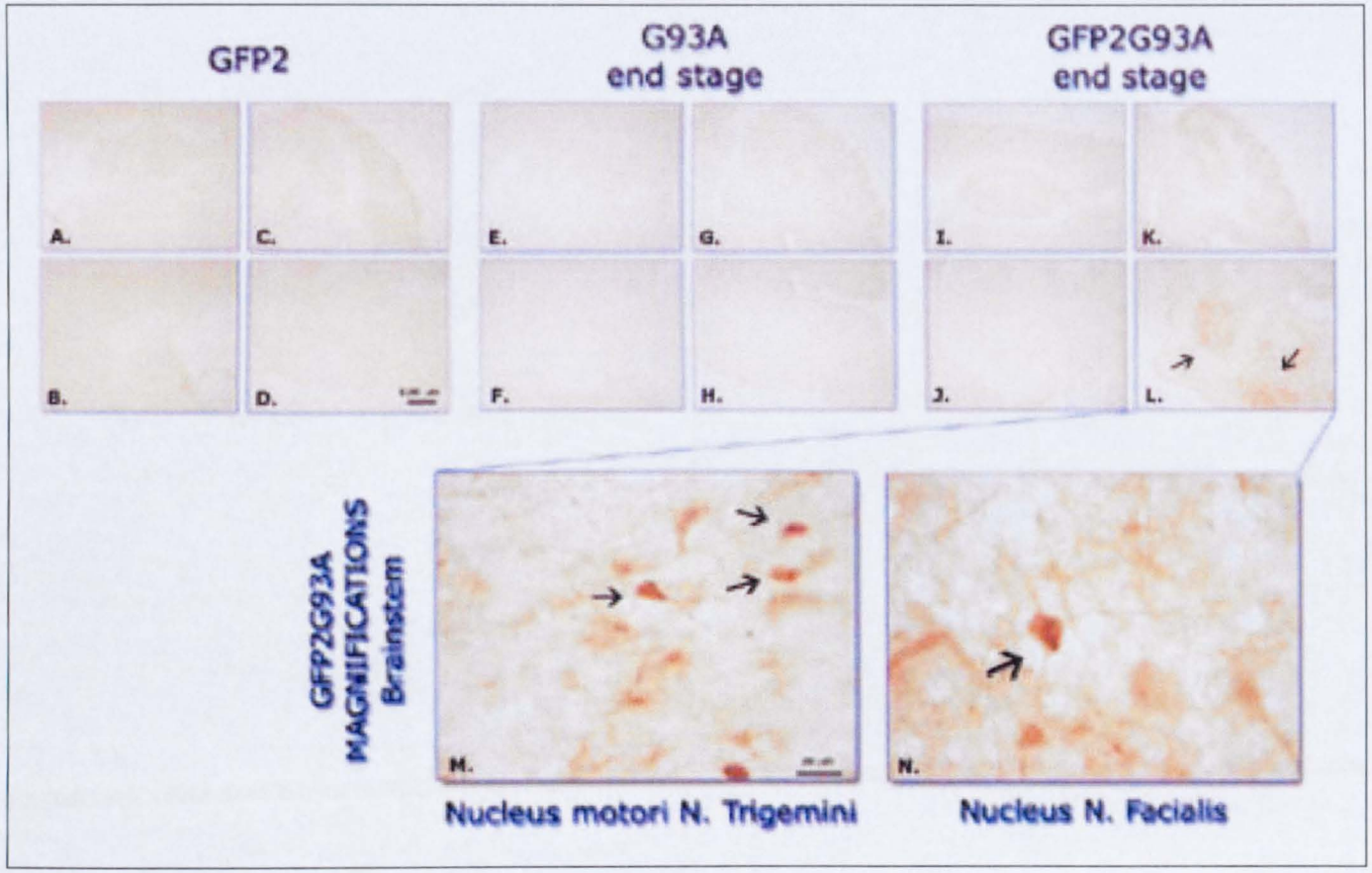

Figure 5.31: Microphotographs of GFP labelling in the brain of GFP2 (A-D), G93A (E-H) and GFP2G93A (I-N) mice at the end stage of disease progression. Scale bar 500 μm (A-L) and 20 μm (M, N). The GFP signal is not detectable in the brain of GFP2 and G93A mice, while GFP-positive cells are present in the brainstem of GFP2G93A sections (arrows in L-N).

5.4.11 Measurement of Ub^{G76V}-GFP transcript in double transgenic mice

5.4.11.1 Real-time PCR experiments

For changes in Ub^{G76V}-GFP protein levels to be an accurate measure of UPP activity, alterations in protein production must be minimal relative to those in protein degradation; for this reason, experiments were performed in order to evaluate the levels of Ub^{G76V}-GFP transcript by real time PCR. Real-time PCR data on the lumbar spinal cord and hippocampus of GFPG93A mice in comparison with GFP littermates are reported in Fig. 5.32.

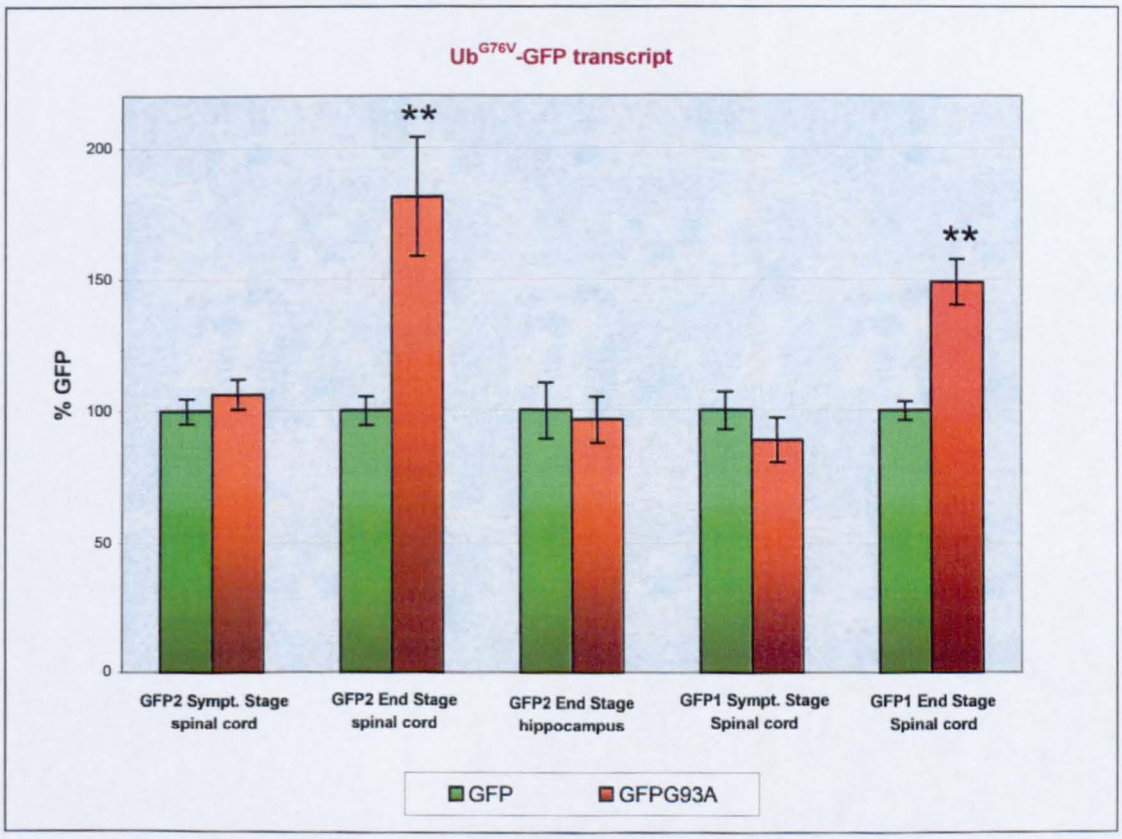

Figure 5.32 Real-time PCR for Ub^{G76V}-GFP transcript in the lumbar spinal cord and hippocampus of GFPG93A mice and GFP littermates at the symptomatic or end stage of disease progression. Data were normalized versus β-actin and expressed as percentage of the value of the GFP. Each histogram shows the mean ± S.E. of at least five mice. Data were analyzed by Student's t-test (** $p<0.01$ compared to GFP).

At the symptomatic stage, no differences were detected between GFP and double transgenic mice in both GFP1 and GFP2 line; on the contrary, at the end stage in the spinal cord of both GFP2G93A and GFP1G93A mice, Ub^{G76V}-GFP transcript resulted significantly increased in respect to GFP littermates. The phenomenon was restricted to the pathological area, since no changes were detected in the hippocampus.

5.4.11.2 In situ hybridization experiments

Real time PCR revealed an increase of Ub^{G76V}-GFP mRNA in double transgenic mice at the end stage and no changes at the symptomatic phase. However, in order to evaluate the quantity of the transcript at the cellular level, an *in situ* hybridization approach was employed.

In Fig. 5.33 are shown representative images of sections from NTg, GFP2 and GFP2G93A mice in which the *in situ* hybridization for GFP was performed. A clear accumulation of grains, higher than the background signal visible in NTg, is noticeable in the cells of GFP2 and GFP2G93A samples, indicating the specificity of the probe for the Ub^{G76V}-GFP mRNA.

The graph (Fig. 5.34) reports the levels of Ub^{G76V}-GFP transcript, quantify as grain density, localized in small (100-250 μm^2 of area) and large cells (>250 μm^2 of area, that could be in part considered as large motor neurons) of the ventral horn in the lumbar spinal cord of GFP2G93A mice compared with GFP2 littermates. At the symptomatic phase, no significant rise of the transcript was noticeable in the large cells of GFP2G93A mice, while augmented levels were detected in the small cells. At the end stage, the density of silver grains resulted significantly increased in both small and large cells; moreover, it was registered a relevant increase in the number of small cells, probably glia, with a signal higher than the background.

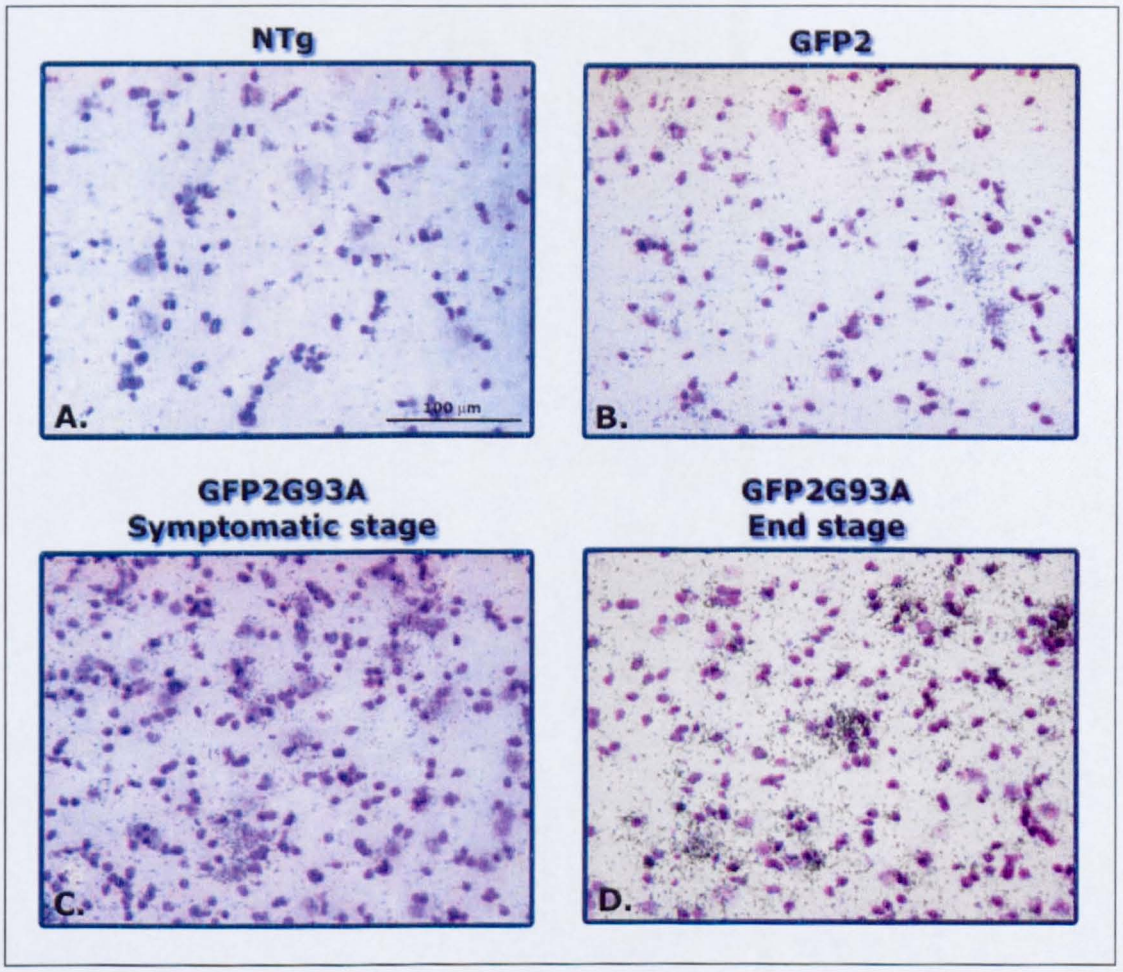

Figure 5.33 Microphotographs of ISH for Ub^{G76V}-GFP on sections from the lumbar spinal cord of NTg (A), GFP2 (B) and GFP2G93A mice at the symptomatic (C) or end stage (D) of the disease.

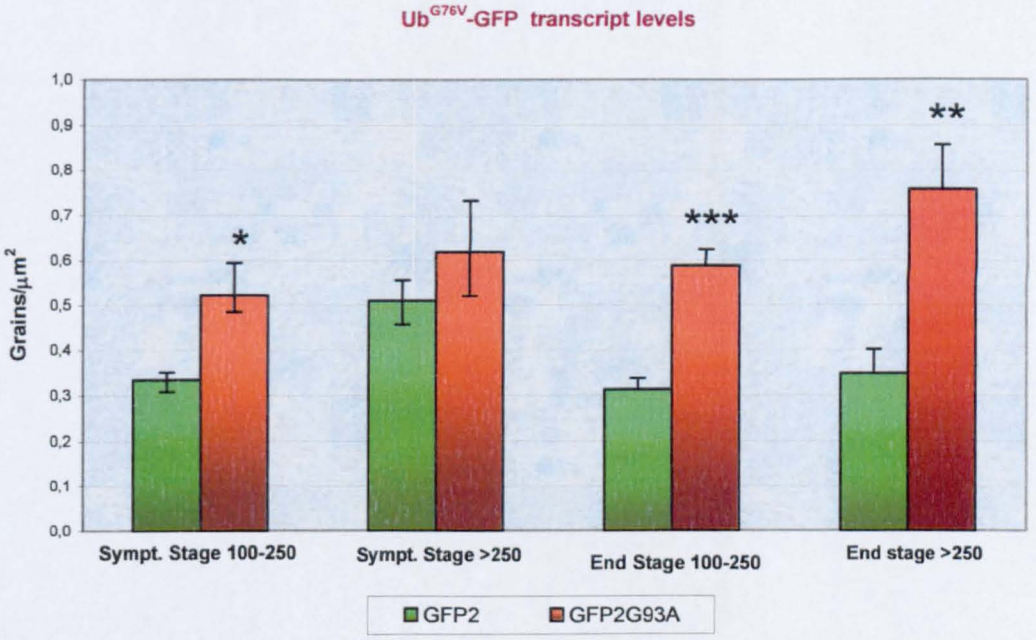

Figure 5.34 Quantification of the grain density in cells from the ventral horn lumbar spinal cord of GFP2 and GFP2G93A mice at the symptomatic or end stage of the disease. Each histogram shows the mean ± S.E. of five mice. Data were analyzed by Student's t-test (* $p<0.05$, ** $p<0.01$, *** $p<0.001$ compared to GFP).

To visualize better the population of cells in respect to the measured grain density, the data are represented also as frequency of cells with increasing values of grain density (Fig. 5.35, 5.36, 5.37, 5.38). At the end stage, as well as for small cells at the symptomatic stage, a shift toward higher values is clearly visible in double transgenic mice for a consistent fraction of cells. On the contrary, for symptomatic motor neurons, only very sporadic GFP2G93A cells with a mild increase of Ub^{G76V}-GFP mRNA are detectable in one sample out of the five analyzed.

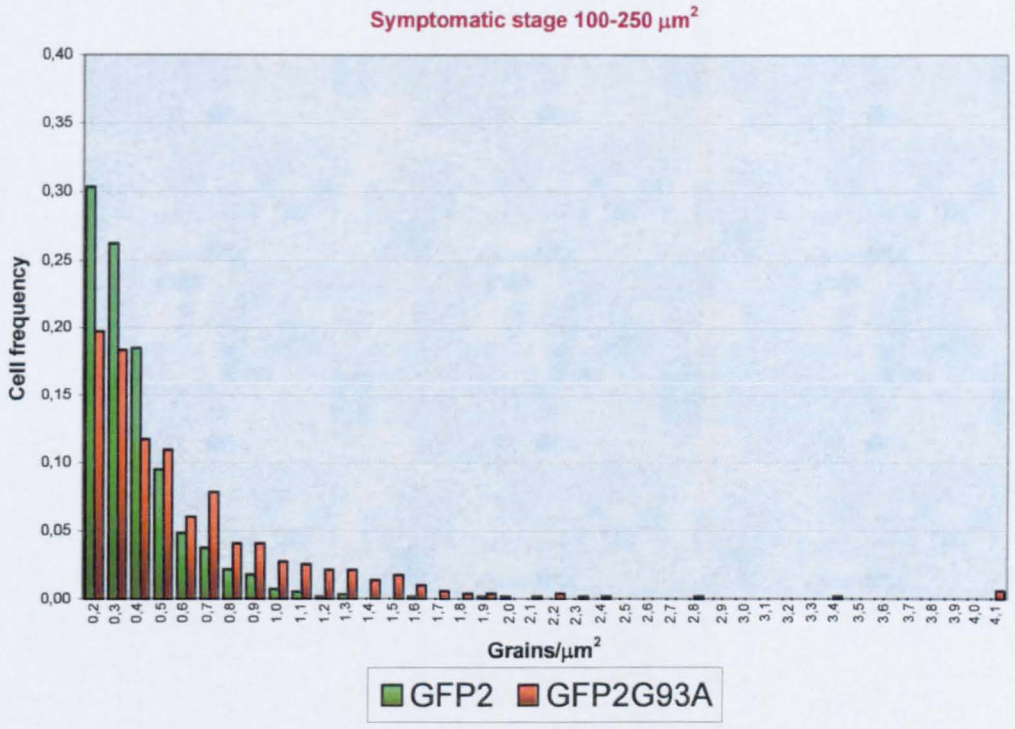

Figure 5.35 Frequency of 100-250 μm²-large cells with various levels of grain density in the lumbar spinal cord of symptomatic GFP2G93A mice compared to GFP2 littermates.

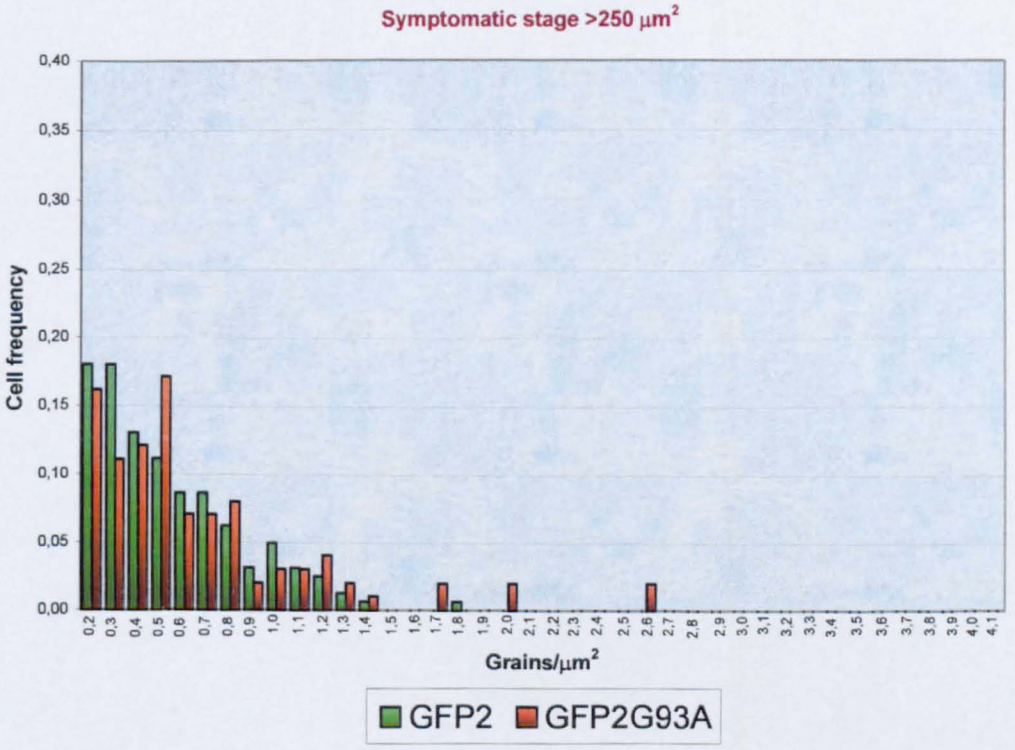

Figure 5.36 Frequency of >250 μm ²-large cells with various levels of grain density in the lumbar spinal cord of symptomatic GFP2G93A mice compared to GFP2 littermates.

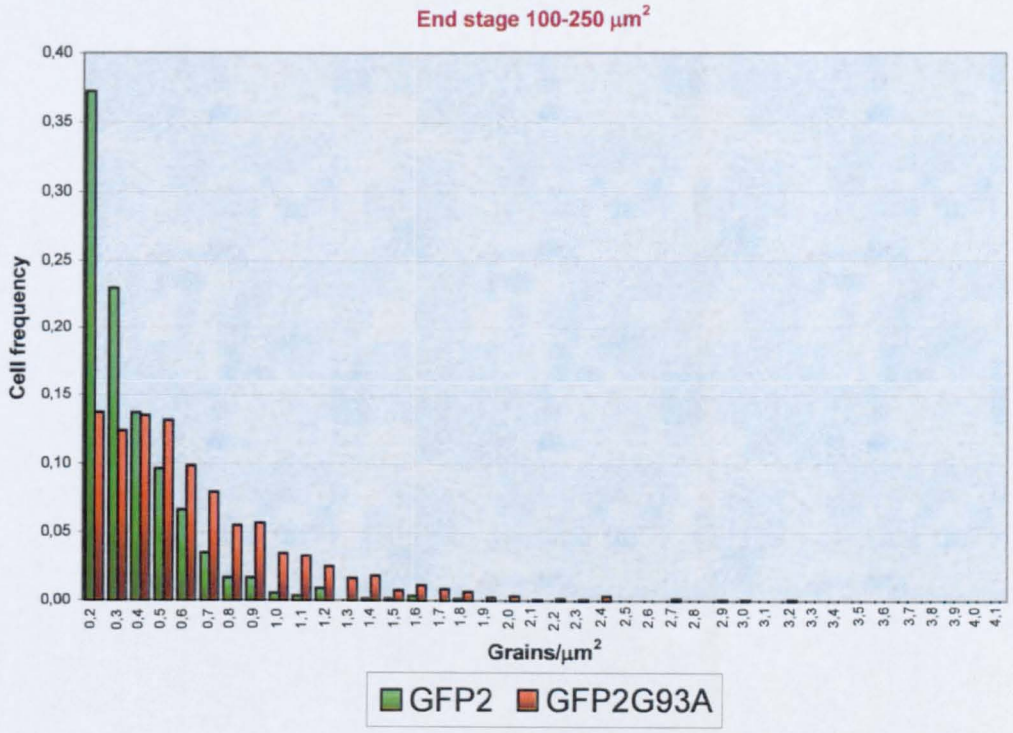

Figure 5.37 Frequency of 100-250 μm²-large cells with various levels of grain density in the lumbar spinal cord of end stage GFP2G93A mice compared to GFP2 littermates.

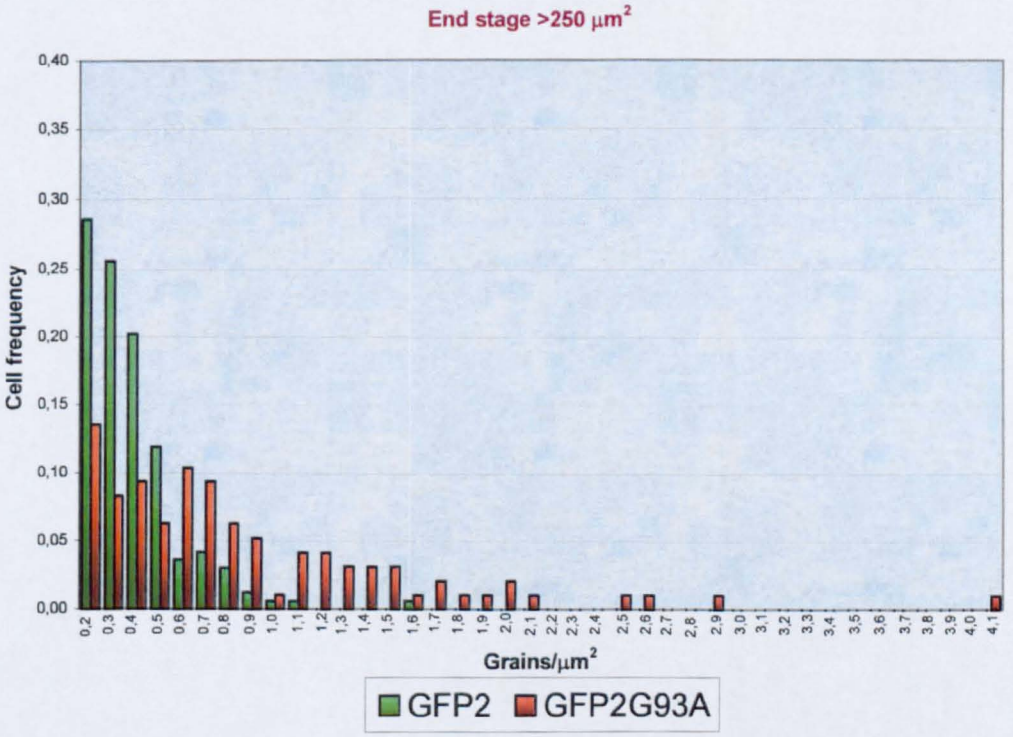

Figure 5.38 Frequency of >250 μm²-large cells with various levels of grain density in the lumbar spinal cord of end stage GFP2G93A mice compared to GFP2 littermates.

5.5 Discussion

As described in the introduction of this chapter, the presence of inclusion bodies of aggregated and ubiquitinated proteins is a well known feature of the motor neurons of ALS patients and murine model of the disease; moreover, it is known that both mutant SOD1 and ubiquitin accumulate in the spinal cord of G93A mice during disease progression (Cheroni et al., 2005).

Analysing by immunohistochemistry the lumbar spinal cord of G93A mice, I observed increasing amounts of ubiquitin-positive deposits as the motor dysfunction progresses, with massive presence of inclusions of ubiquitinated proteins scattered throughout the grey matter at the end stage. It was noticed that, sometimes, the neurons with higher ubiquitin accumulation showed a weak labelling of the neuronal marker NeuN. In fact, it has been reported that NeuN staining can be decreased (for a reduction of its levels or loss of antigenicity) in stressful conditions such as cerebral ischemia (Unal-Cevik et al., 2004) and axotomy (McPhail et al., 2004); therefore, its loss can be considered a sign of cellular suffering. As a consequence, it could be possible that the accumulation of ubiquitin in the neuronal population was underestimated for the lack of NeuN immunostaining.

With the purpose to verify the possible co-localization between ubiquitin and mutant SOD1, triple immunostaining experiments for SOD1, ubiquitin and ChAT or GFAP were done at the end stage of disease progression. However, only sporadically the signals of SOD1 and ubiquitin appeared to be overlapped in motor neuronal cells; in astrocytes, in which ubiquitin inclusions were occasionally detected, SOD1 levels were not found increased (Basso et al., 2006). Proteomic analysis carried out in collaboration with the Proteomic Unit of our institute on the detergent insoluble portion of G93A end stage spinal cord demonstrated that mutant SOD1 is partially mono- and oligo-

ubiquitinated (Basso et al., 2006); on the contrary, poly-ubiquitinated mutant SOD1 does not accumulate in the insoluble portion. It is possible that poly-ubiquitinated SOD1 is instead present in the soluble fraction, or that, when the mutant protein reaches the poly-ubiquitinated state, it is rapidly degraded by the proteasome. On the other hand, it has been demonstrated that proteasome degradation of mutant SOD1 can occur, at least in part, independently from direct poly-ubiquitination: for example, CHIP has been reported to mediate the degradation of mutant SOD1 by the ubiquitination of associated Hsp/Hsc 70 (Choi et al., 2004; Urushitani et al., 2004).

Even if the mutant SOD1 does not accumulate in a poly-ubiqitinated insoluble form, the formation of deposits of ubiquitinated proteins is a clear hallmark of the pathology in SOD1 mutant mice. The most probable reason that could explain such phenomenon is an altered functionality of the ubiquitin-proteasome pathway.

Various studies have tried to analyze the activity of the ubiquitin-proteasome pathway in *in vitro* and *in vivo* models of ALS. So far, contradictory results have been obtained probing the homogenates of G93A spinal cord with fluorogenic peptides, that, as already discussed, can give information only on the proteolytic activity of the 20S proteasome (Kabashi et al., 2004; Cheroni et al., 2005; Puttaparthi and Elliott, 2005; Ahtoniemi et al., 2007). For this reason, we decided to face the problem with a more direct approach, and particularly using Ub^{G76V}-GFP mouse model, that allow an *in vivo* evaluation of the overall functionality of the ubiquitin-proteasome system, after the cross-breeding with G93A mice. Ub^{G76V}-GFP model has already been used to demonstrate that proteasome impairment does not contribute to the neurodegeneration in a mouse model of SCA7 (Bowman et al., 2005) and to

detect a functional UPP dysfunction in prion-infected mice (Kristiansen et al., 2007).

Immunohistochemical analysis of the basal levels of the reporter protein in GFP1 and GFP2 spinal cord revealed differences between the two lines; GFP2 mice were considered more appropriate to detect possible increases of the reporter protein, so this line was used for the majority of the analyses.

Experiments on GFP2 primary cultures confirmed the accumulation of the reporter protein in response to proteasome inhibition in the spinal motor neurons.

The analysis of body weight, motor function impairment and survival in GFP1G93A mice compared to G93A did not show any differences. Therefore, the presence of a transgene coding for a protein that must be degraded by the UPP does not modify the time course of the motor decline in the G93A model.

Since disease progression is contemporaneous in G93A and GFPG93A mice, the levels of the reporter protein in double transgenic samples were analyzed at the same end points established for G93A.

Western blot measure of Ub^{G76V}-GFP in the lumbar spinal cord of double transgenic mice did not reveal substantial changes of the reporter protein at the symptomatic stage of the disease, thus excluding a major and generalized impairment of UPP functionality. However, a trend to an increase was detected in double transgenic mice, suggesting that a UPP dysfunction may occur selectively in specific cell populations.

In fact, while in sections from the lumbar spinal cord of double transgenic mice at the pre-symptomatic stage there was not a clear increase of the reporter protein, at the symptomatic stage a few GFP-positive cells were found and were identified prevalently as large neurons of the ventral horns. These

data were confirmed both in GFP1G93A and GFP2G93A mice, thus excluding a possible line-specific effect.

Interestingly, co-localization studies on serial sections demonstrated a partial association between the presence of the reporter protein and markers of neurodegeneration, such as ubiquitin deposits and perikaryal accumulation of phosphorylated neurofilaments. The connection between increased levels of the reporter protein and accumulation of ubiquitin strengthen the hypothesis of UPP alterations in these cells. In addition, it was observed that sometimes cells with high levels of Ub^{G76V}-GFP were characterized by a weak NeuN staining. All these indications point out that the accumulation of the reporter protein occurs prevalently in damaged cells.

At the end stage of the disease, GFP-positive cells were more numerous and localized both in the ventral and dorsal horns. Co-localization experiments revealed increased levels of Ub^{G76V}-GFP in neuronal but not in glial cells, in association with the presence of ubiquitin deposits; however, only few motor neurons resulted GFP-positive.

In the brain, an augment of Ub^{G76V}-GFP was detected only at the end stage in the motor nuclei of the brainstem, thus further demonstrating the association with the pathology. As already noticed at the same stage for the spinal cord, also in the brainstem GFP staining was noticeable prevalently in small neuronal-like cells.

To assure that the increased levels of Ub^{G76V}-GFP were due to an inhibition of its degradation and not to a change in its production, the transcription of the transgene was monitored. Real-time PCR experiments in the lumbar spinal cord of GFPG93A mice highlighted no changes at the symptomatic stage, while augmented mRNA levels were detected at the end stage selectively in the lumbar spinal cord. When mRNA levels were measured at the cellular level by

in situ hybridization experiments, a clear increase of Ub^{G76V}-GFP mRNA was registered in both small cells and motor neurons of the ventral horns from end stage mice. The transcriptional induction of the transgene renders it difficult to evaluate if this is the only phenomenon that determines the increase of the reporter protein or if an alteration of the degradation contributes to it.

Conversely, at the symptomatic stage, motor neuronal cells did not show significant increase of Ub^{G76V}-GFP mRNA, demonstrating that the augmented levels of the reporter protein detected in these cells are due to an inhibition of its degradation.

At the end stage, the rise of Ub^{G76V}-GFP transcript observed in double transgenic mice appears to be a phenomenon strictly related to the pathology, since it occurs selectively in the lumbar spinal cord and not in the hippocampus. It could be speculated that this event reflects generalized pathological changes in the transcriptional machinery; however, in the motor neuronal population, at the end stage of the disease a marked degree of transcriptional repression has been found (Ferraiuolo et al., 2007). On the other hand, it could not be excluded a selective induction of the transgene due to the action of cytokines or other signalling pathways activated during the disease progression. In fact, the CMV promoter, whose enhancer is present in Ub^{G76V}-GFP construct, could be induced by TNFα through NFkB transcription factor (Ramanathan et al., 2005).

At the symptomatic and, even more evidently, at the end stage of the disease, an increase in Ub^{G76V}-GFP mRNA was noticed in a consistent number of small cells, among which probably glia. However, Ub^{G76V}-GFP protein was never found increased in astrocytes and microglia, thus suggesting that, differentially from neurons, they are able to get rid of even large amounts of proteasome substrates.

Stage of disease progression	Marker	Co-localization with Ub^{G76V}-GFP
Symptomatic stage	Ubiquitin	+++
	SMI-31	++
	CHOP	-
End stage	ChAT	+
	Calretinin	+
	GFAP	-
	CD11b	-
	Ubiquitin	+++

-: no co-localization

+: rare co-localization

++: frequent co-localization

+++: very frequent co-localization

Table 5.3: Co-localization of Ub^{G76V}-GFP with various markers in the spinal cord of GFPG93A mice at the symptomatic or end stage of disease progression.

Table 5.3 recapitulates the co-localization studies carried on on double transgenic mice. In summary, the analysis of the protein and mRNA levels of Ub^{G76V}-GFP reporter points out a subtle dysfunction of the ubiquitin proteasome pathway in the lumbar spinal cord of double transgenic symptomatic mice. This finding is in agreement with what observed by Sau and colleagues, that described increased levels of the YFP^{u} reporter for UPP functionality in NSC34 cell lines expressing mutant SOD1 (Sau et al., 2007).

Even if high levels of Ub^{G76V}-GFP were noticeable only in a fraction of the vulnerable cell population, this phenomenon could be relevant in the context of a chronic neurodegenerative disease, in which the pathological changes and the loss of the motor neurons are dispersed in a long time span.

The detection of GFP staining required the use of amplification techniques, indicating that the accumulation of the reporter protein was not massive; this moderate rise of Ub^{G76V}-GFP suggests a mild dysfunction of UPP rather than a complete block of the system. However, even subtle perturbations of UPP could alter the appropriate protein turnover, especially in cells dealing with mutant and aggregation-prone proteins or exposed to other stresses. Indeed, it has been demonstrated that the presence of mutant SOD1 increases the vulnerability to proteasome dysfunction (Aquilano et al., 2003; Hyun et al., 2003). Moreover, a partial inhibition of the proteasome is sufficient to provoke the accumulation and aggregation of mutant SOD1 in cell cultures (Johnston et al., 2000; Hyun et al., 2003) and in organotypic slices from G93A spinal cord (Puttaparthi et al., 2003).

The dysfunction of the ubiquitin-proteasome pathway may be due to a decrease of 20S levels or catalytic activity. In support to this hypothesis, a marked decline of constitutive 20S staining was observed in the motor neurons of G93A mice during disease progression (Kabashi et al., 2004; Cheroni et al., 2005). Also the catalytic activity of 20S proteasome was found diminished in lumbar spinal cord homogenates of the same model (Kabashi et al., 2004). However, it is important to remind that Ub^{G76V}-GFP requires to be poly-ubiquitinated and recognized by the 26S complex to be degraded. Therefore, a failure in other steps of this process, like the availability of free ubiquitin, the action of ubiquitinating enzymes, the delivery of the substrate to the proteasome and the functionality of 19S subunit may be involved.

The decline of UPP activity probably contributes to the accumulation and aggregation of mutant SOD1 and ubiquitinated proteins that occurs during disease progression (Cheroni et al., 2005). Moreover, since it is known that UPP functionality can be impaired by protein aggregates (Bence et al., 2001), a

negative feed-back mechanism could arise. Given the fundamental role of the ubiquitin-proteasome system in the regulation of the cells homeostasis, its dysfunction could have profound consequences on cell physiology, altering the levels of a variety of proteins, such as chaperones, transcription factors and key regulatory proteins.

The selectivity of the involvement of the spinal cord in the described phenomenon could be related to the reduction of 20S catalytic activity found in this region as compared to other disctricts (Puttaparthi et al., 2003). Furthermore, in organotypic cultures, motor neurons are more sensitive to a short term proteasome inhibition than the other cell types (Tsuji et al., 2005).

It has been demonstrated that mild alterations of UPP function could be linked to ER stress (Menendez-Benito et al., 2005). CHOP-positive large neurons were visible in the ventral horns of G93A spinal cord already at the pre-symptomatic stage and their number increased with the worsening of the motor dysfunction. Nevertheless, at the symptomatic stage, no co-localization between CHOP and GFP was found. Therefore, ER stress maybe an early event in the processes of motor neuron degeneration produced by mutant SOD1. In fact, it has been demonstrated that mutant SOD1 could accumulate and aggregate in the ER (Kikuchi et al., 2006) and ER abnormalities have been reported in human patients and in the murine model (Dal Canto and Gurney, 1995; Engelhardt et al., 1997). Furthermore, various studies have reported the presence of markers of ER stress in SOD1 mutant mice (Vlug et al., 2005; Atkin et al., 2006; Kikuchi et al., 2006). Nonetheless, the induction of CHOP and the dysfunction of the UPP, detectable as Ub^{G76V}-GFP accumulation, appear not to be contemporaneous events.

In conclusion, this is the first study that demonstrates *in vivo* an impairment of the ubiquitin-proteasome pathway in a mouse model of ALS. Even if subtle,

this dysfunction could contribute in the events that determine the motor neuron degeneration in G93A mice. While the motor neurons may suffer from an impairment of UPP activity, the glial cells appear able to eliminate large amounts of proteasome substrate.

CHAPTER VI

ROLE OF THE INDUCTION OF THE IMMUNOPROTEASOME

6.1 INTRODUCTION

In a recent study, analyzing by western blot the levels of proteasome subunits in the spinal cord of end stage G93A mice, we observed that the decrease of 20S constitutive catalytic subunits β1, β2 and β5 was mirrored by an increase in their inducible counterparts LMP2, LMP10 and LMP7 (Cheroni et al., 2005). These findings were confirmed by Puttaparthi and colleagues in G93A low expressor mice (Puttaparthi and Elliott, 2005) and Ahtoniemi and colleagues in G93A rats (Ahtoniemi et al., 2007).

While constitutive proteasomes are typical of tissues and cell types with a low immunological activity (Rock et al., 1994), immunoproteasomes are especially expressed in lymphoid organs (Eleuteri et al., 1997; Cascio et al., 2001). As regards to the CNS, in physiological situations constitutive proteasome is predominant; however, immunoproteasome can be up-regulated in activated microglia (Stohwasser et al., 2000). Moreover, although the levels of MHC class I and II are very low in the normal CNS parenchyma, neuronal injury leads to a massive increase of these molecules on the activated microglia (McGeer et al., 1989; Kaur and Ling, 1992), which can serve as competent antigen-presenting cells (Ford et al., 1996; Dangond et al., 1997). Traditionally, it was thought that neurons did not express MHC class I molecules and were unable of presenting antigens to CD8+ T-cells (Joly and Oldstone, 1992); however, more recent studies in developing CNS have revealed a functional and highly ordered expression of MHC I, suggesting a role in brain development and neuronal plasticity (Corriveau et al., 1998; Huh et al., 2000; Oliveira et al., 2004). Furthermore, MHC I expression is reported increased in motor neurons and glia of aged rat spinal cords (Edstrom et al., 2004).

A rise of LMP2 and LMP7 was found in cortical pyramidal neurons of a conditional mouse model of Huntington's disease (Diaz-Hernandez et al.,

2003). The authors suggested that this may be a common feature of degenerative processes characterized by the accumulation of protein aggregates, as a compensatory mechanism of the affected neurons trying to counteract the decreased clearance of proteins, or alternatively as a response to pro-inflammatory cytokines released by activated glia. However, it is still unknown whether the capacity of the inducible proteasome to degrade disease-related aggregates is distinct from the constitutive proteasome, as well as it is unclear the effect of the substitution of constitutive with inducible subunits on the CNS physiology.

As regards to ALS, immunohistochemical studies in the spinal cord of animal models revealed that the augmented signal for LMP7 co-localizes with astrocytic and microglial markers (Ahtoniemi et al., 2007; Puttaparthi et al., 2007). In NSC-34 cells expressing mutant SOD1, a decrease of LMP7 (but not LMP2) and increase of β5 protein levels was found; moreover, RT-PCR in both NSC-34 cells and motor neurons from human fALS samples confirmed the LMP7 decline (Allen et al., 2003). In another cell model (PC12 cells), LMP2 co-expressed with G85R mutant resulted sequestered into SOD1 aggregates (Matsumoto et al., 2005).

Various experiments have been done to try to explain the mechanisms involved in the induction of immunoproteasome levels and its importance during the progression of motor dysfunction in SOD1 mutant mice. In organotypic spinal cord slice cultures from both G93A and NTg mice, the administration of TNFα or IFNγ was able to induce LMP2 and LMP7, suggesting an important role played by cytokines. Indeed, IFNγ treatment has been demonstrated to induce the immunoproteasome in microglia (Stohwasser et al., 2000). Dysregulation in various cytokines, among which TNFα and IFNγ, has been found in G93A spinal cord (Hensley et al., 2002).

The treatment of G93A rats with the anti-inflammatory drug pyrrolidine dithiocarbamate determined an earlier onset of the disease and a decrease of the survival (by 15%) in the treated group. This effect was accompanied by increased levels of ubiquitinated proteins and by the prevention of the induction of LMP7 during disease progression (Ahtoniemi et al., 2007). However, largely due to the non-specificity of the drug, this study did not provide a definitive answer to the importance of immunoproteasome induction on disease course. Using a genetic approach, Puttaparthi and colleagues cross-bred G93A mice (low expressor line) with LMP2 knock out mice. Knock out mice lacking LMP2, LMP10 or LMP7 subunits are viable, show modest reduction in proteasome activity as well as in immunological function but do not manifest neurological deficits (Van Kaer et al., 1994; Stohwasser et al., 2000; Martin et al., 2004). The loss of LMP2 in G93A mice determined a mild decrease in proteasome function in spinal cord and a compensatory induction of LMP7, but did not significantly impact motor function or survival (Puttaparthi et al., 2007).

6.2 Aim

The aim of this section of experiments was the investigation of the role of the shift from constitutive proteasome to immunoproteasome in G93A mice.

In order to evaluate a possible transcriptional regulation, the levels of the transcripts for constitutive and inducible β catalytic 20S subunits, as well as an α non catalytic subunit, were examined in the spinal cord of G93A mice at different stages of disease progression. To complete the information about the entire 26S complex, I analyzed also components of the 19S and 11S particles and the proteasome maturation protein POMP, whose presence is important for the correct assembly of the proteasome complex.

It is known that the increment of immunoproteasome occurs following changes in the cytokine network, which may result from glia activation. Therefore, I measured the transcript levels of TNFα and of markers of the glial population (GFAP for astrocytes and CD68 for phagocytic cells). Finally, since immunoproteasome is involved in the antigenic presentation, I investigated the presence of CD8+ lymphocytes.

6.3 METHODS

Real time PCR experiments were performed exploiting SYBR Green as fluorescent dye or using TaqMan assays, as described in the paragraphs 4.4.5 and 4.4.6.

In table 6.1 are reported the primer sequences used in SYBR Green experiments or the number of the chosen TaqMan Gene Expression Assays.

Gene	Accession n°	Forward (5'→ 3')	Reverse (5'→ 3')
β-actin (Actb)	NM_007393	GCCCTGAGGCTCTTTTCCAG	TGCCACAGGATTCCATACCC
β1 subunit of 20S (Psmb1)	NM_011185	TAATTGGCTGCAGTGGTTTCC	AAGCGCCGTGAGTACAGGAT
β2 subunit of 20S (Psmb2)	NM_011970	GATGAAGGACGATCATGACAAGAT	TGGGAGACAATTCATATCCATTCC
β5 subunit of 20S (Psmb5)	NM_011186	CGCAGCAGCCTCCAAACT	GAAGGCGGTCCCAGAGATC
LMP2 subunit of 20S (Psmb9)	NM_013585	TAGCTGACATGGCCGCCTA	TGGTCCCAGCCAGCTACTATG
LMP7 subunit of 20S (Psmb8)	NM_010724	AAGGATGAACAAAGTGATCGAGATT	TGCTGCAGACACGGAGATG
LMP10 subunit of 20S (Pmsb10)	NM_013640	GGAACCCACAGGAGGCTTCT	GTCCGCTCCCAGGATGACT
α5 subunit of 20S (Psma5)	NM_011967	AGTCCTCGCTCATCATCCTCA	ACGGCTCCTTCTTAAATGTCCTT
S1 subunit of 19S (Psmd1)	NM_027357	TGTTGGATAATCCAGCACGAGT	GGTTCCACGAGTTCTTCAACGT
α Subunit of 11S (Psme1)	NM_011189	GGCTTCCACACGCAGATCTC	TCTCCATGACCATCAGACGG
POMP	NM_025624	GTGTGCTCAGCATAGTTGCCTG	AGCTTTGCTATAACCTCAGAACCAC
CD8 α chain (Cd8a)	NM_001081110	CTATTCAAACCACTGCCGCAG	CCGAGGTTCGACCTGACATTAC
Gene	**Accession n°**	**TaqMan Gene expression assay n°**	
β-actin (Actb)	NM_007393	4352341E	
GFAP	NM_010277	Mm00546086_m1	
CD68	NM_009853	Mm00839636_g1	
TNF α	NM_013693	Mm00546086_m1	

Table 6.1: Primer sequences and TaqMan Gene Expression Assay number for real-time PCR experiments

6.4 RESULTS

6.4.1 Measure of the transcript levels of 26S proteasome components

To obtain information about the rate of transcription of various components of the 26S complex in G93A mice during disease progression, the following transcripts were measured: constitutive catalytic β1, β2 and β5 subunits of 20S particle; inducible catalytic LMP2, LMP10 and LMP7 subunits of 20S particle; non-catalytic α5 subunit of 20S particle; non-ATPAse S1 subunit of the base of 19S complex (homolog of S. Cerevisiae Rnp2); α subunit of 11S complex; POMP protein.

I. Pre-symptomatic stage

In the lumbar spinal cord of G93A mice prior to symptom onset, no changes were found for the catalytic subunits of the 20S proteasome (Fig. 6.1 and 6.2), nor for the non-catalytic α5. However, both S1 subunit of 19S and α subunit of 11S resulted significantly decreased (Fig. 6.3).

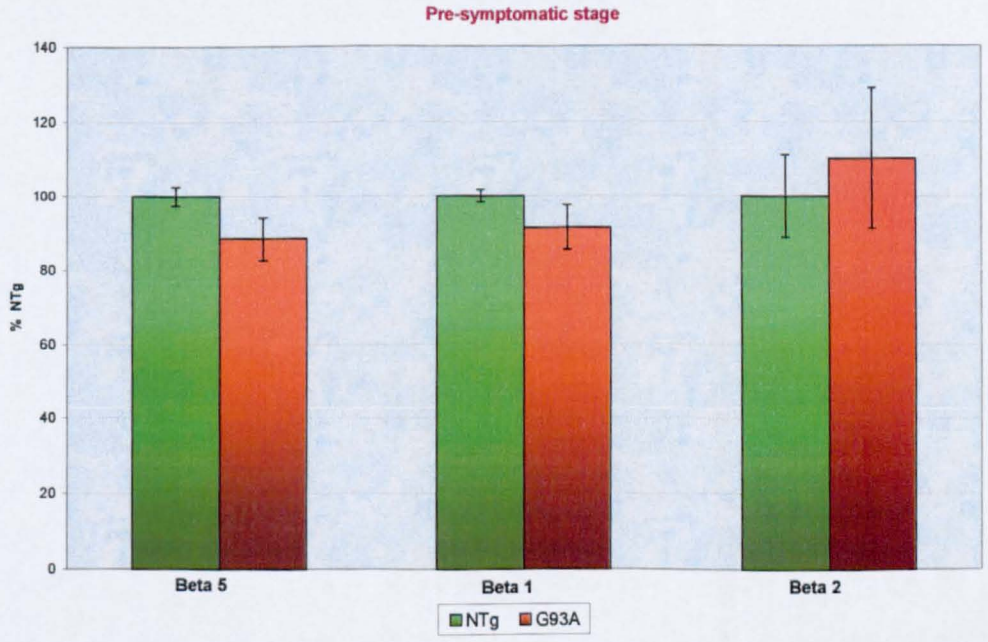

Figure 6.1: Real-time PCR for β5, β1 and β2 transcripts in the lumbar spinal cord of pre-symptomatic G93A mice and NTg littermates. Data were normalized versus β-actin and expressed as percentage of the value of the NTg. Each histogram shows the mean ± S.E. of at least four mice. Data were analyzed by Student's t-test.

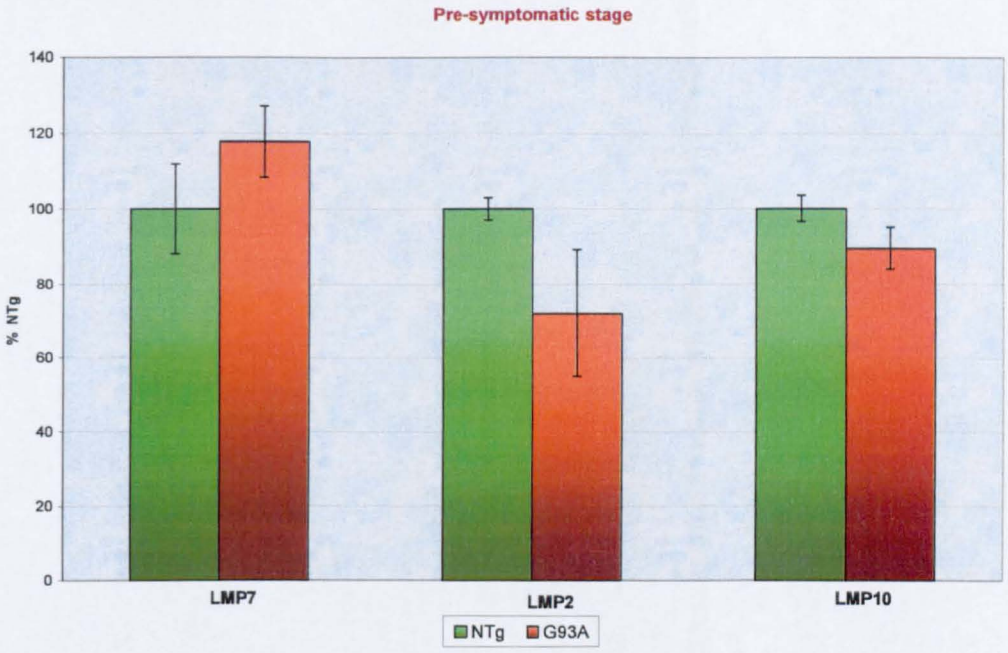

Figure 6.2: Real-time PCR for LMP7, LMP2 and LMP10 transcripts in the lumbar spinal cord of pre-symptomatic G93A mice and NTg littermates. Data were normalized versus β-actin and expressed as percentage of the value of the NTg. Each histogram shows the mean ± S.E. of at least four mice. Data were analyzed by Student's t-test.

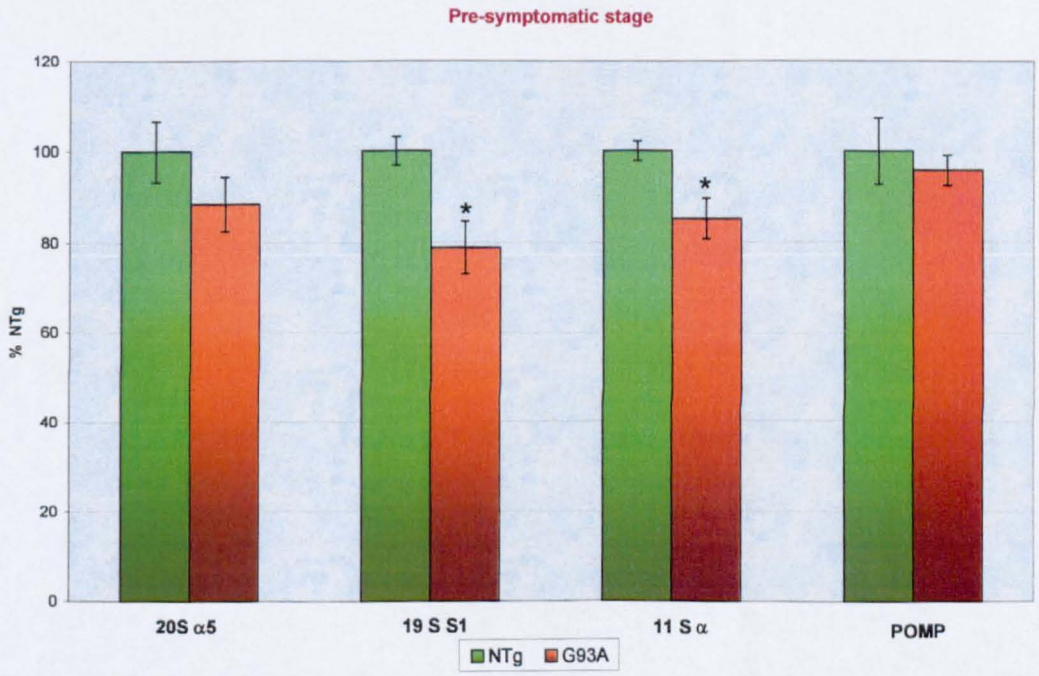

Figure 6.3: Real-time PCR for α5 subunit of 20S, S1 subunit of 19S, α subunit of 11S and POMP transcripts in the lumbar spinal cord of pre-symptomatic G93A mice and NTg littermates. Data were normalized versus β-actin and expressed as percentage of the value of the NTg. Each histogram shows the mean ± S.E. of at least four mice. Data were analyzed by Student's t-test (* $p<0.05$ compared to NTg).

II. Symptomatic stage

At the symptomatic stage, the mRNA levels of catalytic constitutive 20S proteasome subunits were not different between the lumbar spinal cord of G93A and NTg littermates (Fig. 6.4). On the contrary, LMP7 and LMP10 transcripts were found significantly up-regulated in G93A (Fig 6.5), while the non-catalytic α subunit was decreased (Fig 6.6).

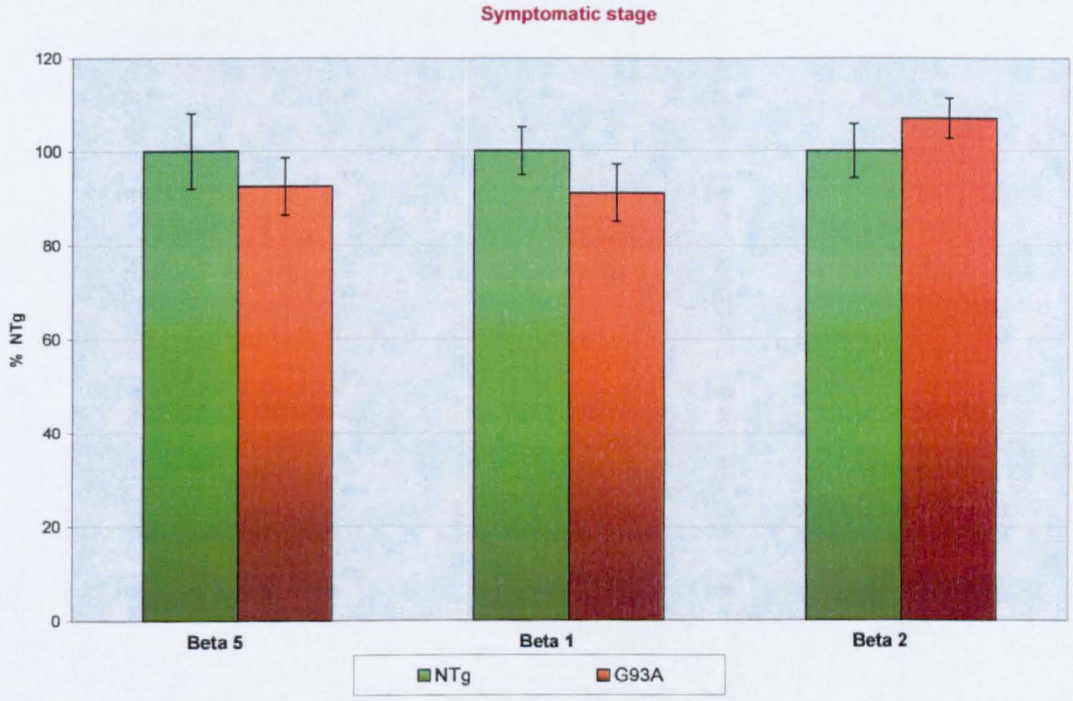

Figure 6.4: Real-time PCR for β5, β1 and β2 transcripts in the lumbar spinal cord of symptomatic G93A mice and NTg littermates. Data were normalized versus β-actin and expressed as percentage of the value of the NTg. Each histogram shows the mean ± S.E. of at least four mice. Data were analyzed by Student's t-test.

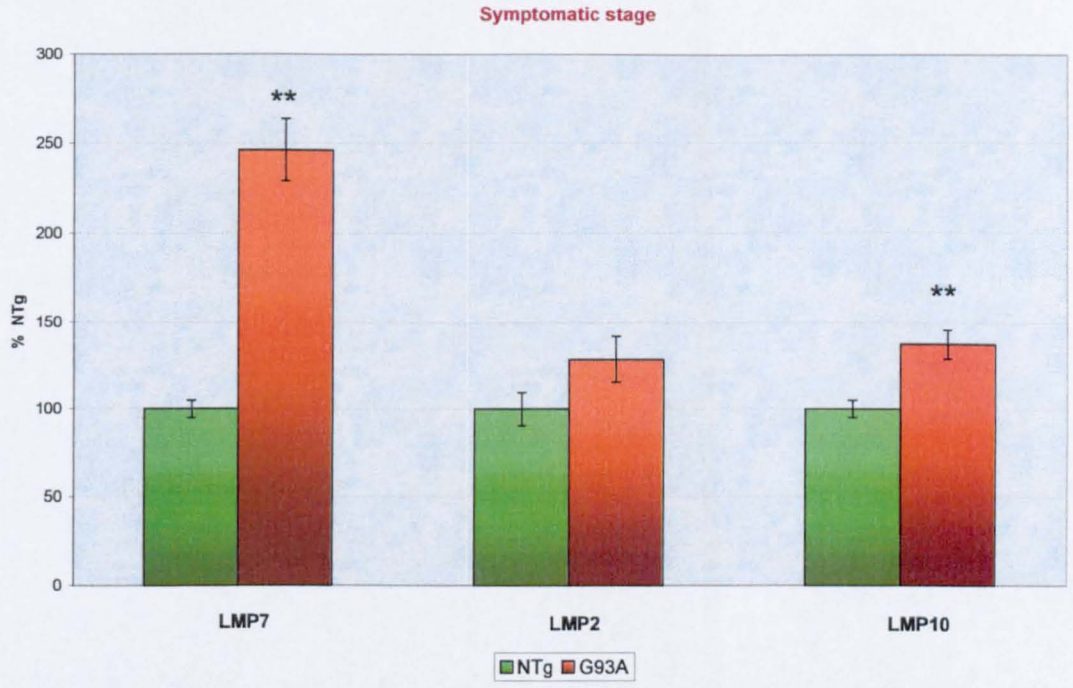

Figure 6.5: Real-time PCR for LMP7, LMP2 and LMP10 transcripts in the lumbar spinal cord of symptomatic G93A mice and NTg littermates. Data were normalized versus β-actin and expressed as percentage of the value of the NTg. Each histogram shows the mean ± S.E. of at least four mice. Data were analyzed by Student's t-test (** $p<0.01$ compared to NTg).

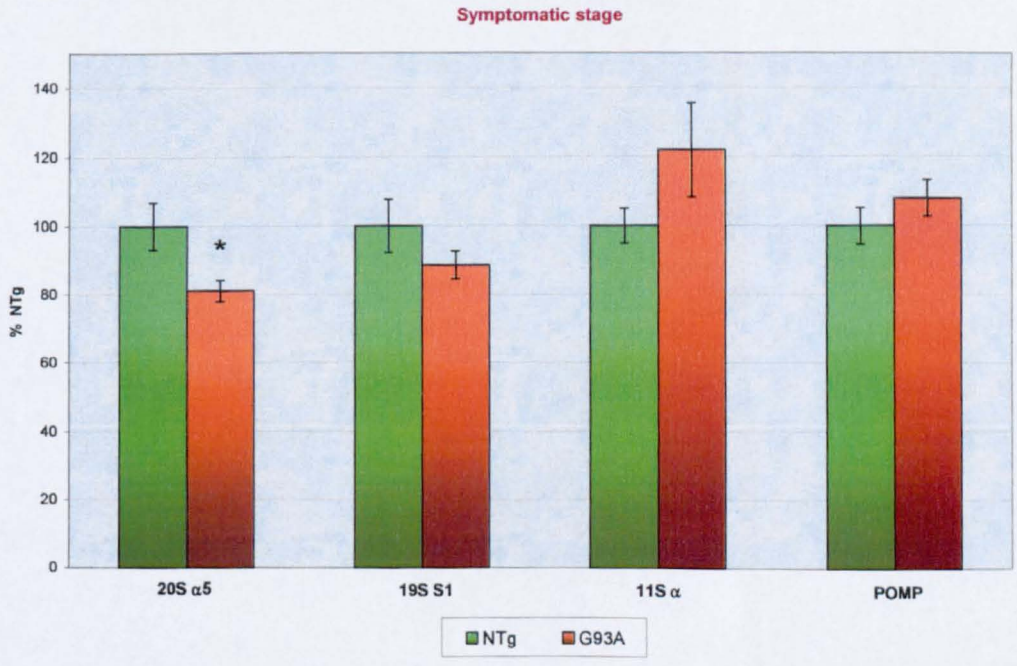

Figure 6.6: Real-time PCR for α5 subunit of 20S, S1 subunit of 19S, α subunit of 11S and POMP transcripts in the lumbar spinal cord of symptomatic G93A mice and NTg littermates. Data were normalized versus β-actin and expressed as percentage of the value of the NTg. Each histogram shows the mean ± S.E. of at least four mice. Data were analyzed by Student's t-test (* $p<0.05$ compared to NTg).

III. End stage

The analysis of the transcript levels in the lumbar spinal cord of G93A mice at the end stage of disease progression in comparison to NTg littermates revealed a general tendency to a decrease of the constitutive subunits and to an increase of the inducible counterparts. The data reached the statistical significance for β5, β1 and LMP7 transcripts (Fig 6.7 and 6.8). Also the levels of 19S and POMP were decreased (Fig 6.9).

These changes were restricted to the pathological area, since no alterations were detected in the hippocampus (β5, LMP7, α5 and 19S tested).

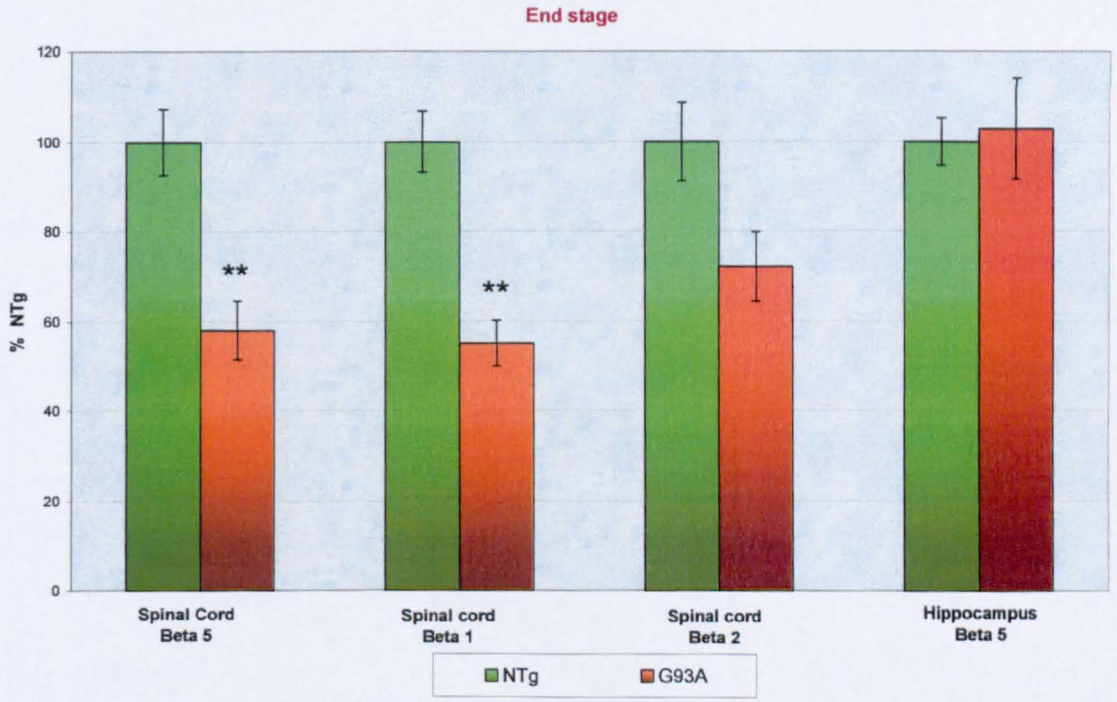

Figure 6.7: Real-time PCR for β5, β1 and β2 transcripts in the lumbar spinal cord and hippocampus of end stage G93A mice and NTg littermates. Data were normalized versus β-actin and expressed as percentage of the value of the NTg. Each histogram shows the mean ± S.E. of at least four mice. Data were analyzed by Student's t-test (** $p<0.01$ compared to NTg)

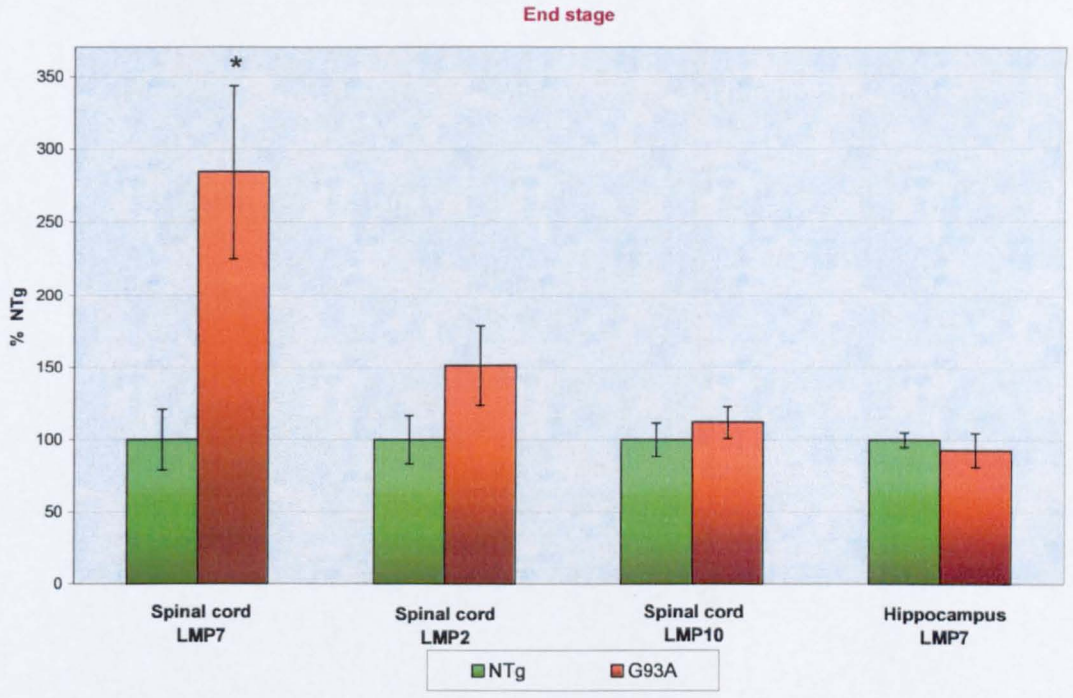

Figure 6.8: Real-time PCR for LMP7, LMP2 and LMP10 transcripts in the lumbar spinal cord and hippocampus of end stage G93A mice and NTg littermates. Data were normalized versus β-actin and expressed as percentage of the value of the NTg. Each histogram shows the mean ± S.E. of at least four mice. Data were analyzed by Student's t-test (* $p<0.05$ compared to NTg).

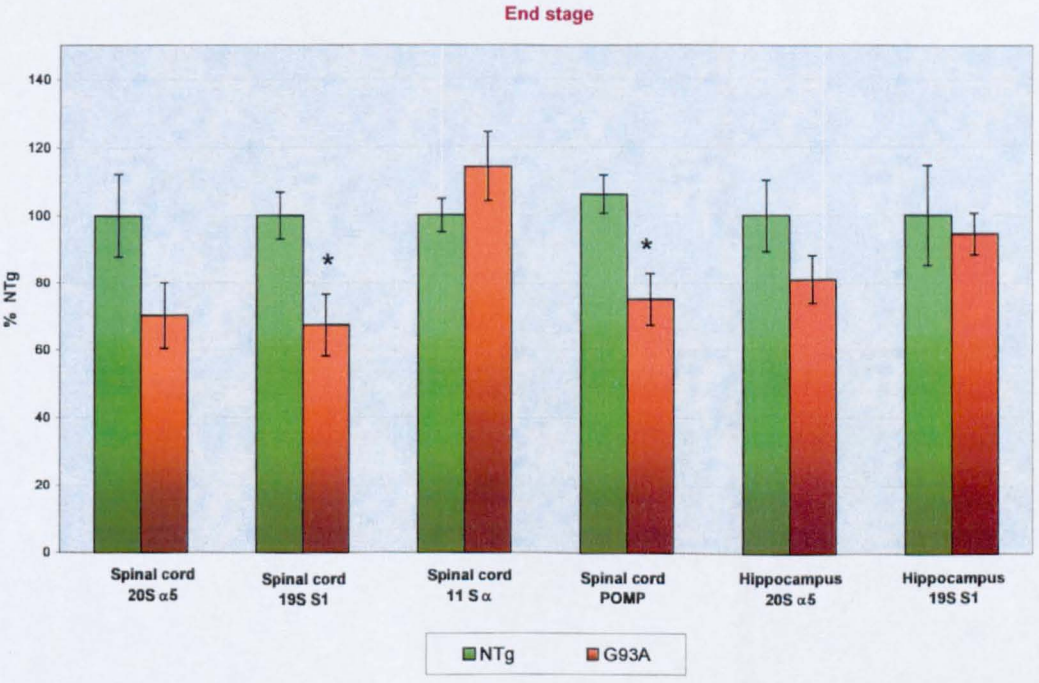

Figure 6.9: Real-time PCR for α5 subunit of 20S, S1 subunit of 19S, α subunit of 11S and POMP transcripts in the lumbar spinal cord and hippocampus of end stage G93A mice and NTg littermates. Data were normalized versus β-actin and expressed as percentage of the value of the NTg. Each histogram shows the mean ± S.E. of at least four mice. Data were analyzed by Student's t-test (* $p<0.05$ compared to NTg).

6.4.2 Measure of the transcript levels of glia and immunological markers

To investigate whether the induction of immunoproteasome correlates with alterations of the immuno-inflammatory system, the levels of the pro-inflammatory cytokine TNFα were measured in the lumbar spinal cord of G93A mice. The presence of astrocytic cells (evaluated by GFAP marker), of phagocytic cells (CD68-positive cells) and of T lymphocytes (evaluated by CD8 marker) was also investigated.

The results showed that, already at the pre-symptomatic stage, TNFα, CD68 and GFAP were up-regulated in transgenic mice (Fig. 6.10). The phenomenon became remarkably prominent with the progression of the disease (Fig. 6.11, 6.12). On the contrary, changes of CD8 level were never found (Fig 6.10, 6.11, 6.12).

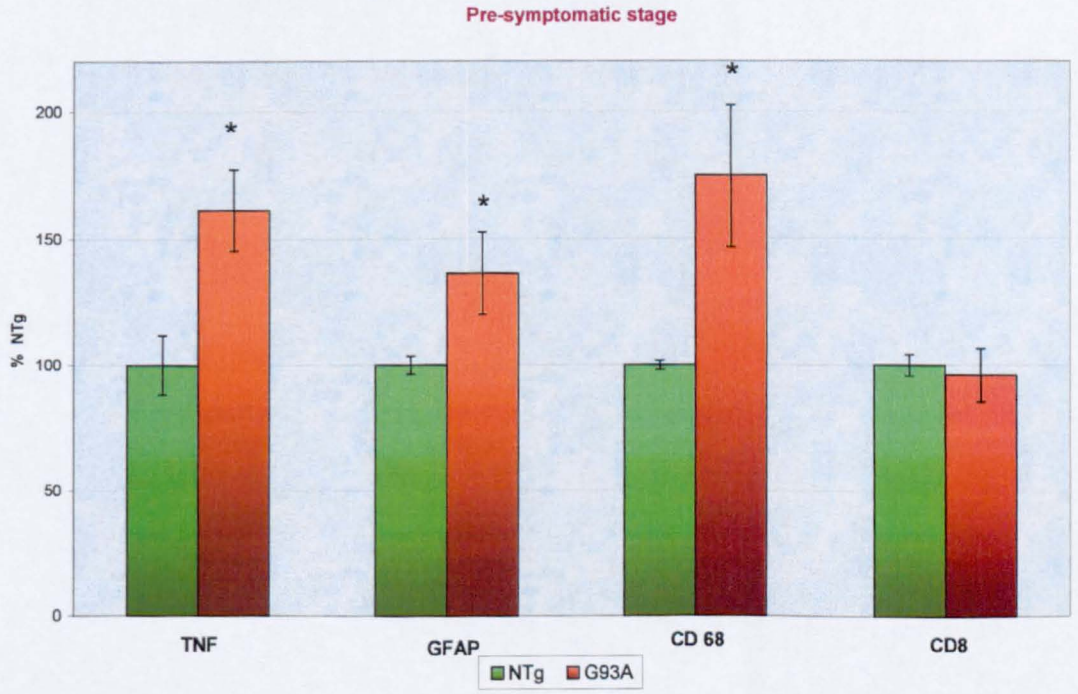

Figure 6.10: Real-time PCR for TNFα, GFAP, CD68 and CD8 transcripts in the lumbar spinal cord of pre-symptomatic G93A mice and NTg littermates. Data were normalized versus β-actin and expressed as percentage of the value of the NTg. Each histogram shows the mean ± S.E. of at least five mice. Data were analyzed by Student's t-test (* $p<0.05$ compared to NTg).

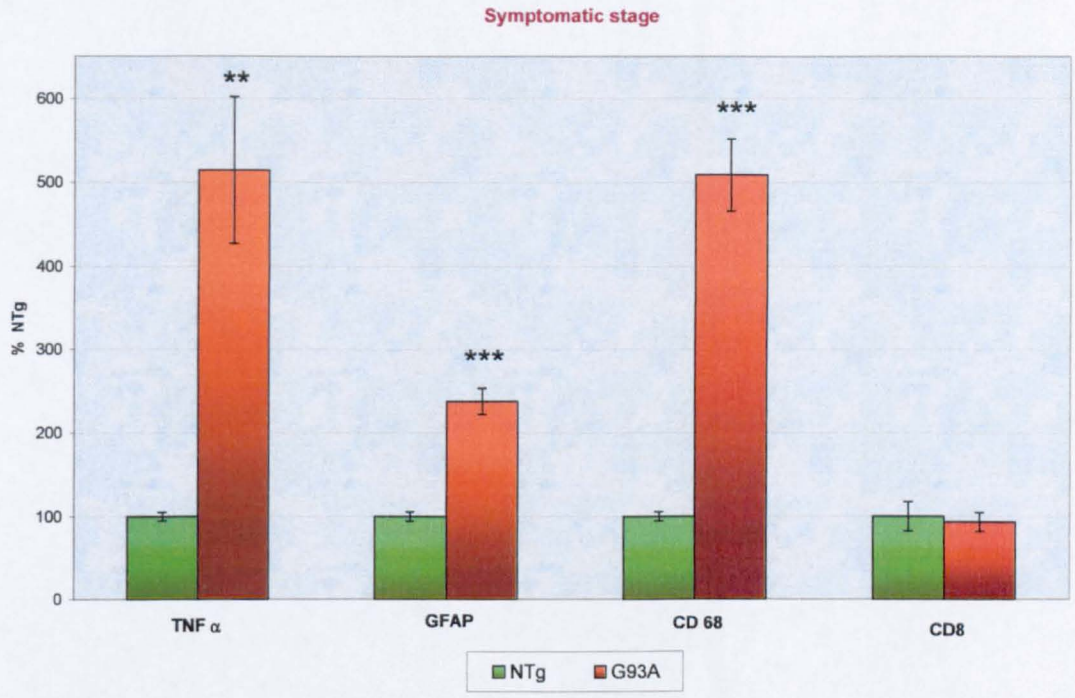

Figure 6.11: Real-time PCR for TNFα, GFAP, CD68 and CD8 transcripts in the lumbar spinal cord of symptomatic G93A mice and NTg littermates. Data were normalized versus β-actin and expressed as percentage of the value of the NTg. Each histogram shows the mean ± S.E. of at least five mice. Data were analyzed by Student's t-test (** p<0.01, *** p<0.001 compared to NTg).

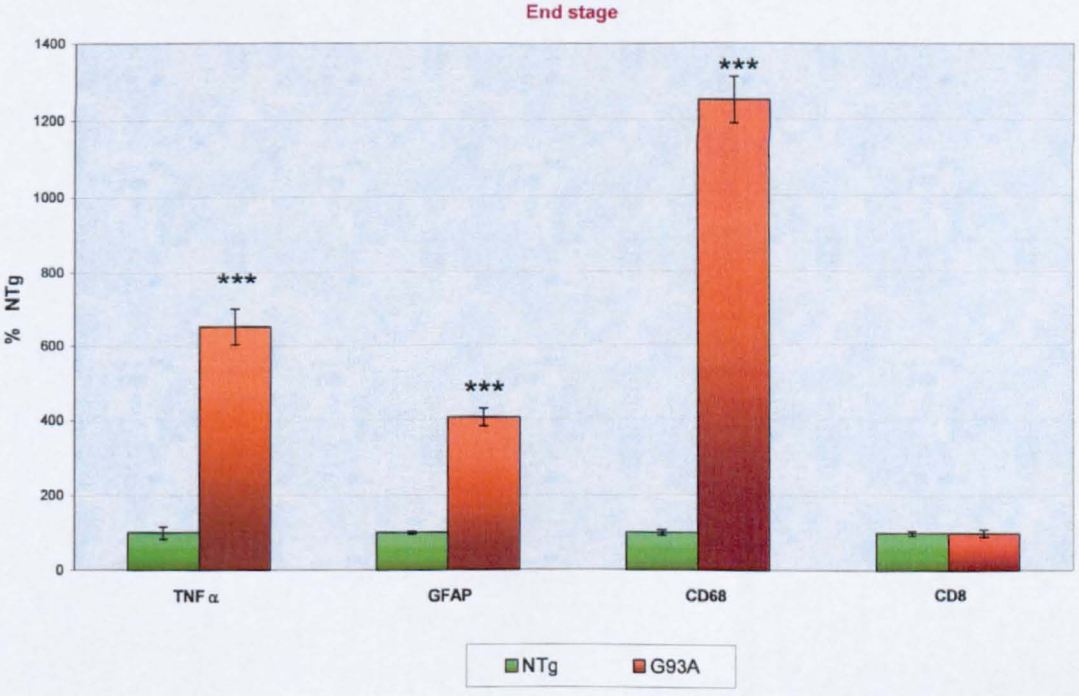

Figure 6.12: Real-time PCR for TNFα, GFAP, CD68 and CD8 transcripts in the lumbar spinal cord of end stage G93A mice and NTg littermates. Data were normalized versus β-actin and expressed as percentage of the value of the NTg. Each histogram shows the mean ± S.E. of at least five mice. Data were analyzed by Student's t-test (*** p<0.001 compared to NTg).

6.5 Discussion

Real-time PCR experiments on the lumbar spinal cord of G93A mice compared to NTg littermates revealed no changes in the levels of 20S proteasome catalytic constitutive subunits (β1, β2 and β5) at the pre-symptomatic and symptomatic stage of the disease, while a decrease was detected at the end stage. These data are in agreement to what found in a recent study for the protein levels (Cheroni, 2005). The reduction of constitutive proteasome could not be only ascribed to the loss of motor neurons, that is relevant already in the symptomatic phase. Indeed, a decline of the immunolabelling for 20S constitutive proteasome was registered in the spinal motor neurons of G93A with the progression of the motor dysfunction (Cheroni et al., 2005).

Unlike for the constitutive subunits, a significant up-regulation of LMP7 and LMP10 is present already at the symptomatic stage in the lumbar spinal cord but not in a non-vulnerable area such as the hippocampus. Since mutant SOD1 is over-expressed both in the spinal cord and the hippocampus, it appears clear that this effect is strictly associated with pathological features. Moreover, these data, for the first time, permit to conclude that the changes in the protein levels of constitutive and inducible 20S catalytic subunits revealed by our and other groups (Cheroni et al., 2005; Puttaparthi and Elliott, 2005; Ahtoniemi et al., 2007) are regulated at transcriptional level.

The mechanisms that control the transcription of constitutive subunits of 20S proteasome are poorly understood; it is believed that the various subunits are transcripted in a coordinated fashion and that can be induced in stress situations through the antioxidant response element (Kwak et al., 2003a; Kwak et al., 2003b). On the other hand, it is well known that inducible proteasome can be up-regulated in response to inflammatory cytokines (Bochtler et al., 1999). Among the inducible subunits, LMP7 showed the

strongest induction, with a 2.5-fold increase in the lumbar spinal cord of symptomatic and end stage G93A mice compared to NTg littermates. Since the induction of the other subunits was more limited, it is possible that mixed 20S particles formed. In fact, the presence in the CNS not only of homogeneous immunoproteasome, but also of heterogeneous particles incorporating LMP7 but not LMP2 and LMP10 has been reported (Griffin et al., 1998; Piccinini et al., 2003). However, at the moment, the specific properties and biological functions of heterogeneous immunoproteasome are not known.

As regards to the non-catalytic α5 subunit, a modest decrease was observed in all the disease stages analyzed, and reached the statistical significance at the symptomatic phase. Since the various 20S subunits must assembly in stochiometric amounts, it is possible that the scarcity of non catalytic subunits is limiting in the process of building new proteasome particles, even when the rate of transcription of catalytic subunits is not affected. Moreover, at the end stage, also POMP results diminished of about 20% in respect to NTg littermates; given its role in the biogenesis of 20S proteasome, the decrease in its levels could be a further element that contributes to reduce the availability of assembled proteasomes.

The S1 non-ATPase subunit of 19S and the α subunit of 11S resulted mild diminished already at the pre-symptomatic phase, being the first detectable change. The decrease in 19S correlated with immunohistochemical data (Cheroni et al., 2005), which revealed reduced levels in the ventral horns of G93A spinal cord. Since 19S is necessary for the physiological degradation of ubiquitinated proteins, its reduction could have consequences on UPP functionality; however, it has been reported that a minority of proteins could be degraded directly by 20S proteasome (Orlowski and Wilk, 2003). More puzzling appears to be the change in 11S, that behaved differentially from the

other inducible components of the UPP. Although 11S is known to enhance the ability of 20S to hydrolyze small peptides *in vitro* (Ma et al., 1992), its *in vivo* function has not been unravelled yet.

In parallel with the up-regulation of LMP7, I have found an increase of TNFα already at the pre-symptomatic stage; the induction became prominent during disease progression (6-fold increase compared to NTg littermates). These data are in line with other studies (Elliott, 2001; Ishigaki et al., 2002). It is known that TFNα is able to determine an up-regulation of LMP7 in the astrocytes and microglia of both NTg and G93A spinal cord slices (Cheroni et al., 2005; Puttaparthi and Elliott, 2005; Ahtoniemi et al., 2007); therefore, the increase of TNFα is probably contributing to the induction of the immunoproteasome in G93A spinal cord.

GFAP and CD68 were found increased in transgenic mice already at the pre-symptomatic stage, when proliferation of glia is difficult to reveal by immunohistochemistry. CD68 is a Lamp protein expressed on phagocytic cells and could be considered as a marker of monocytes, macrophages, activated microglia and dendritic cells; its rise is the most relevant, since at the end stage a 12-fold increase in its levels could be detected. These data confirmed the increase of C68 transcription revealed both in SOD1 mutant mice (Henkel et al., 2006) and in ALS patients (Henkel et al., 2004); in the latter case, CD68-positive cells were found to densely infiltrate both the white and the grey matter regions of the spinal cord (Graves et al., 2004).

Since there is a strong correlation between LMP7 up-regulation and massive increase of glial markers in a phase of disease in which the motor neurons are dying, it appears highly probable that, differently of what has been reported for Huntington's disease (Diaz-Hernandez et al., 2003), in mutant SOD1 model the induction of immunoproteasome takes place in the glial population. The

literature confirms this view for LMP7 (Puttaparthi and Elliott, 2005; Ahtoniemi et al., 2007), while no data are to date available for the other two subunits; therefore, at the moment, the localization of LMP10 and LMP2 is not known and it is not possible to totally exclude an involvement of the motor neuronal population.

As antigen-presenting cells, microglia is known to normally express immunoproteasome and to further up-regulate its subunits after activation (Stohwasser et al., 2000); for this reason, it is possible that these cells are involved in starting an immune response against modified proteins. This scenario would require the influx of CD8+ T-lymphocytes specific for the antigens presented on the surface of the microglia; however, by real time PCR, no changes of CD8 transcript were found in the spinal cord of G93A mice.

In ALS patients, the influx of peripheral lymphocytes is a rare event only associated with end stage of the disease (Kawamata et al., 1992; Graves et al., 2004; Zhang et al., 2005). The presence of CD8+ cytotoxic T cells has never been investigated before in the mouse model; immunohistochemical studies performed by Alexianu and colleagues (Alexianu et al., 2001) revealed the sporadic presence of a small number of CD3+ T cells only at the end stage. Therefore, even if it is not possible to exclude the infiltration of rare cells not detectable by real time PCR due to sensitivity limitations, it can be concluded that, unlike macrophagic cells, CD8+ lymphocytes seems not to play a relevant role in immune-inflammatory reaction observed in SOD1 mutant mice.

CHAPTER VII

CONCLUSIONS

The main focus of this thesis was to unravel the role of the ubiquitin-proteasome pathway in the mechanisms that lead to motor neuron degeneration in the G93A mouse model of ALS.

The expression of Ub^{G76V}-GFP reporter of UPP functionality made it possible to identify subtle alterations of the ubiquitin-proteasome system in the spinal cord of G93A mice in the symptomatic phase, mainly in the motor neuronal population. Even if a generalized and total impairment of the UPP was never observed, it is important to consider that a not completely efficient UPP could represent a critical weakness for cells that are dealing with large amounts of misfolded and aggregation-prone proteins.

Accumulation of the reporter protein was never detected in the glial population, even in presence of augmented mRNA levels. It is possible that the capability of the glial cells to preserve a full functioning UPP is related to their capacity to induce the immunoproteasome. In fact, the measure of transcript levels revealed a decrease of constitutive proteasome subunits and an increase of their inducible counterparts in the lumbar spinal cord of G93A mice during disease progression; the changes in proteasome composition were accompanied by a substantial increase of glial markers and TNFα.

BIBLIOGRAPHY

Abrahams S, Leigh PN, Goldstein LH (2005) *Cognitive change in ALS: a prospective study.* Neurology 64:1222-1226.

Ahmad-Annuar A, Tabrizi SJ, Fisher EM (2003) *Mouse models as a tool for understanding neurodegenerative diseases.* Curr Opin Neurol 16:451-458.

Ahtoniemi T, Goldsteins G, Keksa-Goldsteine V, Malm T, Kanninen K, Salminen A, Koistinaho J (2007) *Pyrrolidine dithiocarbamate inhibits induction of immunoproteasome and decreases survival in a rat model of amyotrophic lateral sclerosis.* Mol Pharmacol 71:30-37.

Aksoy H, Dean G, Elian M, Deng HX, Deng G, Juneja T, Storey E, McKinlay Gardner RJ, Jacob RL, Laing NG, Siddique T (2003) *A4T mutation in the SOD1 gene causing familial amyotrophic lateral sclerosis.* Neuroepidemiology 22:235-238.

Al-Chalabi A, Andersen PM, Nilsson P, Chioza B, Andersson JL, Russ C, Shaw CE, Powell JF, Leigh PN (1999) *Deletions of the heavy neurofilament subunit tail in amyotrophic lateral sclerosis.* Hum Mol Genet 8:157-164.

Alexander GM, Deitch JS, Seeburger JL, Del Valle L, Heiman-Patterson TD (2000) *Elevated cortical extracellular fluid glutamate in transgenic mice expressing human mutant (G93A) Cu/Zn superoxide dismutase.* J Neurochem 74:1666-1673.

Alexianu ME, Kozovska M, Appel SH (2001) *Immune reactivity in a mouse model of familial ALS correlates with disease progression.* Neurology 57:1282-1289.

Allen S, Heath PR, Kirby J, Wharton SB, Cookson MR, Menzies FM, Banks RE, Shaw PJ (2003) *Analysis of the cytosolic proteome in a cell culture model of familial amyotrophic lateral sclerosis reveals alterations to the proteasome, antioxidant defenses, and nitric oxide synthetic pathways.* J Biol Chem 278:6371-6383.

Andersen PM, Nilsson P, Ala-Hurula V, Keranen ML, Tarvainen I, Haltia T, Nilsson L, Binzer M, Forsgren L, Marklund SL (1995) *Amyotrophic lateral*

sclerosis associated with homozygosity for an Asp90Ala mutation in CuZn-superoxide dismutase. Nat Genet 10:61-66.

Andersen PM, Sims KB, Xin WW, Kiely R, O'Neill G, Ravits J, Pioro E, Harati Y, Brower RD, Levine JS, Heinicke HU, Seltzer W, Boss M, Brown RH, Jr. (2003) *Sixteen novel mutations in the Cu/Zn superoxide dismutase gene in amyotrophic lateral sclerosis: a decade of discoveries, defects and disputes.* Amyotroph Lateral Scler Other Motor Neuron Disord 4:62-73.

Andrus PK, Fleck TJ, Gurney ME, Hall ED (1998) *Protein oxidative damage in a transgenic mouse model of familial amyotrophic lateral sclerosis.* J Neurochem 71:2041-2048.

Aquilano K, Rotilio G, Ciriolo MR (2003) *Proteasome activation and nNOS down-regulation in neuroblastoma cells expressing a Cu,Zn superoxide dismutase mutant involved in familial ALS.* J Neurochem 85:1324-1335.

Arisato T, Okubo R, Arata H, Abe K, Fukada K, Sakoda S, Shimizu A, Qin XH, Izumo S, Osame M, Nakagawa M (2003) *Clinical and pathological studies of familial amyotrophic lateral sclerosis (FALS) with SOD1 H46R mutation in large Japanese families.* Acta Neuropathol (Berl) 106:561-568.

Arnesano F, Banci L, Bertini I, Martinelli M, Furukawa Y, O'Halloran TV (2004) *The unusually stable quaternary structure of human Cu,Zn-superoxide dismutase 1 is controlled by both metal occupancy and disulfide status.* J Biol Chem 279:47998-48003.

Atkin JD, Farg MA, Turner BJ, Tomas D, Lysaght JA, Nunan J, Rembach A, Nagley P, Beart PM, Cheema SS, Horne MK (2006) *Induction of the unfolded protein response in familial amyotrophic lateral sclerosis and association of protein-disulfide isomerase with superoxide dismutase 1.* J Biol Chem 281:30152-30165.

Aviel S, Winberg G, Massucci M, Ciechanover A (2000) *Degradation of the epstein-barr virus latent membrane protein 1 (LMP1) by the ubiquitin-proteasome pathway. Targeting via ubiquitination of the N-terminal residue.* J Biol Chem 275:23491-23499.

Bachmair A, Varshavsky A (1989) *The degradation signal in a short-lived protein.* Cell 56:1019-1032.

Bachmair A, Finley D, Varshavsky A (1986) *In vivo half-life of a protein is a function of its amino-terminal residue.* Science 234:179-186.

Basso M, Massignan T, Samengo G, Cheroni C, De Biasi S, Salmona M, Bendotti C, Bonetto V (2006) *Insoluble mutant SOD1 is partly oligoubiquitinated in amyotrophic lateral sclerosis mice.* J Biol Chem 281:33325-33335.

Baumeister W, Walz J, Zuhl F, Seemuller E (1998) *The proteasome: paradigm of a self-compartmentalizing protease.* Cell 92:367-380.

Beal MF, Palomo T, Kostrzewa RM, Archer T (2000) *Neuroprotective and neurorestorative strategies for neuronal injury.* Neurotox Res 2:71-84.

Beal MF, Ferrante RJ, Browne SE, Matthews RT, Kowall NW, Brown RH, Jr. (1997) *Increased 3-nitrotyrosine in both sporadic and familial amyotrophic lateral sclerosis.* Ann Neurol 42:644-654.

Beaulieu JM, Robertson J, Julien JP (1999) *Interactions between peripherin and neurofilaments in cultured cells: disruption of peripherin assembly by the NF-M and NF-H subunits.* Biochem Cell Biol 77:41-45.

Bebok Z, Mazzochi C, King SA, Hong JS, Sorscher EJ (1998) *The mechanism underlying cystic fibrosis transmembrane conductance regulator transport from the endoplasmic reticulum to the proteasome includes Sec61beta and a cytosolic, deglycosylated intermediary.* J Biol Chem 273:29873-29878.

Beckman JS, Carson M, Smith CD, Koppenol WH (1993) *ALS, SOD and peroxynitrite.* Nature 364:584.

Beers DR, Henkel JS, Xiao Q, Zhao W, Wang J, Yen AA, Siklos L, McKercher SR, Appel SH (2006) *Wild-type microglia extend survival in PU.1 knockout mice with familial amyotrophic lateral sclerosis.* Proc Natl Acad Sci U S A 103:16021-16026.

Bence NF, Sampat RM, Kopito RR (2001) *Impairment of the ubiquitin-proteasome system by protein aggregation.* Science 292:1552-1555.

Bence NF, Bennett EJ, Kopito RR (2005) *Application and analysis of the GFPu family of ubiquitin-proteasome system reporters.* Methods Enzymol 399:481-490.

Bendotti C, Carri MT (2004) *Lessons from models of SOD1-linked familial ALS.* Trends Mol Med 10:393-400.

Bendotti C, Hohmann C, Forloni G, Reeves R, Coyle JT, Oster-Granite ML (1990) *Developmental expression of somatostatin in mouse brain. II. In situ hybridization.* Brain Res Dev Brain Res 53:26-39.

Bendotti C, Atzori C, Piva R, Tortarolo M, Strong MJ, DeBiasi S, Migheli A (2004) *Activated p38MAPK is a novel component of the intracellular inclusions found in human amyotrophic lateral sclerosis and mutant SOD1 transgenic mice.* J Neuropathol Exp Neurol 63:113-119.

Bendotti C, Calvaresi N, Chiveri L, Prelle A, Moggio M, Braga M, Silani V, De Biasi S (2001) *Early vacuolization and mitochondrial damage in motor neurons of FALS mice are not associated with apoptosis or with changes in cytochrome oxidase histochemical reactivity.* J Neurol Sci 191:25-33.

Bochtler M, Ditzel L, Groll M, Hartmann C, Huber R (1999) *The proteasome.* Annu Rev Biophys Biomol Struct 28:295-317.

Boillee S, Yamanaka K, Lobsiger CS, Copeland NG, Jenkins NA, Kassiotis G, Kollias G, Cleveland DW (2006) *Onset and progression in inherited ALS determined by motor neurons and microglia.* Science 312:1389-1392.

Bommel H, Xie G, Rossoll W, Wiese S, Jablonka S, Boehm T, Sendtner M (2002) *Missense mutation in the tubulin-specific chaperone E (Tbce) gene in the mouse mutant progressive motor neuronopathy, a model of human motoneuron disease.* J Cell Biol 159:563-569.

Borchelt DR, Wong PC, Becher MW, Pardo CA, Lee MK, Xu ZS, Thinakaran G, Jenkins NA, Copeland NG, Sisodia SS, Cleveland DW, Price DL, Hoffman PN (1998) *Axonal transport of mutant superoxide dismutase 1 and focal axonal abnormalities in the proximal axons of transgenic mice.* Neurobiol Dis 5:27-35.

Borthwick GM, Johnson MA, Ince PG, Shaw PJ, Turnbull DM (1999) *Mitochondrial enzyme activity in amyotrophic lateral sclerosis: implications for the role of mitochondria in neuronal cell death.* Ann Neurol 46:787-790.

Bowman AB, Yoo SY, Dantuma NP, Zoghbi HY (2005) *Neuronal dysfunction in a polyglutamine disease model occurs in the absence of ubiquitin-proteasome system impairment and inversely correlates with the degree of nuclear inclusion formation.* Hum Mol Genet 14:679-691.

Bronson RT, Lake BD, Cook S, Taylor S, Davisson MT (1993) *Motor neuron degeneration of mice is a model of neuronal ceroid lipofuscinosis* (Batten's disease). Ann Neurol 33:381-385.

Browne SE, Bowling AC, Baik MJ, Gurney M, Brown RH, Jr., Beal MF (1998) *Metabolic dysfunction in familial, but not sporadic, amyotrophic lateral sclerosis.* J Neurochem 71:281-287.

Bruijn LI, Houseweart MK, Kato S, Anderson KL, Anderson SD, Ohama E, Reaume AG, Scott RW, Cleveland DW (1998) *Aggregation and motor neuron toxicity of an ALS-linked SOD1 mutant independent from wild-type SOD1.* Science 281:1851-1854.

Bruijn LI, Becher MW, Lee MK, Anderson KL, Jenkins NA, Copeland NG, Sisodia SS, Rothstein JD, Borchelt DR, Price DL, Cleveland DW (1997) *ALS-linked SOD1 mutant G85R mediates damage to astrocytes and promotes rapidly progressive disease with SOD1-containing inclusions.* Neuron 18:327-338.

Brunialti AL, Poirier C, Schmalbruch H, Guenet JL (1995) *The mouse mutation progressive motor neuronopathy (pmn) maps to chromosome 13.* Genomics 29:131-135.

Bruns CK, Kopito RR (2007) *Impaired post-translational folding of familial ALS-linked Cu, Zn superoxide dismutase mutants.* Embo J 26:855-866.

Buratti E, Baralle FE (2001) *Characterization and functional implications of the RNA binding properties of nuclear factor TDP-43, a novel splicing regulator of CFTR exon 9.* J Biol Chem 276:36337-36343.

Buratti E, Brindisi A, Pagani F, Baralle FE (2004) *Nuclear factor TDP-43 binds to the polymorphic TG repeats in CFTR intron 8 and causes skipping of exon 9: a functional link with disease penetrance.* Am J Hum Genet 74:1322-1325.

Burri L, Hockendorff J, Boehm U, Klamp T, Dohmen RJ, Levy F (2000) *Identification and characterization of a mammalian protein interacting with 20S proteasome precursors.* Proc Natl Acad Sci U S A 97:10348-10353.

Carri MT, Ferri A, Battistoni A, Famhy L, Gabbianelli R, Poccia F, Rotilio G (1997) *Expression of a Cu,Zn superoxide dismutase typical of familial amyotrophic lateral sclerosis induces mitochondrial alteration and increase of*

cytosolic Ca2+ concentration in transfected neuroblastoma SH-SY5Y cells. FEBS Lett 414:365-368.

Casciati A, Ferri A, Cozzolino M, Celsi F, Nencini M, Rotilio G, Carri MT (2002) *Oxidative modulation of nuclear factor-kappaB in human cells expressing mutant fALS-typical superoxide dismutases.* J Neurochem 83:1019-1029.

Cascio P, Hilton C, Kisselev AF, Rock KL, Goldberg AL (2001) *26S proteasomes and immunoproteasomes produce mainly N-extended versions of an antigenic peptide.* Embo J 20:2357-2366.

Cascio P, Call M, Petre BM, Walz T, Goldberg AL (2002) Properties of the hybrid form of the 26S proteasome containing both 19S and PA28 complexes. Embo J 21:2636-2645.

Chambers DM, Peters J, Abbott CM (1998) *The lethal mutation of the mouse wasted (wst) is a deletion that abolishes expression of a tissue-specific isoform of translation elongation factor 1alpha, encoded by the Eef1a2 gene.* Proc Natl Acad Sci U S A 95:4463-4468.

Chan HY, Warrick JM, Andriola I, Merry D, Bonini NM (2002) *Genetic modulation of polyglutamine toxicity by protein conjugation pathways in Drosophila.* Hum Mol Genet 11:2895-2904.

Chen P, Hochstrasser M (1996) *Autocatalytic subunit processing couples active site formation in the 20S proteasome to completion of assembly.* Cell 86:961-972.

Chen YZ, Bennett CL, Huynh HM, Blair IP, Puls I, Irobi J, Dierick I, Abel A, Kennerson ML, Rabin BA, Nicholson GA, Auer-Grumbach M, Wagner K, De Jonghe P, Griffin JW, Fischbeck KH, Timmerman V, Cornblath DR, Chance PF (2004) *DNA/RNA helicase gene mutations in a form of juvenile amyotrophic lateral sclerosis (ALS4).* Am J Hum Genet 74:1128-1135.

Cheroni C, Peviani M, Cascio P, Debiasi S, Monti C, Bendotti C (2005) *Accumulation of human SOD1 and ubiquitinated deposits in the spinal cord of SOD1G93A mice during motor neuron disease progression correlates with a decrease of proteasome.* Neurobiol Dis 18:509-522.

Choi JS, Cho S, Park SG, Park BC, Lee DH (2004) *Co-chaperone CHIP associates with mutant Cu/Zn-superoxide dismutase proteins linked to*

familial amyotrophic lateral sclerosis and promotes their degradation by proteasomes. Biochem Biophys Res Commun 321:574-583.

Chou SM (1992) *Immunohistochemical and ultrastructural classification of peripheral neuropathies with onion-bulbs.* Clin Neuropathol 11:109-114.

Chung J, Yang H, de Beus MD, Ryu CY, Cho K, Colon W (2003) *Cu/Zn superoxide dismutase can form pore-like structures.* Biochem Biophys Res Commun 312:873-876.

Ciavarro GL, Calvaresi N, Botturi A, Bendotti C, Andreoni G, Pedotti A (2003) *The densitometric physical fractionator for counting neuronal populations: application to a mouse model of familial amyotrophic lateral sclerosis.* J Neurosci Methods 129:61-71.

Ciechanover A, Heller H, Elias S, Haas AL, Hershko A (1980a) *ATP-dependent conjugation of reticulocyte proteins with the polypeptide required for protein degradation.* Proc Natl Acad Sci U S A 77:1365-1368.

Ciechanover A, Elias S, Heller H, Ferber S, Hershko A (1980b) *Characterization of the heat-stable polypeptide of the ATP-dependent proteolytic system from reticulocytes.* J Biol Chem 255:7525-7528.

Clement AM, Nguyen MD, Roberts EA, Garcia ML, Boillee S, Rule M, McMahon AP, Doucette W, Siwek D, Ferrante RJ, Brown RH, Jr., Julien JP, Goldstein LS, Cleveland DW (2003) *Wild-type nonneuronal cells extend survival of SOD1 mutant motor neurons in ALS mice.* Science 302:113-117.

Cleveland DW, Rothstein JD (2001) *From Charcot to Lou Gehrig: deciphering selective motor neuron death in ALS.* Nat Rev Neurosci 2:806-819.

Cook JC, Chock PB (1992) *Isoforms of mammalian ubiquitin-activating enzyme.* J Biol Chem 267:24315-24321.

Cook SA, Johnson KR, Bronson RT, Davisson MT (1995) *Neuromuscular degeneration (nmd): a mutation on mouse chromosome 19 that causes motor neuron degeneration.* Mamm Genome 6:187-191.

Corbo M, Hays AP (1992) *Peripherin and neurofilament protein coexist in spinal spheroids of motor neuron disease.* J Neuropathol Exp Neurol 51:531-537.

Corcia P, Mayeux-Portas V, Khoris J, de Toffol B, Autret A, Muh JP, Camu W, Andres C (2002) *Abnormal SMN1 gene copy number is a susceptibility factor for amyotrophic lateral sclerosis.* Ann Neurol 51:243-246.

Corriveau RA, Huh GS, Shatz CJ (1998) *Regulation of class I MHC gene expression in the developing and mature CNS by neural activity.* Neuron 21:505-520.

Cote F, Collard JF, Julien JP (1993) *Progressive neuronopathy in transgenic mice expressing the human neurofilament heavy gene: a mouse model of amyotrophic lateral sclerosis.* Cell 73:35-46.

Couillard-Despres S, Meier J, Julien JP (2000) *Extra axonal neurofilaments do not exacerbate disease caused by mutant Cu,Zn superoxide dismutase.* Neurobiol Dis 7:462-470.

Couillard-Despres S, Zhu Q, Wong PC, Price DL, Cleveland DW, Julien JP (1998) *Protective effect of neurofilament heavy gene overexpression in motor neuron disease induced by mutant superoxide dismutase.* Proc Natl Acad Sci U S A 95:9626-9630.

Cox GA, Mahaffey CL, Frankel WN (1998) *Identification of the mouse neuromuscular degeneration gene and mapping of a second site suppressor allele.* Neuron 21:1327-1337.

Crapo JD, Oury T, Rabouille C, Slot JW, Chang LY (1992) *Copper,zinc superoxide dismutase is primarily a cytosolic protein in human cells.* Proc Natl Acad Sci U S A 89:10405-10409.

Cummings CJ, Mancini MA, Antalffy B, DeFranco DB, Orr HT, Zoghbi HY (1998) *Chaperone suppression of aggregation and altered subcellular proteasome localization imply protein misfolding in SCA1.* Nat Genet 19:148-154.

Dal Canto MC, Gurney ME (1994) *Development of central nervous system pathology in a murine transgenic model of human amyotrophic lateral sclerosis.* Am J Pathol 145:1271-1279.

Dal Canto MC, Gurney ME (1995) *Neuropathological changes in two lines of mice carrying a transgene for mutant human Cu,Zn SOD, and in mice overexpressing wild type human SOD: a model of familial amyotrophic lateral sclerosis (FALS).* Brain Res 676:25-40.

Dangond F, Windhagen A, Groves CJ, Hafler DA (1997) *Constitutive expression of costimulatory molecules by human microglia and its relevance to CNS autoimmunity.* J Neuroimmunol 76:132-138.

Davy A, Bello P, Thierry-Mieg N, Vaglio P, Hitti J, Doucette-Stamm L, Thierry-Mieg D, Reboul J, Boulton S, Walhout AJ, Coux O, Vidal M (2001) *A protein-protein interaction map of the Caenorhabditis elegans 26S proteasome.* EMBO Rep 2:821-828.

Deng HX, Shi Y, Furukawa Y, Zhai H, Fu R, Liu E, Gorrie GH, Khan MS, Hung WY, Bigio EH, Lukas T, Dal Canto MC, O'Halloran TV, Siddique T (2006) *Conversion to the amyotrophic lateral sclerosis phenotype is associated with intermolecular linked insoluble aggregates of SOD1 in mitochondria.* Proc Natl Acad Sci U S A 103:7142-7147.

Desterro JM, Rodriguez MS, Hay RT (1998) *SUMO-1 modification of IkappaBalpha inhibits NF-kappaB activation.* Mol Cell 2:233-239.

Di Giorgio FP, Carrasco MA, Siao MC, Maniatis T, Eggan K (2007) *Non-cell autonomous effect of glia on motor neurons in an embryonic stem cell-based ALS model.* Nat Neurosci 10:608-614.

Di Noto L, Whitson LJ, Cao X, Hart PJ, Levine RL (2005) *Proteasomal degradation of mutant superoxide dismutases linked to amyotrophic lateral sclerosis.* J Biol Chem 280:39907-39913.

Diaz-Hernandez M, Hernandez F, Martin-Aparicio E, Gomez-Ramos P, Moran MA, Castano JG, Ferrer I, Avila J, Lucas JJ (2003) *Neuronal induction of the immunoproteasome in Huntington's disease.* J Neurosci 23:11653-11661.

Dick TP, Nussbaum AK, Deeg M, Heinemeyer W, Groll M, Schirle M, Keilholz W, Stevanovic S, Wolf DH, Huber R, Rammensee HG, Schild H (1998) *Contribution of proteasomal beta-subunits to the cleavage of peptide substrates analyzed with yeast mutants.* J Biol Chem 273:25637-25646.

Ditzel L, Huber R, Mann K, Heinemeyer W, Wolf DH, Groll M (1998) *Conformational constraints for protein self-cleavage in the proteasome.* J Mol Biol 279:1187-1191.

Doble A, Kennel P (2000) *Animal models of amyotrophic lateral sclerosis.* Amyotroph Lateral Scler Other Motor Neuron Disord 1:301-312.

Durham HD, Roy J, Dong L, Figlewicz DA (1997) *Aggregation of mutant Cu/Zn superoxide dismutase proteins in a culture model of ALS.* J Neuropathol Exp Neurol 56:523-530.

Ebneth A, Godemann R, Stamer K, Illenberger S, Trinczek B, Mandelkow E (1998) *Overexpression of tau protein inhibits kinesin-dependent trafficking of vesicles, mitochondria, and endoplasmic reticulum: implications for Alzheimer's disease.* J Cell Biol 143:777-794.

Edstrom E, Kullberg S, Ming Y, Zheng H, Ulfhake B (2004) *MHC class I, beta2 microglobulin, and the INF-gamma receptor are upregulated in aged motoneurons.* J Neurosci Res 78:892-900.

Eleuteri AM, Kohanski RA, Cardozo C, Orlowski M (1997) *Bovine spleen multicatalytic proteinase complex (proteasome). Replacement of X, Y, and Z subunits by LMP7, LMP2, and MECL1 and changes in properties and specificity.* J Biol Chem 272:11824-11831.

Elliott JL (2001) *Cytokine upregulation in a murine model of familial amyotrophic lateral sclerosis.* Brain Res Mol Brain Res 95:172-178.

Engelhardt JI, Siklos L, Appel SH (1997) *Altered calcium homeostasis and ultrastructure in motoneurons of mice caused by passively transferred anti-motoneuronal IgG.* J Neuropathol Exp Neurol 56:21-39.

Estevez AG, Crow JP, Sampson JB, Reiter C, Zhuang Y, Richardson GJ, Tarpey MM, Barbeito L, Beckman JS (1999) *Induction of nitric oxide-dependent apoptosis in motor neurons by zinc-deficient superoxide dismutase.* Science 286:2498-2500.

Fei E, Jia N, Yan M, Ying Z, Sun Q, Wang H, Zhang T, Ma X, Ding H, Yao X, Shi Y, Wang G (2006) *SUMO-1 modification increases human SOD1 stability and aggregation.* Biochem Biophys Res Commun 347:406-412.

Ferdous A, Gonzalez F, Sun L, Kodadek T, Johnston SA (2001) *The 19S regulatory particle of the proteasome is required for efficient transcription elongation by RNA polymerase II.* Mol Cell 7:981-991.

Ferraiuolo L, Heath PR, Holden H, Kasher P, Kirby J, Shaw PJ (2007) *Microarray analysis of the cellular pathways involved in the adaptation to and progression of motor neuron injury in the SOD1 G93A mouse model of familial ALS.* J Neurosci 27:9201-9219.

Ferrante RJ, Browne SE, Shinobu LA, Bowling AC, Baik MJ, MacGarvey U, Kowall NW, Brown RH, Jr., Beal MF (1997) *Evidence of increased oxidative*

damage in both sporadic and familial amyotrophic lateral sclerosis. J Neurochem 69:2064-2074.

Ford AL, Foulcher E, Lemckert FA, Sedgwick JD (1996) *Microglia induce CD4 T lymphocyte final effector function and death.* J Exp Med 184:1737-1745.

Forman HJ, Fridovich I (1973) *Superoxide dismutase: a comparison of rate constants.* Arch Biochem Biophys 158:396-400.

Fray AE, Ince PG, Banner SJ, Milton ID, Usher PA, Cookson MR, Shaw PJ (1998) *The expression of the glial glutamate transporter protein EAAT2 in motor neuron disease: an immunohistochemical study.* Eur J Neurosci 10:2481-2489.

Fu H, Reis N, Lee Y, Glickman MH, Vierstra RD (2001) *Subunit interaction maps for the regulatory particle of the 26S proteasome and the COP9 signalosome.* Embo J 20:7096-7107.

Fujita Y, Okamoto K (2005) *Golgi apparatus of the motor neurons in patients with amyotrophic lateral sclerosis and in mice models of amyotrophic lateral sclerosis.* Neuropathology 25:388-394.

Furukawa Y, O'Halloran TV (2005) *Amyotrophic lateral sclerosis mutations have the greatest destabilizing effect on the apo- and reduced form of SOD1, leading to unfolding and oxidative aggregation.* J Biol Chem 280:17266-17274.

Gillardon F, Kloss A, Berg M, Neumann M, Mechtler K, Hengerer B, Dahlmann B (2007) *The 20S proteasome isolated from Alzheimer's disease brain shows post-translational modifications but unchanged proteolytic activity.* J Neurochem 101:1483-1490.

Gillette TG, Huang W, Russell SJ, Reed SH, Johnston SA, Friedberg EC (2001) *The 19S complex of the proteasome regulates nucleotide excision repair in yeast.* Genes Dev 15:1528-1539.

Glickman MH, Rubin DM, Coux O, Wefes I, Pfeifer G, Cjeka Z, Baumeister W, Fried VA, Finley D (1998) *A subcomplex of the proteasome regulatory particle required for ubiquitin-conjugate degradation and related to the COP9-signalosome and eIF3.* Cell 94:615-623.

Goldberg AL, Cascio P, Saric T, Rock KL (2002) *The importance of the proteasome and subsequent proteolytic steps in the generation of antigenic peptides.* Mol Immunol 39:147-164.

Goldknopf IL, Busch H (1977) *Isopeptide linkage between nonhistone and histone 2A polypeptides of chromosomal conjugate-protein A24.* Proc Natl Acad Sci U S A 74:864-868.

Gong YH, Parsadanian AS, Andreeva A, Snider WD, Elliott JL (2000) *Restricted expression of G86R Cu/Zn superoxide dismutase in astrocytes results in astrocytosis but does not cause motoneuron degeneration.* J Neurosci 20:660-665.

Goodsell DS, Olson AJ (2000) *Structural symmetry and protein function.* Annu Rev Biophys Biomol Struct 29:105-153.

Graves MC, Fiala M, Dinglasan LA, Liu NQ, Sayre J, Chiappelli F, van Kooten C, Vinters HV (2004) *Inflammation in amyotrophic lateral sclerosis spinal cord and brain is mediated by activated macrophages, mast cells and T cells.* Amyotroph Lateral Scler Other Motor Neuron Disord 5:213-219.

Griffin TA, Nandi D, Cruz M, Fehling HJ, Kaer LV, Monaco JJ, Colbert RA (1998) *Immunoproteasome assembly: cooperative incorporation of interferon gamma (IFN-gamma)-inducible subunits.* J Exp Med 187:97-104.

Groll M, Ditzel L, Lowe J, Stock D, Bochtler M, Bartunik HD, Huber R (1997) *Structure of 20S proteasome from yeast at 2.4 A resolution.* Nature 386:463-471.

Groll M, Bajorek M, Kohler A, Moroder L, Rubin DM, Huber R, Glickman MH, Finley D (2000) *A gated channel into the proteasome core particle.* Nat Struct Biol 7:1062-1067.

Grune T (2000) *Oxidative stress, aging and the proteasomal system.* Biogerontology 1:31-40.

Grune T, Blasig IE, Sitte N, Roloff B, Haseloff R, Davies KJ (1998) *Peroxynitrite increases the degradation of aconitase and other cellular proteins by proteasome.* J Biol Chem 273:10857-10862.

Gurney ME, Pu H, Chiu AY, Dal Canto MC, Polchow CY, Alexander DD, Caliendo J, Hentati A, Kwon YW, Deng HX, et al. (1994) *Motor neuron*

degeneration in mice that express a human Cu,Zn superoxide dismutase mutation. Science 264:1772-1775.

Hadano S, Benn SC, Kakuta S, Otomo A, Sudo K, Kunita R, Suzuki-Utsunomiya K, Mizumura H, Shefner JM, Cox GA, Iwakura Y, Brown RH, Jr., Ikeda JE (2006) *Mice deficient in the Rab5 guanine nucleotide exchange factor ALS2/alsin exhibit age-dependent neurological deficits and altered endosome trafficking.* Hum Mol Genet 15:233-250.

Hadano S, Hand CK, Osuga H, Yanagisawa Y, Otomo A, Devon RS, Miyamoto N, Showguchi-Miyata J, Okada Y, Singaraja R, Figlewicz DA, Kwiatkowski T, Hosler BA, Sagie T, Skaug J, Nasir J, Brown RH, Jr., Scherer SW, Rouleau GA, Hayden MR, Ikeda JE (2001) *A gene encoding a putative GTPase regulator is mutated in familial amyotrophic lateral sclerosis 2.* Nat Genet 29:166-173.

Hafezparast M, Klocke R, Ruhrberg C, Marquardt A, Ahmad-Annuar A, Bowen S, Lalli G, Witherden AS, Hummerich H, Nicholson S, Morgan PJ, Oozageer R, Priestley JV, Averill S, King VR, Ball S, Peters J, Toda T, Yamamoto A, Hiraoka Y, Augustin M, Korthaus D, Wattler S, Wabnitz P, Dickneite C, Lampel S, Boehme F, Peraus G, Popp A, Rudelius M, Schlegel J, Fuchs H, Hrabe de Angelis M, Schiavo G, Shima DT, Russ AP, Stumm G, Martin JE, Fisher EM (2003) *Mutations in dynein link motor neuron degeneration to defects in retrograde transport.* Science 300:808-812.

Hall ED, Oostveen JA, Gurney ME (1998) *Relationship of microglial and astrocytic activation to disease onset and progression in a transgenic model of familial ALS.* Glia 23:249-256.

Hallermalm K, Seki K, Wei C, Castelli C, Rivoltini L, Kiessling R, Levitskaya J (2001) *Tumor necrosis factor-alpha induces coordinated changes in major histocompatibility class I presentation pathway, resulting in increased stability of class I complexes at the cell surface.* Blood 98:1108-1115.

Hammer RP, Jr., Tomiyasu U, Scheibel AB (1979) *Degeneration of the human Betz cell due to amyotrophic lateral sclerosis.* Exp Neurol 63:336-346.

Handley-Gearhart PM, Stephen AG, Trausch-Azar JS, Ciechanover A, Schwartz AL (1994) *Human ubiquitin-activating enzyme, E1. Indication of potential nuclear and cytoplasmic subpopulations using epitope-tagged cDNA constructs.* J Biol Chem 269:33171-33178.

Hatakeyama S, Nakayama KI (2003) *U-box proteins as a new family of ubiquitin ligases.* Biochem Biophys Res Commun 302:635-645.

Hayward LJ, Rodriguez JA, Kim JW, Tiwari A, Goto JJ, Cabelli DE, Valentine JS, Brown RH, Jr. (2002) *Decreased metallation and activity in subsets of mutant superoxide dismutases associated with familial amyotrophic lateral sclerosis.* J Biol Chem 277:15923-15931.

Heink S, Ludwig D, Kloetzel PM, Kruger E (2005) *IFN-gamma-induced immune adaptation of the proteasome system is an accelerated and transient response.* Proc Natl Acad Sci U S A 102:9241-9246.

Henkel JS, Beers DR, Siklos L, Appel SH (2006) *The chemokine MCP-1 and the dendritic and myeloid cells it attracts are increased in the mSOD1 mouse model of ALS.* Mol Cell Neurosci 31:427-437.

Henkel JS, Engelhardt JI, Siklos L, Simpson EP, Kim SH, Pan T, Goodman JC, Siddique T, Beers DR, Appel SH (2004) *Presence of dendritic cells, MCP-1, and activated microglia/macrophages in amyotrophic lateral sclerosis spinal cord tissue.* Ann Neurol 55:221-235.

Hensley K, Floyd RA, Gordon B, Mou S, Pye QN, Stewart C, West M, Williamson K (2002) *Temporal patterns of cytokine and apoptosis-related gene expression in spinal cords of the G93A-SOD1 mouse model of amyotrophic lateral sclerosis.* J Neurochem 82:365-374.

Hershko A, Ciechanover A, Heller H, Haas AL, Rose IA (1980) *Proposed role of ATP in protein breakdown: conjugation of protein with multiple chains of the polypeptide of ATP-dependent proteolysis.* Proc Natl Acad Sci U S A 77:1783-1786.

Hervias I, Beal MF, Manfredi G (2006) *Mitochondrial dysfunction and amyotrophic lateral sclerosis.* Muscle Nerve 33:598-608.

Hicke L (2001) *Protein regulation by monoubiquitin.* Nat Rev Mol Cell Biol 2:195-201.

Higgins CM, Jung C, Ding H, Xu Z (2002) *Mutant Cu, Zn superoxide dismutase that causes motoneuron degeneration is present in mitochondria in the CNS.* J Neurosci 22:RC215.

Hirano A, Nakano I, Kurland LT, Mulder DW, Holley PW, Saccomanno G (1984) *Fine structural study of neurofibrillary changes in a family with amyotrophic lateral sclerosis.* J Neuropathol Exp Neurol 43:471-480.

Hirano K, Fukuta M, Adachi T, Hayashi K, Sugiura M, Mori Y, Toyoshi K (1985) *In vitro synthesis of superoxide dismutases of rat liver.* Biochem Biophys Res Commun 129:89-94.

Hishikawa N, Niwa J, Doyu M, Ito T, Ishigaki S, Hashizume Y, Sobue G (2003) *Dorfin localizes to the ubiquitylated inclusions in Parkinson's disease, dementia with Lewy bodies, multiple system atrophy, and amyotrophic lateral sclerosis.* Am J Pathol 163:609-619.

Hoffman EK, Wilcox HM, Scott RW, Siman R (1996) *Proteasome inhibition enhances the stability of mouse Cu/Zn superoxide dismutase with mutations linked to familial amyotrophic lateral sclerosis.* J Neurol Sci 139:15-20.

Hofmann K, Falquet L (2001) *A ubiquitin-interacting motif conserved in components of the proteasomal and lysosomal protein degradation systems.* Trends Biochem Sci 26:347-350.

Holzhutter HG, Frommel C, Kloetzel PM (1999) *A theoretical approach towards the identification of cleavage-determining amino acid motifs of the 20 S proteasome.* J Mol Biol 286:1251-1265.

Howland DS, Liu J, She Y, Goad B, Maragakis NJ, Kim B, Erickson J, Kulik J, DeVito L, Psaltis G, DeGennaro LJ, Cleveland DW, Rothstein JD (2002) *Focal loss of the glutamate transporter EAAT2 in a transgenic rat model of SOD1 mutant-mediated amyotrophic lateral sclerosis (ALS).* Proc Natl Acad Sci U S A 99:1604-1609.

Huang TT, Wuerzberger-Davis SM, Wu ZH, Miyamoto S (2003) *Sequential modification of NEMO/IKKgamma by SUMO-1 and ubiquitin mediates NF-kappaB activation by genotoxic stress.* Cell 115:565-576.

Hudson AJ (1981) *Amyotrophic lateral sclerosis and its association with dementia, parkinsonism and other neurological disorders: a review.* Brain 104:217-247.

Huh GS, Boulanger LM, Du H, Riquelme PA, Brotz TM, Shatz CJ (2000) *Functional requirement for class I MHC in CNS development and plasticity.* Science 290:2155-2159.

Hyun DH, Lee M, Halliwell B, Jenner P (2003) *Proteasomal inhibition causes the formation of protein aggregates containing a wide range of proteins, including nitrated proteins.* J Neurochem 86:363-373.

Ii K, Ito H, Tanaka K, Hirano A (1997) *Immunocytochemical co-localization of the proteasome in ubiquitinated structures in neurodegenerative diseases and the elderly.* J Neuropathol Exp Neurol 56:125-131.

Inai Y, Nishikimi M (2002) *Increased degradation of oxidized proteins in yeast defective in 26 S proteasome assembly.* Arch Biochem Biophys 404:279-284.

Ishigaki S, Niwa J, Ando Y, Yoshihara T, Sawada K, Doyu M, Yamamoto M, Kato K, Yotsumoto Y, Sobue G (2002) *Differentially expressed genes in sporadic amyotrophic lateral sclerosis spinal cords--screening by molecular indexing and subsequent cDNA microarray analysis.* FEBS Lett 531:354-358.

Ishihara T, Hong M, Zhang B, Nakagawa Y, Lee MK, Trojanowski JQ, Lee VM (1999) *Age-dependent emergence and progression of a tauopathy in transgenic mice overexpressing the shortest human tau isoform.* Neuron 24:751-762.

Jaarsma D, Rognoni F, van Duijn W, Verspaget HW, Haasdijk ED, Holstege JC (2001) *CuZn superoxide dismutase (SOD1) accumulates in vacuolated mitochondria in transgenic mice expressing amyotrophic lateral sclerosis-linked SOD1 mutations.* Acta Neuropathol (Berl) 102:293-305.

Jaarsma D, Haasdijk ED, Grashorn JA, Hawkins R, van Duijn W, Verspaget HW, London J, Holstege JC (2000) *Human Cu/Zn superoxide dismutase (SOD1) overexpression in mice causes mitochondrial vacuolization, axonal degeneration, and premature motoneuron death and accelerates motoneuron disease in mice expressing a familial amyotrophic lateral sclerosis mutant SOD1.* Neurobiol Dis 7:623-643.

Jackson M, Morrison KE, Al-Chalabi A, Bakker M, Leigh PN (1996) *Analysis of chromosome 5q13 genes in amyotrophic lateral sclerosis: homozygous NAIP deletion in a sporadic case.* Ann Neurol 39:796-800.

Jackson PK, Eldridge AG, Freed E, Furstenthal L, Hsu JY, Kaiser BK, Reimann JD (2000) *The lore of the RINGs: substrate recognition and catalysis by ubiquitin ligases.* Trends Cell Biol 10:429-439.

Jahngen-Hodge J, Obin MS, Gong X, Shang F, Nowell TR, Jr., Gong J, Abasi H, Blumberg J, Taylor A (1997) *Regulation of ubiquitin-conjugating enzymes by glutathione following oxidative stress.* J Biol Chem 272:28218-28226.

Jana NR, Zemskov EA, Wang G, Nukina N (2001) *Altered proteasomal function due to the expression of polyglutamine-expanded truncated N-terminal huntingtin induces apoptosis by caspase activation through mitochondrial cytochrome c release.* Hum Mol Genet 10:1049-1059.

Joazeiro CA, Weissman AM (2000) *RING finger proteins: mediators of ubiquitin ligase activity.* Cell 102:549-552.

Johnson ES, Bartel B, Seufert W, Varshavsky A (1992) *Ubiquitin as a degradation signal.* Embo J 11:497-505.

Johnston JA, Dalton MJ, Gurney ME, Kopito RR (2000) *Formation of high molecular weight complexes of mutant Cu, Zn-superoxide dismutase in a mouse model for familial amyotrophic lateral sclerosis.* Proc Natl Acad Sci U S A 97:12571-12576.

Joly E, Oldstone MB (1992) *Neuronal cells are deficient in loading peptides onto MHC class I molecules.* Neuron 8:1185-1190.

Jonsson PA, Graffmo KS, Andersen PM, Brannstrom T, Lindberg M, Oliveberg M, Marklund SL (2006) *Disulphide-reduced superoxide dismutase-1 in CNS of transgenic amyotrophic lateral sclerosis models.* Brain 129:451-464.

Jung C, Higgins CM, Xu Z (2002) *Mitochondrial electron transport chain complex dysfunction in a transgenic mouse model for amyotrophic lateral sclerosis.* J Neurochem 83:535-545.

Kabashi E, Agar JN, Taylor DM, Minotti S, Durham HD (2004) *Focal dysfunction of the proteasome: a pathogenic factor in a mouse model of amyotrophic lateral sclerosis.* J Neurochem 89:1325-1335.

Kabuta T, Suzuki Y, Wada K (2006) *Degradation of amyotrophic lateral sclerosis-linked mutant Cu,Zn-superoxide dismutase proteins by macroautophagy and the proteasome.* J Biol Chem 281:30524-30533.

Kanekura K, Hashimoto Y, Niikura T, Aiso S, Matsuoka M, Nishimoto I (2004) *Alsin, the product of ALS2 gene, suppresses SOD1 mutant neurotoxicity through RhoGEF domain by interacting with SOD1 mutants.* J Biol Chem 279:19247-19256.

Kato S, Saito M, Hirano A, Ohama E (1999) *Recent advances in research on neuropathological aspects of familial amyotrophic lateral sclerosis with superoxide dismutase 1 gene mutations: neuronal Lewy body-like hyaline inclusions and astrocytic hyaline inclusions.* Histol Histopathol 14:973-989.

Kaur C, Ling EA (1992) *Activation and re-expression of surface antigen in microglia following an epidural application of kainic acid in the rat brain.* J Anat 180 (Pt 2):333-342.

Kawamata T, Akiyama H, Yamada T, McGeer PL (1992) *Immunologic reactions in amyotrophic lateral sclerosis brain and spinal cord tissue.* Am J Pathol 140:691-707.

Keller GA, Warner TG, Steimer KS, Hallewell RA (1991) *Cu,Zn superoxide dismutase is a peroxisomal enzyme in human fibroblasts and hepatoma cells.* Proc Natl Acad Sci U S A 88:7381-7385.

Keller JN, Markesbery WR (2000) *Proteasome inhibition results in increased poly-ADP-ribosylation: implications for neuron death.* J Neurosci Res 61:436-442.

Keller JN, Huang FF, Markesbery WR (2000a) D*ecreased levels of proteasome activity and proteasome expression in aging spinal cord.* Neuroscience 98:149-156.

Keller JN, Hanni KB, Markesbery WR (2000b) I*mpaired proteasome function in Alzheimer's disease.* J Neurochem 75:436-439.

Keller JN, Huang FF, Zhu H, Yu J, Ho YS, Kindy TS (2000c) *Oxidative stress-associated impairment of proteasome activity during ischemia-reperfusion injury.* J Cereb Blood Flow Metab 20:1467-1473.

Kennel PF, Finiels F, Revah F, Mallet J (1996) *Neuromuscular function impairment is not caused by motor neurone loss in FALS mice: an electromyographic study.* Neuroreport 7:1427-1431.

Kiernan JA, Hudson AJ (1991) *Changes in sizes of cortical and lower motor neurons in amyotrophic lateral sclerosis.* Brain 114 (Pt 2):843-853.

Kikuchi H, Almer G, Yamashita S, Guegan C, Nagai M, Xu Z, Sosunov AA, McKhann GM, 2nd, Przedborski S (2006) *Spinal cord endoplasmic reticulum stress associated with a microsomal accumulation of mutant superoxide dismutase-1 in an ALS model.* Proc Natl Acad Sci U S A 103:6025-6030.

Kilani M, Micallef J, Soubrouillard C, Rey-Lardiller D, Demattei C, Dib M, Philippot P, Ceccaldi M, Pouget J, Blin O (2004) *A longitudinal study of the evolution of cognitive function and affective state in patients with amyotrophic lateral sclerosis.* Amyotroph Lateral Scler Other Motor Neuron Disord 5:46-54.

Kitada T, Asakawa S, Hattori N, Matsumine H, Yamamura Y, Minoshima S, Yokochi M, Mizuno Y, Shimizu N (1998) *Mutations in the parkin gene cause autosomal recessive juvenile parkinsonism.* Nature 392:605-608.

Kohler A, Bajorek M, Groll M, Moroder L, Rubin DM, Huber R, Glickman MH, Finley D (2001) *The substrate translocation channel of the proteasome.* Biochimie 83:325-332.

Kolde G, Bachus R, Ludolph AC (1996) *Skin involvement in amyotrophic lateral sclerosis.* Lancet 347:1226-1227.

Komatsu T, Bi Z, Reiss CS (1996) *Interferon-gamma induced type I nitric oxide synthase activity inhibits viral replication in neurons.* J Neuroimmunol 68:101-108.

Kong J, Xu Z (2000) *Overexpression of neurofilament subunit NF-L and NF-H extends survival of a mouse model for amyotrophic lateral sclerosis.* Neurosci Lett 281:72-74.

Kristiansen M, Deriziotis P, Dimcheff DE, Jackson GS, Ovaa H, Naumann H, Clarke AR, van Leeuwen FW, Menendez-Benito V, Dantuma NP, Portis JL, Collinge J, Tabrizi SJ (2007) *Disease-associated prion protein oligomers inhibit the 26S proteasome.* Mol Cell 26:175-188.

Krogan NJ, Lam MH, Fillingham J, Keogh MC, Gebbia M, Li J, Datta N, Cagney G, Buratowski S, Emili A, Greenblatt JF (2004) *Proteasome involvement in the repair of DNA double-strand breaks.* Mol Cell 16:1027-1034.

Kurland LT, Molgaard CA (1982) *Guamanian ALS: hereditary or acquired?* Adv Neurol 36:165-171.

Kurtzke JF (1991) *Risk factors in amyotrophic lateral sclerosis.* Adv Neurol 56:245-270.

Kwak MK, Wakabayashi N, Greenlaw JL, Yamamoto M, Kensler TW (2003a) *Antioxidants enhance mammalian proteasome expression through the Keap1-Nrf2 signaling pathway.* Mol Cell Biol 23:8786-8794.

Kwak MK, Wakabayashi N, Itoh K, Motohashi H, Yamamoto M, Kensler TW (2003b) *Modulation of gene expression by cancer chemopreventive dithiolethiones through the Keap1-Nrf2 pathway. Identification of novel gene clusters for cell survival.* J Biol Chem 278:8135-8145.

Kwak S, Masaki T, Ishiura S, Sugita H (1991) *Multicatalytic proteinase is present in Lewy bodies and neurofibrillary tangles in diffuse Lewy body disease brains.* Neurosci Lett 128:21-24.

Lai C, Xie C, McCormack SG, Chiang HC, Michalak MK, Lin X, Chandran J, Shim H, Shimoji M, Cookson MR, Huganir RL, Rothstein JD, Price DL, Wong PC, Martin LJ, Zhu JJ, Cai H (2006) *Amyotrophic lateral sclerosis 2-deficiency leads to neuronal degeneration in amyotrophic lateral sclerosis through altered AMPA receptor trafficking.* J Neurosci 26:11798-11806.

Lambrechts D, Storkebaum E, Morimoto M, Del-Favero J, Desmet F, Marklund SL, Wyns S, Thijs V, Andersson J, van Marion I, Al-Chalabi A, Bornes S, Musson R, Hansen V, Beckman L, Adolfsson R, Pall HS, Prats H, Vermeire S, Rutgeerts P, Katayama S, Awata T, Leigh N, Lang-Lazdunski L, Dewerchin M, Shaw C, Moons L, Vlietinck R, Morrison KE, Robberecht W, Van Broeckhoven C, Collen D, Andersen PM, Carmeliet P (2003) *VEGF is a modifier of amyotrophic lateral sclerosis in mice and humans and protects motoneurons against ischemic death.* Nat Genet 34:383-394.

Lanier LL (2005) *NK cell recognition.* Annu Rev Immunol 23:225-274.

Lariviere RC, Beaulieu JM, Nguyen MD, Julien JP (2003) *Peripherin is not a contributing factor to motor neuron disease in a mouse model of amyotrophic lateral sclerosis caused by mutant superoxide dismutase.* Neurobiol Dis 13:158-166.

Lashuel HA, Hartley D, Petre BM, Walz T, Lansbury PT, Jr. (2002) *Neurodegenerative disease: amyloid pores from pathogenic mutations.* Nature 418:291.

Lederer CW, Torrisi A, Pantelidou M, Santama N, Cavallaro S (2007) *Pathways and genes differentially expressed in the motor cortex of patients with sporadic amyotrophic lateral sclerosis.* BMC Genomics 8:26.

Leigh PN, Dodson A, Swash M, Brion JP, Anderton BH (1989) *Cytoskeletal abnormalities in motor neuron disease. An immunocytochemical study.* Brain 112 (Pt 2):521-535.

Lepock JR, Arnold LD, Torrie BH, Andrews B, Kruuv J (1985) *Structural analyses of various Cu2+, Zn2+-superoxide dismutases by differential scanning calorimetry and Raman spectroscopy.* Arch Biochem Biophys 241:243-251.

Lewis J, McGowan E, Rockwood J, Melrose H, Nacharaju P, Van Slegtenhorst M, Gwinn-Hardy K, Paul Murphy M, Baker M, Yu X, Duff K, Hardy J, Corral A, Lin WL, Yen SH, Dickson DW, Davies P, Hutton M (2000) *Neurofibrillary tangles, amyotrophy and progressive motor disturbance in mice expressing mutant (P301L) tau protein.* Nat Genet 25:402-405.

Ligon LA, LaMonte BH, Wallace KE, Weber N, Kalb RG, Holzbaur EL (2005) *Mutant superoxide dismutase disrupts cytoplasmic dynein in motor neurons.* Neuroreport 16:533-536.

Lin CL, Bristol LA, Jin L, Dykes-Hoberg M, Crawford T, Clawson L, Rothstein JD (1998) *Aberrant RNA processing in a neurodegenerative disease: the cause for absent EAAT2, a glutamate transporter, in amyotrophic lateral sclerosis.* Neuron 20:589-602.

Lindberg MJ, Tibell L, Oliveberg M (2002) *Common denominator of Cu/Zn superoxide dismutase mutants associated with amyotrophic lateral sclerosis: decreased stability of the apo state.* Proc Natl Acad Sci U S A 99:16607-16612.

Lindberg MJ, Normark J, Holmgren A, Oliveberg M (2004) *Folding of human superoxide dismutase: disulfide reduction prevents dimerization and produces marginally stable monomers.* Proc Natl Acad Sci U S A 101:15893-15898.

Lindberg MJ, Bystrom R, Boknas N, Andersen PM, Oliveberg M (2005) *Systematically perturbed folding patterns of amyotrophic lateral sclerosis (ALS)-associated SOD1 mutants.* Proc Natl Acad Sci U S A 102:9754-9759.

Lindsten K, Menendez-Benito V, Masucci MG, Dantuma NP (2003) *A transgenic mouse model of the ubiquitin/proteasome system.* Nat Biotechnol 21:897-902.

Liu J, Li Z, Yan H, Wang L, Chen J (1999) *The design and synthesis of ALS inhibitors from pharmacophore models.* Bioorg Med Chem Lett 9:1927-1932.

Liu J, Lillo C, Jonsson PA, Vande Velde C, Ward CM, Miller TM, Subramaniam JR, Rothstein JD, Marklund S, Andersen PM, Brannstrom T, Gredal O, Wong PC, Williams DS, Cleveland DW (2004) *Toxicity of familial ALS-linked SOD1 mutants from selective recruitment to spinal mitochondria.* Neuron 43:5-17.

Liu Y, Fallon L, Lashuel HA, Liu Z, Lansbury PT, Jr. (2002) *The UCH-L1 gene encodes two opposing enzymatic activities that affect alpha-synuclein degradation and Parkinson's disease susceptibility.* Cell 111:209-218.

Lomen-Hoerth C, Murphy J, Langmore S, Kramer JH, Olney RK, Miller B (2003) *Are amyotrophic lateral sclerosis patients cognitively normal?* Neurology 60:1094-1097.

Lorick KL, Jensen JP, Fang S, Ong AM, Hatakeyama S, Weissman AM (1999) *RING fingers mediate ubiquitin-conjugating enzyme (E2)-dependent ubiquitination.* Proc Natl Acad Sci U S A 96:11364-11369.

Lowe J, Stock D, Jap B, Zwickl P, Baumeister W, Huber R (1995) *Crystal structure of the 20S proteasome from the archaeon T. acidophilum at 3.4 A resolution.* Science 268:533-539.

Ma CP, Slaughter CA, DeMartino GN (1992) *Identification, purification, and characterization of a protein activator (PA28) of the 20 S proteasome (macropain).* J Biol Chem 267:10515-10523.

Ma J, Lindquist S (2001) *Wild-type PrP and a mutant associated with prion disease are subject to retrograde transport and proteasome degradation.* Proc Natl Acad Sci U S A 98:14955-14960.

Ma J, Wollmann R, Lindquist S (2002) *Neurotoxicity and neurodegeneration when PrP accumulates in the cytosol.* Science 298:1781-1785.

Martin N, Jaubert J, Gounon P, Salido E, Haase G, Szatanik M, Guenet JL (2002) *A missense mutation in Tbce causes progressive motor neuronopathy in mice.* Nat Genet 32:443-447.

Martin S, Gee JR, Bruce-Keller AJ, Keller JN (2004) *Loss of an individual proteasome subunit alters motor function but not cognitive function or ambulation in mice.* Neurosci Lett 357:76-78.

Matsumoto G, Kim S, Morimoto RI (2006) *Huntingtin and mutant SOD1 form aggregate structures with distinct molecular properties in human cells.* J Biol Chem 281:4477-4485.

Matsumoto G, Stojanovic A, Holmberg CI, Kim S, Morimoto RI (2005) *Structural properties and neuronal toxicity of amyotrophic lateral sclerosis-associated Cu/Zn superoxide dismutase 1 aggregates.* J Cell Biol 171:75-85.

McGeer PL, Akiyama H, Itagaki S, McGeer EG (1989) *Immune system response in Alzheimer's disease.* Can J Neurol Sci 16:516-527.

McGuire V, Longstreth WT, Jr., Koepsell TD, van Belle G (1996) *Incidence of amyotrophic lateral sclerosis in three counties in western Washington state.* Neurology 47:571-573.

McNaught KS, Jenner P (2001) *Proteasomal function is impaired in substantia nigra in Parkinson's disease.* Neurosci Lett 297:191-194.

McPhail LT, McBride CB, McGraw J, Steeves JD, Tetzlaff W (2004) *Axotomy abolishes NeuN expression in facial but not rubrospinal neurons.* Exp Neurol 185:182-190.

Meacham GC, Patterson C, Zhang W, Younger JM, Cyr DM (2001) *The Hsc70 co-chaperone CHIP targets immature CFTR for proteasomal degradation.* Nat Cell Biol 3:100-105.

Mendonca DM, Chimelli L, Martinez AM (2006) *Expression of ubiquitin and proteasome in motorneurons and astrocytes of spinal cords from patients with amyotrophic lateral sclerosis.* Neurosci Lett 404:315-319.

Menendez-Benito V, Verhoef LG, Masucci MG, Dantuma NP (2005) *Endoplasmic reticulum stress compromises the ubiquitin-proteasome system.* Hum Mol Genet 14:2787-2799.

Mennini T, Bigini P, Ravizza T, Vezzani A, Calvaresi N, Tortarolo M, Bendotti C (2002) *Expression of glutamate receptor subtypes in the spinal cord of control and mnd mice, a model of motor neuron disorder.* J Neurosci Res 70:553-560.

Mercado PA, Ayala YM, Romano M, Buratti E, Baralle FE (2005) *Depletion of TDP 43 overrides the need for exonic and intronic splicing enhancers in the human apoA-II gene.* Nucleic Acids Res 33:6000-6010.

Messer A, Strominger NL, Mazurkiewicz JE (1987) *Histopathology of the late-onset motor neuron degeneration (Mnd) mutant in the mouse.* J Neurogenet 4:201-213.

Migheli A, Autilio-Gambetti L, Gambetti P, Mocellini C, Vigliani MC, Schiffer D (1990) *Ubiquitinated filamentous inclusions in spinal cord of patients with motor neuron disease.* Neurosci Lett 114:5-10.

Migheli A, Atzori C, Piva R, Tortarolo M, Girelli M, Schiffer D, Bendotti C (1999) *Lack of apoptosis in mice with ALS.* Nat Med 5:966-967.

Mitsumoto H, Bradley WG (1982) *Murine motor neuron disease (the wobbler mouse): degeneration and regeneration of the lower motor neuron.* Brain 105 (Pt 4):811-834.

Mitsumoto H, Chad DA, Pioro EP (1998) *Amyotrophic Lateral Sclerosis.* New York: Oxford Univ. Press.

Miyazaki K, Fujita T, Ozaki T, Kato C, Kurose Y, Sakamoto M, Kato S, Goto T, Itoyama Y, Aoki M, Nakagawara A (2004) *NEDL1, a novel ubiquitin-protein isopeptide ligase for dishevelled-1, targets mutant superoxide dismutase-1.* J Biol Chem 279:11327-11335.

Moretta L, Bottino C, Pende D, Vitale M, Mingari MC, Moretta A (2004) *Different checkpoints in human NK-cell activation.* Trends Immunol 25:670-676.

Mourelatos Z, Hirano A, Rosenquist AC, Gonatas NK (1994) F*ragmentation of the Golgi apparatus of motor neurons in amyotrophic lateral sclerosis (ALS). Clinical studies in ALS of Guam and experimental studies in deafferented neurons and in beta,beta'-iminodipropionitrile axonopathy.* Am J Pathol 144:1288-1300.

Murakami T, Warita H, Hayashi T, Sato K, Manabe Y, Mizuno S, Yamane K, Abe K (2001) *A novel SOD1 gene mutation in familial ALS with low penetrance in females.* J Neurol Sci 189:45-47.

Nagai M, Re DB, Nagata T, Chalazonitis A, Jessell TM, Wichterle H, Przedborski S (2007) *Astrocytes expressing ALS-linked mutated SOD1 release factors selectively toxic to motor neurons.* Nat Neurosci 10:615-622.

Nakamura S, Kawamoto Y, Nakano S, Ikemoto A, Akiguchi I, Kimura J (1997) *Cyclin-dependent kinase 5 in Lewy body-like inclusions in anterior horn cells of a patient with sporadic amyotrophic lateral sclerosis.* Neurology 48:267-270.

Nakano I, Hirano A (1987) *Atrophic cell processes of large motor neurons in the anterior horn in amyotrophic lateral sclerosis: observation with silver impregnation method.* J Neuropathol Exp Neurol 46:40-49.

Neumann M, Sampathu DM, Kwong LK, Truax AC, Micsenyi MC, Chou TT, Bruce J, Schuck T, Grossman M, Clark CM, McCluskey LF, Miller BL, Masliah E, Mackenzie IR, Feldman H, Feiden W, Kretzschmar HA, Trojanowski JQ, Lee VM (2006) *Ubiquitinated TDP-43 in frontotemporal lobar degeneration and amyotrophic lateral sclerosis.* Science 314:130-133.

Nishimura AL, Mitne-Neto M, Silva HC, Richieri-Costa A, Middleton S, Cascio D, Kok F, Oliveira JR, Gillingwater T, Webb J, Skehel P, Zatz M (2004) *A mutation in the vesicle-trafficking protein VAPB causes late-onset spinal muscular atrophy and amyotrophic lateral sclerosis.* Am J Hum Genet 75:822-831.

Niwa J, Ishigaki S, Hishikawa N, Yamamoto M, Doyu M, Murata S, Tanaka K, Taniguchi N, Sobue G (2002) *Dorfin ubiquitylates mutant SOD1 and prevents mutant SOD1-mediated neurotoxicity.* J Biol Chem 277:36793-36798.

Oliveira AL, Thams S, Lidman O, Piehl F, Hokfelt T, Karre K, Linda H, Cullheim S (2004) *A role for MHC class I molecules in synaptic plasticity and regeneration of neurons after axotomy.* Proc Natl Acad Sci U S A 101:17843-17848.

Oosthuyse B, Moons L, Storkebaum E, Beck H, Nuyens D, Brusselmans K, Van Dorpe J, Hellings P, Gorselink M, Heymans S, Theilmeier G, Dewerchin M, Laudenbach V, Vermylen P, Raat H, Acker T, Vleminckx V, Van Den Bosch L, Cashman N, Fujisawa H, Drost MR, Sciot R, Bruyninckx F, Hicklin DJ, Ince C, Gressens P, Lupu F, Plate KH, Robberecht W, Herbert JM, Collen D, Carmeliet P (2001) *Deletion of the hypoxia-response element in the vascular*

endothelial growth factor promoter causes motor neuron degeneration. Nat Genet 28:131-138.

Orlowski M, Wilk S (2003) *Ubiquitin-independent proteolytic functions of the proteasome.* Arch Biochem Biophys 415:1-5.

Orrell RW (2000) *Amyotrophic lateral sclerosis: copper/zinc superoxide dismutase (SOD1) gene mutations.* Neuromuscul Disord 10:63-68.

Otomo A, Hadano S, Okada T, Mizumura H, Kunita R, Nishijima H, Showguchi-Miyata J, Yanagisawa Y, Kohiki E, Suga E, Yasuda M, Osuga H, Nishimoto T, Narumiya S, Ikeda JE (2003) *ALS2, a novel guanine nucleotide exchange factor for the small GTPase Rab5, is implicated in endosomal dynamics.* Hum Mol Genet 12:1671-1687.

Oyadomari S, Mori M (2004) *Roles of CHOP/GADD153 in endoplasmic reticulum stress.* Cell Death Differ 11:381-389.

Oyanagi K, Wada M (1999) *Neuropathology of parkinsonism-dementia complex and amyotrophic lateral sclerosis of Guam: an update.* J Neurol 246 Suppl 2:II19-27.

Oyanagi K, Ikuta F, Horikawa Y (1989) *Evidence for sequential degeneration of the neurons in the intermediate zone of the spinal cord in amyotrophic lateral sclerosis: a topographic and quantitative investigation.* Acta Neuropathol (Berl) 77:343-349.

Parham P (2005) *Immunogenetics of killer cell immunoglobulin-like receptors.* Mol Immunol 42:459-462.

Pasinelli P, Brown RH (2006) *Molecular biology of amyotrophic lateral sclerosis: insights from genetics.* Nat Rev Neurosci 7:710-723.

Pasinelli P, Belford ME, Lennon N, Bacskai BJ, Hyman BT, Trotti D, Brown RH, Jr. (2004) *Amyotrophic lateral sclerosis-associated SOD1 mutant proteins bind and aggregate with Bcl-2 in spinal cord mitochondria.* Neuron 43:19-30.

Peng J, Schwartz D, Elias JE, Thoreen CC, Cheng D, Marsischky G, Roelofs J, Finley D, Gygi SP (2003) *A proteomics approach to understanding protein ubiquitination.* Nat Biotechnol 21:921-926.

Piccinini M, Mostert M, Croce S, Baldovino S, Papotti M, Rinaudo MT (2003) *Interferon-gamma-inducible subunits are incorporated in human brain 20S proteasome.* J Neuroimmunol 135:135-140.

Pickart CM, Eddins MJ (2004) *Ubiquitin: structures, functions, mechanisms.* Biochim Biophys Acta 1695:55-72.

Plaitakis A, Caroscio JT (1987) *Abnormal glutamate metabolism in amyotrophic lateral sclerosis.* Ann Neurol 22:575-579.

Pramatarova A, Laganiere J, Roussel J, Brisebois K, Rouleau GA (2001) *Neuron-specific expression of mutant superoxide dismutase 1 in transgenic mice does not lead to motor impairment.* J Neurosci 21:3369-3374.

Puttaparthi K, Elliott JL (2005) *Non-neuronal induction of immunoproteasome subunits in an ALS model: possible mediation by cytokines.* Exp Neurol 196:441-451.

Puttaparthi K, Van Kaer L, Elliott JL (2007) *Assessing the role of immuno-proteasomes in a mouse model of familial ALS.* Exp Neurol 206:53-58.

Puttaparthi K, Wojcik C, Rajendran B, DeMartino GN, Elliott JL (2003) *Aggregate formation in the spinal cord of mutant SOD1 transgenic mice is reversible and mediated by proteasomes.* J Neurochem 87:851-860.

Rakhit R, Crow JP, Lepock JR, Kondejewski LH, Cashman NR, Chakrabartty A (2004) *Monomeric Cu,Zn-superoxide dismutase is a common misfolding intermediate in the oxidation models of sporadic and familial amyotrophic lateral sclerosis.* J Biol Chem 279:15499-15504.

Rakhit R, Cunningham P, Furtos-Matei A, Dahan S, Qi XF, Crow JP, Cashman NR, Kondejewski LH, Chakrabartty A (2002) *Oxidation-induced misfolding and aggregation of superoxide dismutase and its implications for amyotrophic lateral sclerosis.* J Biol Chem 277:47551-47556.

Ramanathan M, Hasko G, Leibovich SJ (2005) *Analysis of signal transduction pathways in macrophages using expression vectors with CMV promoters: a cautionary tale.* Inflammation 29:94-102.

Ramos PC, Hockendorff J, Johnson ES, Varshavsky A, Dohmen RJ (1998) *Ump1p is required for proper maturation of the 20S proteasome and becomes its substrate upon completion of the assembly.* Cell 92:489-499.

Ranta S, Zhang Y, Ross B, Lonka L, Takkunen E, Messer A, Sharp J, Wheeler R, Kusumi K, Mole S, Liu W, Soares MB, Bonaldo MF, Hirvasniemi A, de la Chapelle A, Gilliam TC, Lehesjoki AE (1999) *The neuronal ceroid*

lipofuscinoses in human EPMR and mnd mutant mice are associated with mutations in CLN8. Nat Genet 23:233-236.

Ray SS, Nowak RJ, Strokovich K, Brown RH, Jr., Walz T, Lansbury PT, Jr. (2004) *An intersubunit disulfide bond prevents in vitro aggregation of a superoxide dismutase-1 mutant linked to familial amytrophic lateral sclerosis.* Biochemistry 43:4899-4905.

Raynor EM, Shefner JM (1994) *Recurrent inhibition is decreased in patients with amyotrophic lateral sclerosis.* Neurology 44:2148-2153.

Reaume AG, Elliott JL, Hoffman EK, Kowall NW, Ferrante RJ, Siwek DF, Wilcox HM, Flood DG, Beal MF, Brown RH, Jr., Scott RW, Snider WD (1996) *Motor neurons in Cu/Zn superoxide dismutase-deficient mice develop normally but exhibit enhanced cell death after axonal injury.* Nat Genet 13:43-47.

Richardson JS, Richardson DC, Thomas KA, Silverton EW, Davies DR (1976) *Similarity of three-dimensional structure between the immunoglobulin domain and the copper, zinc superoxide dismutase subunit.* J Mol Biol 102:221-235.

Rideout HJ, Larsen KE, Sulzer D, Stefanis L (2001) *Proteasomal inhibition leads to formation of ubiquitin/alpha-synuclein-immunoreactive inclusions in PC12 cells.* J Neurochem 78:899-908.

Rippon GA, Scarmeas N, Gordon PH, Murphy PL, Albert SM, Mitsumoto H, Marder K, Rowland LP, Stern Y (2006) *An observational study of cognitive impairment in amyotrophic lateral sclerosis.* Arch Neurol 63:345-352.

Ripps ME, Huntley GW, Hof PR, Morrison JH, Gordon JW (1995) *Transgenic mice expressing an altered murine superoxide dismutase gene provide an animal model of amyotrophic lateral sclerosis.* Proc Natl Acad Sci U S A 92:689-693.

Robberecht W, Aguirre T, Van den Bosch L, Tilkin P, Cassiman JJ, Matthijs G (1996) *D90A heterozygosity in the SOD1 gene is associated with familial and apparently sporadic amyotrophic lateral sclerosis.* Neurology 47:1336-1339.

Rock KL, Gramm C, Rothstein L, Clark K, Stein R, Dick L, Hwang D, Goldberg AL (1994) *Inhibitors of the proteasome block the degradation of most cell proteins and the generation of peptides presented on MHC class I molecules.* Cell 78:761-771.

Rodriguez JA, Valentine JS, Eggers DK, Roe JA, Tiwari A, Brown RH, Jr., Hayward LJ (2002) *Familial amyotrophic lateral sclerosis-associated mutations decrease the thermal stability of distinctly metallated species of human copper/zinc superoxide dismutase.* J Biol Chem 277:15932-15937.

Rodriguez JA, Shaw BF, Durazo A, Sohn SH, Doucette PA, Nersissian AM, Faull KF, Eggers DK, Tiwari A, Hayward LJ, Valentine JS (2005) *Destabilization of apoprotein is insufficient to explain Cu,Zn-superoxide dismutase-linked ALS pathogenesis.* Proc Natl Acad Sci U S A 102:10516-10521.

Rosen DR, Siddique T, Patterson D, Figlewicz DA, Sapp P, Hentati A, Donaldson D, Goto J, O'Regan JP, Deng HX, et al. (1993) *Mutations in Cu/Zn superoxide dismutase gene are associated with familial amyotrophic lateral sclerosis.* Nature 362:59-62.

Ross CA, Poirier MA (2005) Opinion: *What is the role of protein aggregation in neurodegeneration?* Nat Rev Mol Cell Biol 6:891-898.

Roth RA, Koshland ME (1981) *Role of disulfide interchange enzyme in immunoglobulin synthesis.* Biochemistry 20:6594-6599.

Rothstein JD, Tsai G, Kuncl RW, Clawson L, Cornblath DR, Drachman DB, Pestronk A, Stauch BL, Coyle JT (1990) *Abnormal excitatory amino acid metabolism in amyotrophic lateral sclerosis.* Ann Neurol 28:18-25.

Rutkowski DT, Kaufman RJ (2004) *A trip to the ER: coping with stress.* Trends Cell Biol 14:20-28.

Saigoh K, Wang YL, Suh JG, Yamanishi T, Sakai Y, Kiyosawa H, Harada T, Ichihara N, Wakana S, Kikuchi T, Wada K (1999) *Intragenic deletion in the gene encoding ubiquitin carboxy-terminal hydrolase in gad mice.* Nat Genet 23:47-51.

Salomons FA, Verhoef LG, Dantuma NP. (2005) *Fluorescent reporters for the ubiquitin-proteasome system.* Essays Biochem. 41:113-28.

Santacruz K, Lewis J, Spires T, Paulson J, Kotilinek L, Ingelsson M, Guimaraes A, DeTure M, Ramsden M, McGowan E, Forster C, Yue M, Orne J, Janus C, Mariash A, Kuskowski M, Hyman B, Hutton M, Ashe KH (2005) *Tau suppression in a neurodegenerative mouse model improves memory function.* Science 309:476-481.

Sasaki S, Maruyama S (1991) *Immunocytochemical and ultrastructural studies of hyaline inclusions in sporadic motor neuron disease.* Acta Neuropathol (Berl) 82:295-301.

Sasaki S, Maruyama S (1993) *A fine structural study of Onuf's nucleus in sporadic amyotrophic lateral sclerosis.* J Neurol Sci 119:28-37.

Sasaki S, Iwata M (1996) *Synaptic loss in anterior horn neurons in lower motor neuron disease.* Acta Neuropathol (Berl) 91:416-421.

Sato-Harada R, Okabe S, Umeyama T, Kanai Y, Hirokawa N (1996) *Microtubule-associated proteins regulate microtubule function as the track for intracellular membrane organelle transports.* Cell Struct Funct 21:283-295.

Sato T, Nakanishi T, Yamamoto Y, Andersen PM, Ogawa Y, Fukada K, Zhou Z, Aoike F, Sugai F, Nagano S, Hirata S, Ogawa M, Nakano R, Ohi T, Kato T, Nakagawa M, Hamasaki T, Shimizu A, Sakoda S (2005) *Rapid disease progression correlates with instability of mutant SOD1 in familial ALS.* Neurology 65:1954-1957.

Sau D, De Biasi S, Vitellaro-Zuccarello L, Riso P, Guarnieri S, Porrini M, Simeoni S, Crippa V, Onesto E, Palazzolo I, Rusmini P, Bolzoni E, Bendotti C, Poletti A (2007) *Mutation of SOD1 in ALS: a gain of a loss of function.* Hum Mol Genet 16:1604-1618.

Scheffner M, Nuber U, Huibregtse JM (1995) *Protein ubiquitination involving an E1-E2-E3 enzyme ubiquitin thioester cascade.* Nature 373:81-83.

Schmalbruch H, Jensen HJ, Bjaerg M, Kamieniecka Z, Kurland L (1991) *A new mouse mutant with progressive motor neuronopathy.* J Neuropathol Exp Neurol 50:192-204.

Schmitt-John T, Drepper C, Mussmann A, Hahn P, Kuhlmann M, Thiel C, Hafner M, Lengeling A, Heimann P, Jones JM, Meisler MH, Jockusch H (2005) *Mutation of Vps54 causes motor neuron disease and defective spermiogenesis in the wobbler mouse.* Nat Genet 37:1213-1215.

Schnell JD, Hicke L (2003) *Non-traditional functions of ubiquitin and ubiquitin-binding proteins.* J Biol Chem 278:35857-35860.

Schochet SS, Jr., Hardman JM, Ladewig PP, Earle KM (1969) *Intraneuronal conglomerates in sporadic motor neuron disease. A light and electron microscopic study.* Arch Neurol 20:548-553.

Schreiber H, Gaigalat T, Wiedemuth-Catrinescu U, Graf M, Uttner I, Muche R, Ludolph AC (2005) *Cognitive function in bulbar- and spinal-onset amyotrophic lateral sclerosis. A longitudinal study in 52 patients.* J Neurol 252:772-781.

Schwarz K, Eggers M, Soza A, Koszinowski UH, Kloetzel PM, Groettrup M (2000) *The proteasome regulator PA28alpha/beta can enhance antigen presentation without affecting 20S proteasome subunit composition.* Eur J Immunol 30:3672-3679.

Seilhean D, Takahashi J, El Hachimi KH, Fujigasaki H, Lebre AS, Biancalana V, Durr A, Salachas F, Hogenhuis J, de The H, Hauw JJ, Meininger V, Brice A, Duyckaerts C (2004) *Amyotrophic lateral sclerosis with neuronal intranuclear protein inclusions.* Acta Neuropathol (Berl) 108:81-87.

Shang F, Taylor A (1995) *Oxidative stress and recovery from oxidative stress are associated with altered ubiquitin conjugating and proteolytic activities in bovine lens epithelial cells.* Biochem J 307 (Pt 1):297-303.

Shaw PJ, Ince PG, Falkous G, Mantle D (1995) *Oxidative damage to protein in sporadic motor neuron disease spinal cord.* Ann Neurol 38:691-695.

Shibata N (2001) *Transgenic mouse model for familial amyotrophic lateral sclerosis with superoxide dismutase-1 mutation.* Neuropathology 21:82-92.

Shinder GA, Lacourse MC, Minotti S, Durham HD (2001) *Mutant Cu/Zn-superoxide dismutase proteins have altered solubility and interact with heat shock/stress proteins in models of amyotrophic lateral sclerosis.* J Biol Chem 276:12791-12796.

Shringarpure R, Grune T, Mehlhase J, Davies KJ (2003) *Ubiquitin conjugation is not required for the degradation of oxidized proteins by proteasome.* J Biol Chem 278:311-318.

Siddons MA, Pickering-Brown SM, Mann DM, Owen F, Cooper PN (1996) *Debrisoquine hydroxylase gene polymorphism frequencies in patients with amyotrophic lateral sclerosis.* Neurosci Lett 208:65-68.

Siklos L, Engelhardt J, Harati Y, Smith RG, Joo F, Appel SH (1996) *Ultrastructural evidence for altered calcium in motor nerve terminals in amyotropic lateral sclerosis.* Ann Neurol 39:203-216.

Sitte N, Huber M, Grune T, Ladhoff A, Doecke WD, Von Zglinicki T, Davies KJ (2000) *Proteasome inhibition by lipofuscin/ceroid during postmitotic aging of fibroblasts.* Faseb J 14:1490-1498.

Sobue G, Hashizume Y, Yasuda T, Mukai E, Kumagai T, Mitsuma T, Trojanowski JQ (1990) *Phosphorylated high molecular weight neurofilament protein in lower motor neurons in amyotrophic lateral sclerosis and other neurodegenerative diseases involving ventral horn cells.* Acta Neuropathol (Berl) 79:402-408.

Son M, Puttaparthi K, Kawamata H, Rajendran B, Boyer PJ, Manfredi G, Elliott JL (2007) *Overexpression of CCS in G93A-SOD1 mice leads to accelerated neurological deficits with severe mitochondrial pathology.* Proc Natl Acad Sci U S A 104:6072-6077.

Spittaels K, Van den Haute C, Van Dorpe J, Bruynseels K, Vandezande K, Laenen I, Geerts H, Mercken M, Sciot R, Van Lommel A, Loos R, Van Leuven F (1999) *Prominent axonopathy in the brain and spinal cord of transgenic mice overexpressing four-repeat human tau protein.* Am J Pathol 155:2153-2165.

Steffan JS, Agrawal N, Pallos J, Rockabrand E, Trotman LC, Slepko N, Illes K, Lukacsovich T, Zhu YZ, Cattaneo E, Pandolfi PP, Thompson LM, Marsh JL (2004) *SUMO modification of Huntingtin and Huntington's disease pathology.* Science 304:100-104.

Stephens B, Guiloff RJ, Navarrete R, Newman P, Nikhar N, Lewis P (2006) *Widespread loss of neuronal populations in the spinal ventral horn in sporadic motor neuron disease. A morphometric study.* J Neurol Sci 244:41-58.

Stieber A, Gonatas JO, Gonatas NK (2000) *Aggregates of mutant protein appear progressively in dendrites, in periaxonal processes of oligodendrocytes, and in neuronal and astrocytic perikarya of mice expressing the SOD1(G93A) mutation of familial amyotrophic lateral sclerosis.* J Neurol Sci 177:114-123.

Stohwasser R, Giesebrecht J, Kraft R, Muller EC, Hausler KG, Kettenmann H, Hanisch UK, Kloetzel PM (2000) *Biochemical analysis of proteasomes from mouse microglia: induction of immunoproteasomes by interferon-gamma and lipopolysaccharide.* Glia 29:355-365.

Stokin GB, Lillo C, Falzone TL, Brusch RG, Rockenstein E, Mount SL, Raman R, Davies P, Masliah E, Williams DS, Goldstein LS (2005) *Axonopathy and*

transport deficits early in the pathogenesis of Alzheimer's disease. Science 307:1282-1288.

Strange RW, Antonyuk S, Hough MA, Doucette PA, Rodriguez JA, Hart PJ, Hayward LJ, Valentine JS, Hasnain SS (2003) *The structure of holo and metal-deficient wild-type human Cu, Zn superoxide dismutase and its relevance to familial amyotrophic lateral sclerosis.* J Mol Biol 328:877-891.

Strong MJ, Kesavapany S, Pant HC (2005) *The pathobiology of amyotrophic lateral sclerosis: a proteinopathy?* J Neuropathol Exp Neurol 64:649-664.

Subramaniam JR, Lyons WE, Liu J, Bartnikas TB, Rothstein J, Price DL, Cleveland DW, Gitlin JD, Wong PC (2002) *Mutant SOD1 causes motor neuron disease independent of copper chaperone-mediated copper loading.* Nat Neurosci 5:301-307.

Sumi H, Nagano S, Fujimura H, Kato S, Sakoda S (2006) *Inverse correlation between the formation of mitochondria-derived vacuoles and Lewy-body-like hyaline inclusions in G93A superoxide-dismutase-transgenic mice.* Acta Neuropathol (Berl) 112:52-63.

Swerdlow RH, Parks JK, Cassarino DS, Trimmer PA, Miller SW, Maguire DJ, Sheehan JP, Maguire RS, Pattee G, Juel VC, Phillips LH, Tuttle JB, Bennett JP, Jr., Davis RE, Parker WD, Jr. (1998) *Mitochondria in sporadic amyotrophic lateral sclerosis.* Exp Neurol 153:135-142.

Tainer JA, Getzoff ED, Beem KM, Richardson JS, Richardson DC (1982) *Determination and analysis of the 2 A-structure of copper, zinc superoxide dismutase.* J Mol Biol 160:181-217.

Tiwari A, Hayward LJ (2003) *Familial amyotrophic lateral sclerosis mutants of copper/zinc superoxide dismutase are susceptible to disulfide reduction.* J Biol Chem 278:5984-5992.

Tobisawa S, Hozumi Y, Arawaka S, Koyama S, Wada M, Nagai M, Aoki M, Itoyama Y, Goto K, Kato T (2003) *Mutant SOD1 linked to familial amyotrophic lateral sclerosis, but not wild-type SOD1, induces ER stress in COS7 cells and transgenic mice.* Biochem Biophys Res Commun 303:496-503.

Tofaris GK, Layfield R, Spillantini MG (2001) *alpha-synuclein metabolism and aggregation is linked to ubiquitin-independent degradation by the proteasome.* FEBS Lett 509:22-26.

Tomik B, Adamek D, Pierzchalski P, Banares S, Duda A, Partyka D, Pawlik W, Kaluza J, Krajewski S, Szczudlik A (2005) *Does apoptosis occur in amyotrophic lateral sclerosis? TUNEL experience from human amyotrophic lateral sclerosis (ALS) tissues.* Folia Neuropathol 43:75-80.

Topp JD, Gray NW, Gerard RD, Horazdovsky BF (2004) *Alsin is a Rab5 and Rac1 guanine nucleotide exchange factor.* J Biol Chem 279:24612-24623.

Tortarolo M, Veglianese P, Calvaresi N, Botturi A, Rossi C, Giorgini A, Migheli A, Bendotti C (2003) *Persistent activation of p38 mitogen-activated protein kinase in a mouse model of familial amyotrophic lateral sclerosis correlates with disease progression.* Mol Cell Neurosci 23:180-192.

Toyoshima I, Sugawara M, Kato K, Wada C, Hirota K, Hasegawa K, Kowa H, Sheetz MP, Masamune O (1998) *Kinesin and cytoplasmic dynein in spinal spheroids with motor neuron disease.* J Neurol Sci 159:38-44.

Tseng BP, Green KN, Chan JL, Blurton-Jones M, Laferla FM (2007) *Abeta inhibits the proteasome and enhances amyloid and tau accumulation.* Neurobiol Aging.

Tsuji S, Kikuchi S, Shinpo K, Tashiro J, Kishimoto R, Yabe I, Yamagishi S, Takeuchi M, Sasaki H (2005) *Proteasome inhibition induces selective motor neuron death in organotypic slice cultures.* J Neurosci Res 82:443-451.

Tudor EL, Perkinton MS, Schmidt A, Ackerley S, Brownlees J, Jacobsen NJ, Byers HL, Ward M, Hall A, Leigh PN, Shaw CE, McLoughlin DM, Miller CC (2005) *ALS2/Alsin regulates Rac-PAK signaling and neurite outgrowth.* J Biol Chem 280:34735-34740.

Turano C, Coppari S, Altieri F, Ferraro A (2002) *Proteins of the PDI family: unpredicted non-ER locations and functions.* J Cell Physiol 193:154-163.

Tyers M, Willems AR (1999) *One ring to rule a superfamily of E3 ubiquitin ligases.* Science 284:601, 603-604.

Unal-Cevik I, Kilinc M, Gursoy-Ozdemir Y, Gurer G, Dalkara T (2004) Loss *of NeuN immunoreactivity after cerebral ischemia does not indicate neuronal cell loss: a cautionary note.* Brain Res 1015:169-174.

Urushitani M, Kurisu J, Tsukita K, Takahashi R (2002) *Proteasomal inhibition by misfolded mutant superoxide dismutase 1 induces selective motor neuron death in familial amyotrophic lateral sclerosis.* J Neurochem 83:1030-1042.

Urushitani M, Sik A, Sakurai T, Nukina N, Takahashi R, Julien JP (2006) *Chromogranin-mediated secretion of mutant superoxide dismutase proteins linked to amyotrophic lateral sclerosis.* Nat Neurosci 9:108-118.

Urushitani M, Kurisu J, Tateno M, Hatakeyama S, Nakayama K, Kato S, Takahashi R (2004) *CHIP promotes proteasomal degradation of familial ALS-linked mutant SOD1 by ubiquitinating Hsp/Hsc70.* J Neurochem 90:231-244.

Van Kaer L, Ashton-Rickardt PG, Eichelberger M, Gaczynska M, Nagashima K, Rock KL, Goldberg AL, Doherty PC, Tonegawa S (1994) *Altered peptidase and viral-specific T cell response in LMP2 mutant mice.* Immunity 1:533-541.

Veglianese P, Lo Coco D, Bao Cutrona M, Magnoni R, Pennacchini D, Pozzi B, Gowing G, Julien JP, Tortarolo M, Bendotti C (2006) *Activation of the p38MAPK cascade is associated with upregulation of TNF alpha receptors in the spinal motor neurons of mouse models of familial ALS.* Mol Cell Neurosci 31:218-231.

Verma R, Aravind L, Oania R, McDonald WH, Yates JR, 3rd, Koonin EV, Deshaies RJ (2002) *Role of Rpn11 metalloprotease in deubiquitination and degradation by the 26S proteasome.* Science 298:611-615.

Vlug AS, Jaarsma D (2004) *Long term proteasome inhibition does not preferentially afflict motor neurons in organotypical spinal cord cultures.* Amyotroph Lateral Scler Other Motor Neuron Disord 5:16-21.

Vlug AS, Teuling E, Haasdijk ED, French P, Hoogenraad CC, Jaarsma D (2005) *ATF3 expression precedes death of spinal motoneurons in amyotrophic lateral sclerosis-SOD1 transgenic mice and correlates with c-Jun phosphorylation, CHOP expression, somato-dendritic ubiquitination and Golgi fragmentation.* Eur J Neurosci 22:1881-1894.

Wang J, Xu G, Borchelt DR (2002) *High molecular weight complexes of mutant superoxide dismutase 1: age-dependent and tissue-specific accumulation.* Neurobiol Dis 9:139-148.

Wang J, Slunt H, Gonzales V, Fromholt D, Coonfield M, Copeland NG, Jenkins NA, Borchelt DR (2003) *Copper-binding-site-null SOD1 causes ALS in transgenic mice: aggregates of non-native SOD1 delineate a common feature.* Hum Mol Genet 12:2753-2764.

Wang J, Xu G, Slunt HH, Gonzales V, Coonfield M, Fromholt D, Copeland NG, Jenkins NA, Borchelt DR (2005) *Coincident thresholds of mutant protein for paralytic disease and protein aggregation caused by restrictively expressed superoxide dismutase cDNA.* Neurobiol Dis 20:943-952.

Wang XZ, Ron D (1996) *Stress-induced phosphorylation and activation of the transcription factor CHOP (GADD153) by p38 MAP Kinase.* Science 272:1347-1349.

Watanabe M, Dykes-Hoberg M, Culotta VC, Price DL, Wong PC, Rothstein JD (2001) *Histological evidence of protein aggregation in mutant SOD1 transgenic mice and in amyotrophic lateral sclerosis neural tissues.* Neurobiol Dis 8:933-941.

Welchman RL, Gordon C, Mayer RJ (2005) *Ubiquitin and ubiquitin-like proteins as multifunctional signals.* Nat Rev Mol Cell Biol 6:599-609.

Wharton SP (2003) *Pathology of motor neuron disorders.* Philadelphia: Butterworth-Heinemann.

Wiedau-Pazos M, Goto JJ, Rabizadeh S, Gralla EB, Roe JA, Lee MK, Valentine JS, Bredesen DE (1996) *Altered reactivity of superoxide dismutase in familial amyotrophic lateral sclerosis.* Science 271:515-518.

Wilkinson KD, Rose IA (1980) *Glucose exchange and catalysis by two crystalline hexokinase x glucose complexes. Evidence for an obligatory ATP-dependent conformational change in catalysis.* J Biol Chem 255:7569-7574.

Williamson E, Westrich GM, Viney JL (1999) *Modulating dendritic cells to optimize mucosal immunization protocols.* J Immunol 163:3668-3675.

Williamson TL, Bruijn LI, Zhu Q, Anderson KL, Anderson SD, Julien JP, Cleveland DW (1998) *Absence of neurofilaments reduces the selective vulnerability of motor neurons and slows disease caused by a familial amyotrophic lateral sclerosis-linked superoxide dismutase 1 mutant.* Proc Natl Acad Sci U S A 95:9631-9636.

Witherden AS, Hafezparast M, Nicholson SJ, Ahmad-Annuar A, Bermingham N, Arac D, Rankin J, Iravani M, Ball S, Peters J, Martin JE, Huntley D, Hummerich H, Sergot M, Fisher EM (2002) *An integrated genetic, radiation hybrid, physical and transcription map of a region of distal mouse chromosome*

12, including an imprinted locus and the 'Legs at odd angles' (Loa) mutation. Gene 283:71-82.

Witt E, Zantopf D, Schmidt M, Kraft R, Kloetzel PM, Kruger E (2000) *Characterisation of the newly identified human Ump1 homologue POMP and analysis of LMP7(beta 5i) incorporation into 20 S proteasomes.* J Mol Biol 301:1-9.

Wong GH (1995) *Protective roles of cytokines against radiation: induction of mitochondrial MnSOD.* Biochim Biophys Acta 1271:205-209.

Wootz H, Hansson I, Korhonen L, Napankangas U, Lindholm D (2004) *Caspase-12 cleavage and increased oxidative stress during motoneuron degeneration in transgenic mouse model of ALS.* Biochem Biophys Res Commun 322:281-286.

Xu Z, Cork LC, Griffin JW, Cleveland DW (1993) *Involvement of neurofilaments in motor neuron disease.* J Cell Sci Suppl 17:101-108.

Yang Y, Hentati A, Deng HX, Dabbagh O, Sasaki T, Hirano M, Hung WY, Ouahchi K, Yan J, Azim AC, Cole N, Gascon G, Yagmour A, Ben-Hamida M, Pericak-Vance M, Hentati F, Siddique T (2001) *The gene encoding alsin, a protein with three guanine-nucleotide exchange factor domains, is mutated in a form of recessive amyotrophic lateral sclerosis.* Nat Genet 29:160-165.

Yao T, Cohen RE (2002) *A cryptic protease couples deubiquitination and degradation by the proteasome.* Nature 419:403-407.

Yedidia Y, Horonchik L, Tzaban S, Yanai A, Taraboulos A (2001) *Proteasomes and ubiquitin are involved in the turnover of the wild-type prion protein.* Embo J 20:5383-5391.

Young P, Deveraux Q, Beal RE, Pickart CM, Rechsteiner M (1998) *Characterization of two polyubiquitin binding sites in the 26 S protease subunit 5a.* J Biol Chem 273:5461-5467.

Zhang FL, Kirschmeier P, Carr D, James L, Bond RW, Wang L, Patton R, Windsor WT, Syto R, Zhang R, Bishop WR (1997) *Characterization of Ha-ras, N-ras, Ki-Ras4A, and Ki-Ras4B as in vitro substrates for farnesyl protein transferase and geranylgeranyl protein transferase type I.* J Biol Chem 272:10232-10239.

Zhang R, Gascon R, Miller RG, Gelinas DF, Mass J, Hadlock K, Jin X, Reis J, Narvaez A, McGrath MS (2005) *Evidence for systemic immune system alterations in sporadic amyotrophic lateral sclerosis (sALS).* J Neuroimmunol 159:215-224.

LIST OF PUBLICATIONS

Publication arisen from the work reported in this thesis

Basso M, Massignan T, Samengo G, Cheroni C, De Biasi S, Salmona M, Bendotti C, Bonetto V (2006) *Insoluble mutant SOD1 is partly oligoubiquitinated in amyotrophic lateral sclerosis mice.* J Biol Chem 281:33325-33335.

Publications not strictly related to this thesis

Peviani M, Cheroni C, Troglio F, Quarto M, Pelicci G, Bendotti C (2007) *Lack of changes in the PI3K/AKT survival pathway in the spinal cord motor neurons of a mouse model of familial amyotrophic lateral sclerosis.* Mol Cell Neurosci 34:592-602

Cheroni C, Peviani M, Cascio P, Debiasi S, Monti C, Bendotti C (2005) *Accumulation of human SOD1 and ubiquitinated deposits in the spinal cord of SOD1G93A mice during motor neuron disease progression correlates with a decrease of proteasome.* Neurobiol Dis 18:509-522.

Bendotti C, Bao Cutrona M, Cheroni C, Grignaschi G, Lo Coco D, Peviani M, Tortarolo M, Veglianese P, Zennaro E (2005) *Inter- and intracellular signaling in amyotrophic lateral sclerosis: role of p38 mitogen-activated protein kinase.* Neurodegener Dis 2:128-134.

Casoni F, Basso M, Massignan T, Gianazza E, Cheroni C, Salmona M, Bendotti C, Bonetto V (2005) *Protein nitration in a mouse model of familial amyotrophic lateral sclerosis: possible multifunctional role in the pathogenesis.* J Biol Chem 280:16295-16304.